o-Nitrobenzyl Functionalized Photo-patternable Conjugated Polymers

A dissertation submitted by

Zachary Craig Smith

in partial fulfillment of the requirements for the degree of

Doctor of Philosophy

In

Chemistry

TUFTS UNIVERSITY

May 2015

Advisor: Professor Samuel W. Thomas III

Abstract

Organic electronics often use conjugated polymers to enable optoelectronic activity. It is a common practice to modify a polymer with alkyl side chains that improve its solubility so that solution processing can be used to make solid state samples. While this approach has proven useful, it introduces some additional issues: i) if the device contains multiple layers, any solution based processing must not perturb already existing layers, and ii) the solubilizing side chains occupy space in the solid state with atoms that have no optoelectronic activity. This thesis describes a novel technique where conjugated polymers are functionalized with solubilizing side chains that can be removed by irradiating the polymer with ultraviolet light.

Chapter 2 describes the use of photocleavable *o*-nitrobenzyl (NB) ester solubilizing side chains on a polythiophene backbone. This methodology works in both solution leading to aggregation, and in the solid state leading to an insoluble film. Prior work on changing the solubility of polythiophene relied on using heat as the external stimulus to initiate the side chain cleavage. Chapter 3 describes the further exploration of NB side chains on polythiophene. This work examines the modification of the NB group to increase the rate of photocleavage, the use of donor-accepter polymer backbones, and patterning. Finally, Chapter 4 describes the application of this methodology to new low-bandgap conjugated polymers that absorb light in the near-infrared (NIR) region.

Acknowledgements

The first person I need to thank is my advisor, Sam Thomas. Sam has always believed in me and encouraged me to pursue any avenue that would further my career. From the minute I joined the lab, Sam always wanted to make sure I was happy, and this attitude helped foster an amazing lab atmosphere. For all of his support, I am truly thankful. I would also like to thank Professor Clay Bennett and Professor Elena Rybak-Akimova for their support throughout my time at Tufts, and Professor Erik Berda for graciously being my outside committee member. I would also like to thank Dr. Stefanie Sydlik for always being super positive and encouraging throughout this past year. I cannot wait to work for you at CMU and help you establish setup the lab!

I would also like to thank all the members of Team Thomas: Patty Gumbley, Rob Pawle, Jingjing Zhang, Esra Altinok, Xioran Hu, Rom Baral, Fanny Frausto, Brendan Duran, Matt Feeney, Seth Sharber, and the many undergraduates I got to interact with over the years. I would like to specifically thank Rob, Patty, and Jingjing for all helping to train me over the years. You all were incredibly helpful and welcoming in the beginning. I would also like to thank Esra for always being my confidant, as we came through the lab side by side. Lastly, I would like to thank Trey Lawrence for being a great friend and excellent mentee.

I would also like to thank all of my friends in the department. There are too many people to name everyone, but I would specifically like to thank Kyle, Glen, and Maël for being an awesome group of senior guys who took me under

their wings in my first few years of grad school. I would also like to thank Sean McHugh for being my own personal trainer, getting me into better shape, and for being an awesome friend who has made my last two years of grad school an absolute joy.

I would like to thank my family for all of their support over the years. Thank you for all of the times you have been encouraging, and for understanding my work schedule. It has been a tremendous boon to have you all so close by these past five years and I will truly miss being near you all over the next few years.

Finally, I would like to thank my girlfriend, Melissa Weiner. Melissa and I started dating during my first month at Tufts so she has been by my side the whole way. Thank you so much for always being there for me, putting up with my ever changing work schedule (especially this past fall), and for always listening to me talk about work. You have no idea how much it means to me that you are genuinely interested and curious when it comes to me talking about chemistry. I absolutely cannot wait to move to Pittsburgh with you and begin the next chapter of our lives together!

Table of Contents

List of Tables

List of Figures

List of Charts

List of Schemes

List of Common Abbreviations

AFM ..... Atomic Force Microscopy
CP ..... Conjugated Polymer
DCC ..... *N*,*N*′-Dicyclohexylcarbodiimide
DCM ..... Dichloromethane
DMAP 4-Dimethylaminopyridine
DMF ..... Dimethylformamide
DMSO ..... Dimethyl Sulfoxide
GPC ..... Gel Permeation Chromatography
HMDS ..... Hexamethyldisilazane
HOMO ..... Highest Occupied Molecular Orbital
HRMS ..... High Resolution Mass Spectrometry
I_{SD} ..... Source-Drain Current
I-V ..... Current-Voltage
LBCP ..... Low Bandgap Conjugated Polymer
LUMO ..... Lowest Unoccupied Molecular Orbital
M_n ..... Number Average Molecular Weight
MNB ..... Methylated *o*-Nitrobenzyl
NB ..... *o*-Nitrobenzyl
NBS ..... *N*-Bromosuccinimde
NIR ..... Near-Infrared
NMR ..... Nuclear Magnetic Resonance
OD ..... Optical Density
OLED ..... Organic Light-Emitting Diode
OPV ..... Organic Photovoltaic
OTFT ..... Organic Thin Film Transistor
P3HT ..... Poly-(3-hexylthiophene)
PCE ..... Power Conversion Efficiency
PDI ..... Polydispersity Index
PEN ..... Polyethylene Naphthalate
PET ..... Polyethylene Terephthalate
PLA ..... Polylactic Acid
PT ..... Polythiophene
R2R ..... Roll-to-Roll
THF ..... Tetrahydrofuran
TQ ..... Thiadiazoloquinoxaline
UV ..... Ultraviolet
V_{DS} ..... Source-Drain Voltage
V_{GS} ..... Gate-Source Voltage
ε ..... Molar Extinction Coefficient
Φ_F ..... Quantum Yield of Fluorescence
Φ_P ..... Quantum Yield of Photocleavage

o-Nitrobenzyl Functionalized Photo-patternable Conjugated Polymers

Chapter 1:

Introduction to Photoresponsive Conjugated Polymers

1.1 Introduction to Conjugated Polymers

Conjugated polymers (CPs) are macromolecules that have a fully conjugated backbone comprised of sp or sp^2 hybridized carbon atoms. The conjugated nature of CPs give them many unique properties that can include: conducting electricity, absorbing light, and emitting light. Some examples of conjugated polymers can be seen in Chart 1.1.

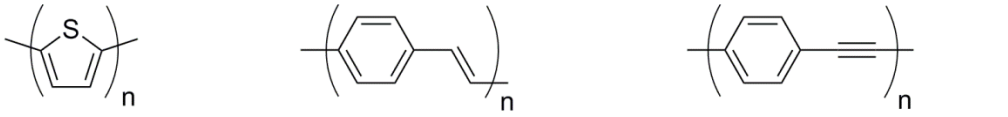

Polythiophene (PT) Polyphenylene vinylene (PPV) Polyphenylene ethynylene (PPE)

Chart 1.1 Examples of conjugated polymers comprised of three different structure types: i) only aromatic rings (PT), ii) aromatic rings and exocyclic double bonds (PPV), and iii) aromatic rings and exocyclic triple bonds (PPE).

Due to their ability to exhibit semiconducting properties, conjugated polymers are often compared to inorganic semiconducting materials, which are traditionally used when making electronic devices. However, there is a current movement to try to transition some electronics from inorganic materials to organic materials. This is driven by three key factors: cost, processability, and flexibility of the material.[1,2] Organic materials are typically less expensive, easier to manufacture, less energy intensive to fabricate, lighter weight, and more flexible than their inorganic counterparts.[3,4] The main drawbacks of organic electronics are device stability and efficiency. However, since the use of organic materials in electronic devices is a much newer field than inorganic materials, there still is a large discrepancy in the performances of the materials. That being

said, there has been huge progress in recent years in developing better organic electronics.

1.1.1 Photophysical Properties of Conjugated Polymers

Beyond their semiconducting properties, conjugated polymers exhibit many unique optoelectronic properties as well. Conjugated polymers typically absorb light in the visible region of the electromagnetic spectrum and many emit light through a process known as fluorescence. A schematic showing the typical processes of absorption and emission can be seen in the Jablonski diagram shown in Figure 1.1. The polymer at its ground electronic state (S_0) absorbs a photon with enough energy to promote the polymer to an excited electronic state (S_1, S_2, …). The excited state accessed is directly related to the energy of photon absorbed by the polymer. The excitation is often to an excited vibrational level within an excited electronic state. The polymer can then give off the excess energy in the form of radiative and non-radiative decay. Non-radiative decay can involve giving off the excess energy as vibration, or heat, while radiative decay results in the emission of a photon. In most excited fluorescent molecules, energy is first given off in a non-radiative decay in a process known as internal conversion. This brings the excited molecule back down to its S_1 excited state. The molecule can then undergo radiative decay in the form of fluorescence to relax back down to a vibrational level of S_0, the ground electronic state. The amount of energy given off by the emission determines the wavelength of the photon generated. This is why an emission spectrum is over a range of wavelengths and not a single line at

a single wavelength. The same correlation can be made when discussing an absorbance spectrum which is directly tied to the amount of energy of the absorbed photon.

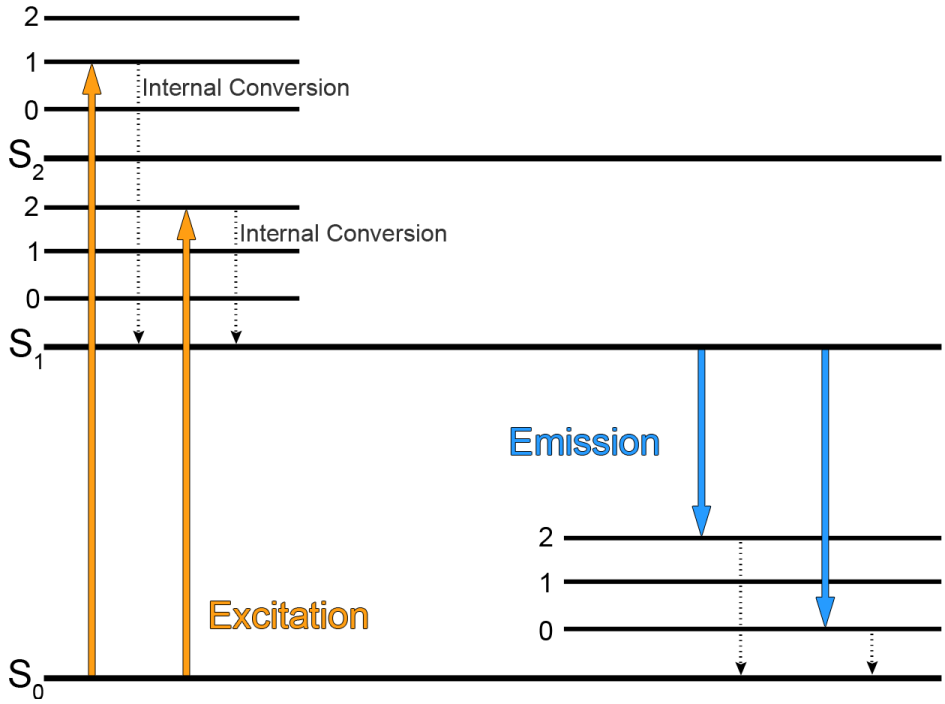

Figure 1.1 A Jablonski diagram depicting the excitation (orange) and emission (blue) of a fluorophore.

One metric that is often used to characterize fluorescent molecules is the quantum yield of fluorescence (Φ_F). This property is described by the following equation:

$$\Phi_F = \frac{\#\text{ of photons emitted}}{\#\text{ of photons absorbed}} \qquad (1)$$

Therefore, if a molecule emits a photon for every absorbed photon, it has a quantum yield of fluorescence of 1.0. The quantum yield of fluorescence of a molecule is dependent on the ratio of the rate of radiative decay and the rate of

non-radiative decay. The desired Φ_F varies greatly depending on the application. In applications that rely on fluorescence output, like displays or sensors, a higher Φ_F is desirable. This would require a molecule with a relative fast rate of radiative decay. However, in applications where the excited state energy is to be harnessed for purposes other than fluorescence, like organic photovoltaics, a lower Φ_F is desirable. These types of applications necessitate a faster rate of non-radiative decay or slower rate of fluorescence.[5]

1.1.2 Electronic Properties of Conjugated Polymers

The electronic properties of conjugated polymers have been of great interest since the initial conductivity measurements of doped polyacetylene in 1977 by Shirakawa, MacDiarmid, and Heeger.[6] Since that discovery there have been many advances in improving the stability, flexibility, processing, and conductivity of electrically conductive or semiconductive conjugated polymers. The conductivity or semiconductivity of a CP is directly related to its bandgap.

The bandgap of a polymer is defined as the energy gap between the highest occupied molecular orbital (HOMO) and lowest unoccupied molecular orbital (LUMO). In materials science these states are often referred to as the valence band and the conduction band, respectively. Thus, the bandgap defines the amount of energy required to transfer an electron from the HOMO to the LUMO.

The bandgap of a polymer is dependent on many factors; one of the most important factors is the length of the conjugated polymer. Huckel theory dictates

that π-electrons can delocalize along adjacent π-bonds and that the activation energy or bandgap between the HOMO and LUMO decreases as the conjugation length increases.[7] Another key factor in modifying the bandgap of a polymer is the structure and substituents of the polymer itself.

The structure of a conducting polymer is often designed to decrease the bandgap of the polymer by enforcing planarity, thus increasing conjugation length and quinoidal character, or by using alternating electron rich and electron poor units, which are often referred to as donor-acceptor polymers.[8,9] Research on conjugated polymers focused on decreasing the bandgap of the materials has led to the creation of a new class of polymer, known as low-bandgap conjugated polymers (LBCPs). The smallest recorded bandgap for an LBCP has been around 1.0 eV, with most other LBCPs exhibiting a bandgap below 1.5 eV.[10] This makes these types of polymers ideal candidates for semiconductors as the optimal bandgap for semiconductors in organic photovoltaics (OPVs) is thought to be 1.0-1.5 eV in order to maximize the light absorbed by the polymer.[11,12] For comparison, conducting metals have no bandgap.

There are many electronic characteristics that differentiate metals from conjugated polymers. One of the properties that differentiate conjugated polymers and metals is that they are conductively anisotropic, meaning that the polymer conducts electricity along a specific axis, in this case, the axis of conjugation.[7] This is in contrast to metals which are conductively isotropic, meaning that conductive metals have no directional preference for conductivity. While each of these properties has distinct advantages and disadvantages, the anisotropy of

conjugated polymers make them attractive candidates for applications that require very small and controlled connections, such as molecular wires.[13]

1.1.3 Applications of Conjugated Polymers

The main applications of conjugated polymers are in organic electronic devices. These devices come in a range of different fields such as sensors, display technologies, transistors, and photovoltaics.

The area that has received much of the interest in organic electronics recently is the field of organic photovoltaics (OPVs). The best OPVs have a power conversion efficiency (PCE) of around 9 %.[14,15] In contrast, the best monocrystalline Silicon based solar cells have a PCE around 25-27 %.[16] Part of this discrepancy is due to the fact that silicon photovoltaic devices have been studied since the mid-1950s while OPVs were first described in the mid-1980s. Even though the field of organic photovoltaics is young, there is a large interest mostly due to the promise of low-cost solar cells.

Currently in the OPV field there are three major concerns with any potential device: processability, stability, and efficiency.[17] Processability specifically refers to how easy it is to manufacture the device. In recent years this idea of processability can be directly linked to roll-to-roll manufacturing (R2R). R2R is a method of manufacturing electronic devices on thin sheets of plastic. The process is very similar to that of an inkjet printer but instead of ink and paper it utilizes a solution containing the material of interest and large rolls of thin plastic.[18] R2R represents a very easy and inexpensive way to manufacture OPVs

as long as the necessary materials are soluble in the organic solvents used in the printing process. Polyethylene terephthalate (PET) is an ideal substrate to use for R2R because it is cheap, easily processed, and ubiquitous.[19] The stability of the OPV is important since the device will most likely be left exposed to the elements for the extent of its lifetime. If the material used in the OPV cannot withstand its environment then it is not a good candidate for OPVs. The final criterion is the overall efficiency of the device. It has proven quite difficult to find materials that fit all of these criteria.

1.1.4 Introduction to Polythiophene

In recent years this focus has been on polythiophene (PT) based materials because of their many unique optoelectronic properties.[20] These properties include: a low band gap (~2 eV), high optical absorbance, and excellent stability.[21] The main drawback of PT is that it is insoluble in most organic solvents used for solution processing. This led to the development of substituted polythiophenes designed for improved solubility in organic solvents. The most widely used PT derivative is poly-(3-hexylthiophene) (P3HT). P3HT is soluble in several organic solvents due to each thiophene ring containing a hexyl side chain, while still retaining many of the unique optoelectronic properties of bare polythiophene.[22]

1.1.5 Polythiophene Synthesis and Optoelectronic Properties

Numerous techniques have been used to synthesize polythiophene, including both step growth and chain growth polymerizations.[23,24] The research presented in this dissertation has focused on two different step-growth polymerization techniques: the Suzuki and Stille cross-coupling reactions.

1.2 Introduction to Conjugated Polymer Solubility

Many organic electronic devices are fabricated on a large scale using solution processing to print thin films of each layer of the device. This method of fabrication requires that the CPs be soluble in the solvent(s) used during fabrication. This solubility is normally accomplished by adding long alkyl side chains to the polymer backbone, and while this approach works quite well, it can lead to issues since most organic electronics require the deposition of multiple layers of different materials. This can be problematic because the deposition of the second layer in an organic solvent must not disturb the previously deposited layer(s).[25] This problem is compounded as the number of layers required by the device increases. One way of addressing this issue is to use polymers that are orthogonally soluble in different solvents.

Orthogonal solubility refers to the use polymers in a multilayer device where each layer is specifically designed to be soluble in a very specific solvent that is intended to not perturb the previous layers.[26] This allows for the deposition of each subsequent layer without disturbing the previous layer due to the specific solvents used.

Another method for solution processing polymers into a multilayer device involves using cross-linking to covalently bind the polymer chains together, and thus rendering them insoluble.[27] This is usually accomplished by adding a cross-linking reagent to a polymer film that is designed to react with functionality present on the polymer backbone in order to covalently link separate polymer chains. Cross-linking reagents often contain functionalities that are amenable to post-polymerization functionalization. Some examples of common cross-linking functionalization include amines, maleimides, thiols, and double bonds.[28-30]

The addition of these side chains has distinct disadvantages: i) the addition of side chains to the polymer add a new pathway for oxidative degradation of the conjugated backbone of the polymer,[31,32] ii) in multi-layer devices the deposition of each subsequent layer should not disturb any of the previous layers which requires developing polymers that display orthogonal solubility, and iii) the side chains occupy a large amount of space in the solid state and they do not contribute to the optoelectronic properties of the material. However, the alkyl side chains are often necessary for solution processing of the material. The two approaches typically used for changing the solubility of a conjugated polymer are to cross-link the polymer chains after deposition, or to remove the solubilizing side-chains from the polymer backbone using some sort of external stimulus.

1.2.1 Crosslinking Conjugated Polymers

The most common approach to rendering a film insoluble is to cross-link the polymer chains after deposition. This technique has been demonstrated with

many different side chains and polymer backbones, but some examples include polyspirobifluorene-*co*-fluorene functionalized with oxetane-based crosslinkers and polythiophene functionalized with conjugated crosslinkers.[33,34] An example of oxetane based crosslinkers can be seen in Scheme 1.1.

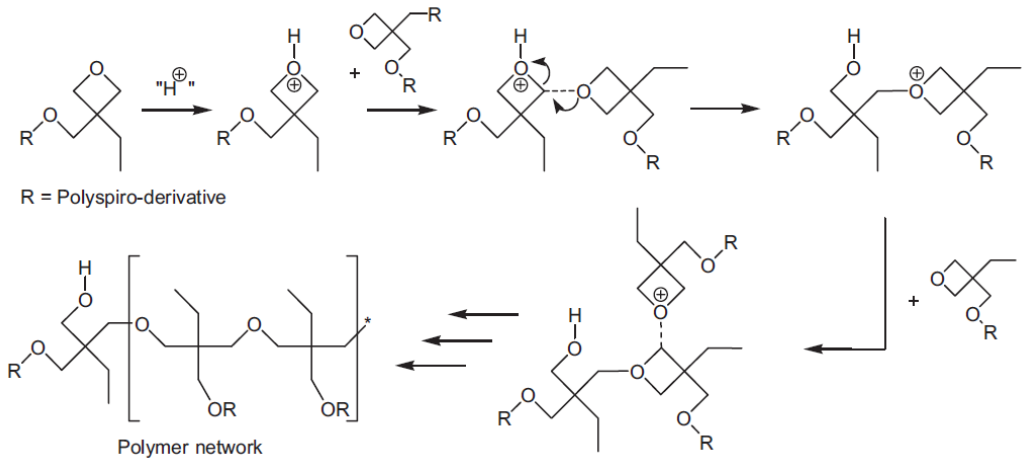

Scheme 1.1 The process of cationic ring opening polymerization (CROP) of oxetanes. Oxetanes are popular functionalities used in crosslinking conjugated polymers. Figure adapted from Gather *et al*.[35]

However, most crosslinking approaches have several potential drawbacks: i) solubilizing side chains are not removed from the polymer, ii) crosslinking often requires the addition of external crosslinking chemicals, and iii) the crosslinkers and side-chains occupy space with material that is usually electronically and optically inert, which do not benefit the conjugated polymer.

1.2.2 Thermocleavable Side Chains

While cross-linking can render a CP insoluble, it is beneficial to completely remove the solubilizing side chain if possible. The removal of the side chain can drastically increase the lifetime of the conjugate polymer. Stability

studies have shown that a dithienylthienopyrazine-thiophene copolymer has its lifetime increased from over 300 hours before cleavage to over 1000 hours after cleavage. Work by Frechét and Krebs has shown that solubilizing side chains composed of tertiary esters are capable of thermocleavage at temperatures around 200 °C.[19,36,37] This method of thermocleavage leaves behind carboxylic acid moieties along the polythiophene backbone which can also be cleaved off at temperatures around 300 °C. A schematic depicting this process can be seen in Figure 1.2.

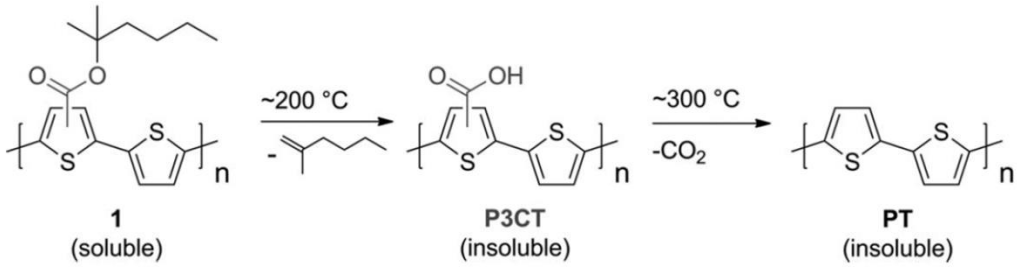

Figure 1.2 The thermocleavage and decarboxylation of tertiary ester-functionalized polythiophene. Reproduced with permission.[38] Copyright 2011, John Wiley and Sons.

One drawback to this approach is that it requires prohibitively high temperatures that severely limit the choice of substrate that can be used in making the device. Many popular substrates like poly(lactic acid) (PLA), polyethylene terephthalate (PET), and poly(ethylene naphthalenate) (PEN) would undergo a glass transition at the temperatures necessary for thermocleavage.[19] However, this methodology has been iterated on in recent years by Krebs to function at lower temperatures by utilizing an acid catalyst or by using a silane-based side chain.[38,39]

The method of using thermocleavable side chains relies on an external stimulus. Polymers that utilize an external stimulus to enact a physical change in the polymer are called stimuli responsive materials. Many different stimuli can be used including: temperature,[40,41] pH,[42] mechanical force,[43,44] and light.[45-48]

1.3 Introduction to Photocleavable Groups in Polymers

There are several advantages to using light as an external stimulus: i) light is a remote and permeable stimulus, ii) fine control over intensity and wavelength of light used, and iii) spatiotemporal control of what area is exposed. These advantages make light responsive materials ideal candidates for patterning. Light responsive materials are often fabricated by the incorporation of photocleavable groups within the material.

Photocleavable groups can be incorporated into a polymer in two ways: directly into the polymer backbone, or as part of a side chain attached to the polymer backbone. Irradiation of a photocleavable group results in the breaking of a covalent bond. Therefore, if incorporated into a polymer backbone, irradiation will result in breaking the polymer backbone, and if incorporated into a side chain, irradiation will result in cleavage of the side chain.

1.3.1 Photochemical Reactions

A photochemical reaction is a reaction where photons act as a reagent. A equation summarizing a typical photochemical reaction can be seen below:

$$R + h\nu \rightarrow R^* \rightarrow P$$

Where a photon (*hv*) is absorbed by a molecule (R) which promotes an electron from the HOMO to the LUMO, generating the electronically excited molecule (R*). The excited molecule can then lead to the formation of the photoproduct of the reaction (P). A schematic representation of the reaction pathway of the reaction can be seen in Figure 1.3. The reaction pathway for a photochemical reaction consists of at least two hypothetical surfaces, one representing the ground state pathway and one for each electronic excited state pathway.

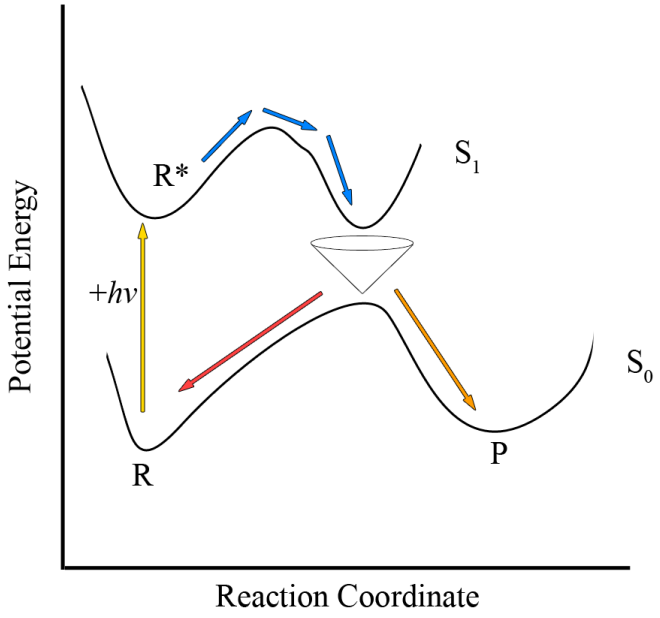

Figure 1.3 The schematic representation of a typical photochemical reaction where R is the starting material in the S_0 ground electronic state, R* is the starting material in the S_1 first electronic excited state, and P is the product of the photochemical reaction.

The photochemical reaction begins with starting material R absorbing a photon (yellow arrow) and being promoted to the first electronic excited state of R*. R* can then move along its energy surface (blue arrows) to a local minimum that is similar in energy to a local maximum on the energy surface of R. The R* is then

able to “funnel” or “jump” through a radiationless transition from the S_1 excited state energy surface to a similar geometry on the S_0 ground state energy surface.[49] From this point, the structure can revert back to the starting material R (red arrow) or continue on to form product P (orange arrow).

1.3.2 *o*-Nitrobenzyl Groups

One of the most popular photocleavable moieties is the *o*-nitrobenzyl (NB) group. The NB group has been very thoroughly researched since its discovery in the mid-1960s by Baltrop *et al*.[50-52] Upon irradiation with UV light, the nitrobenzyl group undergoes cleavage resulting in an *o*-nitrosoaldehyde and a second byproduct that depends on the structure of the initial NB group.

1.3.2a Photocleavage Mechanism of NB Groups

A general schematic for the NB photocleavage can be seen in Figure 1.4. The photocleavage of a NB group follows a Norrish type II mechanism.[53] The photocleavage starts when the nitrobenzyl group (1) absorbs a photon of light. This leads to the conversion of the nitro group into a nitro diradical (2). The radical oxygen atom then abstracts a γ-hydrogen from the benzylic position to generate a 1,4-diradical structure (3), which also has a resonance structure (4). This reactive intermediate can then undergo cyclization (5), which can then open to yield the nitrosobenzaldehyde and the hydroxyl containing group as the products.

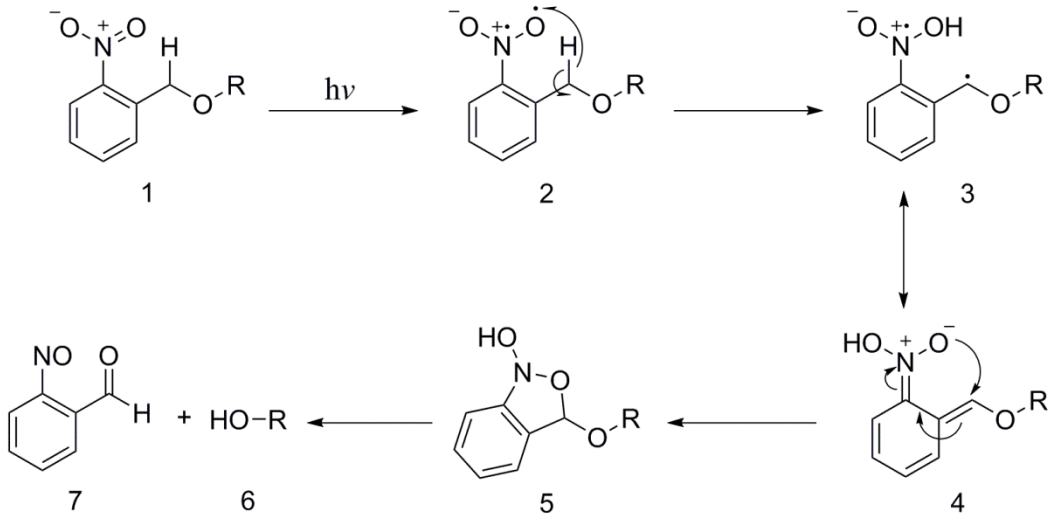

Figure 1.4 The general mechanism of photocleavage for nitrobenzyl derivatives.

1.3.2b Advantages and Disadvantages of NB Groups

o-Nitrobenzyl groups have been thoroughly studied and are thus very well understood. While the *o*-nitrobenzyl ester is the most commonly used derivative, there is a whole class of NB groups that include: amides, amines, carbamate, carbonates, and ethers.[54] The NB ester derivative's popularity is due mostly to its ease of synthesis. However, the NB ester has one of the slowest reaction rates relative to the other NB derivatives, and it is more sensitive to its chemical environment which can limit the reaction conditions used when a NB ester is present. Another possible challenge when working NB groups is the necessity of UV light to induce the photoreaction. However, it has been shown that the absorbance of the NB group can be adjusted by the addition of different substituents to the aromatic ring, and the NB can be made to be two-photon active by attaching a phenyl ring para to the nitro group.[55-57]

1.3.2c Applications of NB Groups

o-Nitrobenzyl groups have been used in many different fields of chemistry for a wide variety of applications. Some of the common uses of NB groups include: i) protecting functionality for organic synthesis,[53,58] ii) remote uncaging of functionality in biological systems,[59,60] iii) photolithography in materials chemistry,[61,62] and iv) as a linker allowing the dissolution of block copolymers, hydrogels, and micelles.[63-66]

1.4 Photolithography

Photolithography is technique that allows patterning of a material using light by means of a photoreactive molecule known as a photoresist.[67] The photoresist is typically a material that is separate from the electronic material and it is simply used to pattern the material(s) of interest. The two major classes of photoresist are known as negative or positive. Negative photoresists are materials that become insoluble in the developer upon irradiation. Positive photoresists are materials that become soluble in the developer upon irradiation. The molecules discussed in this dissertation are all negative photoresists.

Photolithography is used in the fabrication of most modern inorganic electronics, which makes it of great interest for organic electronics as well since it is a well understood and ubiquitous technique.

1.5 Conclusion

Conjugated polymers functionalized with *o*-nitrobenzyl solubilizing side-chains have a lot of potential when it comes to fabricating organic electronics. The use of light as the external stimulus enables many unique techniques such as photolithography without the necessity of an external photoresist. In this dissertation we describe the use of *o*-nitrobenzyl photocleavable groups to control the solubility of polythiophene-based conjugated polymers in solution, and the solid state. These novel materials also allow for the fabrication of multilayer films and photopatterning.

1.6 References

1. Chizu, S.; Yoshiaki, T.; Takeshi, Y.; Makoto, K.; Shuji, D. *Science and Technology of Advanced Materials* **2014**, *15*, 034203.

2. Kamyshny, A.; Magdassi, S. *Small* **2014**, *10*, 3515.

3. Takimiya, K.; Osaka, I.; Nakano, M. *Chem. Mater.* **2014**, *26*, 587.

4. Kumar, B.; Kaushik, B.; Negi, Y. S. *J Mater Sci: Mater Electron* **2014**, *25*, 1.

5. Hill, C. M.; Zhu, Y.; Pan, S. *ACS Nano* **2011**, *5*, 942.

6. Shirakawa, H.; Louis, E. J.; Macdiarmid, A. G.; Chiang, C. K.; Heeger, A. J. *J. Chem. Soc.-Chem. Commun.* **1977**, 578.

7. Carraher, C. E. *Introduction to Polymer Chemistry, Second Edition*; CRC Press, 2011.

8. Kranthiraja, K.; Gunasekar, K.; Cho, W.; Song, M.; Park, Y. G.; Lee, J. Y.; Shin, Y.; Kang, I.-N.; Kim, A.; Kim, H.; Kim, B.; Jin, S.-H. *Macromolecules* **2014**, *47*, 7060.

9. Boudreault, P.-L. T.; Najari, A.; Leclerc, M. *Chem. Mater.* **2011**, *23*, 456.

10. Steckler, T. T.; Henriksson, P.; Mollinger, S.; Lundin, A.; Salleo, A.; Andersson, M. R. *J. Am. Chem. Soc.* **2013**, *136*, 1190.

11. Zdanowicz, T.; Rodziewicz, T.; Zabkowska-Waclawek, M. *Sol. Energy Mater. Sol. Cells* **2005**, *87*, 757.

12. Kastor, L.; Mihailetchi, V.; Blom, P. The optimal band gap for plastic photovoltaics. *SPIE Newsroom* [Online Early Access]. DOI: 10.1117/2.1200701.0528. Published Online: 2007. http://spie.org/x8479.xml?ArticleID=x8479 (accessed March 15, 2015).

13. Yao, J.; Li, Y.; Zou, Z.; Wang, H.; Shen, Y. *Superlattices Microstruct.* **2012**, *51*, 396.

14. He, Z.; Zhong, C.; Su, S.; Xu, M.; Wu, H.; Cao, Y. *Nat Photon* **2012**, *6*, 591.

15. Dou, L.; Gao, J.; Richard, E.; You, J.; Chen, C.-C.; Cha, K. C.; He, Y.; Li, G.; Yang, Y. *J. Am. Chem. Soc.* **2012**, *134*, 10071.

16. Mazzio, K. A.; Luscombe, C. K. *Chem. Soc. Rev.* **2015**, *44*, 78.

17. Günes, S.; Neugebauer, H.; Sariciftci, N. S. *Chem. Rev.* **2007**, *107*, 1324.

18. Krebs, F. C.; Gevorgyan, S. A.; Alstrup, J. *J. Mater. Chem.* **2009**, *19*, 5442.

19. Krebs, F. C.; Norrman, K. *ACS Appl. Mater. Interfaces* **2010**, *2*, 877.

20. Kim, Y.; Cook, S.; Tuladhar, S. M.; Choulis, S. A.; Nelson, J.; Durrant, J. R.; Bradley, D. D. C.; Giles, M.; McCulloch, I.; Ha, C.-S.; Ree, M. *Nat Mater* **2006**, *5*, 197.

21. Manceau, M.; Bundgaard, E.; Carle, J. E.; Hagemann, O.; Helgesen, M.; Sondergaard, R.; Jorgensen, M.; Krebs, F. C. *J. Mater. Chem.* **2011**, *21*, 4132.

22. Sirringhaus, H.; Brown, P. J.; Friend, R. H.; Nielsen, M. M.; Bechgaard, K.; Langeveld-Voss, B. M. W.; Spiering, A. J. H.; Janssen, R. A. J.; Meijer, E. W.; Herwig, P.; de Leeuw, D. M. *Nature* **1999**, *401*, 685.

23. Roncali, J. *Chem. Rev.* **1992**, *92*, 711.

24. McCullough, R. D.; Lowe, R. D.; Jayaraman, M.; Anderson, D. L. *The Journal of Organic Chemistry* **1993**, *58*, 904.

25. Newby, C.; Lee, J.-K.; Ober, C. *Macromol. Res.* **2013**, *21*, 248.

26. Sax, S.; Rugen-Penkalla, N.; Neuhold, A.; Schuh, S.; Zojer, E.; List, E. J. W.; Müllen, K. *Adv. Mater.* **2010**, *22*, 2087.

27. Huang, F.; Cheng, Y.-J.; Zhang, Y.; Liu, M. S.; Jen, A. K. Y. *J. Mater. Chem.* **2008**, *18*, 4495.

28. Hammer, N.; Brandl, F. P.; Kirchhof, S.; Messmann, V.; Goepferich, A. M. *Macromolecular Bioscience* **2015**, *15*, 405.

29. Xu, J.; Boyer, C. *Macromolecules* **2015**, *48*, 520.

30. Darensbourg, D. J.; Wang, Y. *Polymer Chemistry* **2015**, *6*, 1768.

31. Manceau, M.; Rivaton, A.; Gardette, J.-L.; Guillerez, S.; Lemaître, N. *Polym. Degrad. Stab.* **2009**, *94*, 898.

32. Aoyama, Y.; Yamanari, T.; Koumura, N.; Tachikawa, H.; Nagai, M.; Yoshida, Y. *Polym. Degrad. Stab.* **2013**, *98*, 899.

33. Li, Y.; Zou, Y. *Adv. Mater.* **2008**, *20*, 2952.

34. Muller, C. D.; Falcou, A.; Reckefuss, N.; Rojahn, M.; Wiederhirn, V.; Rudati, P.; Frohne, H.; Nuyken, O.; Becker, H.; Meerholz, K. *Nature* **2003**, *421*, 829.

35. Gather, M. C.; Köhnen, A.; Falcou, A.; Becker, H.; Meerholz, K. *Adv. Funct. Mater.* **2007**, *17*, 191.

36. Petersen, M. H.; Gevorgyan, S. A.; Krebs, F. C. *Macromolecules* **2008**, *41*, 8986.

37. Liu, J. S.; Kadnikova, E. N.; Liu, Y. X.; McGehee, M. D.; Frechet, J. M. J. *J. Am. Chem. Soc.* **2004**, *126*, 9486.

38. Sondergaard, R. R.; Norrman, K.; Krebs, F. C. *Journal of Polymer Science, Part A: Polymer Chemistry* **2012**, *50*, 1127.

39. Bundgaard, E.; Hagemann, O.; Bjerring, M.; Nielsen, N. C.; Andreasen, J. W.; Andreasen, B.; Krebs, F. C. *Macromolecules* **2012**, *45*, 3644.

40. Garbern, J. C.; Hoffman, A. S.; Stayton, P. S. *Biomacromolecules* **2010**, *11*, 1833.

41. Sun, L.; Huang, W. M. *Soft Matter* **2010**, *6*, 4403.

42. Yang, X.; Grailer, J. J.; Rowland, I. J.; Javadi, A.; Hurley, S. A.; Matson, V. Z.; Steeber, D. A.; Gong, S. *ACS Nano* **2010**, *4*, 6805.

43. Bünsow, J.; Erath, J.; Biesheuvel, P. M.; Fery, A.; Huck, W. T. S. *Angew. Chem. Int. Ed.* **2011**, *50*, 9629.

44. Kean, Z. S.; Black Ramirez, A. L.; Yan, Y.; Craig, S. L. *J. Am. Chem. Soc.* **2012**, *134*, 12939.

45. Lee, J.; Han, H.; Lee, J.; Yoon, S. C.; Lee, C. *Journal of Materials Chemistry C* **2014**, *2*, 1474.

46. Johnson, R. S.; Finnegan, P. S.; Wheeler, D. R.; Dirk, S. M. *Chem. Commun.* **2011**, *47*, 3936.

47. Lee, S. K.; Jung, B.-J.; Ahn, T.; Song, I.; Shim, H.-K. *Macromolecules* **2003**, *36*, 9252.

48. Bouffard, J.; Watanabe, M.; Takaba, H.; Itami, K. *Macromolecules* **2010**, *43*, 1425.

49. Turro, N. J. *Modern Molecular Photochemistry*; University Science Books, 1991.

50. Barltrop, J. A.; Plant, P. J.; Schofiel.P *Chem. Commun.* **1966**, 822.

51. Rich, D. H.; Gurwara, S. K. *J. Chem. Soc., Chem. Commun.* **1973**, 610.

52. Patchornik, A.; Amit, B.; Woodward, R. B. *J. Am. Chem. Soc.* **1970**, *92*, 6333.

53. Klán, P.; Šolomek, T.; Bochet, C. G.; Blanc, A.; Givens, R.; Rubina, M.; Popik, V.; Kostikov, A.; Wirz, J. *Chem. Rev.* **2012**, *113*, 119.

54. Solomek, T.; Mercier, S.; Bally, T.; Bochet, C. G. *Photoch. Photobio. Sci.* **2012**, *11*, 548.

55. Holmes, C. P. *The Journal of Organic Chemistry* **1997**, *62*, 2370.

56. Donato, L.; Mourot, A.; Davenport, C. M.; Herbivo, C.; Warther, D.; Leonard, J.; Bolze, F.; Nicoud, J. F.; Kramer, R. H.; Goeldner, M.; Specht, A. *Angew. Chem.-Int. Edit.* **2012**, *51*, 1840.

57. Schelkle, K. M.; Becht, S.; Faraji, S.; Petzoldt, M.; Mullen, K.; Buckup, T.; Dreuw, A.; Motzkus, M.; Hamburger, M. *Macromol. Rapid Commun.* **2015**, *36*, 31.

58. Hasan, A.; Stengele, K.-P.; Giegrich, H.; Cornwell, P.; Isham, K. R.; Sachleben, R. A.; Pfleiderer, W.; Foote, R. S. *Tetrahedron* **1997**, *53*, 4247.

59. Pelliccioli, A. P.; Wirz, J. *Photoch. Photobio. Sci.* **2002**, *1*, 441.

60. Zhao, Y.; Zheng, Q.; Dakin, K.; Xu, K.; Martinez, M. L.; Li, W.-H. *J. Am. Chem. Soc.* **2004**, *126*, 4653.

61. Besson, E.; Gue, A.-M.; Sudor, J.; Korri-Youssoufi, H.; Jaffrezic, N.; Tardy, J. *Langmuir* **2006**, *22*, 8346.

62. Kim, M.; Choi, J.-C.; Jung, H.-R.; Katz, J. S.; Kim, M.-G.; Doh, J. *Langmuir* **2010**, *26*, 12112.

63. Gumbley, P.; Hu, X.; Lawrence, J. A.; Thomas, S. W. *Macromol. Rapid Commun.* **2013**, *34*, 1838.

64. Zhao, H.; Sterner, E. S.; Coughlin, E. B.; Theato, P. *Macromolecules* **2012**, *45*, 1723.

65. Xuan, J.; Han, D.; Xia, H.; Zhao, Y. *Langmuir* **2014**, *30*, 410.

66. Gao, Y.; Qiu, H.; Zhou, H.; Li, X.; Harniman, R.; Winnik, M. A.; Manners, I. *J. Am. Chem. Soc.* **2015**, *137*, 2203.

67. Gates, B. D.; Xu, Q.; Stewart, M.; Ryan, D.; Willson, C. G.; Whitesides, G. M. *Chem. Rev.* **2005**, *105*, 1171.

Chapter 2:

Photoinduced Aggregation of Polythiophenes

2.1 Controlling Conjugated Polymer Solubility Using Light

Conjugated polymers (CPs) have useful optoelectronic properties that make them increasingly important in a variety of applications.[1,2] Although the organic materials in these applications often do not outperform that of more traditional inorganic materials, organics offer exceptional control over properties through the tools of synthetic chemistry, as well as the potential for inexpensive solution based processing over large areas onto lightweight and mechanically flexible substrates. Polythiophenes (PTs) are among the most popular of conjugated materials; this trend is due to their high carrier mobility, good photo-oxidative stability, and the availability of techniques for well-controlled synthesis.

Solubilizing side chains on conjugated polymers are ubiquitous because of solution-based processing: the parent structures of materials such as PT and poly(phenylenevinylene) are insoluble without them. These side chains, however, affect the performance of potential devices that utilize these materials. For example, it is challenging to make layered structures that contain several soluble materials since the deposition of a layer often disturbs the previous layer. Solutions to this problem have included polymers that are orthogonally soluble, and polymer cross-linking upon deposition.[3] Solubilizing side chains also occupy volume in the solid state with optoelectronically inert moieties that do not contribute to the unique characteristics of the polymer, and they contribute to the photochemical degradation of conjugated polymers.[4] In summary, solubilizing side-chains are beneficial for solution based processing but are often detrimental

once the polymer is in the solid state. Therefore, it would be advantageous to remove the solubilizing side chain after polymer deposition.

Previously published work has shown that the solubility of PT derivatives functionalized with tertiary ester solubilizing side chains can be modified by thermally cleaving the side chain, resulting in loss of the solubilizing ester side chain and improved stability of devices prepared in this manner.[5-7] Further heating results in decarboxylation to yield the parent poly(thiophene) structure.[8] However, the temperatures required for this approach greatly limits the available substrates that the polymer can be deposited on. Visible or infrared light can also thermocleave the side chains of PT derivatives with tertiary esters[9] or tetrahydropyran[10,11] protecting groups locally for photopatternable materials. In addition, there are a variety of other strategies for photoinduced changes in CP solubility,[12,13] such as photo-cross-linking and photochemical schemes for conversion of soluble precursor polymers to insoluble CPs.[14-16]

The photochemical cleavage of nitrobenzyl groups is a versatile reaction that has found utility in applications from targeted delivery of therapeutics to surface patterning.[17,18] Cleavage of nitrobenzyl groups from fluorophores is also a known strategy for "uncaging" the fluorescence of dyes and other emitters.[19-22] For example, ortho-nitrobenzyl esters can yield photochemically modulated solubility of phenyleneethynylene/phenylene-vinylene conjugated oligomers.[23] These compounds showed photoinduced increased fluorescence efficiency upon cleavage of NB groups with UV light due to the cleavage of the fluorescence quenching nitroaromatic groups from the fluorophore. In this study, we

demonstrate UV-mediated photocleavage of nitrobenzyl groups substituted with solubilizing alkyl chains from both oligothiophenes and polythiophenes. Our hypothesis was that photolysis of solubilizing chains would yield insoluble polythiophenes. To begin to test this hypothesis, we prepared symmetrically substituted quarterthiophene derivatives (4 ring thiophene oligomers) containing solubilizing alkyl chains that incorporated photolabile nitrobenzyl esters or photoinert alkyl esters at the 3- or 5-position of the terminal thiophene rings.

2.2 Synthesis of NB Containing Quarterthiophenes

Alkylation of commercially available 5-hydroxy-2-nitrobenzaldehyde with bromooctane yielded solubilized nitrobenzyl aldehyde **1**, which $NaBH_4$ reduced to yield nitrobenzyl alcohol **2** (Scheme 2.1).

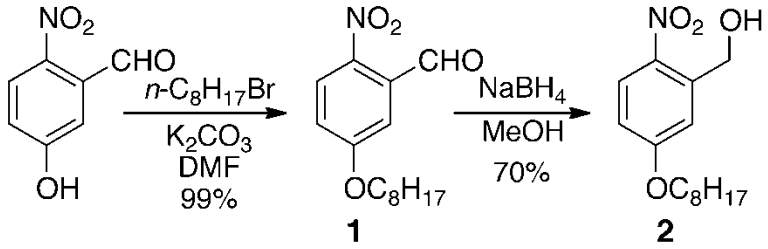

Scheme 2.1 Synthesis of nitrobenzyl alcohol **2**.

Condensation of **2** and 2-bromothiophene-3-carboxylic acid gave ester **3** (Scheme 2.2), which upon palladium-catalyzed cross-coupling with 5,5′-bis(tributylstannyl)-2,2′-bithiophene gave quarterthiophene **O3** with photolabile solubilizing groups. For synthesis of derivative **O4** with photoinert carboxylic esters, acid-catalyzed esterification of 5-bromothiophene-2-carboxylic acid with n-BuOH gave ester **4**, which upon Stille coupling yielded quarterthiophene **O4**. A

similar synthetic strategy yielded **O5** and **O6**, quarterthiophenes with photocleavable or photoinert esters in the 5-positions of the terminal rings, respectively (Scheme 2.2).

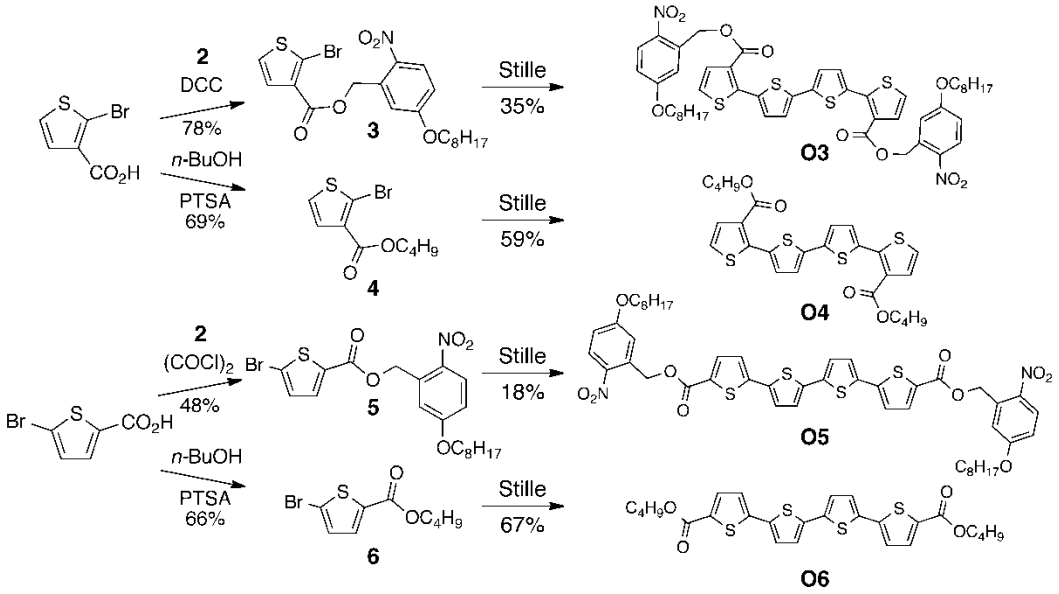

Scheme 2.2 Synthesis of quaterthiophene oligomers **O3-O6**. "Stille": 5,5′-bis(tributylstannyl)-2,2′-bithiophene, $Pd(PPh_3)_4$, DMF.

2.3 Synthesis of NB Containing Polythiophenes

We extended our approach to analogous polythiophenes with either photolabile or photoinert solubilizing esters on alternating rings. N,N′-dicyclohexylcarbodiimide (DCC)-mediated esterification of 2,5-dibromothiophene-3-carboxylic acid with nitrobenzyl alcohol **2** yielded photolabile monomer **7** (Scheme 2.3), whereas acid-catalyzed esterification of 2,5-dibromothiophene-3-carboxylic acid with n-BuOH yielded the photoinert monomer **8**. Each of these monomers was amenable to stepgrowth polymerization with 2,5-bis(trialkylstannyl)thiophene under Stille coupling conditions with either

$Pd(PPh_3)_4$ or $Pd_2(dba)_3/P(o\text{-}tolyl)_3$ to yield polythiophenes **P7** and **P8** (Scheme 2.3).

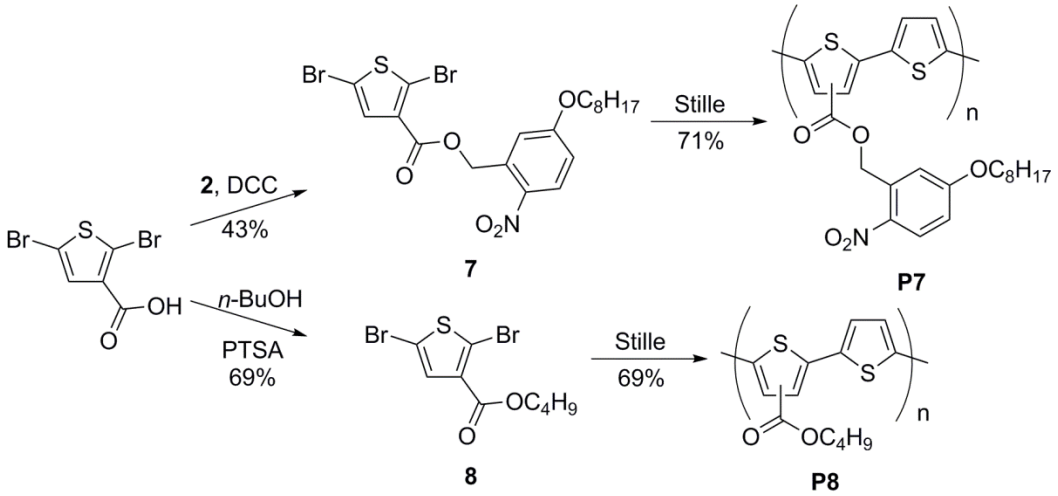

Scheme 2.3 Synthesis of polythiophenes **P7** and **P8**. "Stille": Pd catalyst, 2,5-bis(trialkylstannyl)thiophene.

2.4 Spectral Properties of Synthesized Compounds

The height-normalized absorbance and emission spectra of nitrobenzyl oligomer **O3** and polymer **P7** in CH_2Cl_2 can be seen in Figure 2.1.

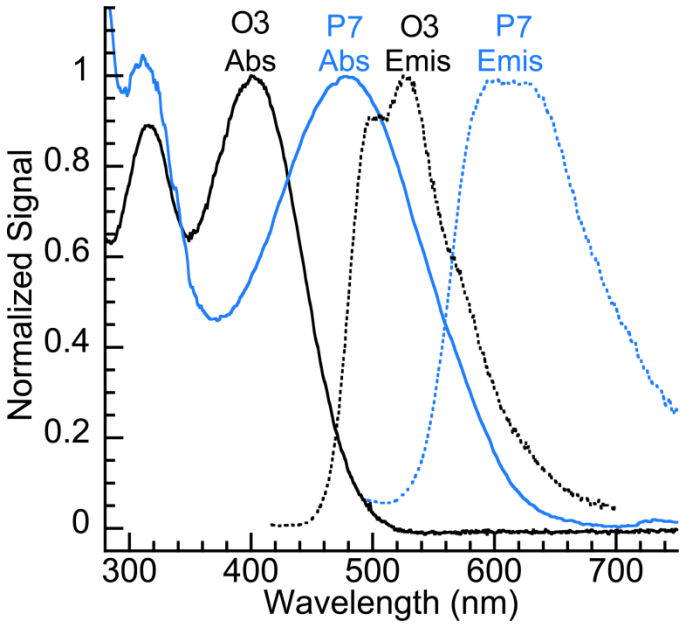

Figure 2.1 Normalized absorbance and fluorescence spectra of quarterthiophene oligomer **O3** and polythiophene **P7** in CH_2Cl_2.

The absorbance spectra of these materials are consistent with expectations based on their chemical structures. Each compound has a band in the visible region of the spectrum corresponding to the (π,π*) excitation of conjugated thiophene chains; the bands of the quarterthiophene oligomers (λ_{max} 400−425 nm) are at higher energy than the polymers (λ_{max} 480 nm), consistent with extended conjugation in the structures. Table 2.1 summarizes relevant optical data of all conjugated thiophene materials. In addition, **O3**, **O5**, and **P7** show an additional band at ~315 nm due to the presence of the nitrobenzyl group.

Table 2.1 Optical properties of conjugated thiophene-based materials.

	λ_{max} (abs)[a]/nm	ε[a]/$M^{-1}cm^{-1}$	λ_{max} (em)[a]/nm	Φ_F[b]			
				C_6H_6	THF	DCM	ACN
O3	402	20700	530	0.16	0.14	0.06	0.03
O4	394	25400	521	0.20	0.18	0.20	0.15
O5	425	41900	522	0.25	0.25	0.16	0.11
O6	421	49000	516	0.26	0.26	0.24	0.26
P7	480	-	610	0.29	0.34	0.29	0.06
P8	469	-	587	0.35	0.35	0.33	-

[a] In CH_2Cl_2. [b] Reported relative to Coumarin 6 in EtOH or Rhodamine 6G in EtOH.

To further understand the effect of the nitroaromatic groups on the excited state of the conjugated thiophene backbones, we characterized the fluorescence spectra of these materials (Table 2.1). Like the UV/vis spectra, the fluorescence emission spectra of polymers **P7** and **P8** is red-shifted (610 nm and 587 nm) from the quarterthiophene oligomers. The excitation spectra of **O3**, **O5**, and **P7** show no peaks attributable to the nitrobenzyl group, which indicates that energy transfer from the photocleavable moieties is not competitive with other excited-state processes and that, besides competitive absorbance of the UV light, the coupling of the two chromophores should not interfere with photocleavage. The quantum yields of fluorescence (Φ_F) of nitrobenzyl-substitued **O3**, **O5**, and **P7** depend strongly on solvent, with quenching more efficient in more polar solvents (CH_2Cl_2 and CH_3CN) than in the less polar solvent benzene. Those fluorophores without nitrobenzyl groups (**O4**, **O6**, and **P8**) had fluorescence quantum yields that did not vary as a function of solvent polarity. These trends are consistent with photoinduced electron transfer quenching of the nitrobenzyl-substituted fluorophores due to more polar solvents stabilizing the resultant charge separated state.[20]

2.5 Oligomer Nitrobenzyl Photocleavage

To photocleave solubilizing nitrobenzyl groups from conjugated thiophene-based materials, we irradiated samples with 365 nm light from a Hg/Xe lamp with a power density of 10 mW/cm^2. To minimize the photo-oxidative degradation that is known to occur with conjugated materials, we deoxygenated all solution based samples by sparging with argon gas. We monitored absorbance, fluorescence emission, and excitation spectra as a function of irradiation time. Figure 2.2 shows the response of both the absorbance and fluorescence emission spectra of oligomer **O3** in CH_2Cl_2 as a function of UV irradiation time. Regioisomer **O5** showed qualitatively similar behavior to that described below for **O3**.

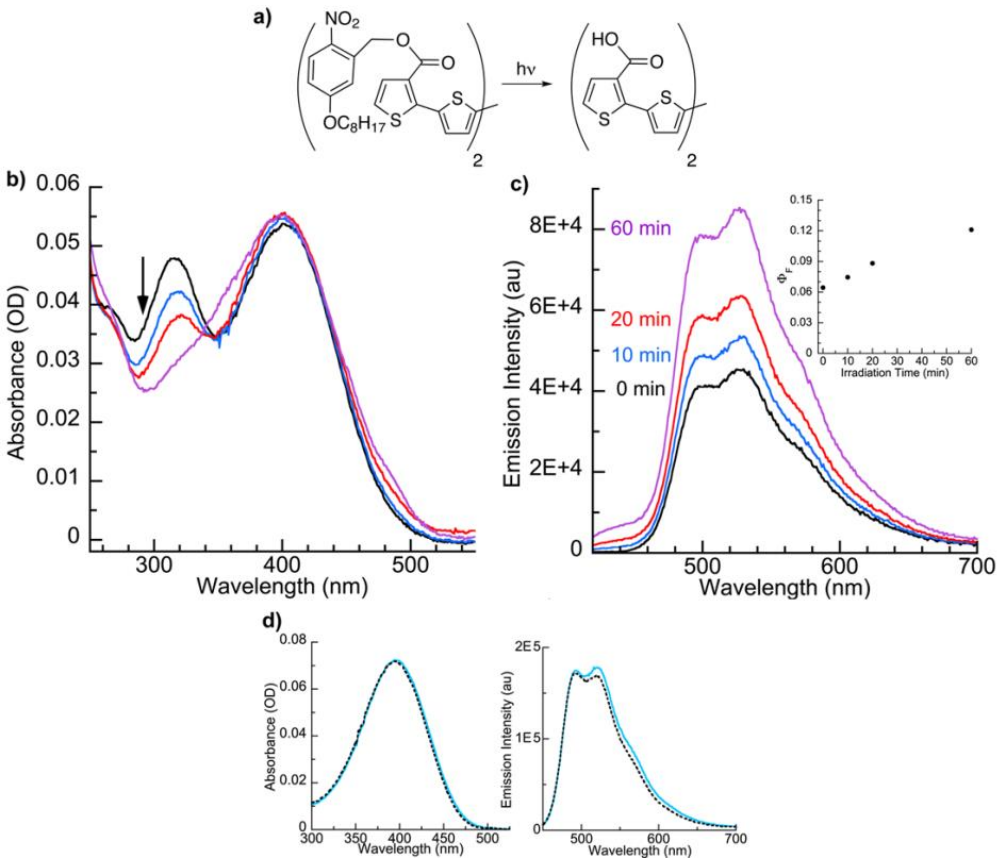

Figure 2.2 a) Photolysis of oligomer **O3**, b) response of absorbance spectrum and c) response of emission spectrum of a deoxygenated sample of **O3** in CH_2Cl_2 to 365 nm light at 0, 10, 20, and 60 minutes of irradiation. The quantum yield of fluorescence versus irradiation time can be seen as an inset. d) Absorbance and emission spectra of **O4** before (solid blue line) and after (black dashed line) 60 min of irradiation at 365 nm.

The absorbance band at 315 nm decreased, consistent with photolysis of the nitrobenzyl group, while the absorbance band at 400 nm did not decrease; we attribute the slight increase to byproducts from the nitrosoaromatic photolysis product. We therefore conclude that photochemical decomposition was not significant under these reaction conditions. Figure 2.2d, which shows that both the absorbance and emission spectra of control oligomer **O4** decreased less than 10% upon irradiation for 60 min, also supports this conclusion. Thiophene-based

materials are more photochemically stable than phenylene-vinylene-based materials because they lack labile main chain exocyclic double bonds, which can easily undergo photo-oxidation. In addition, there was no significant shift in the absorbance peak, which indicated that the products of **O3** photolysis remained well-solvated. ^{1}H NMR spectroscopy of the photolysis reaction of **O3** in DMSO-d_6 was consistent with conversion to the dicarboxylic acid of the quaterthiophene, which we prepared independently by basic hydrolysis of **O4** (Figure 2.3).

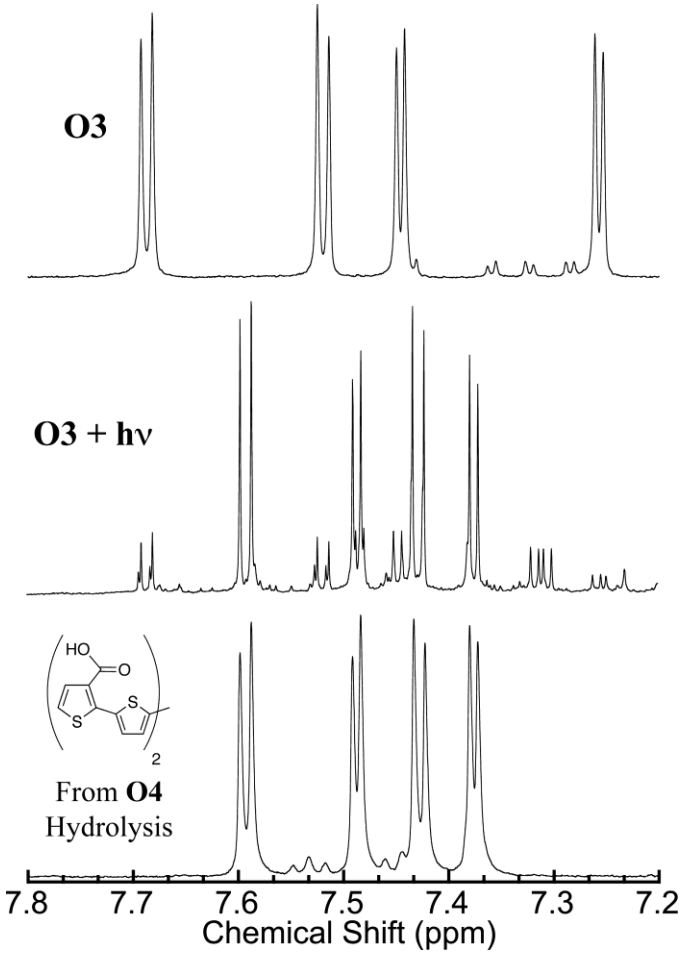

Figure 2.3 ^{1}H NMR spectra in deoxygentated DMSO-d_6 of nitrobenzyl oligomer **O3** (top), the crude photoproducts of photolysis of **O3** at 365 nm in deoxygenated DMSO-d_6 after 480 minutes of irradiation (middle), and independently synthesized quarterthiophene diacid from basic hydrolysis of **O4** in DMSO-d_6 (bottom).

During the irradiation, the fluorescence spectrum of **O3** retained the same spectral shape, but increased in intensity by a factor of 2 after 60 min of photolysis (Figure 2.2c). This corresponds to an increase in fluorescence quantum yield from 0.06 to 0.12. Given that the emission spectrum of **O4** shows <10% change upon identical irradiation conditions, these observations are consistent with cleavage of the nitrobenzyl ester quencher from the conjugated oligothiophene backbone preventing photoinduced electron transfer, and thus increasing fluorescence emission. This result is analogous to previously reported nitrobenzyl-functionalized conjugated oligomers studied in our lab.[23]

2.6 Polymer Nitrobenzyl Photocleavage

Nitrobenzyl ester functionalized polymer **P7**, which is structurally analogous to oligomer **O3**, showed significantly different behavior upon photolysis (Figure 2.4). The maximal absorbance decreased by approximately 20% and red-shifted to λ_{max} = 507 nm after 60 min of irradiation at 365 nm in deoxygenated CH_2Cl_2 (Figure 2.4b). **P7** also showed similar behavior in toluene, while in THF **P7** showed a slight blue shift. In addition, the UV/vis spectrum of **P8**, which does not have photoreactive nitrobenzyl ester pendants, showed no change in CH_2Cl_2. We attribute these observations to photoinduced aggregation of **P7** in solvents of low polarity: red-shifted absorbance spectra is typical of aggregates of conjugated polymers,[24,25] and this interpretation is consistent with cleaving solubilizing chains from the backbone of the polythiophene to yield more polar carboxylic acid pendants.

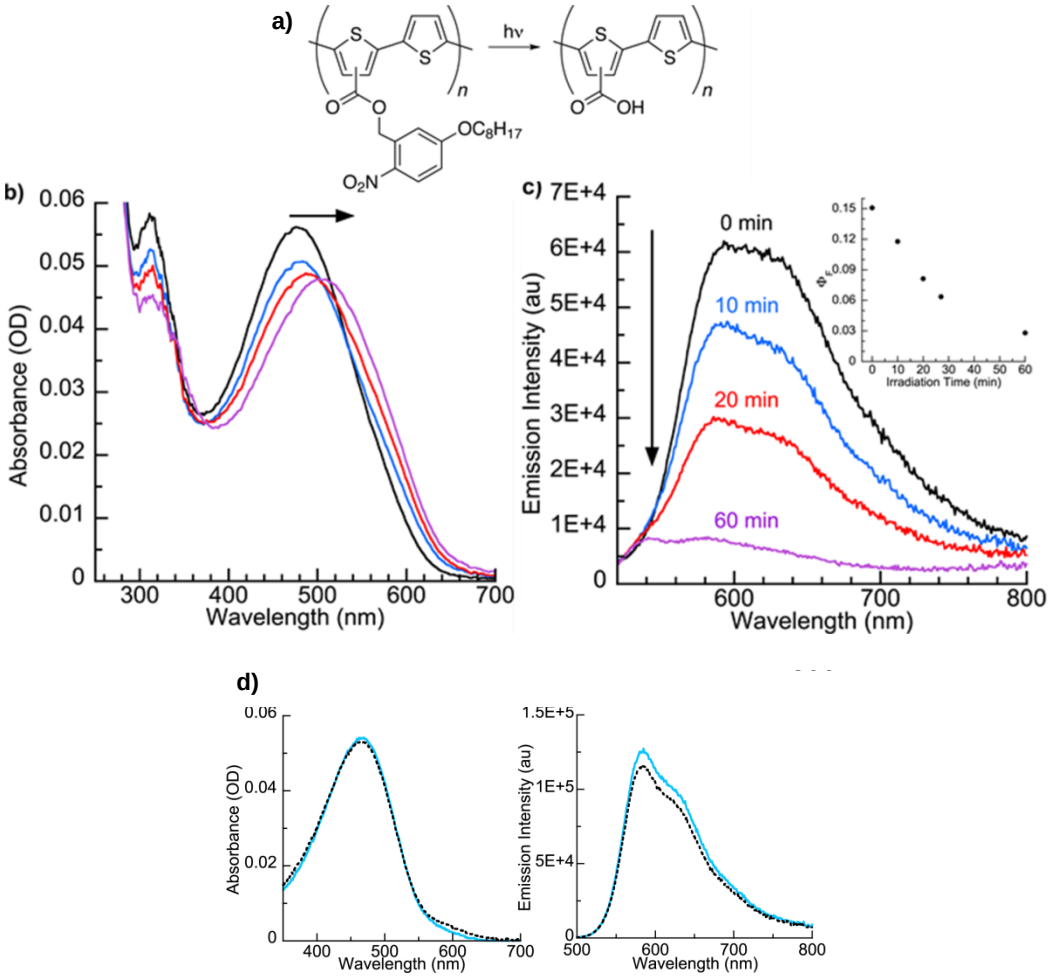

Figure 2.4 (a) Photolysis of polymer **P7**, (b) response of absorbance spectrum, and (c) response of emission spectrum of a deoxygenated sample of **P7** in CH_2Cl_2 to 365 nm light at 0, 10, 20, and 60 min of irradiation. (d) Optical spectra of **P8** before (solid blue line) and after (black dashed line) 60 min of irradiation at 365 nm.

Fluorescence data also supports photoinduced aggregation of polythiophene **P7** in toluene or CH_2Cl_2. In CH_2Cl_2, and in strong contrast to the results with conjugated oligomers **O3** and **O5**, the fluorescence intensity and quantum yield of **P7** decreased by a factor of 8 after 60 min of irradiation (Figure 2.4c). Self-quenching of polymer fluorescence is a common result of the interchain interactions that accompany conjugated polymer aggregation.[25]

Irradiation in toluene yielded similar results at a slower rate of change, while irradiation in THF did not yield fluorescence quenching (Figure 2.5). This lack of quenching is indicative of a lack of aggregation of **P7** in THF, likely due to its ability to solubilize **P7** even after irradiation.

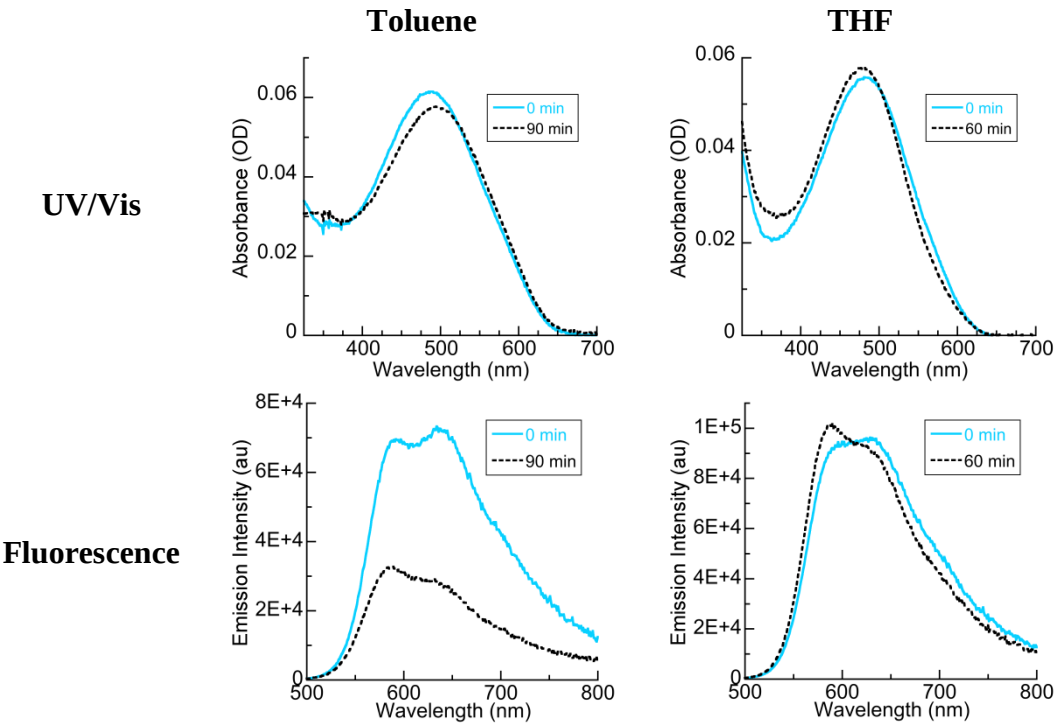

Figure 2.5 Effect of solvent on aggregation of **P7** induced by UV irradiation (365 nm, 10 mW/cm^2) as determined by UV/vis and fluorescence. **P7** shows behavior consistent with light-induced aggregation in toluene—red-shifted absorbance and quenched fluorescence upon irradiation, while the slight changes of the spectra of **P7** in THF do not show evidence of photoinduced aggregation.

2.7 Photoinduced Aggregation of Thin Films

The behavior of these polymers in the solid-state also supports the conclusion that **P7** forms aggregates insoluble in toluene or CH_2Cl_2 upon irradiation: Thin films of **P7** resisted dissolution in these solvents after UV irradiation, as determined by absorbance spectrophotometry, because of the photolytic cleavage of solubilizing groups from the polymer backbone. This can

be effectively demonstrated by irradiating half of a film of **P7** on a glass slide. The side exposed to UV light remains after rinsing, due to its lack of solubility in the rinsing solution, while the side not irradiated is washed away (Figure 2.6).

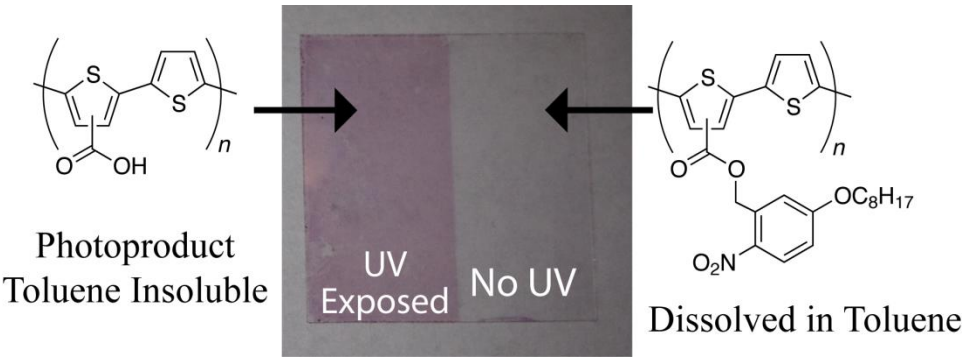

Figure 2.6 An example film of **P7** after toluene rinse where only the left side was irradiated for 30 minutes

As shown in the Figure 2.7, spun-cast films of **P7** on microscope coverslips dissolved readily in organic solvents at room temperature if not irradiated with UV light.

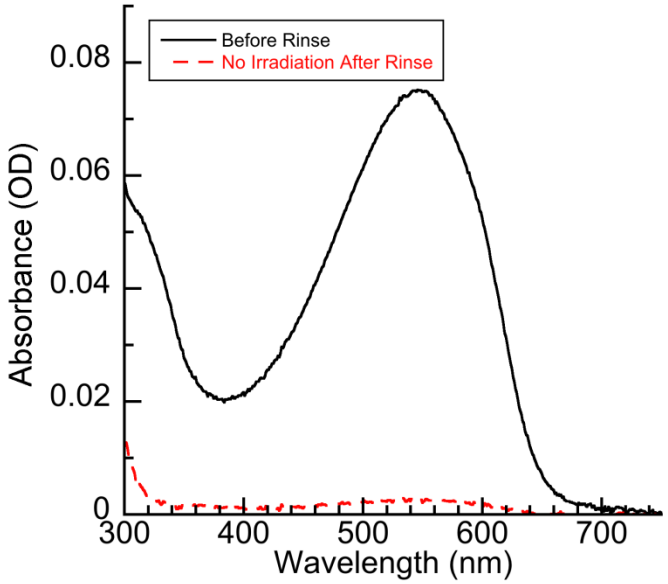

Figure 2.7 UV/vis spectra of spun-cast thin film of **P7** before and after rinsing with toluene without UV irradiation.

However, when these films were irradiated with UV light, they underwent only an 11 ± 3% decrease in optical density after a combination of 30 min of irradiation at 365 nm under ambient conditions and rinsing with toluene (Figure 2.8). We attribute this decrease to the dissolution of shorter polymer chains, and/or the dissolution of chains with some unreacted pendants, while the majority of the polymer chains were rendered insoluble.

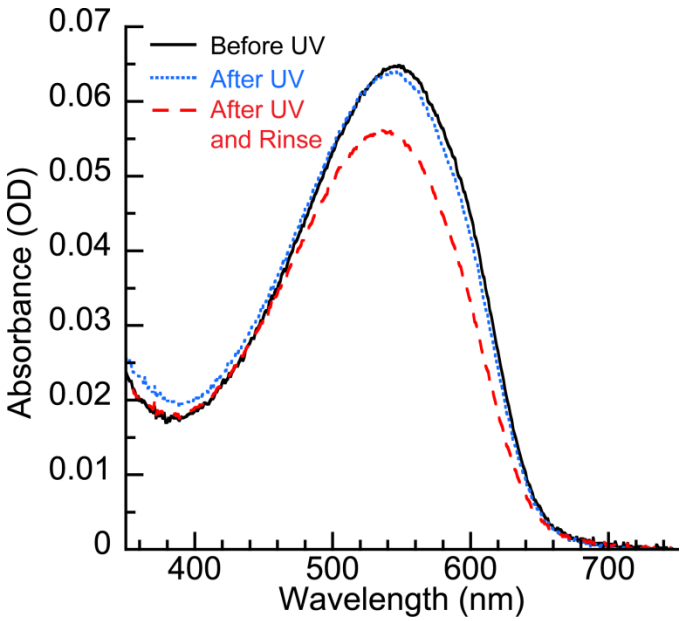

Figure 2.8 UV/vis spectra of a spun-cast film of **P7** before and after exposure to 365 nm light for 30 minutes. Rinsing the irradiated film with toluene resulted in only a 14% decrease in optical density.

As shown in the Figure 2.9, and consistent with the lack of evidence for aggregation in THF as described earlier, polar aprotic solvents such as THF or DMSO significantly solubilize the irradiated polymer films, resulting in a decrease in absorbance of the films by 60−80%.

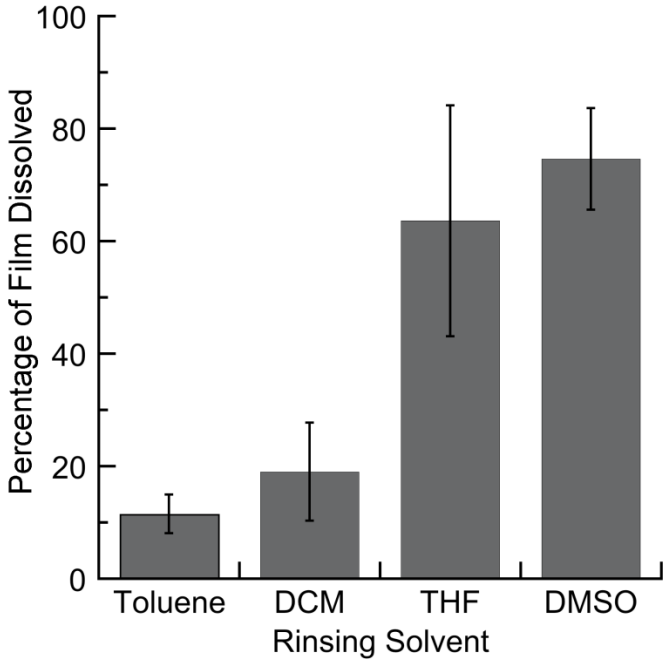

Figure 2.9 Effect of solvent polarity on dissolution of UV-irradiated (365 nm, 30 min, 10 mW/cm^2) spun-cast films of **P7**, as determined by UV/vis spectrophotometry.

2.8 Conclusions

In conclusion, we have demonstrated that incorporating solubilizing side chains through photocleavable linkers on thiophene-based conjugated materials enables photochemical control over intermolecular interactions and solubility of conjugated polymers both in organic solvent and as thin films. While quarterthiophenes remain soluble upon photolysis, an analogous polythiophene aggregates in organic solvents of low polarity upon photochemical cleavage of solubilizing groups. Films of photoresponsive polythiophenes undergo these photoinduced changes with a minimal amount of photobleaching, and resist dissolution upon photolysis. This light based approach complements previously

reported approaches to the stimuli-responsive solubility of conjugated polymers with the added benefit of spatiotemporal control.

2.9 Experimental Considerations

All synthetic manipulations were performed under standard air-free conditions under an atmosphere of argon gas with magnetic stirring unless otherwise mentioned. Flash chromatography was performed using silica gel (230-400 mesh) as the stationary phase. NMR spectra were acquired on a Bruker Avance III 500 or Bruker DPX-300 spectrometer. Chemical shifts are reported relative to residual protonated solvent (7.27 ppm for $CHCl_3$). High-resolution mass spectra (HRMS) were obtained at the MIT Department of Chemistry Instrumentation Facility using a peak-matching protocol to determine the mass and error range of the molecular ion. All reactants and solvents were purchased from commercial suppliers and used without further purification, unless otherwise noted.

All solution optical spectra were acquired of samples in quartz cuvettes (NSG Precision Cells). Electronic absorbance spectra were acquired with a Varian Cary-100 instrument in double-beam mode using a solvent-containing cuvette for background subtraction spectra. Fluorescence emission spectra were obtained by using a PTI Quantum Master 4 equipped with a 75 W Xe lamp. All fluorescence spectra are corrected for the output of the lamp and the dependence of detector response to the wavelength of emitted light. Fluorescence spectra were acquired using sample absorbances less than 0.1 OD. Fluorescence quantum

yields were determined relative to Coumarin 6 in ethanol. Molecular weight distribution measurements of the polymers were conducted with a Shimadzu Gel Permeation Chromatography (GPC) system equipped with a Tosoh TSKgel GMHhr-M mixed-bed column and guard column (5 mm), in addition to both UV and refractive index detectors. The column was calibrated with low polydispersity poly(styrene) standards (Tosoh, PSt Quick Kit) with THF as the mobile phase eluting at 0.75 mL/min. Irradiations of samples to cleave nitrobenzyl ester groups were performed with a 200W Hg/Xe lamp (Newport-Oriel) equipped with a condensing lens, recirculating water filter, manual shutter, and 365 nm interference filter (Semrock) in the light path. All solution samples were deoxygenated by bubbling with Argon gas. Thin films were fabricated using chloroform solutions of **P7** (1–2 mg/mL) that were filtered with a 0.4 μm PTFE syringe filter and spun-cast onto glass cover slips using a Laurell Technologies Corporation spin coater (Model WS-400E-6NPP-Lite) at 2500 rpm for 1 minute.

Synthesis and Characterization

2-Nitro-5-(octyloxy)benzaldehyde (1). A round bottom flask was charged with 5-hydroxy-2-nitrobenzaldehyde (5.0 g, 29.9 mmol) and potassium carbonate (12.4 g, 89.8 mmol). The flask was evacuated and refilled with nitrogen three times. Under nitrogen flow, 100 mL of dimethyl formamide (DMF) and 1-bromooctane (7.8 mL, 8.7 g, 45 mmol) were added. The mixture was left to stir overnight at 50 °C. The reaction mixture was diluted with 1M NaOH (1×100 mL) and extracted

with diethyl ether (3×100 mL). The combined organic layers were then washed with saturated aqueous $NaHCO_3$ (1×100 mL), deionized (DI) water (1×100 mL), and brine (1×100 mL). Drying over $MgSO_4$ and removal of solvent *in vacuo* gave the crude product **1** as a yellow-orange solid. Flash chromatography on silica using 2:1 hexanes:CH_2Cl_2 as eluent gave 8.35 g of **1** (99 %) as a pale yellow solid. ^{1}H NMR ($CDCl_3$, 500 MHz): δ 10.49 (s, 1H), 8.16 (d, *J* = 9 Hz, 1H), 7.31 (d, *J* = 3 Hz, 1H), 7.14 (dd, *J* = 9 Hz, 3 Hz, 1H), 4.10 (t, *J* = 7 Hz, 2H), 1.83 (m, 2H), 1.50-1.44 (m, 2H), 1.38-1.30 (m, 8H), 0.91-0.88 (m, 3H). ^{13}C NMR ($CDCl_3$, 125 MHz): δ 188.6, 163.7, 142.0, 134.4, 127.2, 118.9, 113.7, 69.4, 31.8, 29.2, 29.2, 28.9, 25.8, 22.6, 14.1. HRMS calcd for $C_{15}H_{21}NO_4$ $(M+Na)^+$, 302.1363, found, 302.1370.

(2-Nitro-5-(octyloxy)phenyl)methanol (2). A round bottom flask was charged with **1** (8.35 g, 29.9 mmol), and $NaBH_4$ (1.78 g, 44.8 mmol). The flask was evacuated and refilled with nitrogen three times. Under nitrogen flow, 200 mL of methanol (MeOH) was added. The reaction was left to stir overnight at room temperature. The reaction mixture was diluted with DI water (1 × 100 mL) and brine (1 × 100 mL), and extracted with diethyl ether (3 × 100 mL). The combined organic layers were dried over $MgSO_4$ and solvent was removed *in vacuo* to give the crude product **2** as a yellow solid. Recrystallization of the crude solid from ethanol/water gave 5.88 g of **2** (70 %) as feathery yellow crystals. ^{1}H NMR ($CDCl_3$, 500 MHz): δ 8.19 (d, *J* = 9 Hz, 1H), 7.20 (d, *J* = 2.5 Hz, 1H), 6.89 (dd, *J* = 2.5 Hz, 9 Hz, 1H), 4.99 (s, 2H), 4.08 (t, *J* = 6.5 Hz, 2H), 2.58 (s, 1H), 1.83 (m,

2H), 1.48-1.44 (m, 2H), 1.35-1.30 (m, 8H), 0.91-0.88 (m, 3H). ^{13}C NMR ($CDCl_3$, 125 MHz): δ 163.9, 140.3, 140.1, 128.0, 114.6, 113.5, 68.9, 63.0, 31.8, 29.2, 29.2, 29.0, 25.9, 22.6, 14.0. HRMS calcd for $C_{15}H_{23}NO_4$ $(M+Na)^+$, 304.1519, found, 304.1531.

(2-Nitro-5-(octyloxy)benzyl) 2-bromothiophene-3-carboxylate (3). A round bottom flask was charged with **2** (680 mg, 2.41 mmol), 2-bromothiophene-3-carboxylic acid (500 mg, 2.41 mmol), and DMAP (324 mg, 2.65 mmol). The flask was evacuated and refilled with nitrogen three times. Under nitrogen flow, 30 mL of anhydrous CH_2Cl_2, and *N*,*N*′-dicyclohexylcarbodiimide (DCC) (361 mg, 1.75 mmol) dissolved in 10 mL of anhydrous CH_2Cl_2 were added. The reaction was left to reflux overnight. Upon cooling to room temperature, the reaction mixture was washed with 5% aqueous HCl (2x40 mL), saturated $NaHCO_3$ (2x40 mL), and DI water (2x40 mL). Drying over Na_2SO_4 and removal of solvent *in vacuo* gave the crude product. Flash chromatography on silica using 1:1 hexanes:CH_2Cl_2 as eluent gave 883 mg of **3** (78 %) as a white solid. ^{1}H NMR ($CDCl_3$, 500 MHz): δ 8.20 (d, *J* = 9 Hz, 1H), 7.44 (d, *J* = 5.5 Hz, 1H), 7.26 (d, *J* = 2.5 Hz, 1H), 7.16 (d, *J* = 2.5 Hz, 1H), 6.89 (dd, *J* = 2.5 Hz, *J* = 9 Hz, 1H), 5.77 (s, 2H), 4.02 (t, *J* = 6.5 Hz, 2H), 1.79 (quintet, *J* = 6.5 Hz, 2H), 1.46-1.40 (m, 2H), 1.31-1.27 (m, 8H), 0.89-0.86 (m, 3H). ^{13}C NMR ($CDCl_3$, 125 MHz): δ 163.6, 161.2, 140.1, 135.2, 130.7, 129.5, 128.1, 126.2, 120.4, 114.5, 113.4, 69.0, 63.8, 31.8, 29.2, 29.2, 28.9, 25.9, 22.6, 14.1. HRMS calcd for $C_{20}H_{24}BrNO_5S$ $(M+Na)^+$, 492.0451, found, 492.0447.

Bis(2-nitro-5-(octyloxy)benzyl) [2,2':5',2'':5'',2'''-quaterthiophene]-3,3'''-dicarboxylate (O3). A round bottom flask was charged with **3** (160 mg, 0.34 mmol), and $Pd(PPh_3)_4$ (10 mg, 0.009 mmol). The flask was evacuated and refilled with nitrogen three times. Under nitrogen flow, 5 mL of anhydrous DMF and 5,5′-bis(tributylstannyl)-2,2′-bithiophene (0.10 mL, 122 mg, 0.16 mmol) were added. The reaction was left refluxing overnight. DI water was added to quench the reaction. The solution was then diluted with brine (1x40 mL), and extracted with chloroform (3x40 mL). The combined organic layers were filtered, dried over $MgSO_4$ and solvent was removed *in vacuo*. Flash chromatography on silica using 1:2 hexanes:CH_2Cl_2 as eluent gave 53 mg of **O3** (35 %) as an orange solid. ^{1}H NMR ($CDCl_3$, 500 MHz): δ 8.19 (d, *J* = 9 Hz, 2H), 7.58 (d, *J* = 5.5 Hz, 2H), 7.39 (d, *J* = 4 Hz, 2H), 7.26 (d, *J* = 5.5 Hz, 2H), 7.10 (d, *J* = 4 Hz, 2H), 6.98 (d, *J* = 2.5 Hz, 2H), 6.86 (dd, *J* = 2.5 Hz, *J* = 9 Hz, 2H), 5.74 (s, 4H), 3.97 (t, *J* = 6.5 Hz, 4H), 1.76 (quintet, *J* = 7 Hz, 4H), 1.44-1.38 (m, 4H), 1.33-1.27 (m, 16H), 0.90-0.87 (m, 6H). ^{13}C NMR ($CDCl_3$, 75 MHz): δ 163.5, 162.2, 143.7, 140.0, 139.0, 135.3, 132.9, 130.5, 130.2, 128.0, 127.0, 124.2, 124.2, 114.5, 113.1, 68.9, 63.6, 31.8, 29.3, 29.2, 28.9, 25.9, 22.6, 14.1. HRMS calcd for $C_{48}H_{52}N_2O_{10}S_4$ $(M+Na)^+$, 967.2397, found, 967.2371.

Butyl 2-bromothiophene-3-carboxylate (4). A round bottom flask was charged with 2-bromothiophene-3-carboxylic acid (500 mg, 2.41 mmol), and PTSA (46 mg, 0.24 mmol). The flask was evacuated and refilled with nitrogen three times.

Under nitrogen flow, 20 mL of *n*-butanol was added. The reaction mixture was left to reflux overnight. The reaction mixture was washed with 1 M $NaHCO_3$ (1x30 mL) to quench the reaction. The solution was then extracted with CH_2Cl_2 (2x30 mL) and the combined organic layers were washed with 1 M $NaHCO_3$ (1x30 mL), DI water (1x30 mL), and brine (1x30 mL). Drying over $MgSO_4$ and removal of solvent *in vacuo* gave crude product as a brown oil. Flash chromatography on silica using 1:1 hexanes:CH_2Cl_2as eluent gave 87 mg of **4** (69 %) as a brown oil. ^{1}H NMR ($CDCl_3$, 500 MHz): δ 7.35 (d, *J* = 6 Hz, 1H), 7.20 (d, *J* = 6 Hz, 1H), 4.28 (t, *J* = 6.5 Hz, 2H), 1.72 (quintet, *J* = 7 Hz, 2H), 1.46 (sextet, *J* = 7.5, 2H), 0.96 (t, *J* = 7.5 Hz, 3H). ^{13}C NMR ($CDCl_3$, 75 MHz): δ 162.0, 131.4, 129.4, 125.8, 119.5, 64.8, 30.7, 19.3, 13.7. HRMS calcd for $C_9H_{11}BrO_2S$ $(M+Na)^+$, 284.9555, found, 284.9560.

Dibutyl [2,2':5',2'':5'',2'''-quaterthiophene]-3,3'''-dicarboxylate (O4). A round bottom flask was charged with $Pd(PPh_3)_4$ (10 mg, 0.009 mmol). The flask was evacuated and refilled with nitrogen three times. Under nitrogen flow, **4** (89 mg, 0.34 mmol) dissolved in 5 mL of anhydrous DMF and 5,5′-bis(tributylstannyl)-2,2′-bithiophene (0.1 mL, 122 mg, 0.16 mmol) were added. The reaction was left refluxing overnight. DI water was added to quench the reaction. The solution was then diluted with brine (1x40 mL), and extracted with chloroform (3x40 mL). The combined organic layers, dried over $MgSO_4$ and solvent was removed *in vacuo*. Flash chromatography on silica using 1:1 hexanes:CH_2Cl_2 as eluent gave 50 mg of **O4** (59 %) as a bright orange solid. ^{1}H

NMR ($CDCl_3$, 500 MHz): δ 7.50 (d, *J* = 5.5 Hz, 2H), 7.40 (d, *J* = 4 Hz, 2H), 7.20 (d, *J* = 5.5 Hz, 2H), 7.18 (d, *J* = 4 Hz, 2H), 4.28 (t, *J* = 6.5 Hz, 4H), 1.70 (quintet, *J* = 7.5 Hz, 4H), 1.41 (sextet, *J* = 7.5 Hz, 4H), 0.94 (t, *J* = 7.5 Hz, 6H). ^{13}C NMR ($CDCl_3$, 75 MHz): δ 163.2, 142.7, 139.0, 133.2, 130.6, 130.0, 128.0, 124.0, 123.8, 64.7, 30.7, 19.2, 13.7. HRMS calcd for $C_{26}H_{26}O_4S_4$ $(M+H)^+$, 531.0787, found, 531.0808.

2-Nitro-5-(octyloxy)benzyl 5-bromothiophene-2-carboxylate (5). A round bottom flask was charged with 5-bromothiophene-2-carboxylic acid (500 mg, 2.41 mmol). The flask was evacuated and refilled with nitrogen three times. Under nitrogen flow, 13 mL of anhydrous dichloromethane (DCM), 3 drops of dimethyl formamide (DMF), and oxalyl chloride (0.25 mL, 370 mg, 2.41 mmol) were added. After 4 hours of stirring at room temperature, a solution of **2** (679 mg, 2.41 mmol), *N*,*N*-dimethylaminopyridine (DMAP) (295 mg, 2.41 mmol), and triethylamine (TEA) (0.34 mL, 247 mg, 2.41 mmol) in 15 mL anhydrous CH_2Cl_2 was added to the reaction vessel. The mixture was left to stir overnight at room temperature. The reaction mixture was washed with 5% aqueous HCl, and extracted with CH_2Cl_2 (3×30 mL). The organic extract was washed with deionized (DI) water, saturated aqueous $NaHCO_3$ (2×30 mL), and brine (1×30 mL). Drying over $MgSO_4$ and removal of solvent *in vacuo* gave the crude product **3**. Flash chromatography on silica using 1:1 hexanes:CH_2Cl_2 as eluent gave a white solid that was washed with EtOH to remove remaining starting material. The final wash gave 481 mg of **3** (42%) as a white solid. ^1H NMR ($CDCl_3$, 500

MHz): δ 8.22 (d, *J* = 9 Hz, 1H), 7.65 (d, *J* = 4 Hz, 1H), 7.14 (d, *J* = 4 Hz, 1H), 7.07 (d, *J* = 2 Hz, 1H), 6.91 (dd, *J* = 2.5 Hz, 9.5 Hz, 1H), 5.76 (s, 2H), 4.05 (t, *J* = 6.5 Hz, 2H), 1.82 (m, 2H), 1.48-1.42 (m, 2H), 1.34-1.30 (m, 8H), 0.91-0.88 (m, 3H). ^{13}C NMR ($CDCl_3$, 125 MHz): δ 163.6, 160.3, 140.0, 135.1, 134.4, 134.0, 131.2, 128.1, 121.0, 114.1, 113.3, 69.0, 63.9, 31.8, 29.3, 29.2, 28.9, 25.9, 22.6, 14.1. HRMS calcd for $C_{20}H_{24}BrNO_5S$ $(M+Na)^+$, 492.0451, found, 492.0466.

Bis(2-nitro-5-(octyloxy)benzyl) [2,2':5',2'':5'',2'''-quaterthiophene]-5,5'''-dicarboxylate (O5). A round bottom flask was charged with **5** (170 mg, 0.36 mmol), and $Pd(PPh_3)_4$ (10 mg, 0.009 mmol). . The flask was evacuated and refilled with nitrogen three times. Under nitrogen flow, 5 mL of DMF, and 5,5′-bis(tributylstannyl)-2,2′-bithiophene (0.1 mL, 122 mg, 0.16 mmol) were added. The reaction was left refluxing overnight. DI water was added, and the solution was then diluted with brine (1x40 mL), and extracted with chloroform (3x40 mL). The combined organic layers were dried over $MgSO_4$ and solvent was removed *in vacuo*. The crude solid was then redissolved in CH_2Cl_2, dried over $MgSO_4$, and solvent was removed *in vacuo* to yield crude product as an orange solid. Flash chromatography on silica using 2:1 CH_2Cl_2:hexanes as eluent gave an orange solid that was washed with EtOH to remove remaining starting material. The final wash gave 28 mg of **O5** (18%) as an orange solid. ^{1}H NMR ($CDCl_3$, 500 MHz): δ 8.24 (d, *J* = 9 Hz, 2H), 7.82 (d, *J* = 4 Hz, 2H), 7.25 (d, *J* = 4 Hz, 2H), 7.21 (d, *J* = 4 Hz, 2H), 7.17 (d, *J* = 3.5 Hz, 2H), 7.12 (d, *J* = 2.5 Hz, 2H), 6.92 (dd, *J* = 3 Hz, 9.5 Hz, 2H), 5.80 (s, 4H), 4.06 (t, *J* = 6.5 Hz, 4H), 1.82 (m, 4H), 1.48-1.42 (m,

4H), 1.36-1.26 (m, 16H), 0.89-0.86 (m, 6H). ^{13}C NMR ($CDCl_3$, 125 MHz): δ 163.6, 161.2, 144.2, 140.0, 137.4, 135.5, 135.4, 135.0, 130.9, 128.1, 126.2, 125.1, 124.2, 114.1, 113.3, 69.0, 63.8, 31.8, 29.3, 29.2, 28.9, 25.9, 22.6, 14.1. HRMS calcd for $C_{48}H_{52}N_2O_{10}S_4$ $(M+Na)^+$, 967.2397, found, 967.2387.

Butyl 5-bromothiophene-2-carboxylate (6). A round bottom flask was charged with 5-bromothiophene-2-carboxylic acid (500 mg, 2.41 mmol), and p-toluenesulfonic acid (PTSA) (83 mg, 0.48 mmol). The flask was evacuated and refilled with nitrogen three times. Under nitrogen flow, 25 mL of *n*-butanol was added. The reaction mixture was left to reflux overnight. The reaction mixture was washed with 1 M $NaHCO_3$ (1×30 mL) to quench the reaction. The solution was then extracted with CH_2Cl_2 (2×30 mL) and the combined organic layers were washed with 1 M $NaHCO_3$ (1×30 mL), DI water (1×30 mL), and brine (1×30 mL). Drying over $MgSO_4$ and removal of solvent *in vacuo* gave 420 mg of **6** (66 %) as a yellow/brown oil. ^{1}H NMR ($CDCl_3$, 500 MHz): δ 7.52 (d, J = 4 Hz, 1H), 7.04 (d, J = 4 Hz, 1H), 4.26 (t, J = 6.5 Hz, 2H), 1.70 (m, 2H), 1.43 (m, J =, 2H), 0.95 (t, J = 7.5, 3H). ^{13}C NMR ($CDCl_3$, 125 MHz): δ 161.1, 135.2, 133.4, 130.8, 120.0, 65.2, 30.7, 19.2, 13.7. HRMS calcd for $C_9H_{11}BrO_2S$ $(M+Na)^+$, 284.9555, found, 284.9572.

Dibutyl [2,2':5',2'':5'',2'''-quaterthiophene]-5,5'''-dicarboxylate (O6). A round bottom flask was charged with **6** (94 mg, 0.36 mmol), and $Pd(PPh_3)_4$ (10 mg, 0.009 mmol). The flask was evacuated and refilled with nitrogen three times.

Under nitrogen flow, 5 mL of DMF, and5,5′-bis(tributylstannyl)-2,2′-bithiophene (0.1 mL, 122 mg, 0.16 mmol) were added. The reaction was left refluxing overnight. DI water was added to quench the reaction. The solution was then diluted with brine (1×40 mL), and extracted with chloroform (3×40 mL). The combined organic layers were filtered, dried over $MgSO_4$ and solvent was removed *in vacuo*. Some DMF remained so methanol (MeOH) was added to crash out the solid product. The solution was then filtered to give 57 mg of **O6** (67 %) as a bright orange solid. ^{1}H NMR ($CDCl_3$, 500 MHz): δ 7.72 (d, *J* = 4 Hz, 2H), 7.23 (d, *J* = 4 Hz, 2H), 7.17 (d, *J* = 4 Hz, 2H), 7.15 (d, *J* = 3.5, 2H), 4.33 (t, *J* = 7 Hz, 4H), 1.76 (quintet, *J* = 7 Hz, 4H), 1.49 (sextet, *J* = 7.5 Hz, 4H), 1.00 (t, *J* = 7 Hz, 6H). ^{13}C NMR ($CDCl_3$, 125 MHz): δ 162.1, 143.4, 137.1, 135.7, 134.1, 132.1, 125.9, 124.9, 124.0, 65.2, 30.8, 19.2, 13.7. HRMS calcd for $C_{26}H_{26}O_4S_4$ $(M+H)^+$, 531.0787, found, 531.0801.

2-Nitro-5-(octyloxy)benzyl 2,5-dibromothiophene-3-carboxylate (7). A round bottom flask was charged with **2** (492 mg, 1.75 mmol), 2,5-dibromothiophene-3-carboxylic acid (500 mg, 1.75 mmol), and DMAP (214 mg, 1.75 mmol). The flask was evacuated and refilled with nitrogen three times. Under nitrogen flow, 40 mL of anhydrous CH_2Cl_2, and *N*,*N*′-dicyclohexylcarbodiimide (DCC) (361 mg, 1.75 mmol) dissolved in 10 mL of anhydrous CH_2Cl_2 were added. The reaction was left to reflux overnight. The reaction mixture was washed with 5% aqueous HCl (2×40 mL), saturated $NaHCO_3$ (2×40 mL), and DI water (2×40 mL). Drying over $MgSO_4$ and removal of solvent *in vacuo* gave the crude product. Flash

chromatography on silica using 1:1 hexanes:CH_2Cl_2 as eluent gave 414 mg of **7** (43 %) as a white solid. ^{1}H NMR ($CDCl_3$, 500 MHz): δ 8.22 (d, *J* = 9 Hz, 1H), 7.42 (s, 1H), 7.12 (d, *J* = 2.5 Hz, 1H), 6.92 (dd, *J* = 2.5 Hz, 9 Hz, 1H), 5.76 (s, 2H), 4.05 (t, *J* = 6.5 Hz, 2H), 1.82 (quintet, *J* = 7 Hz, 2H), 1.48-1.42 (m, 2H), 1.37-1.29 (m, 8H), 0.91-0.88 (m, 3H). ^{13}C NMR ($CDCl_3$, 125 MHz): δ 163.5, 160.1, 140.1, 134.8, 131.8, 131.3, 128.1, 119.8, 114.7, 113.4, 111.8, 69.0, 64.1, 31.8, 29.2, 29.2, 28.9, 25.9, 22.6, 14.1. HRMS calcd for $C_{20}H_{23}Br_2NO_5S$ $(M+Na)^+$, 571.9544, found, 571.9548.

Butyl 2,5-dibromothiophene-3-carboxylate (8). A round bottom flask was charged with 2,5-dibromothiophene-3-carboxylic acid (243 mg, 0.85 mmol), and PTSA (48 mg, 0.25 mmol). The flask was evacuated and refilled with nitrogen three times. Under nitrogen flow, 15 mL of *n*-butanol was added. The reaction mixture was left to reflux overnight. The reaction mixture was washed with 1 M $NaHCO_3$ (1x30 mL) to quench the reaction. The solution was then extracted with CH_2Cl_2 (2x30 mL) and the combined organic layers were washed with 1 M $NaHCO_3$ (1x30 mL), DI water (1x30 mL), and brine (1x30 mL). Drying over $MgSO_4$ and removal of solvent *in vacuo* gave crude product. Flash chromatography on silica using 1:1 hexanes:CH_2Cl_2 as eluent gave 156 mg of **8** (53 %) as a brown oil. ^{1}H NMR ($CDCl_3$, 500 MHz): δ 7.34 (s, 1H), 4.28 (t, *J* = 7 Hz, 2H), 1.73 (quintet, *J* = 6.5 Hz, 2H), 1.47 (sextet, *J* = 7.5 Hz, 2H), 0.97 (t, *J* = 7.5, 3H). ^{13}C NMR ($CDCl_3$, 125 MHz): δ 160.9, 132.1, 131.8, 118.9, 111.3, 65.1,

30.6, 19.2, 13.7. HRMS calcd for $C_9H_{10}Br_2O_2S$ $(M+Na)^+$, 364.8643, found, 364.8647.

Stille Polymerizations: Stille polymerizations were carried out using two different methods.

Poly((2-nitro-5-(octyloxy)benzyl)thiophene-3-carboxylate-*co*-thiophene (P7).

Method A. A round bottom flask was charged with **7** (54 mg, 0.098 mmol), and $Pd(PPh_3)_4$ (13 mg, 0.011 mmol). The flask was evacuated and refilled with nitrogen three times. Under nitrogen flow, 0.4 mL of anhydrous DMF, 2 mL of anhydrous toluene, and 0.054 mL 2,5-bis(tributylstannyl)thiophene (65 mg, 0.098 mmol) were added. The reaction mixture was left to reflux overnight. Upon completion, the reaction mixture was added dropwise to MeOH to precipitate the polymer. After centrifugation, the polymer was washed by Soxhlet extraction with hexanes for 24 h, followed by Soxhlet extraction with CH_2Cl_2 for 24 hours. After extraction, the solvent was removed *in vacuo* to give 35 mg of **P7** (71 %) as a purple solid. GPC: M_n = 5781, PDI = 1.36. ^{1}H NMR ($CDCl_3$, 500 MHz): δ 8.2-8.1 (1H), 7.7-7.5 (1H), 7.5-7.4 (1H), 7.2-7.1 (1H), 7.1-6.9 (1H), 6.9-6.8 (1H), 5.8-5.7 (2H), 4.1-3.9 (2H), 1.8-1.7 (2H), 1.4-1.3 (2H), 1.3-1.2 (8H), 0.9-0.8 (3H).

Method B. A round bottom flask was charged with **7** (140 mg, 0.26 mmol), tri(*o*-tolyl)phosphine (31 mg, 0.10 mmol), and $Pd_2(dba)_3$ (11 mg, 0.012 mmol). The flask was evacuated and refilled with nitrogen three times. Under nitrogen flow, a solution of 2,5-bis(trimethylstannyl)thiophene (105 mg, 0.26 mmol) in 5 mL of

anhydrous toluene was added. The reaction mixture was left to reflux for 36 h. Upon completion, the reaction mixture was added dropwise to MeOH to precipitate the polymer. After centrifugation, the solvent was removed *in vacuo* to give 114 mg of **P7** (95 %) as a purple solid. GPC: M_n = 9229, PDI = 1.86.

Poly(butyl thiophene-3-carboxylate-*co*-thiophene) (P8).

Method A. Yield: 33 mg (69 %). GPC: M_n = 3154, PDI = 1.18. ^{1}H NMR ($CDCl_3$, 500 MHz): δ 7.8-7.5 (1H), 7.5-7.3 (1H), 7.2-7.0 (1H), 4.4-4.2 (2H), 1.8-1.7 (2H), 1.5-1.4 (2H), 1.1-0.9 (3H).

Method B. Yield: 48 mg (78 %). GPC: M_n = 2451, PDI = 1.61.

2.10 References

1. So, F.; Krummacher, B.; Mathai, M. K.; Poplavskyy, D.; Choulis, S. A.; Choong, V. E. *J. Appl. Phys.* **2007**, *102*, 21.

2. Coakley, K. M.; McGehee, M. D. *Chem. Mater.* **2004**, *16*, 4533.

3. Huang, F.; Wu, H.; Cao, Y. *Chem. Soc. Rev.* **2010**, *39*, 2500.

4. Manceau, M.; Bundgaard, E.; Carle, J. E.; Hagemann, O.; Helgesen, M.; Sondergaard, R.; Jorgensen, M.; Krebs, F. C. *J. Mater. Chem.* **2011**, *21*, 4132.

5. Petersen, M. H.; Gevorgyan, S. A.; Krebs, F. C. *Macromolecules* **2008**, *41*, 8986.

6. Krebs, F. C.; Spanggaard, H. *Chem. Mater.* **2005**, *17*, 5235.

7. Liu, J. S.; Kadnikova, E. N.; Liu, Y. X.; McGehee, M. D.; Frechet, J. M. J. *J. Am. Chem. Soc.* **2004**, *126*, 9486.

8. Bjerring, M.; Nielsen, J. S.; Nielsen, N. C.; Krebs, F. C. *Macromolecules* **2007**, *40*, 6012.

9. Krebs, F. C.; Norrman, K. *ACS Appl. Mater. Interfaces* **2010**, *2*, 877.

10. Gordon, T. J.; Yu, J. F.; Yang, C.; Holdcroft, S. *Chem. Mater.* **2007**, *19*, 2155.

11. Yu, J. F.; Abley, M.; Yang, C.; Holdcroft, S. *Chem. Commun.* **1998**, 1503.

12. Holdcroft, S. *Adv. Mater.* **2001**, *13*, 1753.

13. Xu, Y. Y.; Zhang, F.; Feng, X. L. *Small* **2011**, *7*, 1338.

14. Bouffard, J.; Watanabe, M.; Takaba, H.; Itami, K. *Macromolecules* **2010**, *43*, 1425.

15. Johnson, R. S.; Finnegan, P. S.; Wheeler, D. R.; Dirk, S. M. *Chem. Commun.* **2011**, *47*, 3936.

16. Lee, S. K.; Jung, B. J.; Ahn, T.; Song, I. S.; Shim, H. K. *Macromolecules* **2003**, *36*, 9252.

17. Zhao, H.; Gu, W. Y.; Sterner, E.; Russell, T. P.; Coughlin, E. B.; Theato, P. *Macromolecules* **2011**, *44*, 6433.

18. Zhao, H.; Sterner, E. S.; Coughlin, E. B.; Theato, P. *Macromolecules* **2012**, *45*, 1723.

19. Gee, K. R.; Weinberg, E. S.; Kozlowski, D. J. *Bioorg. Med. Chem. Lett.* **2001**, *11*, 2181.

20. Groff, D.; Wang, F.; Jockusch, S.; Turro, N. J.; Schultz, P. G. *Angew. Chem.-Int. Edit.* **2010**, *49*, 7677.

21. Han, G.; Mokari, T.; Ajo-Franklin, C.; Cohen, B. E. *J. Am. Chem. Soc.* **2008**, *130*, 15811.

22. Krafft, G. A.; Sutton, W. R.; Cummings, R. T. *J. Am. Chem. Soc.* **1988**, *110*, 301.

23. Pawle, R. H.; Eastman, V.; Thomas, S. W. *J. Mater. Chem.* **2011**, *21*, 14041.

24. Nguyen, T. Q.; Doan, V.; Schwartz, B. J. *J. Chem. Phys.* **1999**, *110*, 4068.

25. Wang, F. K.; Bazan, G. C. *J. Am. Chem. Soc.* **2006**, *128*, 15786.

Chapter 2 Appendix

^{1}H and ^{13}C NMR

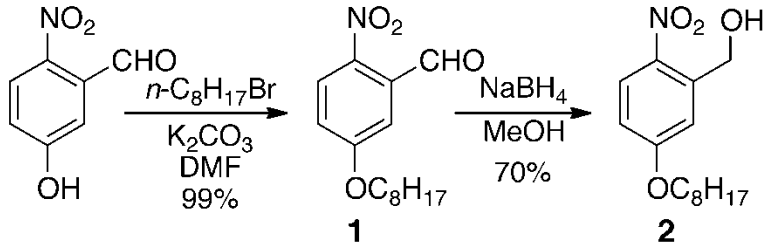

Compound **1**, ^{1}H NMR (500 MHz, $CDCl_3$)

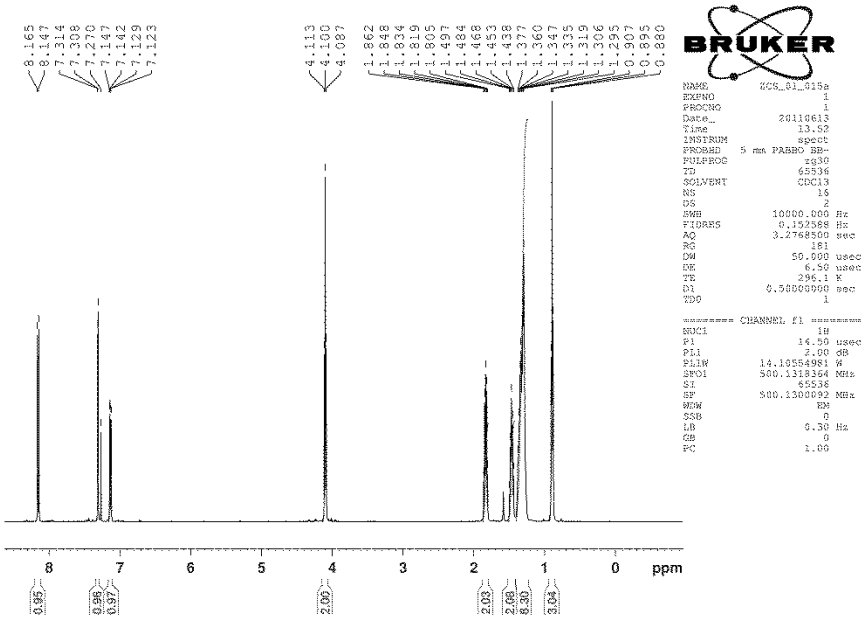

Compound **1**, ^{13}C NMR (125 MHz, $CDCl_3$)

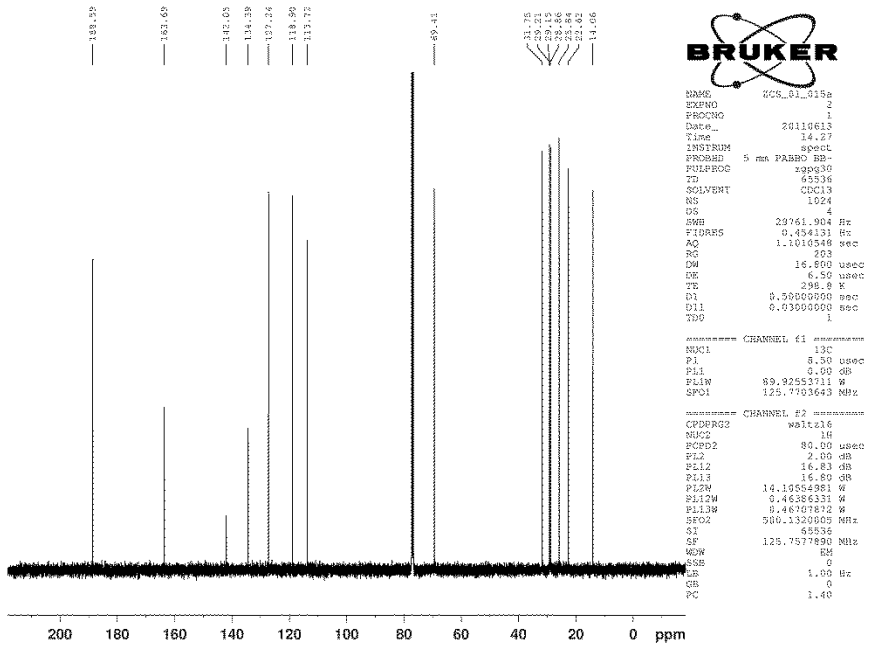

Compound **2**, ^{1}H NMR (500 MHz, $CDCl_3$)

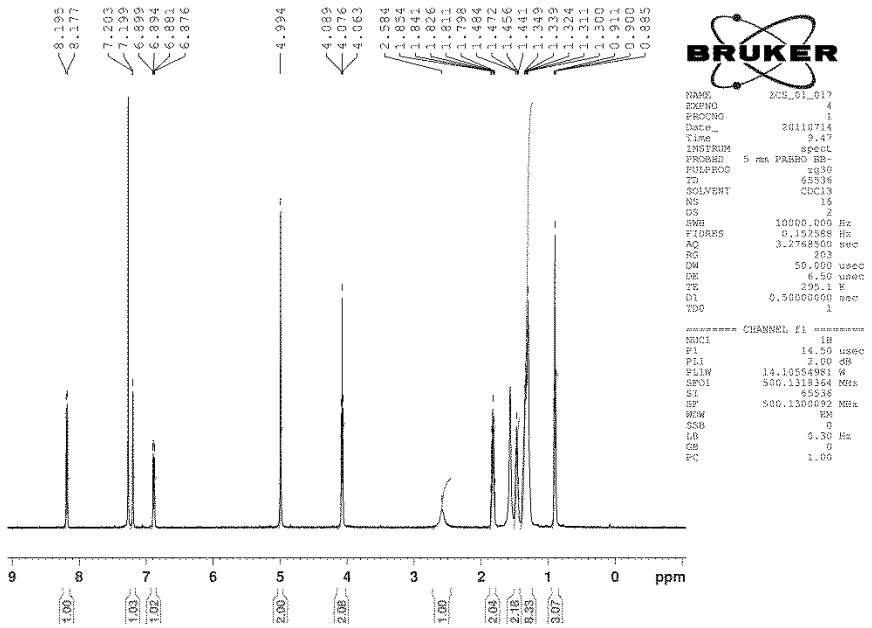

Compound **2**, ^{13}C NMR (125 MHz, $CDCl_3$)

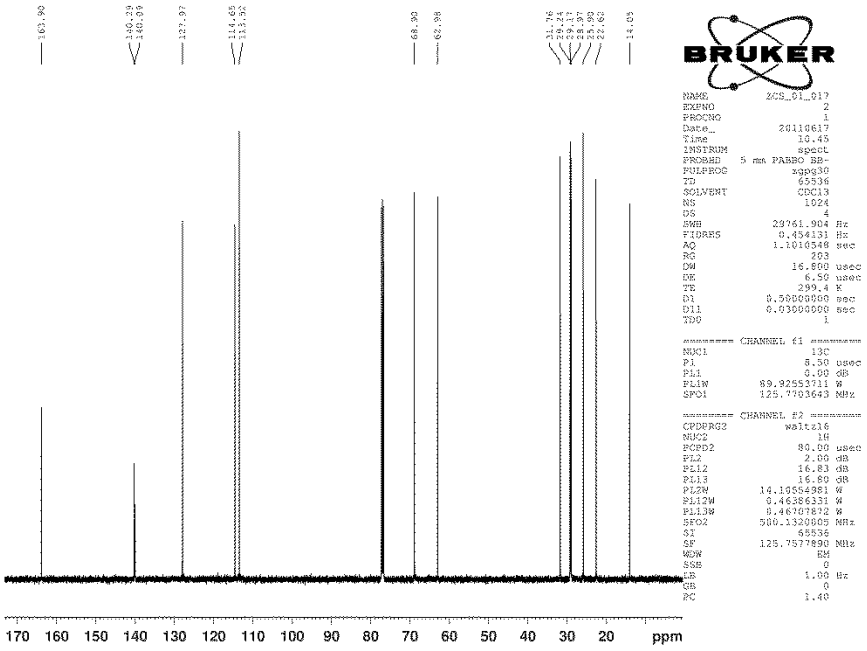

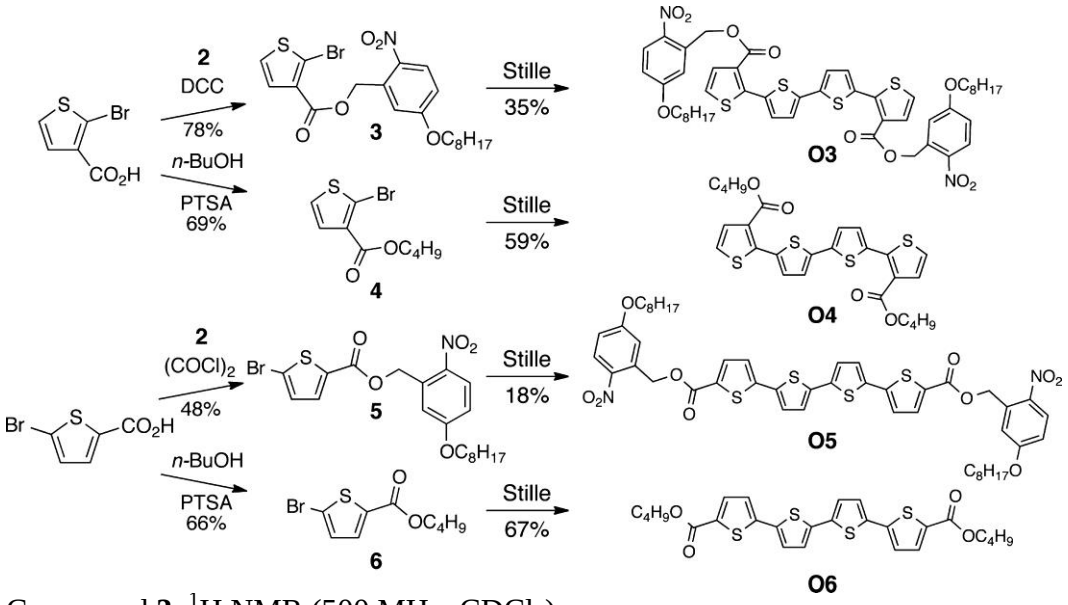

Compound **3**, ^{1}H NMR (500 MHz, $CDCl_3$)

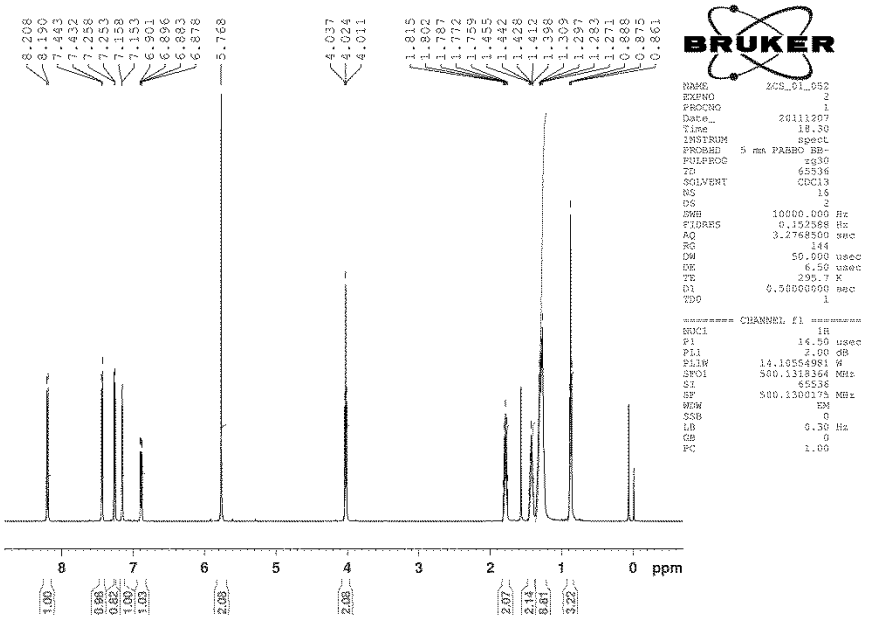

Compound **3**, ^{13}C NMR (125 MHz, $CDCl_3$)

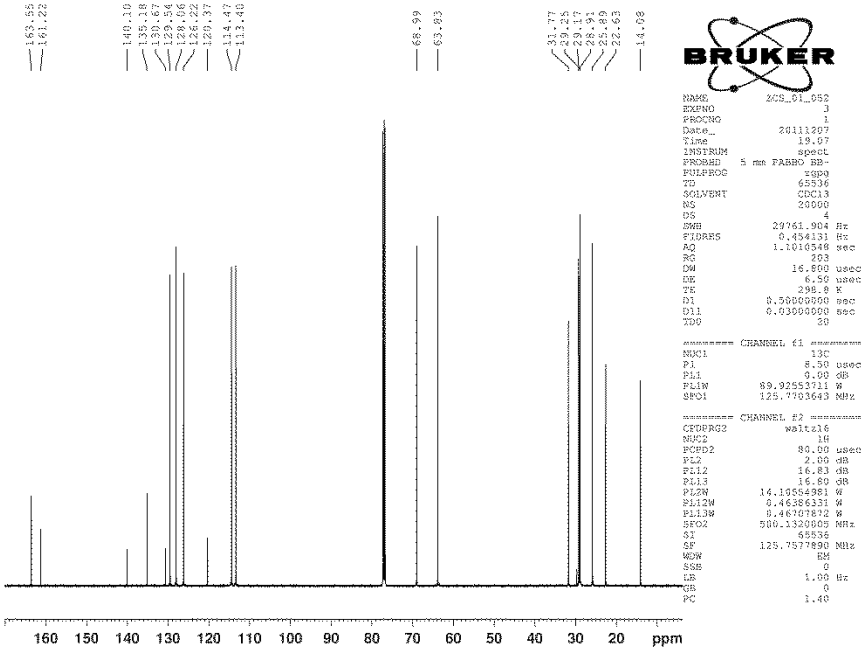

Compound **O3**, ^{1}H NMR (500 MHz, $CDCl_3$)

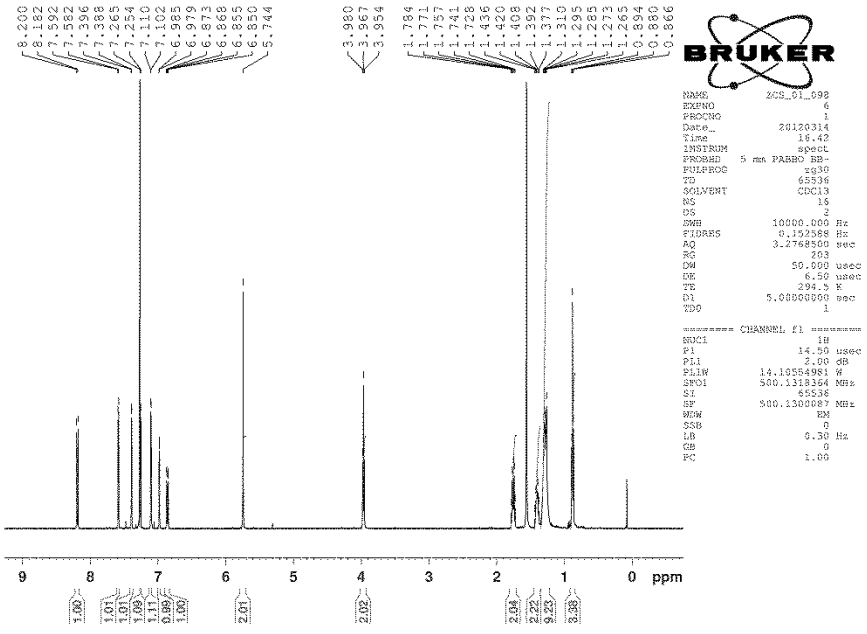

Compound **O3**, ^{13}C NMR (125 MHz, $CDCl_3$)

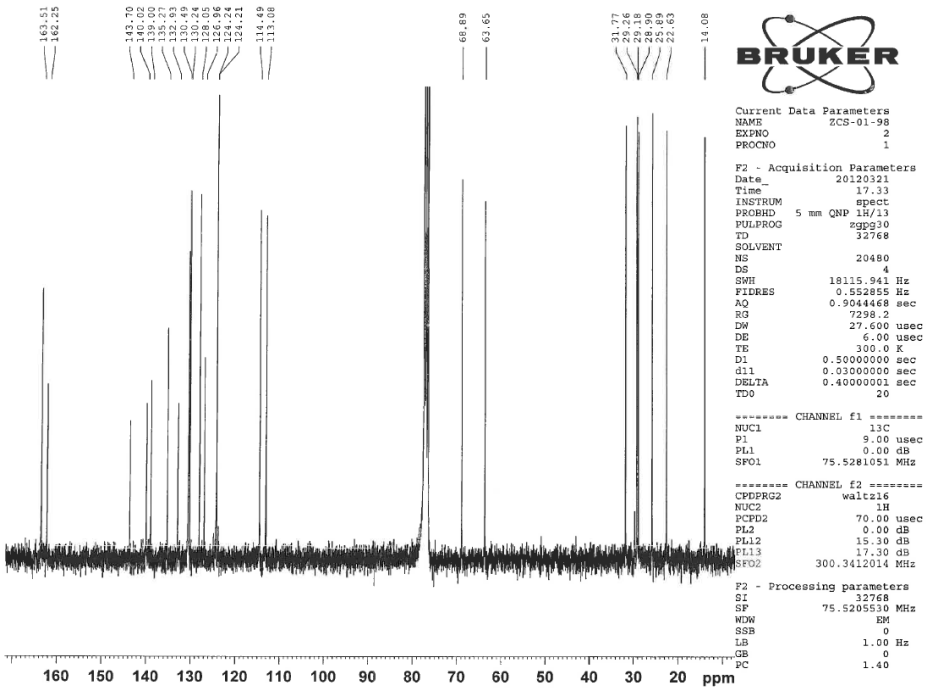

Compound **4**, ^{1}H NMR (500 MHz, $CDCl_3$)

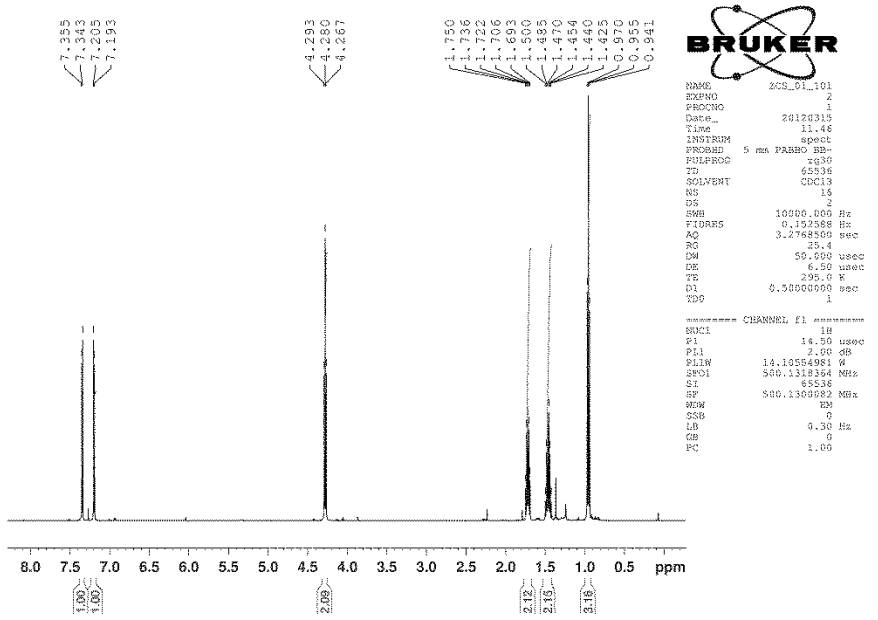

Compound **4**, ^{13}C NMR (125 MHz, $CDCl_3$)

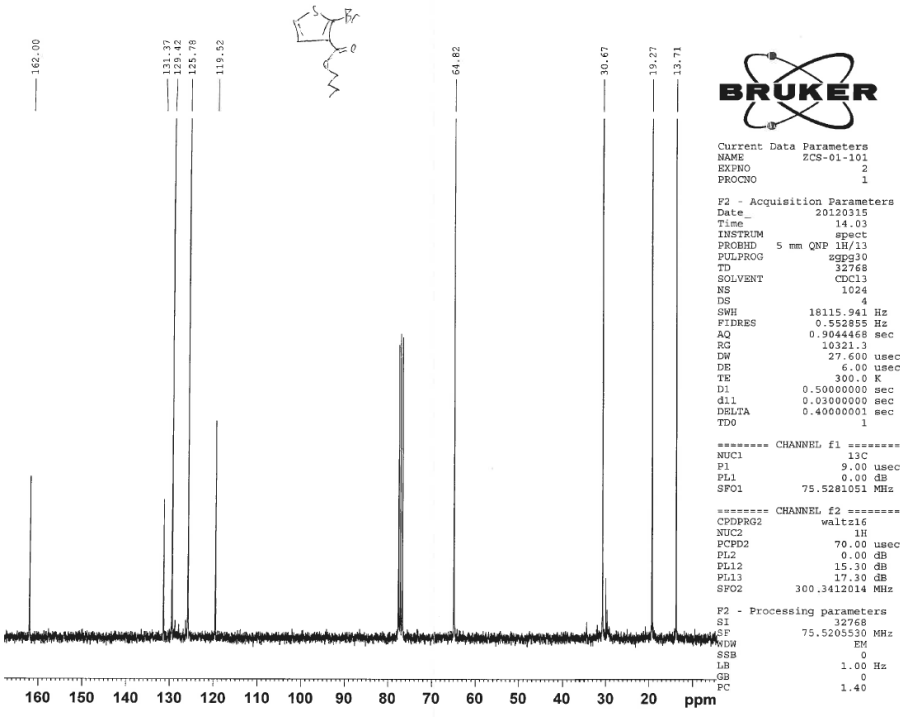

Compound **O4**, ^{1}H NMR (500 MHz, $CDCl_3$)

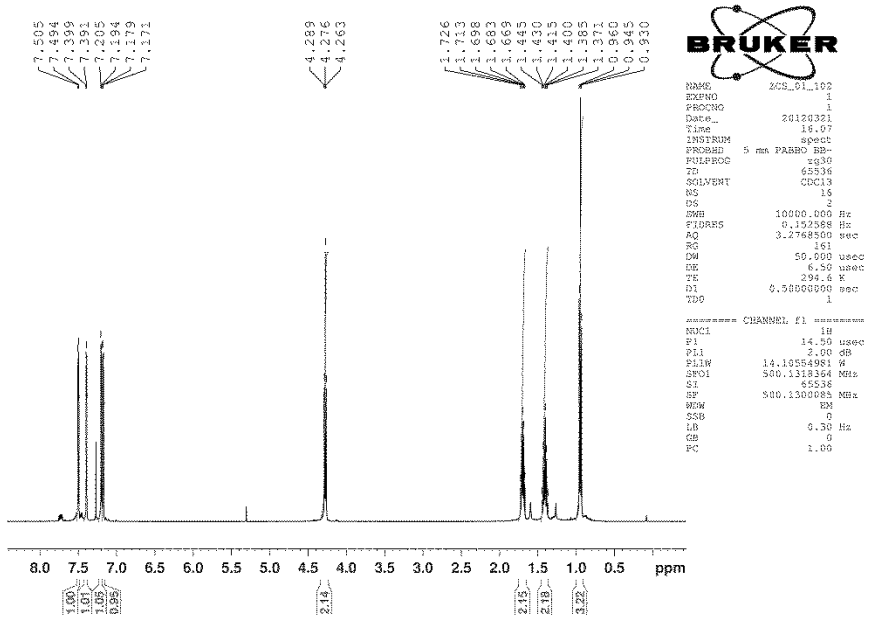

Compound **O4**, ^{13}C NMR (125 MHz, $CDCl_3$)

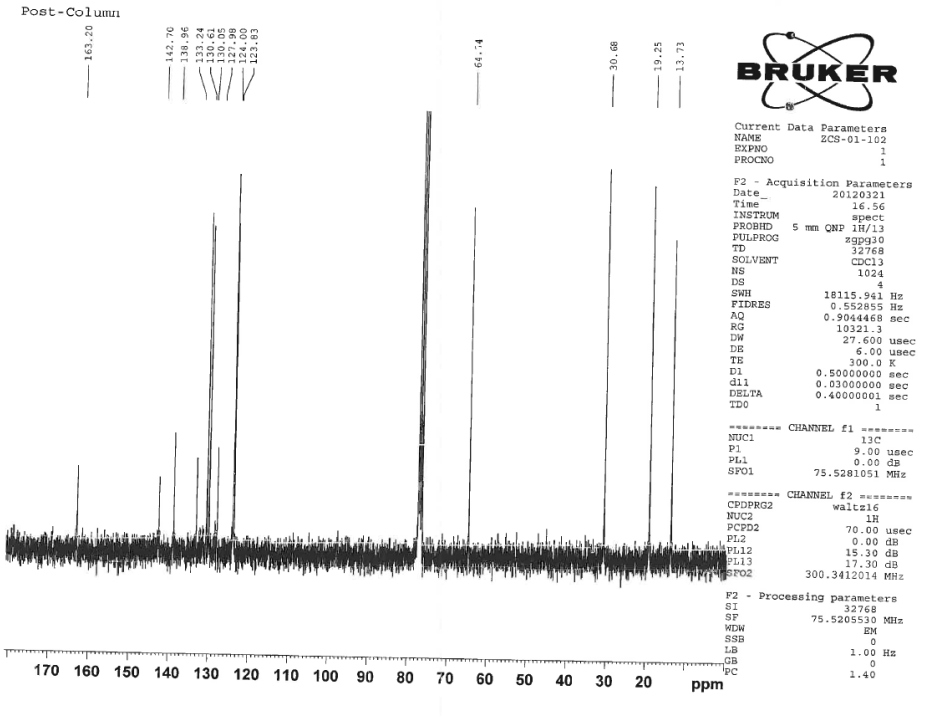

Compound **5**, ^{1}H NMR (500 MHz, $CDCl_3$)

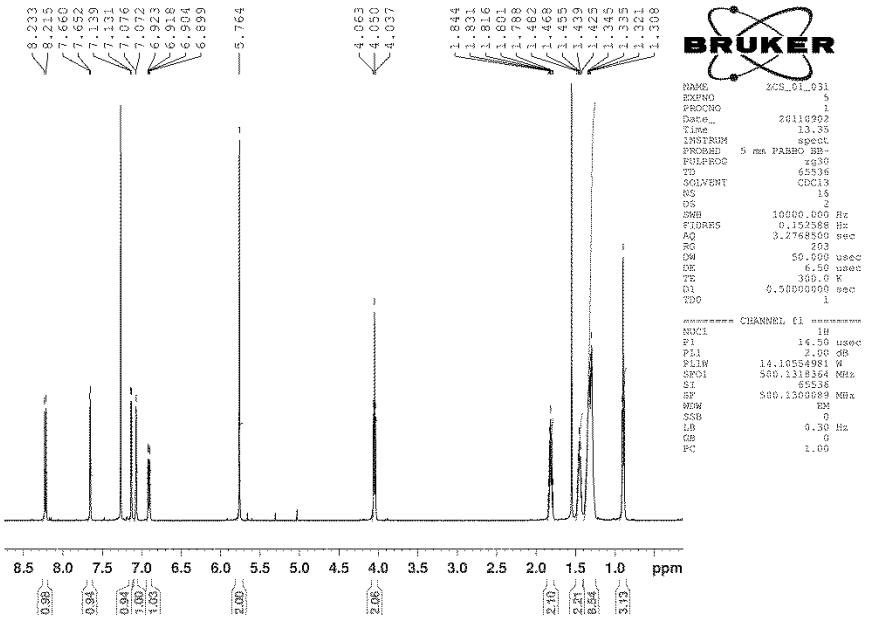

Compound **5**, ^{13}C NMR (125 MHz, $CDCl_3$)

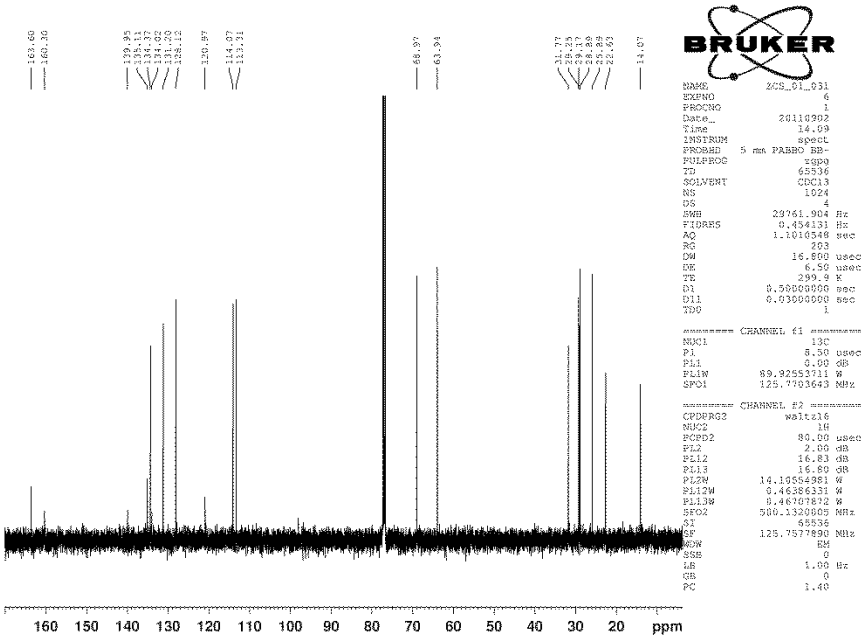

Compound **O5**, ^{1}H NMR (500 MHz, $CDCl_3$)

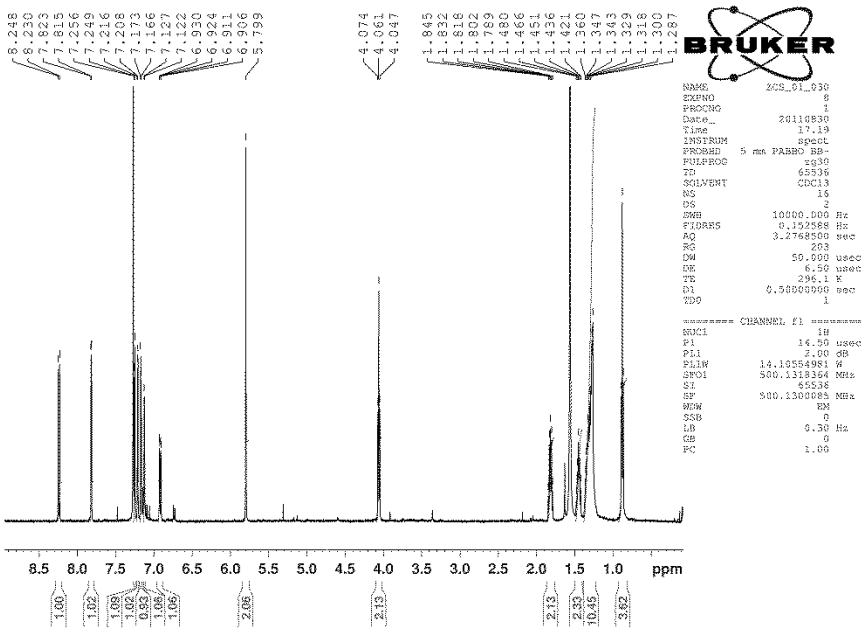

Compound **O5**, ^{13}C NMR (125 MHz, $CDCl_3$)

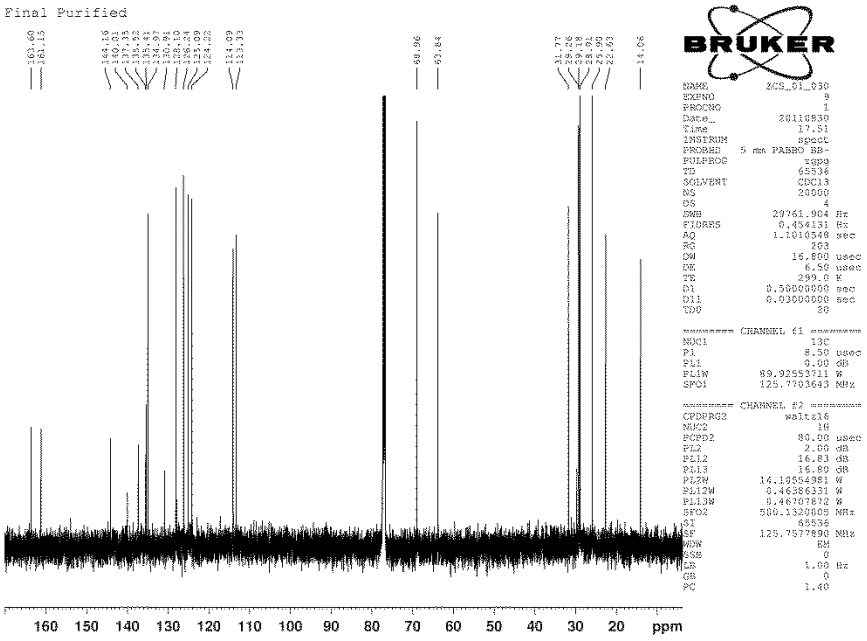

Compound **6**, ^{1}H NMR (500 MHz, $CDCl_3$)

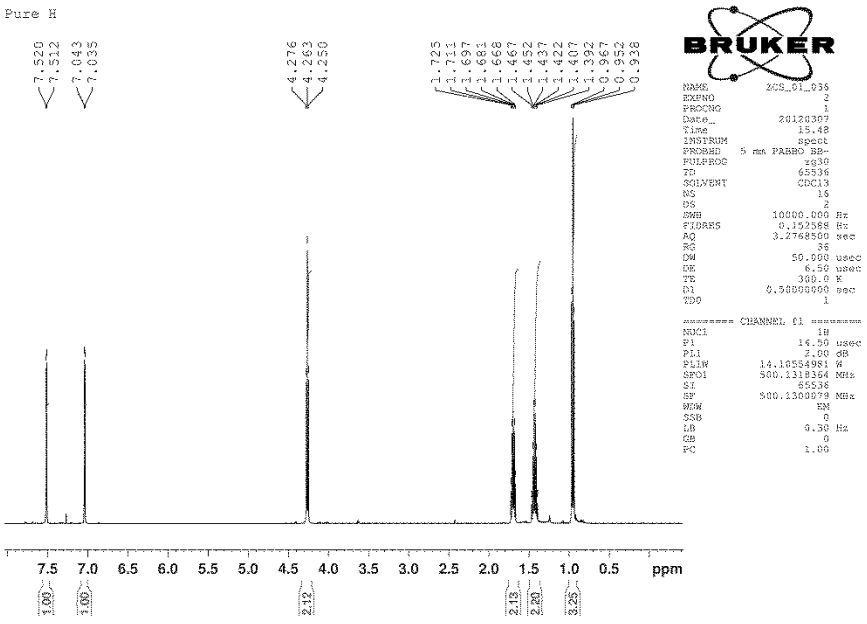

Compound **6**, ^{13}C NMR (125 MHz, $CDCl_3$)

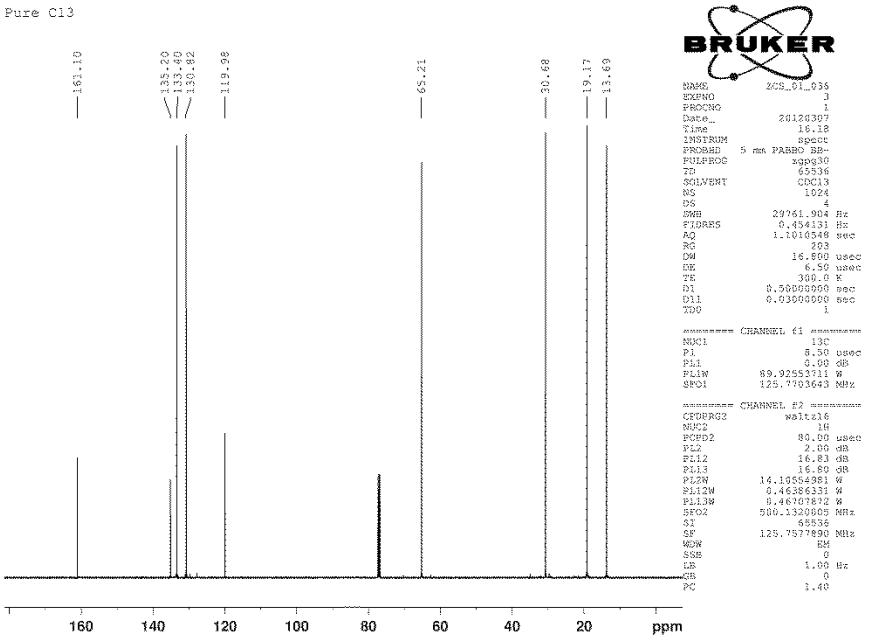

Compound **O6**, ^{1}H NMR (500 MHz, $CDCl_3$)

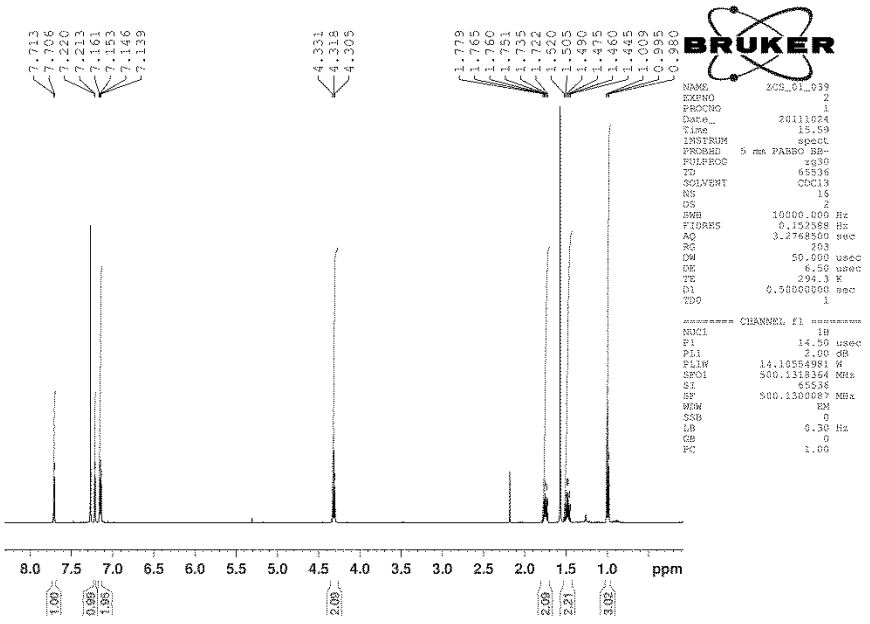

Compound **O6**, ^{13}C NMR (125 MHz, $CDCl_3$)

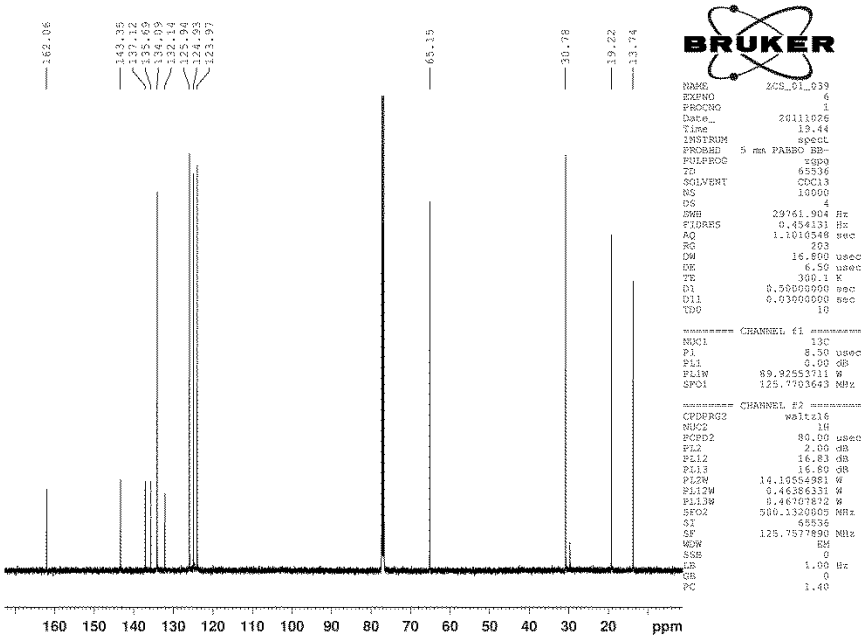

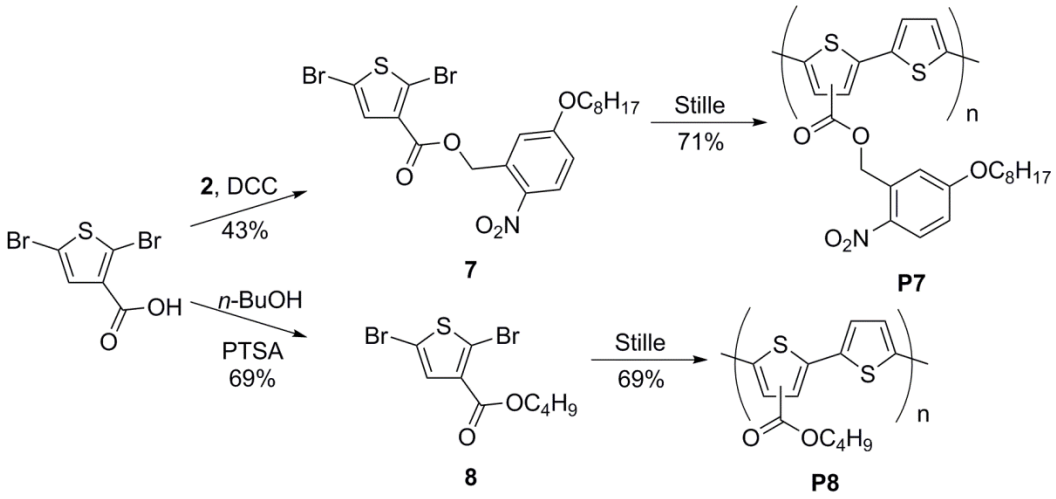

Compound **7**, ^{1}H NMR (500 MHz, $CDCl_3$)

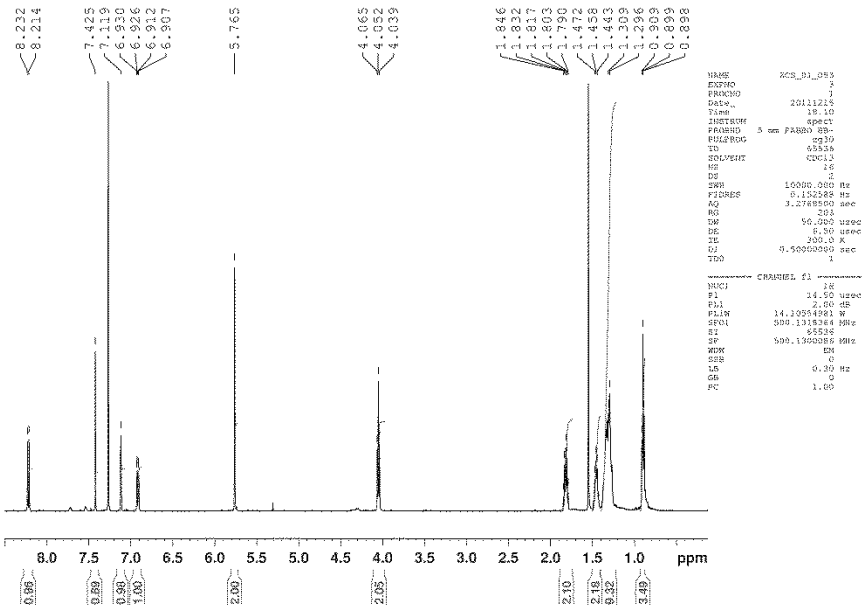

Compound **7**, ^{13}C NMR (125 MHz, $CDCl_3$)

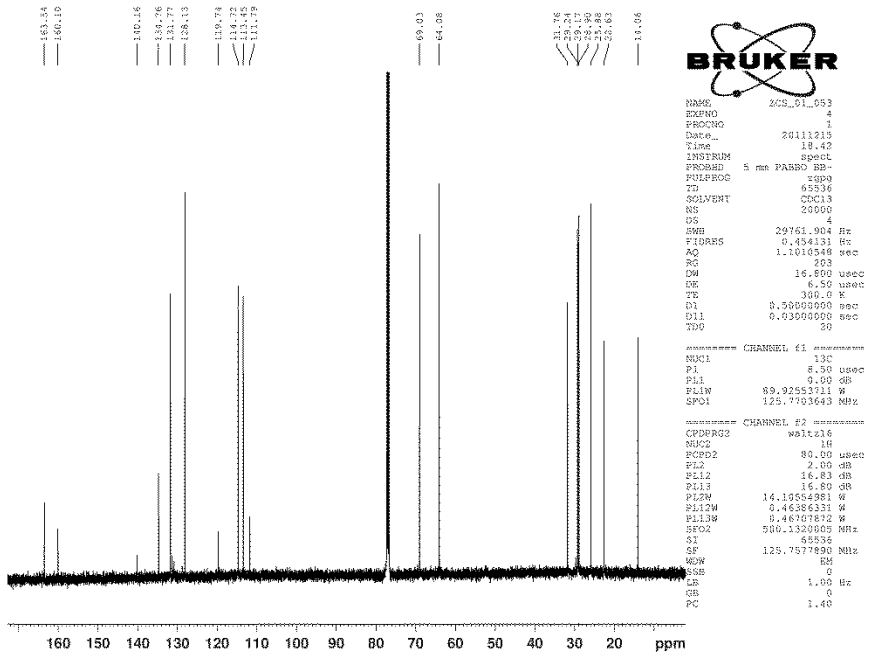

Compound **P7**, ^{1}H NMR (500 MHz, $CDCl_3$)

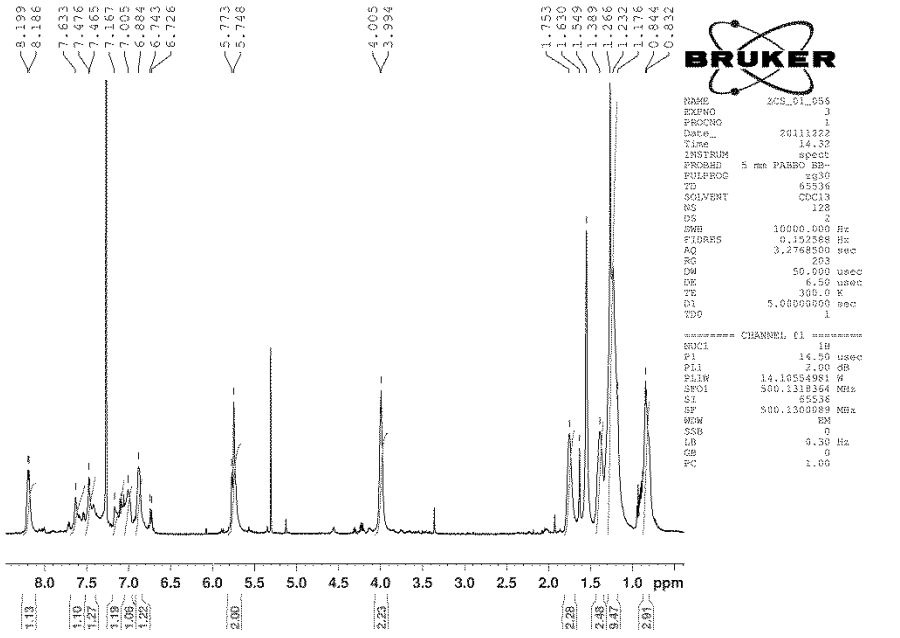

Compound **8**, ^{1}H NMR (500 MHz, $CDCl_3$)

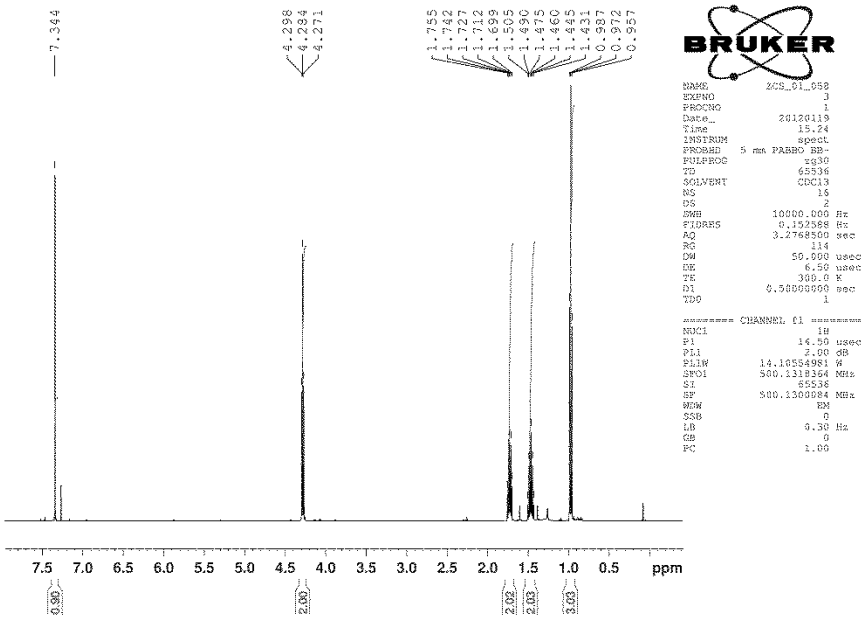

Compound **8**, ^{13}C NMR (125 MHz, $CDCl_3$)

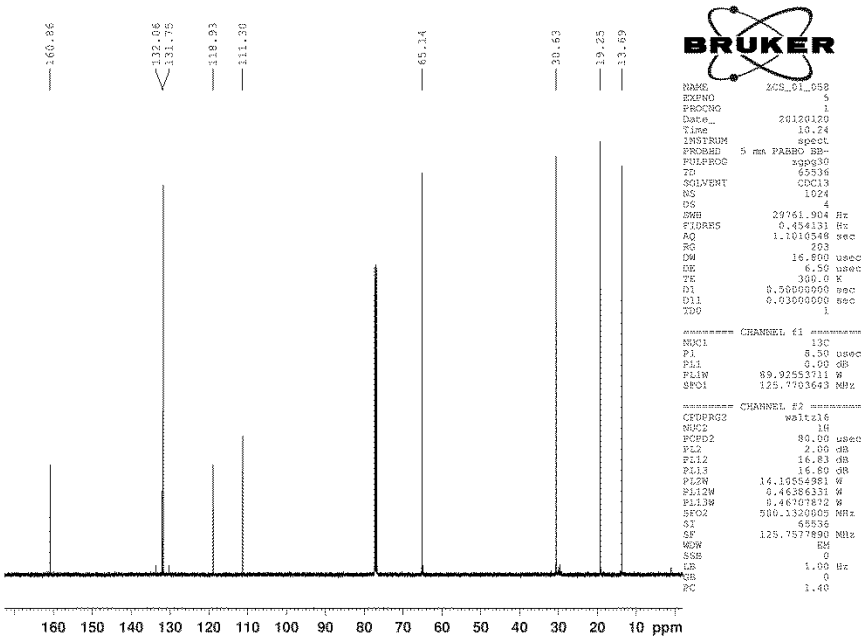

Compound **P8**, ^{1}H NMR (500 MHz, $CDCl_3$)

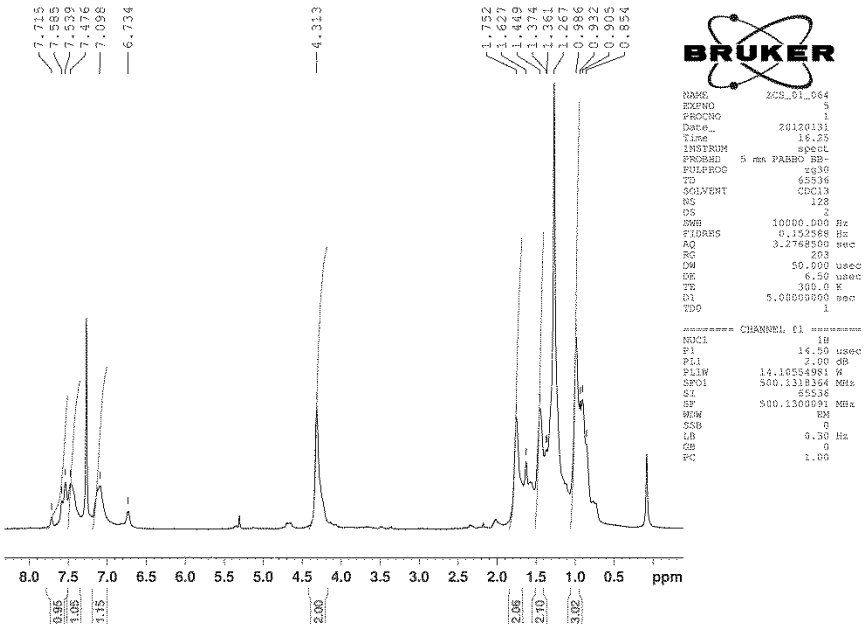
7.715
7.685
7.639
7.476
7.098
6.734
4.313
1.752
1.627
1.449
1.374
1.361
1.267
0.986
0.932
0.905
0.854
8.0 7.5 7.0 6.5 6.0 5.5 5.0 4.5 4.0 3.5 3.0 2.5 2.0 1.5 1.0 0.5 ppm
0.95
1.05
1.15
2.00
2.06
2.10
3.02
BRUKER
NAME 2CS_01_064
EXPNO 5
PROCNO 1
Date_ 20120131
Time 16.25
INSTRUM spect
PROBHD 5 mm PABBO BB-
PULPROG zg30
TD 65536
SOLVENT CDCl3
NS 128
DS 2
SWH 10000.000 Hz
FIDRES 0.152588 Hz
AQ 3.2768500 sec
RG 203
DW 50.000 usec
DE 6.50 usec
TE 300.0 K
D1 5.00000000 sec
TD0 1
======== CHANNEL f1 ========
NUC1 1H
P1 14.50 usec
PL1 2.00 dB
PLW 14.10554981 W
SFO1 500.1318364 MHz
SI 65536
SF 500.1300091 MHz
WDW EM
SSB 0
LB 0.30 Hz
GB 0
PC 1.00

Chapter 3:

Thiophene-Based Conjugated Polymers with Photolabile Solubilizing Side Chains

Reproduced in part with permission from:
Smith, Z.C.; Meyer, D.M.; Simon, M.G.; Staii, C.; Shukla, D.; Thomas, S. W.
Thiophene-Based Conjugated Polymers with
Photolabile Solubilizing Side Chains.
Macromolecules **2015**, *48*, 959-966.

3.1 Comparing Different NB Groups Attached to Conjugated Polymers

This chapter describes conjugated oligomers and polymers (CPs) with solubilizing chains connected to polymer backbone through different photocleavable linkers. Conjugated polymers are active components of a number of solid-state optoelectronic technologies, such as sensors, transistors and photovoltaics.[1-3] Consistent among the vast majority of reported CPs are the presence of long alkyl chains, which impart solubility to these otherwise insoluble materials.[4] Solubility of CPs is critical both during their preparation—precipitation during polymerization can results in low yields and reduced molecular weights —and for solvent-based processing of materials into thin films, which is an important advantage that organic semiconductors have over their inorganic counterparts.[5] Although state of the art semiconducting polymers generally possess them, solubilizing chains can present some drawbacks: i) they restrict fabrication of solution-deposited multilayer films to materials that are orthogonally soluble or cross-linked after deposition,[6] ii) they occupy volume with optoelectronically inactive groups,[7] and iii) they participate in CP degradation processes, such as hydrogen atom abstractions.[8] In a comprehensive study relating chemical structure of CPs to their photochemical stability, Krebs and coworkers recommended limiting the occurrence of side chains to "as low as possible".[7]

Several approaches exist for addressing the drawbacks of solubilizing chains. Cross-linking of polymer films is a popular choice for limiting solubility upon film deposition, although the alkyl chains remain in the film.[9] There have

been a number of examples of thermally cleavable solubilizing chains, focusing on tertiary esters that eliminate olefins and produce insoluble carboxylic acid-functionalized CPs.[10,11] Interestingly, the resultant films can have performances that are superior to the films prior to thermolysis.[10] More recently, acid catalysis for the thermocleavage of solubilizing side chains has been reported using of silane-substituted polythiophenes, thus enabling thermocleavage at much lower temperatures.[12,13] Approaches that do not require high temperatures are important for eventual coating of CPs on inexpensive, flexible substrates such as poly(ethylene terephthalate) or poly(ethylene napthalate).[14] Photochemical approaches to changing the solubility of CPs have the advantage of spatiotemporal control, and the possibility of mild conditions. Some approaches have included photo-oxidative cleavage of the CP backbone,[15] photocleavage of solubilizing xanthate side-chains,[16] and photo-patterning of a conjugated polymer using a photobase generator.[17]

The application of photocleavable groups to the design of light-responsive polymers and surfaces is a rapidly growing area of research.[18,19] Although a number of photocleavable linkers exist, *ortho*-nitrobenzyl (NB) groups are among the most popular, due to their ease of synthesis and their wide range of materials and experimental conditions in which they can function.[20,21] Pauly and Theato have used NB groups in the photopatterning of conjugated poly(phenylacetylene)s.[21] Our group has reported a polythiophene derivative comprising *n*-octyloxy chains connected to the conjugated poly(thiophene)

backbone through photolabile NB esters that cleave upon irradiation at 365 nm (Scheme 3.1).[22]

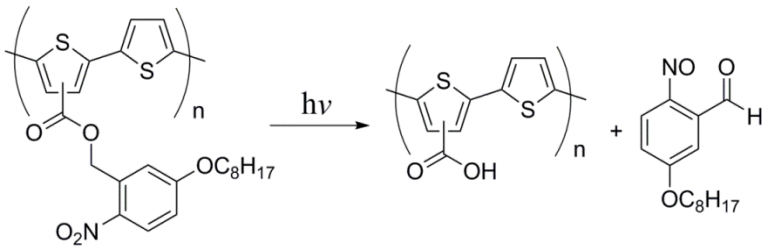

Scheme 3.1 *o*-Nitrobenzyl ester photocleavage reaction of our previously reported polymer (**P1**) resulting in the analogous carboxylic acid containing polythiophene, and the nitroso aldehyde byproduct.

Upon irradiation, films of this polymer became insoluble in toluene without significant photobleaching of the polythiophene backbone. This chapter represents a comprehensive study of the following: i) the effect of the chemical structure of the NB group on the efficiency of photocleavage of solubilizing chains from terthiophenes and polythiophenes, ii) the preparation of multilayer CP films using only one deposition solvent, iii) the photopatterning of CP films, and iv) hole mobility measurements in thin film transistors before and after photocleavage of solubilizing chains.

3.2 Experimental Design

Reducing the time required for photochemical cleavage of solubilizing chains is important for the purposes of efficiency in processing. In addition, because both the CP backbones and photocleavage byproducts compete with NB groups for absorption of light, reducing the number of photons required to render

polymers insoluble also reduces photobleaching. We therefore designed conjugated oligomers and CPs with the photocleavable units shown in **Chart 3.1**.

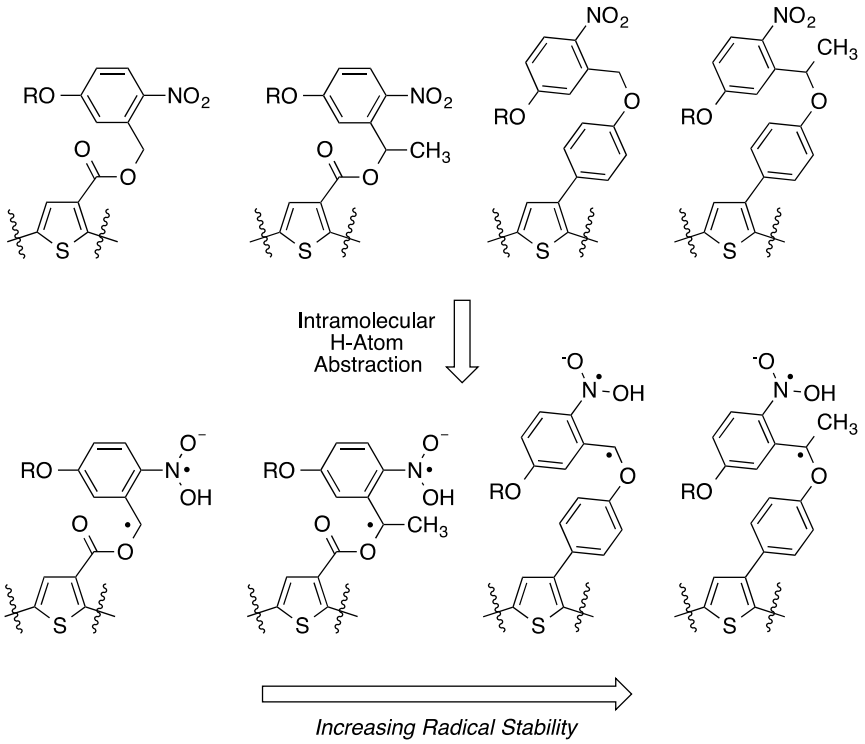

Chart 3.1 Rationale for design of photolabile linkers: increasing radical stability upon intramolecular hydrogen atom abstraction during photocleavage.

The key difference between these NB groups is the stability of the corresponding benzylic radical photolysis intermediate after the initial intramolecular hydrogen atom abstraction**.** Our hypothesis was that linkers with increased substitution or increased electron density at the benzylic position would cleave more efficiently: Bochet and coworkers recently showed a positive correlation between radical stabilization energy of NB radicals and their quantum yields of photocleavage.[23]

3.3 Synthesis of Conjugated Oligomers and Polymers

We prepared nitrobenzyl ester-linked terthiophenes and polythiophenes, that were unsubstituted (**O1** and **P1**) or methylated (**O2** and **P2**) at the benzylic position. The synthesis of these oligomers and polymers is summarized in Scheme 3.2.

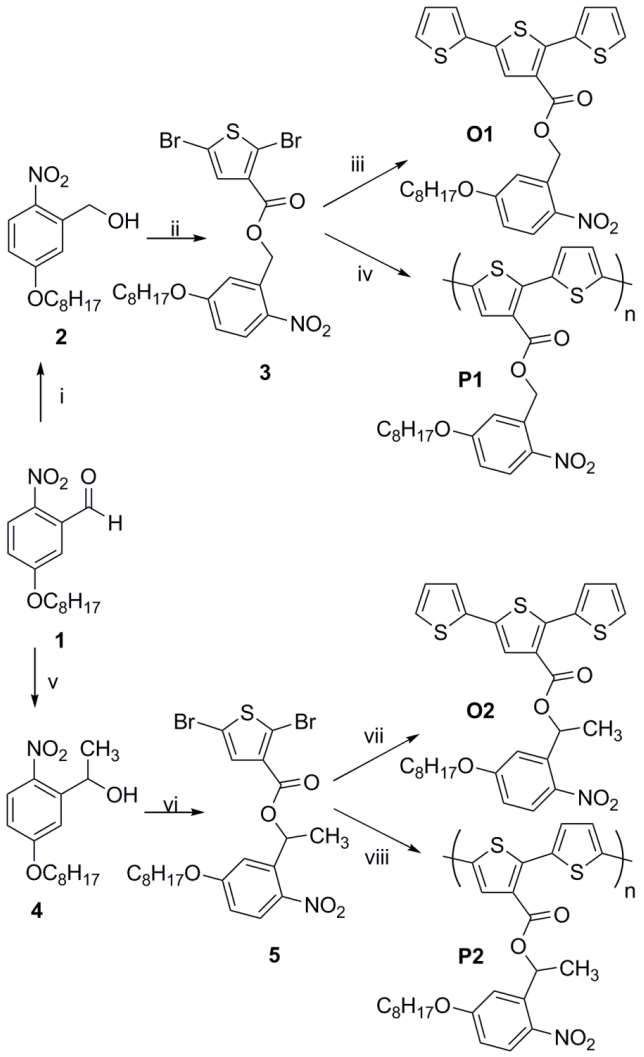

Scheme 3.2 i) $NaBH_4$, MeOH, 70%; ii) 2,5-dibromo-3-thiophenecarboxylic acid, DCC, DMAP, CH_2Cl_2, reflux, 43%; iii) 2-(tributylstannyl)thiophene, $Pd(PPh_3)_4$, DMF, 90°C, 83%; iv) $Pd_2(dba)_3$,tri-*o*-tolylphosphine, 2,5-bis(trimethylstannyl) thiophene, toluene, 90°C, 95%; v) $TiCl_4$, CH_3MgBr, Et_2O, -78°C, 95%; vi) 2,5-dibromo-3-thiophene carboxylic acid, DCC, DMAP, CH_2Cl_2, reflux, 50%; vii) $Pd(PPh_3)_4$, 2-(tributylstannyl)thiophene, DMF, 90°C, 54%; viii) $Pd_2(dba)_3$, tri-*o*-tolylphosphine, 2,5-bis(trimethylstannyl)thiophene, toluene, 90°C, 82%.

The first steps in the synthesis of these targets was to define the substitution pattern at the benzylic position while reducing the aldehyde group of previously described compound **1**; reduction of **1** with $NaBH_4$ yielded primary nitrobenzyl alcohol **2**, while alkylation of **1** with $CH_3MgBr/TiCl_4$ gave the corresponding secondary nitrobenzyl alcohol **4**. Acylation of either **2** or **4** with known compound 2,5-dibromothiophene-3-carboxylic acid[24] gave the nitrobenzyl ester-functionalized dibromide-functionalized monomers **3** and **5**. Stille cross-coupling of **3** with either 2-(tributylstannyl)thiophene or 2,5-bis(trimethylstannyl)thiophene yielded either terthiophene **O1** or polythiophene **P1**, while cross-coupling of **5** under similar reaction conditions yielded terthiophene **O2** and polythiophene **P2**.

The key intermediates to prepare analogous targets with nitrobenzyl ether linkers were 2,5-dibromothiophenes **7** and **9** (Scheme 3.3). Halo-de-hydroxylation reactions of benzyl alcohols **2** and **4** yielded the corresponding benzyl bromides with PBr_3 (**6**) or PPh_3/CBr_4 (**8**). Alkylation of 2,5-dibromo-3-(4-hydroxyphenyl)thiophene with either of these alkyl bromides gave the nitrobenzyl ether-functionalized monomers **7** and **9**. Stille cross-coupling of **7** with the appropriate stannanes yielded terthiophene **O3** and polythiophene **P3**, while cross-coupling of **9** gave analogs **O4** and **P4**, each of which has one methyl group in the benzylic position.

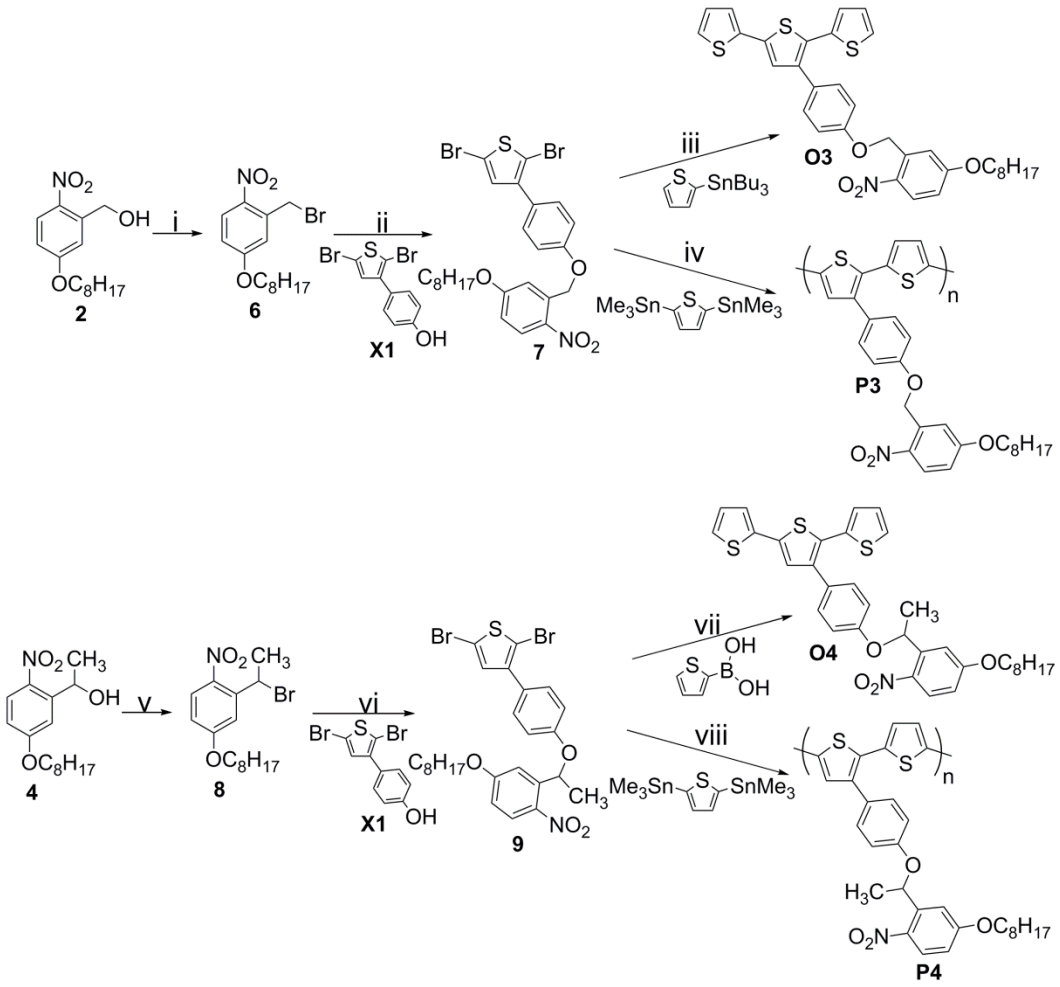

Scheme 3.3 i) PBr_3, 0°C, 46 %; ii) K_2CO_3, DMF, 50°C, 69 %; iii) $Pd(PPh_3)_4$, DMF, 90°C, 43 %; iv) $Pd_2(dba)_3$, tri-*o*-tolylphosphine, toluene, 90°C, 85 %; v) CBr_4, PPh_3, 52 %; vi) K_2CO_3, DMF, 50°C, 84 %; vii) $NaHCO_3$, $Pd(PPh_3)_4$, DMF/H_2O, 80°C, 82 %; viii) $Pd_2(dba)_3$, tri-*o*-tolyl phosphine, toluene, 90°C, 92 %.

Our synthesis of **O4** by Suzuki coupling highlights an advantage of using a nitrobenzyl ether over the more commonly used nitrobenzyl esters. Ethers are more tolerant of the strongly basic conditions that are standard in Suzuki couplings that would readily saponify esters.[25] In addition, the use of Suzuki coupling reactions increases the number of easily accessible polymers because there are more commercially available—and less toxic—diboronic acids and

esters than distannanes. As an example of this extended utility, we synthesized the donor-acceptor polymers **P5** and **P6** using monomers **7** and **9**, respectively, with the commercially available diboronic ester of benzothiadiazole (Scheme 3.4).

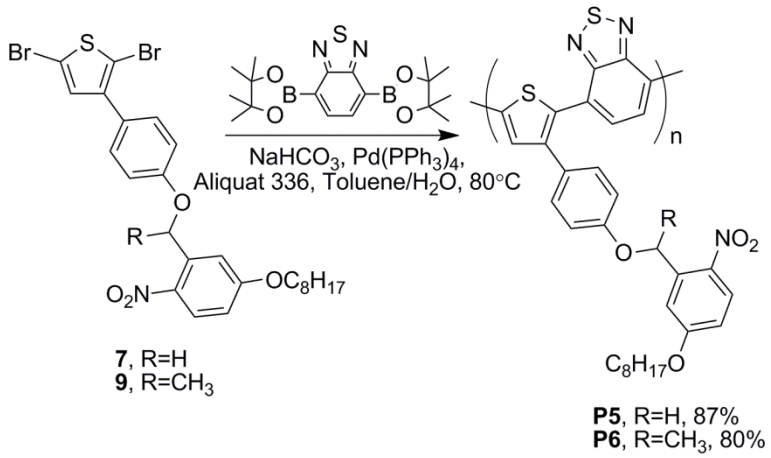

Scheme 3.4 Synthesis of Copolymers P5 and P6.

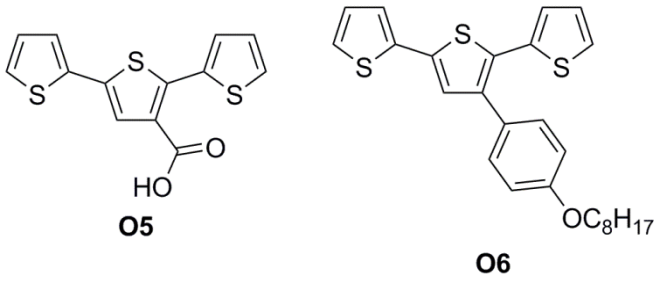

Chart 3.2 The chemical structures of control oligomers **O5** and **O6**.

3.4 Spectral Properties of Synthesized Compounds

Tables 1 and 2 summarize the properties of absorbance and fluorescence emission of the terthiophenes and conjugated polymers studied here, while Figure 3.1 shows absorbance, emission, and excitation spectra of terthiophene **O4**.

Table 3.1 Relevant Properties of Terthiophenes **O1**-**O6**.

	λ_{max} (abs), nm	ε, $M^{-1}cm^{-1}$	λ_{max} (em), nm	Φ_F	Φ_{rxn}
O1	320	15000	469	0.009	0.011
O2	321	17000	438	0.006	0.054
O3	332	21000	438	0.005	0.12
O4	342	17000	434	0.004	0.18
O5	351	15000	476	0.03	-
O6	350	19000	436	0.02	-

Table 3.2 Characterization Details of **P1**-**P7**.

	λ_{max} (abs), nm	λ_{max} (em), nm	Φ_F	M_n, g/mol	PDI
P1	520	627	0.14	18,400	1.20
P2	509	590	0.19	7,000	1.14
P3	529	626	0.10	12,800	2.14
P4	520	579	0.13	14,800	1.58
P5	546	676	0.13	46,400	1.65
P6	544	663	0.17	10,200	2.12
P7	464	581	0.33	6,050	1.42

Absorbance spectra of the NB-containing materials showed bands due to both the NB chromophore in the UV region of the spectrum at approximately 285-320 nm, as well as the conjugated thiophene-containing main chains: terthiophene chromophores absorbed in the UV between 320 and 350 nm, while polythiophenes **P1**-**P4** have absorbance maxima between 510-530 nm, reflecting the extension of the conjugated π-systems from trimers to polymers. The absorbance and fluorescence spectra of the thiophene-*co*-benzothiadiazole polymers (**P5**-**P6**) are significantly red-shifted from those of the polythiophenes

(**P1**-**P4**), which we attribute to their donor-acceptor character. The fluorescence quantum yields of those materials without NB substituents have quantum yields of fluorescence similar to reported terthiophenes[26] and polythiophenes;[27] differences in molecular weight and regioregularity of polythiophenes also contribute to differences in optical properties.

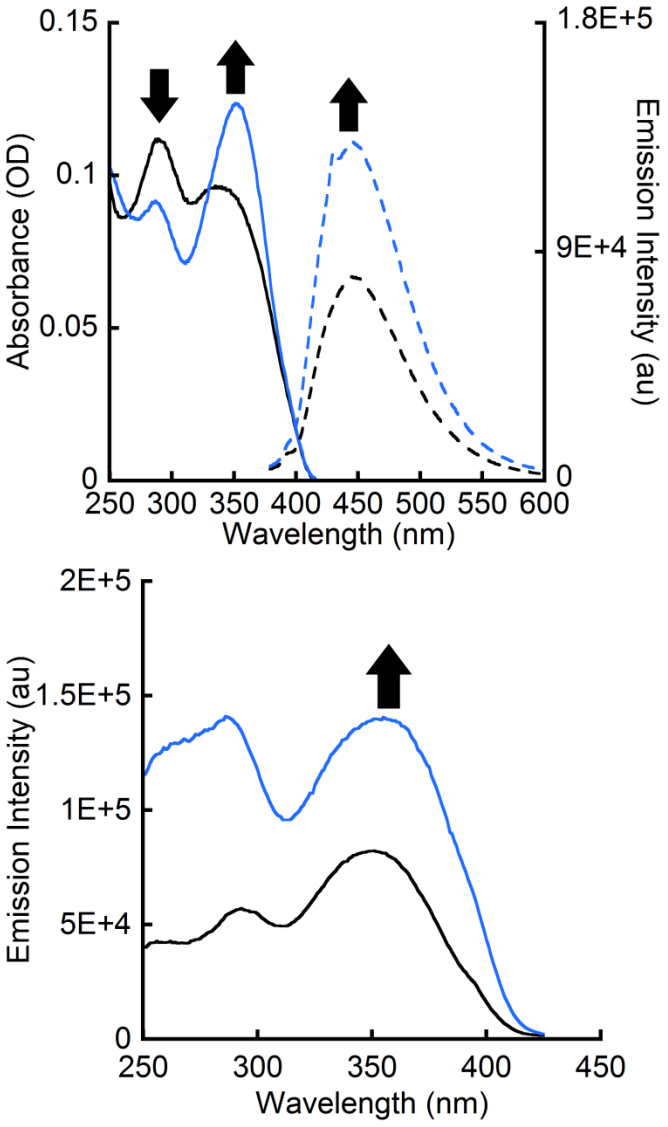

Figure 3.1 *Top*: Absorbance (solid lines), and emission (dashed lines) spectra for **O4**. *Bottom*: excitation spectra for **O4**. Black lines are the spectra of **O4** in dichloromethane before irradiation; blue lines are the spectra of the same sample after 3 minutes of irradiation at 365 nm (40 mW/cm^2). λ_{ex}=350 nm for emission spectra; λ_{em}=450 nm for excitation spectra.

The nature of the interactions between chromophores is key to the study of any multichromophoric material. To help understand the interactions of the NB and thiophene-based chromophores, we compared them to analogous control compounds that did not contain NB groups. Terthiophenes **O5** and **O6**, which do not contain NB groups, had 3-5 fold higher quantum yields of fluorescence than NB-containing analogs **O1**-**O4**; this observation is indicative of photoinduced electron transfer quenching of the fluorescence of the NB-containing fluorophores, as we have observed in previous studies of NB-functionalized conjugated materials, and as is utilized in some photoactivatable dyes.[28] Comparing NB-substituted polythiophenes **P1**-**P4** to control polymer **P7** showed a similar trend.

In contrast to the evidence that the NB group perturbs the excited state of the conjugated backbone by quenching fluorescence, the conjugated thiophene backbones have no more than a small effect on the excited states of NB groups. As shown in Figure 3.1, there is a peak in the same range of absorbance of the nitrobenzyl group of **O4** at 290 nm in the excitation spectrum. Photons absorbed in this range, however, contribute to only a small amount of terthiophene fluorescence, as the intensity of this peak in the excitation spectrum is heavily suppressed relative to its intensity in the absorbance spectrum. In addition, control oligomer **O6**, which has the same terthiophene chromophore, but lacks the NB group, also has a band at 290−300 nm, indicating that the small peak at 290 nm in the excitation spectrum of O4 is mostly due to direct excitation of the

terthiophene and not the NB moiety. We therefore conclude that energy transfer from the NB groups to the terthiophenes is not highly competitive with other photophysical or photochemical pathways, including bond cleavage, indicating the general applicability of using nitrobenzyl-based photocleavable groups in multichromophoric materials.

3.5 NB Cleavage

As we have observed in previous studies of conjugated small molecules bound to nitrobenzyl groups,[22,29] we found that fluorescence emission intensity from the terthiophene of **O4** in solution increased upon irradiation with UV light, as shown in Figure 3.1. After irradiation at 365 nm for 3 minutes in CH_2Cl_2, the emission intensity of the sample increased 3-fold. This observation is consistent with photocleavage of the fluorescence quenching NB groups, as upon their removal from the conjugated terthiophene backbone, the concentrations of any photolysis byproducts in solution are too small for diffusional quenching to compete with the unimolecular relaxation of the terthiophene excited states.

One of our key objectives was to determine the relationship between the structure of the photocleavable NB linkers and the efficiencies of their photocleavage reactions when bound to otherwise identical conjugated terthiophene backbones. We therefore monitored the progress of the photoreaction of each terthiophene oligomer by ^{1}H NMR spectroscopy as a function of the number of photons absorbed from a 200 W Hg/Xe lamp at 365 nm, the flux of which we determined using the potassium ferrioxalate chemical actinometer. As

the reactions proceeded, new resonances corresponding to each terthiophene photoproduct appeared with chemical shifts and multiplicities that matched the resonances observed for the expected terthiophene photoproducts, each of which we synthesized and characterized independently (Figure 3.2). Integrations of the resonances assigned to the starting material and product gave percent conversion.

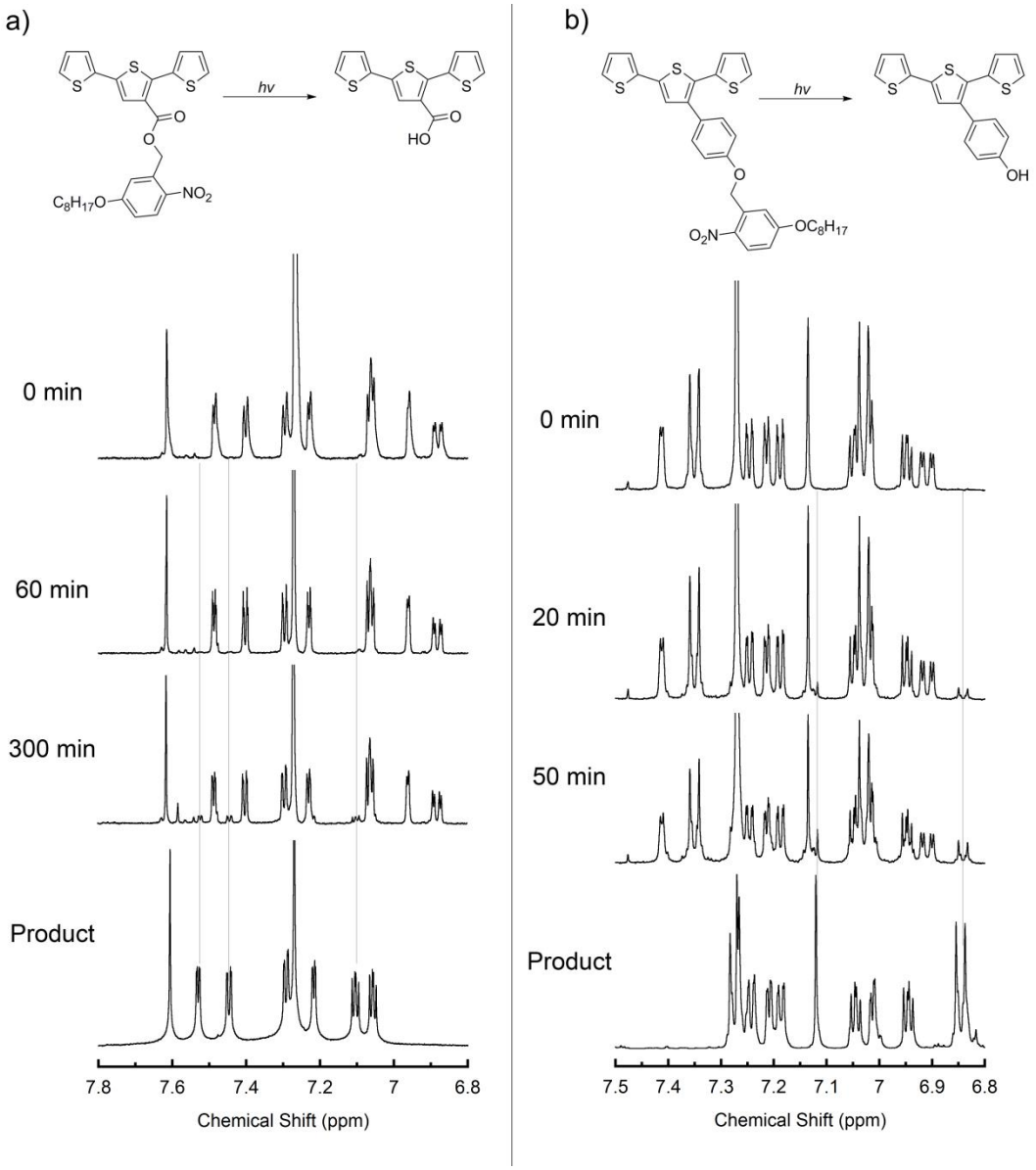

Figure 3.2 NMR spectra from the photolysis of a) **O1** and b) **O3** in $CDCl_3$. Faint vertical lines indicate resonances attributed solely to the terthiophene photoproduct, the integrals of which we used to determine conversion.

Based on our measurements of extinction coefficients of the terthiophene oligomers and model compounds designed to mimic the structures of the NB pendants, the terthiophene chromophores absorb 87–90% of the incident light at 365 nm. Therefore determination of quantum yields required accounting for the percentage of absorbed photons that the nitrobenzyl chromophore absorbed. As samples suitable for NMR spectroscopy were optically dense (OD > 3) at 365 nm, ratios of the extinction coefficients of the oligomeric chromophores and the NB chromophores were sufficient to correct for the competitive absorbance due to the additive nature of the terthiopehene and NB extinction coefficients (See SI). These ratios, combined with the results of chemical actinometry, yielded the rate of photon absorbance of the photocleavable NB pendants.

Table 1 summarizes the quantum yields of photocleavage of the NB groups of **O1**-**O4**. These results are consistent with our expectations detailed in the experimental design section: those structures that yield more stable benzylic radicals upon hydrogen atom abstraction have higher quantum yields of photocleavage than those that yield less stable benzylic radicals. The most dramatic example of this trend is that the NB photocleavage of compound **O4**, which has a methylated nitrobenzyl ether side chain: its photolysis was approximately 18-times more efficient than that of compound **O1**, which has an unmethylated nitrobenzyl ester.

3.6 Photoinduced Film Insolubility

As most applications of conjugated polymers require that they be in the solid state, it is important to understand how structure of the photocleavable groups affects the photo-induced resistance to dissolution of polymer films. Photobleaching, which is often observed upon exposing organic chromophores to light and air simultaneously, is a primary concern in the design of our materials and the execution of these experiments. Addressing this potential problem is an important reason that we focused on thiophene-based polymers, which are known to be relatively resistant to photooxidation.[30] Thin films of our polymers were resistant to photobleaching upon irradiation with UV light under ambient conditions: Figure 3.3 shows that 1-2 nm thick films of **P3** showed less than 7% bleaching of its main absorbance band at 520 nm upon irradiation at 365 nm (39 mW/cm^2, 10 minutes). All polymers described here displayed similar robustness with respect to photobleaching, which we observed during film retention experiments (*vide infra*). Irradiating an identical film of **P3** in an argon atmosphere prevented even this small amount of photobleaching.

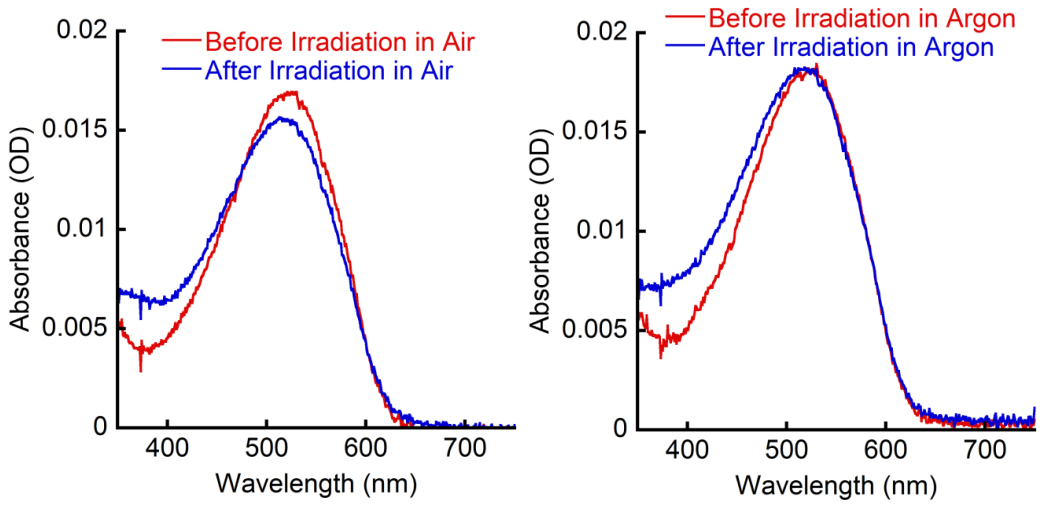

Figure 3.3 Absorbance spectra of films of **P3** before and after 10 minutes of irradiation with a 365 nm spotlight (39 mW/cm^2). The left spectra are from carrying out the irradiation in ambient conditions. The right spectra are from carrying out the irradiation under argon.

Having established the photostability of our materials, we investigated how photocleavable linker structure impacted the efficiency of rendering polythiophene films insoluble with UV irradiation. To do so, we irradiated spun-cast thin films of polymers **P1**-**P4** on glass substrates at 365 nm, followed by rinsing in a bath of $CHCl_3$ for 30 seconds. Comparisons of UV/vis absorbance spectra of films before and after irradiation yielded the degree of photobleaching, while comparisons of spectra before and after rinsing the irradiated films yielded the percent retention of the polymer on the substrate. In all cases, unirradiated spun-cast films were freely soluble in $CHCl_3$.

In agreement with the quantum yields of photocleavage we measured in solution, as well as our expectations based on our experimental design, the solubility of films of polymers with more stable benzylic radical intermediates were more sensitive to UV irradiation than polymers with less stable radical

intermediates. Figure 3.4 shows comparisons that highlights this trend. Results from the thinnest films we prepared (thickness between 3-5 nm) showed that the largest difference of photoinduced insolubility between any two polymers was between **P4** and **P1**: the solubility of **P4**, which has methylated NB ether linkers, decreases significantly faster than that of **P1**, which has unmethylated NB ester linkers, during UV irradiation (Figure 3.4).

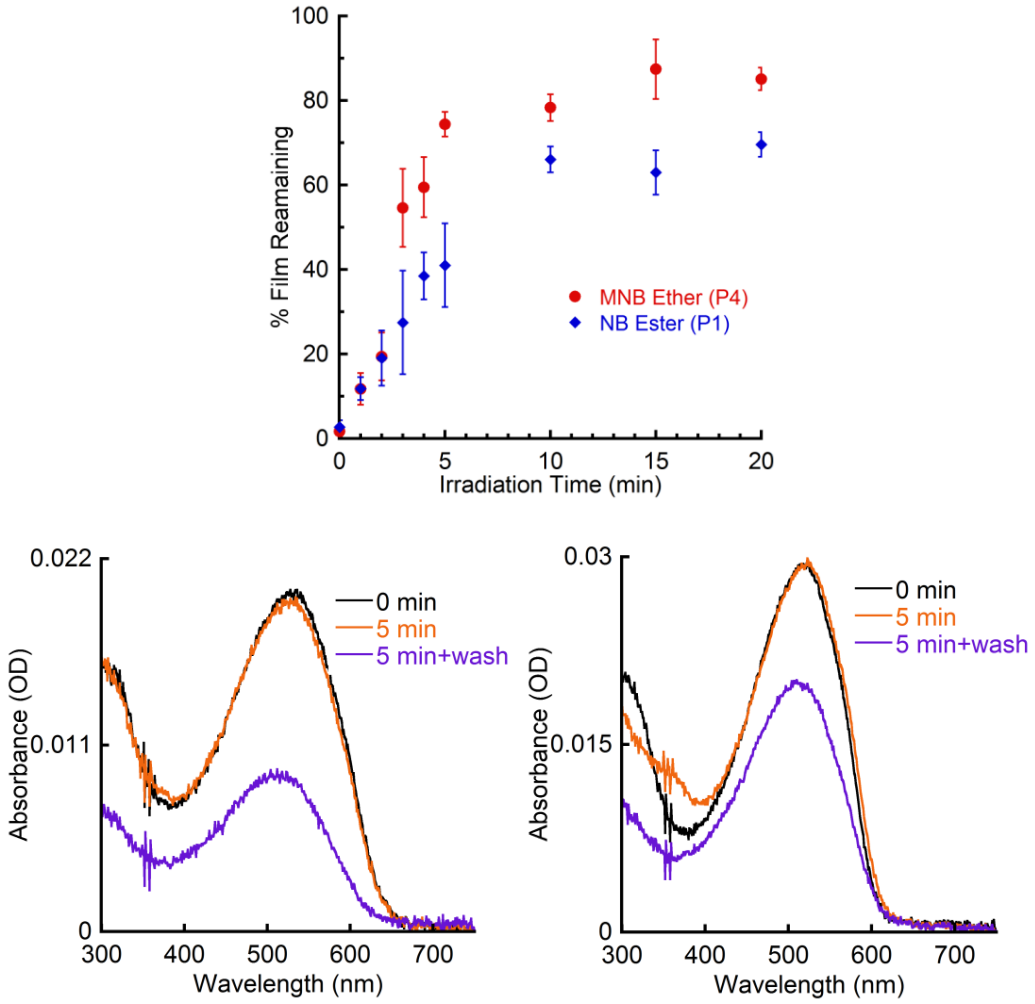

Figure 3.4 Top: Thin film photolysis results for **P1** and **P4**. Three samples of each polymer were made for each irradiation time. These data were then averaged to give the data point and the standard deviation was then used to determine the error bars. Bottom: The absorbance spectra for thin films of **P1** (left) and **P4** (right) for as spun (black), after 5 minutes of irradiation (orange), and after irradiation and $CHCl_3$ wash (purple).

Thicker films showed an even larger difference in photoinduced film retention efficiency, as the comparison of films of **P2** and **P4** in Figure 3.5 shows: after 4 minutes of irradiation followed by rinsing in $CHCl_3$ 3-5 fold more of **P4** is retained in the films. Donor-acceptor polymers **P5** and **P6**, which have NB ether linkers, also showed photoinduced insolubility, with 90% retained of a 27 nm thick film of **P6** after irradiation at 365 nm for 20 minutes and rinsing with $CHCl_3$ (Figure 3.5, Right).

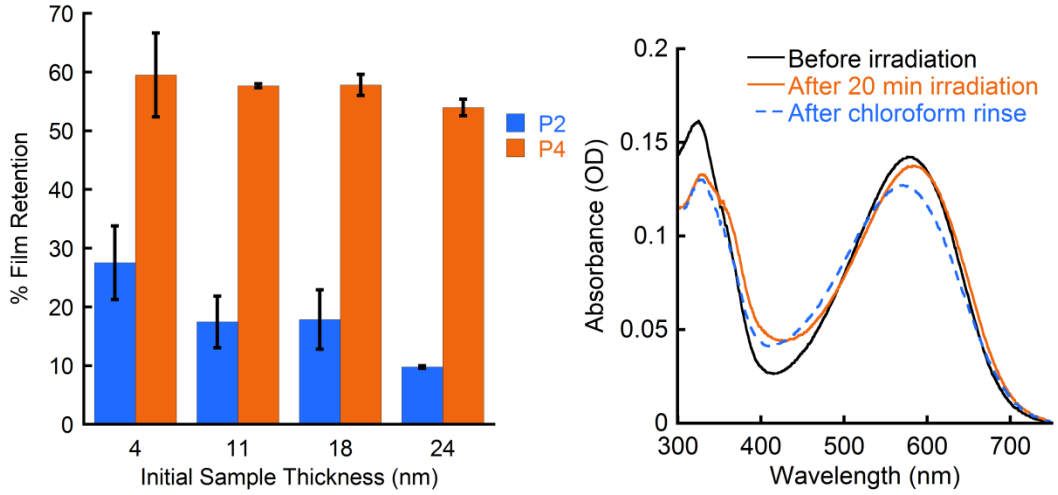

Figure 3.5 *Left*: Film retention of **P2** and **P4** as a function of film thickness under identical irradiation and washing conditions. Each film was irradiated for 4 min and then washed with $CHCl_3$ for 30 s. Film retention was measured by monitoring the change in optical density in peak absorbance. *Right*: The absorbance spectra of a film of **P6** before irradiation (black line), after 20 min of irradiation at 365 nm (orange line), and after washing with chloroform for 30 s (blue dashed line).

Our experiments showed that even after prolonged irradiation times (up to 40 minutes), less than 100% of the polymer film remained after rinsing. UV/vis spectroscopy of the $CHCl_3$ rinsing solution for a film of polymer **P6** that had been irradiated at 365 nm for 20 minutes shows a peak at 325 nm that is due, at least in

part, to the *o*-nitrobenzyl side-chains, and a broad peak with maximum at 565 nm corresponding to the poly(thiophene-*co*-benzothiadiazole) backbone. This peak in the rinsing solution, however, is shifted hypsochromically from the as-synthesized **P6** in $CHCl_3$ by ~16 nm (Figure 3.6).

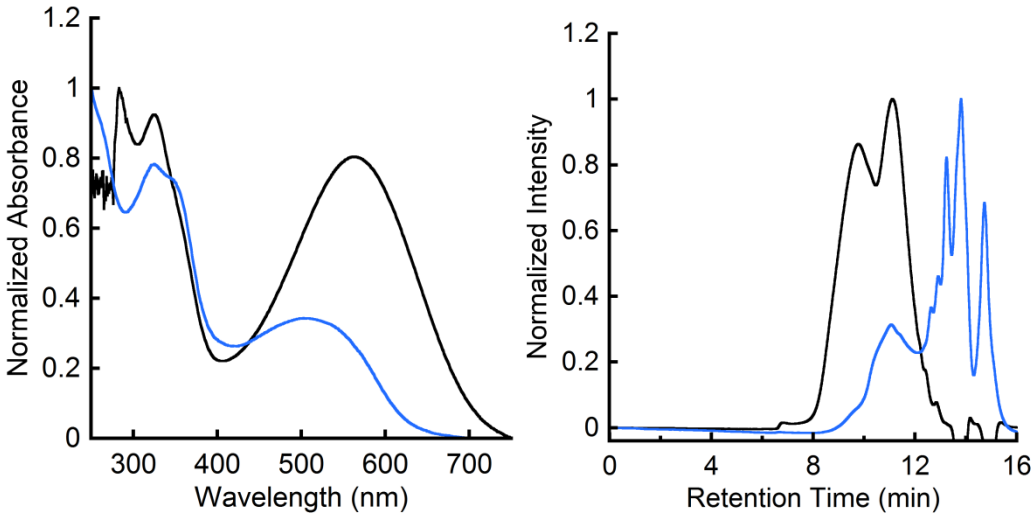

Figure 3.6 *Left:* The normalized absorbance spectra of **P6** in $CHCl_3$ (black) and the rinsing solution from an irradiated film of **P6** (blue). *Right:* The normalized GPC chromatogram for **P6** (black) and its corresponding rinsing solution (blue).

In addition, GPC analysis of the rinsing solution shows low molecular weight polymer chains and small molecule byproducts of photolysis, with less contribution from higher molecular weight chains of the as-synthesized sample of **P6** used to prepare the films. This evidence indicates that some shorter polymer chains remain soluble, even upon NB photolysis, and their dissolution is a primary cause for the 10–20% decrease in absorbance upon rinsing of irradiated films.

3.7 Photopatterning of Conjugated Polymer Films

The patterning of electronically active materials, using photolithography as a key step, is a cornerstone technology of the electronics industry. Conjugated polymers that show light-sensitive solubility open the possibility of semiconducting organic materials that can form intricate patterns easily and directly with minimal additional processing steps.[15,16] Our approach of photocleavage of solubilizing chains enables conjugated polymers to be used as negative photoresists. A cartoon depicting this approach can be seen in Figure 3.7.

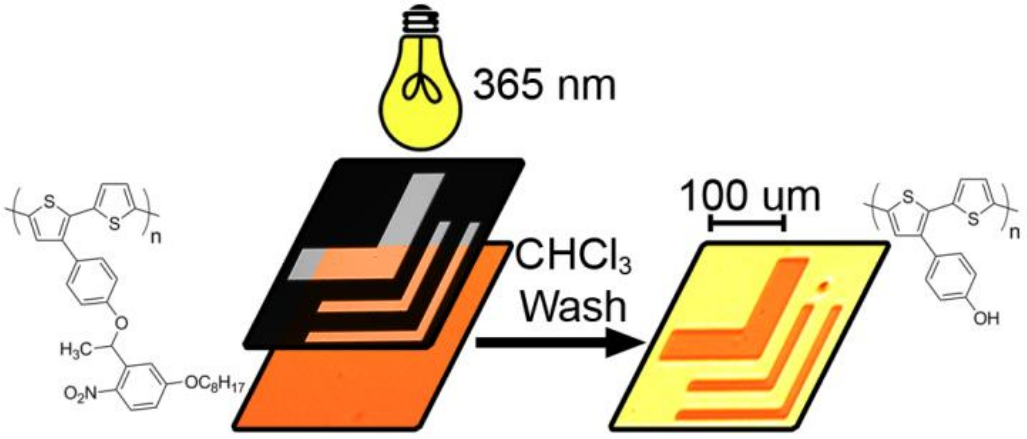

Figure 3.7 A cartoon depicting the process of photopatterning **P4**. First a film of **P4** is spun, and then exposed to 365 nm light through a photomask. This irradiation renders the exposed areas insoluble. The unexposed areas can then be removed with a chloroform wash.

Irradiation of a 23 nm thick of **P4** at 365 nm (34 mW/cm^2) for 20 minutes through a chrome photomask followed by rinsing with $CHCl_3$ for 30 seconds yielded a pattern of conjugated polymer: those areas of polymer film exposed to light remained on the substrate, while those polymers in areas shielded by the mask dissolved. Although imperfections such as rounded corners indicate room for improvement of photolithographic conditions, our non-optimized patterning

procedure could resolve features on the order of 10 μm. Figure 3.8 shows typical results of a photopatterning experiment with polymer **P4**.

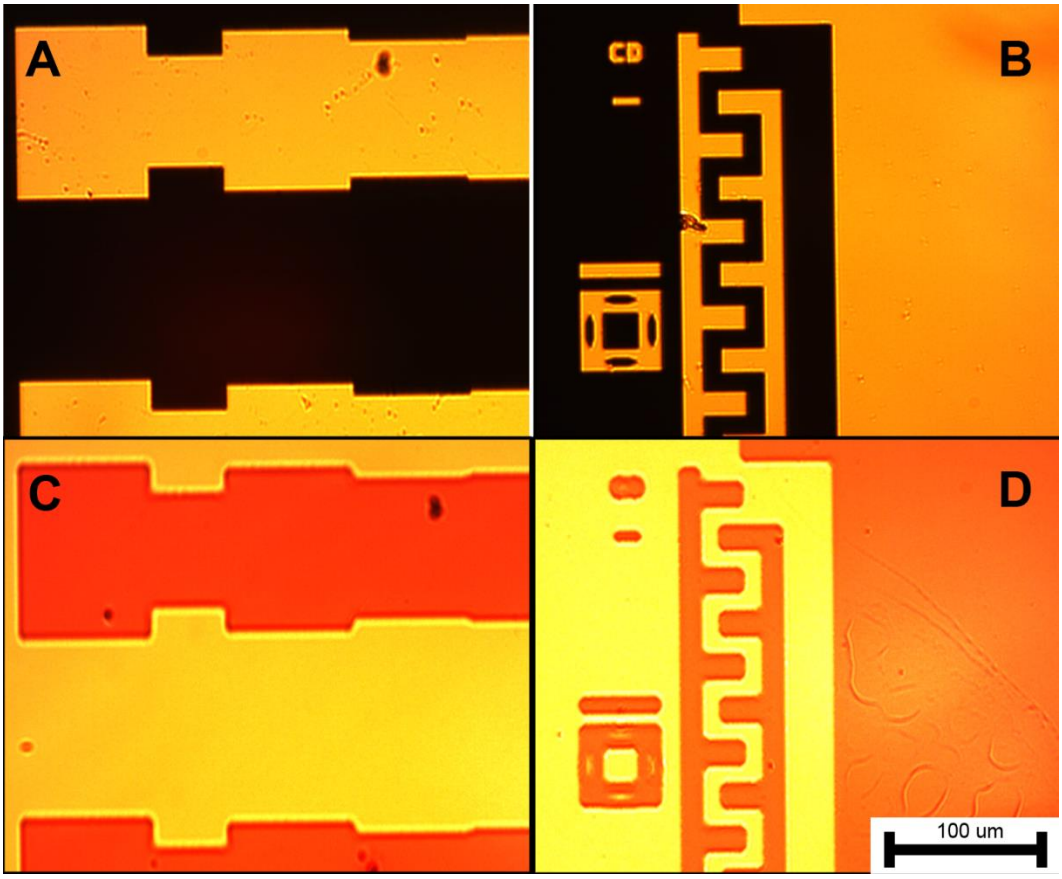

Figure 3.8 Optical microscopy images of a photomask (A and B) and images of films of **P4** photopatterned using the photomask (C and D).

3.8 Multi-layer Films Enabled By Photoinduced Insolubility

Most reported conjugated polymers are soluble in the same group of moderately polar organic solvents. This shared characteristic presents a challenge for using solution-based processes to fabricate films with multiple layers, which organic photovoltaics (OPVs) and organic light emitting devices (OLEDs) often require. The capability to render a solution-cast conjugated polymer film

insoluble in a post-deposition processing step, such as with photochemical crosslinking,[31] or photochemical acid generation leading to a change in polymer solubility,[32] can allow for the preparation of multilayer films from solution while only minimally disturbing previously deposited layers.

Figure 3.9 illustrates the capability of our approach to yield multilayer films with all solution-based processing. We first performed multiple spin-casting steps of a solution of **P6** in $CHCl_3$ onto a glass substrate without any irradiation in between deposition steps. The absorbance of the film did not increase significantly upon spin-casting additional polymer after deposition of the initial film, as the solvent used during each spin-casting step dissolved the previously deposited film. We irradiated the film with 365 nm light (34 mW/cm^2) for ten minutes after the fourth deposition step, which resulted in a decrease of intensity and bathochromic shift of the UV-absorbing band, consistent with cleavage of the NB groups, but no significant change in the band in the visible region of the spectrum, which indicated minimal photobleaching of the conjugated poly(thiophene-*co*-benzothiadiazole) backbone. A subsequent spin casting step of **P6** under identical conditions as used in the first four deposition steps increased the thickness of the film from 38 nm to 62 nm. Rinsing that film with $CHCl_3$ confirmed that this increase in thickness was due to light-induced insolubility of the irradiated film, as the absorbance spectrum of the resultant, thinner film closely resembled that observed after irradiation of the previously deposited film.

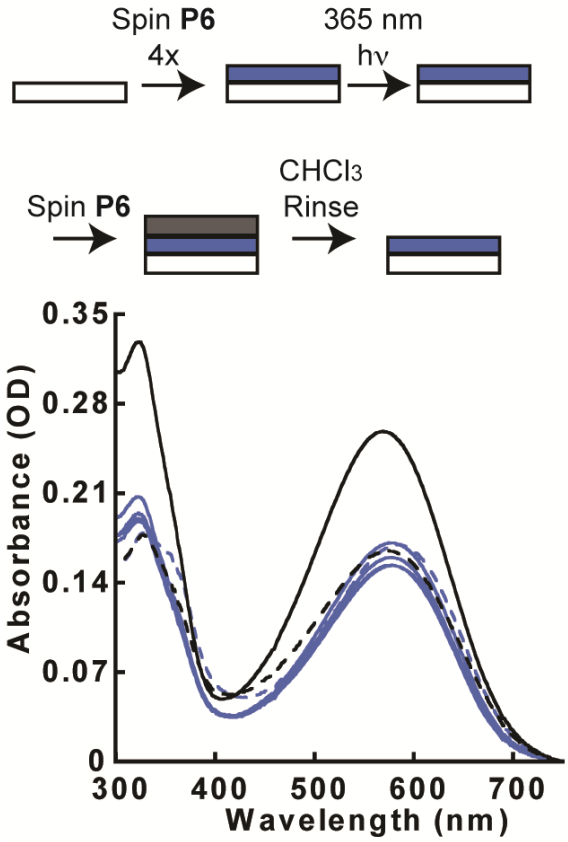

Figure 3.9 Thin film multilayer experiment without irradiation until after spinning **P6** onto the substrate four times.

We could repeat this process multiple times with either the same polymer (**P6**, with final thickness of 11 nm), which has potential utility in the fabrication of thicker films with polymers that have limited solubility (Figure 3.10, Left), or switch between photoreactive polymers that have different optoelectronic properties between deposition/irradiation steps (Figure 3.10, Right; alternating layers of **P4** and **P6**, with final thickness of 90 nm).

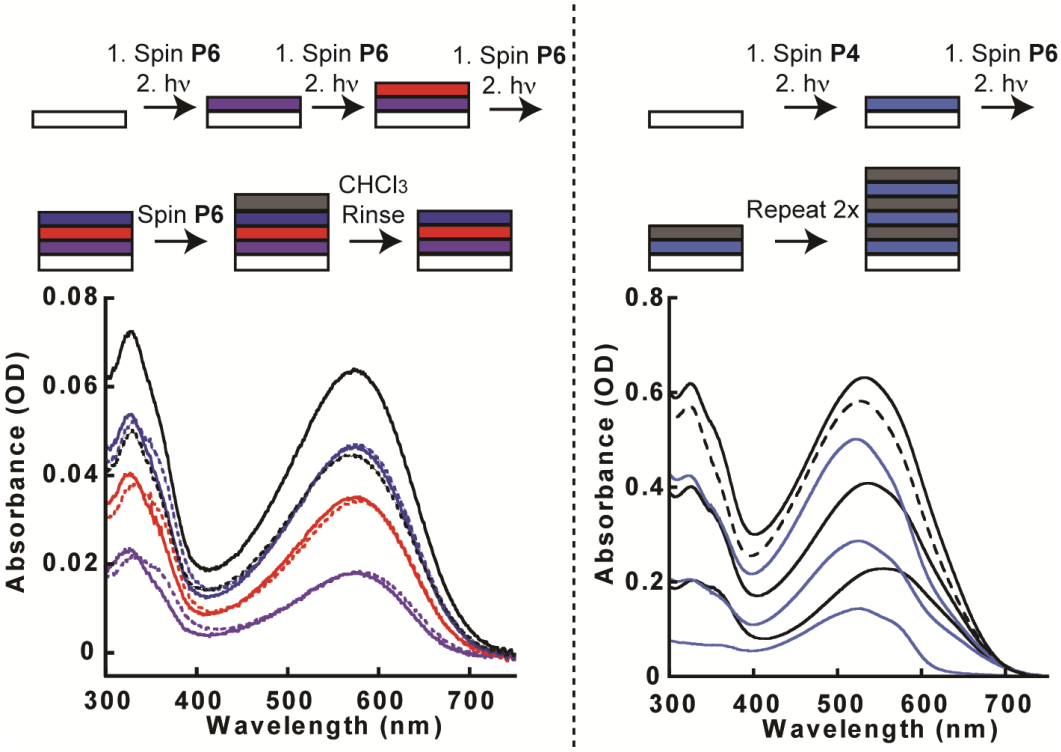

Figure 3.10 Multilayer deposition experiments: *Left:* Thin film multi-layer of **P6** made by sequentially spin coating and irradiating layers for the first three deposition steps. The fourth layer was deposited and then washed away without irradiation, demonstrating the necessity of UV irradiation to retain the film on the substrate. *Right:* Multilayer film made from alternating deposition of **P4** (blue lines) and **P6** (black lines). Each layer was spun on top of the previous layer after a 10 min irradiation at 365 nm. After the final layer was deposited, it was not irradiated and the layer was washed away with chloroform to give the final spectrum (black dashed line).

3.9 Fabrication and Evaluation of Organic Thin Film Transistor Devices

To probe carrier transport properties, p-type thin film organic thin film transistor (OTFT) devices incorporating polymers **P1**, **P2**, **P5**, and **P6** were made by Dianne M. Meyer and Deepak Shukla using the bottom-gate, top-contact geometry, in which heavily doped silicon (resistivity 0.005 – 0.025 Ω-cm) substrate served as the gate electrode. The gate dielectric was a thermally grown SiO_2 layer with a thickness of 190 nm modified with hexamethyldisilazane

(HMDS). **P1**, **P5**, and **P6** showed typical p-type field effect operation with excellent output and transfer characteristics. Representative output characteristics (drain current (I_{SD}) versus source-drain voltage (V_{DS}) curves at different gate voltages (V_{GS})) and transfer characteristics (I_{SD} vs V_{GS} plotted on a logarithmic scale and $(I_{SD})^{1/2}$ vs V_{GS}, at V_{DS} = 100 V) of the transistors based on **P1** at 25 ^{o}C are shown in Figure 3.11.

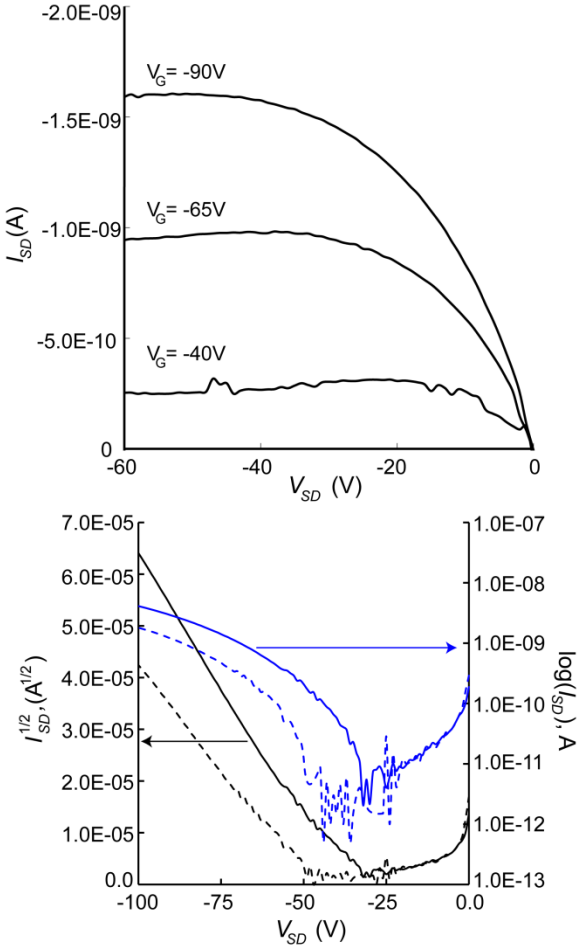

Figure 3.11 I-V characteristics of exemplary OTFT devices based on **P1** coated on HMDS-treated SiO_2/Si substrate with 150 mm channel length and 1000 mm channel width: (a) The output curves at gate voltages VG = – 40, – 65 , and – 90 V. (b) Transfer characteristics, before irradiation (solid lines) and after irradiation and rinsing (dashed lines) for the same device at V_{DS} = – 100 V. All OTFT fabrication and characterization was carried out by Dianne M. Meyer and Deepak Shukla.

For a device with 150 μm channel length (L) and 1000 μm channel width (W), a saturation regime hole mobility of 2.6 (± 0.05) x 10^{-5} $cm^2V^{-1}s^{-1}$ and V_{th} of 52 V and current on/off ratio of 4.5 ×10^3 was extracted for V_{DS} = – 100V. These devices exhibit low contact resistance and as a consequence saturation mobility does not decrease significantly with decreasing channel length. The electrical performance of polymers **P5** and **P6** were similar to **P1** (Table 3.3).

Table 3.3 The characteristics of the transistors fabricated using **P1**, **P6**, and **P5**. All OTFT characterization was carried out by D. M. Meyer and D. Shukla.

		Mobility $cm^2/V.s$	**V_{th}, V**	**I^{on}/I^{off}**
P1	Before Irradiation	2.6 x 10^{-5}	52	10^3
	After Irradiation	1.6 x 10^{-5}	50	10^3
P6	Before Irradiation	3.8 x 10^{-5}	58	10^3
	After Irradiation	1.6 x 10^{-5}	57	10^2
P5	Before Irradiation	2.1 x 10^{-5}	64	10^3

Polymer **P2** did not show any measurable hole mobility in this device architecture, to which impurities in the polymer sample may be a contributing factor. We also compared electrical performance of our polymers with commercially available regioregular P3HT (Aldrich), which showed higher carrier mobility (ca 10^{-3} $cm^2V^{-1}s^{-1}$) than our polymers. Preliminarily, we attribute these differences in mobility in part to higher crystallinity of P3HT, due to the lack of regioregularity and relatively low molecular weights of polymers described in this chapter.

Importantly, the electrical performance of **P1** and **P6** did not degrade significantly after the polymers were exposed to light and rinsed with chloroform

(Figure 3.11, Table 3.3). For example, OTFT devices made with **P1** after exposure to light and rinsing with chloroform did not show any significant change in electrical performance or drop in carrier mobility. Thus, for devices with W = 1000 μm and L = 100 μm, saturation mobility $\mu = 1.6 (\pm 0.05) \times 10^{-5}$ cm^2 V^{-1} s^{-1} was only slightly lower than for devices before irradiation and rinsing.

3.10 Conclusions

This work demonstrates that photocleavable solubilizing side chains can give conjugated polymers the properties of negative photoresists, enabling photopatterning and the fabrication of multilayer films using solution processing. Our observations that photolysis of NB groups need not cause significant photobleaching or complete disruption of the charge transport properties of these materials supports the potential applicability of this approach. Photocleavable side chains generally have the advantages that they neither require the addition of additional compounds in formulations such as photoacid or photobase generators, nor do they depend on degradation of the conjugated backbone. The NB photocleavable moiety has a number of specific advantages in this context: (i) their photolysis efficiencies are not affected significantly by potential energy transfer deactivation pathways to the conjugated material, (ii) they have tunable sensitivity to light through controlling the stabilization of the intermediate benzylic radicals, (iii) their functionalization and installation is straightforward, and (iv) they do not require highly hydrophilic environments to cleave efficiently. Primary impediments to the eventual success of this approach include the

presence of potentially deleterious photolysis byproducts, and the creation of voids within films. Questions this work has not addressed are the potential role of minor extents of photoinduced crosslinking of polymer chains in the thin films due to radical intermediates of NB photolysis, or the sharpness of the interfaces between different polymers in multilayer films, but we anticipate that the degree of interpenetration of polymers may be tunable based on the extent of photolysis. Current work in our laboratory is focused on expanding the classes of monomers that incorporate photocleavable solubilizing chains, as well as the development of conjugated polymers that behave as positive-tone photoresists, which could overcome the challenges described here.

3.11 Experimental Considerations

All synthetic manipulations were performed under standard air-free conditions under an atmosphere of argon gas with magnetic stirring unless otherwise mentioned. Flash chromatography was performed using silica gel (230-400 mesh) as the stationary phase. NMR spectra were acquired on a Bruker Avance III 500 or Bruker DPX-300 spectrometer. Chemical shifts are reported relative to residual protonated solvent (7.27 ppm for $CHCl_3$). High-resolution mass spectra (HRMS) were obtained at the MIT Department of Chemistry Instrumentation Facility using a peak-matching protocol to determine the mass and error range of the molecular ion. All reactants and solvents were purchased from commercial suppliers and used without further purification, unless otherwise noted.

All solution optical spectra were acquired of samples in quartz cuvettes (NSG Precision Cells). Electronic absorbance spectra were acquired with a Varian Cary-100 instrument in double-beam mode using a solvent-containing cuvette for background subtraction spectra. Fluorescence emission spectra were obtained by using a PTI Quantum Master 4 equipped with a 75 W Xe lamp. All fluorescence spectra are corrected for the output of the lamp and the dependence of detector response to the wavelength of emitted light. Fluorescence spectra were acquired using sample absorbances less than 0.1 OD. Fluorescence quantum yields were determined relative to Coumarin 6 in ethanol. Molecular weight distribution measurements of the polymers were conducted with a Shimadzu Gel Permeation Chromatography (GPC) system equipped with a Tosoh TSKgel GMHhr-M mixed-bed column and guard column (5 μm), in addition to both UV and refractive index detectors. The column was calibrated with low polydispersity poly(styrene) standards (Tosoh, PSt Quick Kit) with THF as the mobile phase eluting at 0.75 mL/min. Irradiations of samples to cleave nitrobenzyl ester groups were performed with a 200W Hg/Xe lamp (Newport-Oriel) equipped with a condensing lens, recirculating water filter, manual shutter, and a 365 nm interference filter (Semrock) in the light path. Thin films were fabricated using chloroform solutions of **P1**-**P6** (1–10 mg/mL) that were spun-cast onto glass cover slips using a Laurell Technologies Corporation spin coater (Model WS-400E-6NPP-Lite) at 3000 rpm for 1 minute for thinner films and 1000 rpm for 1 minute for thicker films.

Film thickness was characterized on an Asylum Research MFP-3D-Bio Atomic Force Microscope (Asylum Research, Santa Barbara, CA) in tapping mode using AC160TS-R3 silicon cantilevers (Asylum Research, Santa Barbara, CA) and analyzed in Igor Pro 6.35A5 (Wavemetrics, Lake Oswego, OR, USA). AFM measurements were carried out by Marc G. Simon and Christian Staii. Each film was scratched with a sharp razor to expose the glass surface before scanning. The scratch was visually located and aligned with the cantilever using the AFM top-down camera and followed by a 5x5 μm^2 scan. The AFM measurements were repeated ten times for each film, in different locations. RMS roughness values were calculated from the AFM scan data using Asylum Research MFP3D (Igor Pro.). The film thickness was measured by finding the vertical distance between the exposed glass surface and film surface. Three samples of varying thickness were measured for each polymer. The resulting linear correlations between thickness measured by AFM and absorbance measured by UV/vis spectrophotometry enabled the use of UV/vis to determine approximate film thicknesses. AFM images of **P4** can be seen in Figure 3.12.

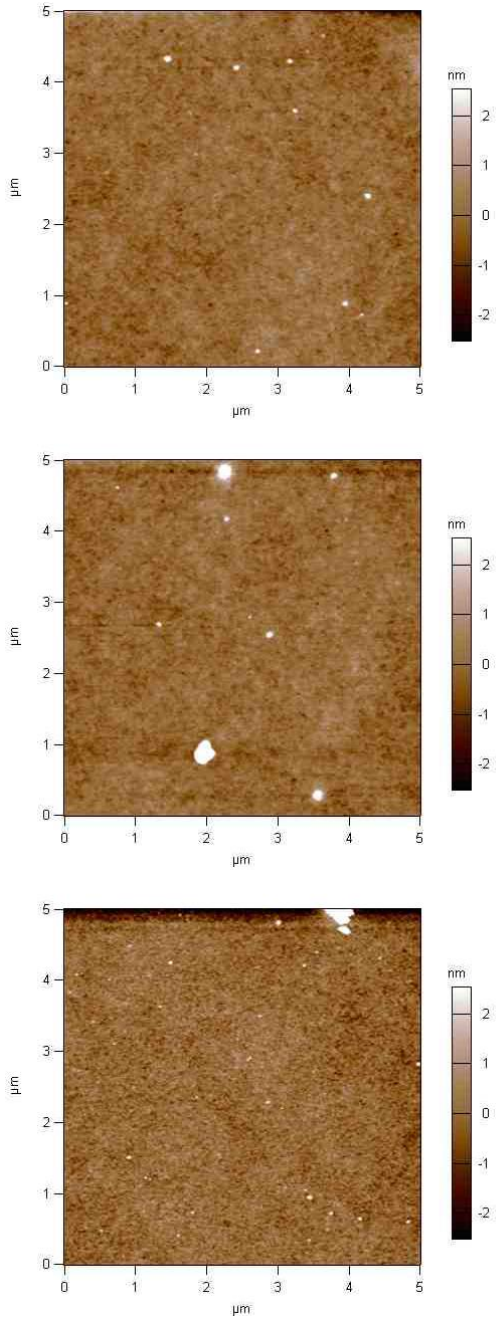

Figure 3.12 Atomic force microscopy images of a film of **P4** before irradiation (top: RMS roughness = 0.3 nm, thickness = 33 nm), after irradiation (middle: RMS roughness = 0.3 nm, thickness = 23 nm), and after chloroform wash (bottom: RMS roughness = 0.4 nm, thickness = 16 nm). AFM images were obtained by Marc G. Simon and Christian Staii.

Fabrication and Characterization of Transistors

Si/SiO_2 wafers were cleaned by immersion in a piranha solution (a mixture of 7:3 (*v/v*) of 98% H_2SO_4 and 30% H_2O_2) for 20 min. at 70 °C. The wafers were then removed from the piranha solution and rinsed five to six times with copious amounts of deionized water. Wafers were blown dry with nitrogen and used immediately. On a clean wafer 90% HMDS solution in toluene (v/v) was spin coated at 4000 rpm for 20 seconds and then heated on a hot plate set at 140°C for 45 minutes. Wafers were cooled and washed in toluene with ultrasonification for 10 minutes followed by washing with ethanol and deionized water. Wafers were then dried with argon and placed on hot plate for 30 minutes at 75°C to remove any excess moisture. Water contact angle after for SiO_2 layer after HDMS treatment increased from ~1° to 60° indicating silanization of SiO_2 surface.

Two samples of 1 wt% solutions of polymers were coated at 3000RPM for 25 s. One of the samples was irradiated for 3 minutes using a 1000W Hg-Xe lamp at 365 nm. The sample was then rinsed gently with chloroform. The samples were annealed for 30 minutes at 70 °C. Gold (Au) source and drain electrodes (60 nm thick, 500 mm × 1000 mm wide) were thermally evaporated through a shadow mask on the organic semiconductor layer. Electrical characterization of the fabricated devices was performed with a Hewlett Packard HP 4145b® parameter analyzer. All measurements were done under ambient atmosphere. The devices were exposed to air prior to testing. For each experiment performed, between 2

and 8 individual devices were tested on each sample prepared, and the results were averaged. For each device, the source-drain current (I_{SD}) was measured as a function of source-drain voltage (V_{SD}) for various values of gate voltage (V_G). For most devices, V_{SD} was swept from 0 V to –100 V for each of the gate voltages measured, typically –40 V, –65 V, and –90 V. In these measurements, the gate current (I_G) was also recorded in order to detect any leakage current through the device. Furthermore, for each device the drain current was measured as a function of gate voltage for various values of source-drain voltage. For most devices, V_G was swept from 0 V to –100 V for each of the drain voltages measured, typically −50 V, −75 V, and −100 V . The saturation field effect mobility, μ_{sat}, was extracted from a straight-line fit to the linear portion of the $\sqrt{I_D}$ versus V_G curve according to the following equation:

$$I_{SD}=C_i\,\mu\,(W/2L)(V_{GS}-V_T)^2$$

Where I_{SD} is the drain current, C_i is the capacitance per unit area of the gate dielectric layer, and V_{GS} and V_T are the gate voltage and threshold voltage, respectively. The threshold of the device was determined from the relationship between the square root of I_D at the saturated regime, and V_{GS} was determined by extrapolating the measured data to $I_{SD} = 0$.

Synthesis and Characterization

2-Nitro-5-(octyloxy)benzaldehyde (1). A round bottom flask was charged with 5-hydroxy-2-nitrobenzaldehyde (5.00 g, 30. mmol) and potassium carbonate (12.4 g, 89.8 mmol). The flask was evacuated and refilled with argon three times.

Under argon flow, 100 mL of dimethyl formamide (DMF) and 1-bromooctane (7.8 mL, 8.7 g, 45 mmol) were added. The mixture was left to stir overnight at 50 °C. The reaction mixture was poured into 1M NaOH (1×100 mL) and extracted with diethyl ether (3×100 mL). The combined organic layers were then washed with saturated aqueous $NaHCO_3$ (1×100 mL), deionized (DI) water (1×100 mL), and brine (1×100 mL). Drying over $MgSO_4$ and removal of solvent *in vacuo* gave the crude product **1** as a yellow-orange solid. Flash chromatography on silica using 2:1 hexanes:CH_2Cl_2 as eluent gave 8.35 g of **1** (99 %) as a pale yellow solid. This compound has been reported.[22] Mp: 55-56 °C. ^{1}H NMR ($CDCl_3$, 500 MHz): δ 10.49 (s, 1H), 8.16 (d, *J* = 9 Hz, 1H), 7.31 (d, *J* = 3 Hz, 1H), 7.14 (dd, *J* = 9 Hz, 3 Hz, 1H), 4.10 (t, *J* = 7 Hz, 2H), 1.83 (m, 2H), 1.50-1.44 (m, 2H), 1.38-1.30 (m, 8H), 0.91-0.88 (m, 3H). ^{13}C NMR ($CDCl_3$, 125 MHz): δ 188.6, 163.7, 142.0, 134.4, 127.2, 118.9, 113.7, 69.4, 31.8, 29.2, 29.2, 28.9, 25.8, 22.6, 14.1. HRMS calcd for $C_{15}H_{21}NO_4$ $(M+Na)^+$, 302.1363, found, 302.1370.

(2-Nitro-5-(octyloxy)phenyl)methanol (2). A round bottom flask was charged with **1** (8.35 g, 29.9 mmol), and $NaBH_4$ (1.78 g, 44.8 mmol). The flask was evacuated and refilled with argon three times. Under argon flow, 200 mL of methanol (MeOH) was added. The reaction was left to stir overnight at room temperature. The reaction mixture was poured into DI water (1 × 100 mL) and brine (1 × 100 mL), and extracted with diethyl ether (3 × 100 mL). The combined organic layers were dried over $MgSO_4$ and solvent was removed *in vacuo* to give the crude product **2** as a yellow solid. Recrystallization of the crude solid from

ethanol/water gave 5.88 g of **2** (70 %) as feathery yellow crystals. This compound has been reported previously.[22] Mp: 50-52 °C. ^{1}H NMR ($CDCl_3$, 500 MHz): δ 8.19 (d, *J* = 9 Hz, 1H), 7.20 (d, *J* = 2.5 Hz, 1H), 6.89 (dd, *J* = 2.5 Hz, 9 Hz, 1H), 4.99 (s, 2H), 4.08 (t, *J* = 6.5 Hz, 2H), 2.58 (s, 1H), 1.83 (m, 2H), 1.48-1.44 (m, 2H), 1.35-1.30 (m, 8H), 0.91-0.88 (m, 3H). ^{13}C NMR ($CDCl_3$, 125 MHz): δ 163.9, 140.3, 140.1, 128.0, 114.6, 113.5, 68.9, 63.0, 31.8, 29.2, 29.2, 29.0, 25.9, 22.6, 14.0. HRMS calcd for $C_{15}H_{23}NO_4$ $(M+Na)^+$, 304.1519, found, 304.1531.

2-Nitro-5-(octyloxy)benzyl 2,5-dibromothiophene-3-carboxylate (3). A round bottom flask was charged with **2** (492 mg, 1.75 mmol), 2,5-dibromothiophene-3-carboxylic acid (500 mg, 1.75 mmol), and DMAP (214 mg, 1.75 mmol). The flask was evacuated and refilled with argon three times. Under argon flow, 40 mL of anhydrous CH_2Cl_2, and *N*,*N*′-dicyclohexylcarbodiimide (DCC) (361 mg, 1.75 mmol) dissolved in 10 mL of anhydrous CH_2Cl_2 were added. The reaction was left to reflux overnight. The reaction mixture was washed with 5% aqueous HCl (2×40 mL), saturated $NaHCO_3$ (2×40 mL), and DI water (2×40 mL). Drying over $MgSO_4$ and removal of solvent *in vacuo* gave the crude product **3**. Flash chromatography on silica using 1:1 hexanes:CH_2Cl_2 as eluent gave 414 mg of **3** (43 %) as a colorless solid. This compound has been reported previously.[22] Mp: 73-76 °C. ^{1}H NMR ($CDCl_3$, 500 MHz): δ 8.22 (d, *J* = 9 Hz, 1H), 7.42 (s, 1H), 7.12 (d, *J* = 2.5 Hz, 1H), 6.92 (dd, *J* = 2.5 Hz, 9 Hz, 1H), 5.76 (s, 2H), 4.05 (t, *J* = 6.5 Hz, 2H), 1.82 (quintet, *J* = 7 Hz, 2H), 1.48-1.42 (m, 2H), 1.37-1.29 (m, 8H), 0.91-0.88 (m, 3H). ^{13}C NMR ($CDCl_3$, 125 MHz): δ 163.5, 160.1, 140.1, 134.8,

131.8, 131.3, 128.1, 119.8, 114.7, 113.4, 111.8, 69.0, 64.1, 31.8, 29.2, 29.2, 28.9, 25.9, 22.6, 14.1. HRMS calcd for $C_{20}H_{23}Br_2NO_5S$ $(M+Na)^+$, 571.9544, found, 571.9548.

2-nitro-5-(octyloxy)benzyl 2,5-bis(2-thienyl)-3-thenoate (O1). A round bottom flask was charged with **3** (150 mg, 0.27 mmol), and $Pd(PPh_3)_4$ (16 mg, 0.014 mmol). The flask was evacuated and refilled with argon three times. Under argon flow, 20 mL of anhydrous DMF was added. 2-(tributylstannyl) thiophene (224 mg, 0.19 mL, 0.60 mmol) was added via syringe. The reaction was heated to 90 °C and left stirring for 18 hours. The reaction mixture was poured into DI H_2O (1 × 200 mL) and extracted with diethyl ether (5 × 50 mL). The combined organic layers were dried over $MgSO_4$ and solvent was removed *in vacuo* to give the crude product **O1** as a yellow solid. Flash chromatography on silica using 2:1 hexanes:CH_2Cl_2 as eluent gave 125 mg of **O1** (83 %) as a bright yellow solid. Mp: 103-105 °C. ^{1}H NMR ($CDCl_3$, 500 MHz): 8.20 (d, *J* = 9 Hz, 1H), 7.61 (d, *J* = 0.5 Hz, 1H), 7.49 (d, *J* = 3.5 Hz, 1H), 7.40 (d, *J* = 5.5 Hz, 1H), 7.30 (d, *J* = 5 Hz, 1H), 7.23 (d, *J* = 3.5 Hz, 1H), 7.06 (m, 2H), 6.96 (d, *J* = 2.5 Hz, 1H), 6.88 (dd, *J* = 2.5 Hz, 9 Hz, 1H), 5.75 (s, 2H), 3.99 (t, *J* = 6.5 Hz, 2H), 1.79 (quintet, *J* = 7 Hz, 2H), 1.65 (m, 1H), 1.30 (m, 9H), 0.89 (t, *J* = 6.5 Hz, 3H). ^{13}C NMR ($CDCl_3$, 125 MHz): δ 163.6, 162.0, 142.4, 135.7, 135.7, 135.4, 133.3, 129.5, 128.1, 128.0, 128.0, 127.4, 127.3, 126.0, 125.5, 124.6, 113.9, 113.3, 68.9, 63.6, 31.8, 29.3, 29.2, 28.9, 25.9, 22.6, 14.1. HRMS calcd for $C_{28}H_{29}NO_5S_3$ $(M+NH_4)^+$, 573.1546, found, 573.1561.

Poly((2-nitro-5-(octyloxy)benzyl)thiophene-3-carboxylate)-*co*-thiophene (P1). A round bottom flask was charged with **3** (120 mg, 0.22 mmol), tri(*o*-tolyl)phosphine (33 mg, 0.11 mmol), and $Pd_2(dba)_3$ (10 mg, 0.011 mmol). The flask was evacuated and refilled with argon three times. Under argon flow, a solution of 2,5-bis(trimethylstannyl)thiophene (89 mg, 0.22 mmol) in 5 mL of anhydrous toluene was added. The reaction mixture was left to reflux for 72 h. Upon completion, the reaction mixture was added dropwise to MeOH to precipitate the polymer. After centrifugation, the solvent was removed *in vacuo* to give 77 mg of **P1** (75 %) as a purple/brown solid. This polymer has been reported previously.[22] GPC: M_n = 18,400, PDI = 1.20. ^{1}H NMR ($CDCl_3$, 500 MHz): δ 8.20-8.19 (1H), 7.70-7.50 (1H), 7.50-7.35 (1H), 7.20-7.10 (1H), 7.10-7.00 (1H), 6.90-6.80 (1H), 5.80-5.70 (2H), 4.10-3.90 (2H), 1.80-1.70 (2H), 1.45-1.35 (2H), 1.35-1.10 (8H), 0.70-1.00 (3H).

1-(2-nitro-5-(octyloxy)phenyl)ethanol (4). A round bottom flask was evacuated and refilled with argon three times. The flask was charged with 40 mL of anhydrous diethyl ether and cooled to -78 °C. $TiCl_4$ (0.12 mL, 1.0 mmol) was added via syringe, followed by the addition of 3.0 M CH_3MgBr in anhydrous diethyl ether (0.35 mL, 1.1 mmol). The solution was left to stir for 30 minutes at -78 °C. **1** (223 mg, 0.80 mmol) was then added and the reaction was left to stir for 3 hours while the reaction gradually warmed to room temperature. The reaction mixture was poured into DI H_2O (1 × 200 mL) and extracted with diethyl ether (3

× 100 mL). The combined organic layers were dried over $MgSO_4$ and solvent was removed *in vacuo* to give 223 mg of **4** (95 %) as a brown oil that was used without further purification. ^{1}H NMR ($CDCl_3$, 500 MHz): δ 8.04 (d, *J* = 9 Hz, 1H), 7.31 (d, *J* = 2.5 Hz, 1H), 6.84 (dd, *J* = 2.5 Hz, *J* = 9 Hz, 1H), 5.56 (q, *J* = 6.5 Hz, 1H), 4.06 (t, *J* = 6.5 Hz, 2H), 2.35 (s, 1H), 1.82 (m, 2H), 1.56 (d, *J* = 6.5 Hz, 3H), 1.49-1.44 (m, 2H), 1.35-1.30 (m, 8H), 0.91-0.88 (m, 3H). ^{13}C NMR ($CDCl_3$, 125 MHz): δ 163.6, 144.7, 140.3, 127.6, 113.4, 112.5, 68.8, 66.0, 31.8, 29.3, 29.2, 29.0, 25.9, 24.1, 22.6, 14.1.

1-(2-nitro-5-(octyloxy)phenyl)ethyl 2,5-dibromothiophene-3-carboxylate (5). A round bottom flask was charged with **4** (195 mg, 0.66 mmol), 2,5-dibromothiophene-3-carboxylic acid (189 mg, 0.66 mmol), and DMAP (81 mg, 0.66 mmol). The flask was evacuated and refilled with argon three times. Under argon flow, *N*,*N*′-dicyclohexylcarbodiimide (DCC) (136 mg, 0.66 mmol), dissolved in 20 mL of anhydrous CH_2Cl_2, was added. The reaction was left to reflux overnight. The reaction mixture was washed with 5% aqueous HCl (2×40 mL), saturated $NaHCO_3$ (2×40 mL), and DI water (2×40 mL). Drying over $MgSO_4$ and removal of solvent *in vacuo* gave the crude product **5** as a pale yellow solid. Flash chromatography on silica using 1:1 hexanes:CH_2Cl_2 as eluent gave 188 mg of **5** (50 %) as a colorless solid. ^{1}H NMR ($CDCl_3$, 500 MHz): δ 8.10 (d, *J* = 9 Hz, 1H), 7.41 (s, 1H), 7.15 (d, *J* = 2.5 Hz, 1H), 6.86 (dd, *J* = 2.5 Hz, 9 Hz, 1H), 6.70 (q, *J* = 6.5 Hz, 1H), 4.03 (t, *J* = 6.5 Hz, 2H), 1.82 (quintet, *J* = 7 Hz, 2H), 1.48-1.42 (m, 2H), 1.37-1.29 (m, 8H), 0.91-0.88 (m, 3H). ^{13}C NMR ($CDCl_3$,

125 MHz): δ 163.5, 160.0, 141.0, 140.1, 131.8, 131.7, 127.8, 119.3, 113.2, 112.8, 111.7, 69.8, 69.0, 31.8, 29.3, 29.2, 28.9, 25.9, 22.6, 22.1, 14.1. HRMS calcd for $C_{21}H_{25}Br_2NO_5S$ $(M+NH_4)^+$, 581.0147, found, 581.0145.

MNB Ester Terthiophene (O2). A round bottom flask was charged with compound **5** (138 mg, 0.24 mmol), and $Pd(PPh_3)_4$ (14 mg, 0.01 mmol). The flask was evacuated and refilled with argon three times. Under argon flow, 15 mL of anhydrous DMF was added. 2-(tributylstannyl) thiophene (201 mg, 0.17 mL, 0.54 mmol) was added via syringe. The reaction was heated to 90 °C and left stirring for 72 hours. The reaction mixture was poured into DI H_2O (1 × 200 mL) and extracted with diethyl ether (5 × 50 mL). The combined organic layers were dried over $MgSO_4$ and solvent was removed *in vacuo* to give the crude product **O2** as a yellow oil. Flash chromatography on silica using 2:1 hexanes:CH_2Cl_2 as eluent gave 75 mg of **O2** (54 %) as a yellow solid. Mp: 105-108 °C. ^{1}H NMR ($CDCl_3$, 500 MHz): δ 8.08 (d, *J* = 9 Hz, 1H), 7.58 (s, 1H), 7.44 (dd, *J* = 1.5 Hz, *J* = 4 Hz, 1H), 7.41 (dd, *J* = 1.5 Hz, *J* = 5 Hz, 1H), 7.29 (dd, *J* = 1 Hz, *J* = 5 Hz, 1H), 7.22 (dd, *J* = 1, *J* = 3.5 Hz, 1H), 7.08-7.05 (m, 2H), 6.94 (d, *J* = 3 Hz, 1H), 6.83 (dd, *J* = 2.5 Hz, *J* = 9 Hz, 1H), 6.68 (q, *J* = 6.5 Hz, 1H), 3.97-3.94 (m, 2H), 1.81-1.76 (m, 2H), 1.67 (d, *J* = 6 Hz, 3H), 1.47-1.42 (m, 2H), 1.37-1.25 (m, 8H), 0.89 (t, *J* = 6.5, 3H). ^{13}C NMR ($CDCl_3$, 125 MHz): δ 163.5, 161.5, 141.6, 141.4, 140.0, 135.8, 135.7, 133.3, 129.6, 128.3, 128.0, 127.9, 127.6, 127.3, 126.0, 125.4, 124.6, 113.3, 112.4, 69.3, 68.8, 31.8, 29.3, 29.2, 29.0, 25.9, 22.6, 22.0, 14.1. HRMS calcd for $C_{29}H_{31}NO_5S_3$ $(M+NH_4)^+$, 587.1703, found 587.1703.

MNB Ester Polythiophene (P2). A round bottom flask was charged with **5** (42 mg, 0.075 mmol), tri(*o*-tolyl)phosphine (14 mg, 0.038 mmol), and $Pd_2(dba)_3$ (5 mg, 0.004 mmol). The flask was evacuated and refilled with argon three times. Under argon flow, a solution of 2,5-bis(trimethylstannyl)thiophene (31 mg, 0.075 mmol) in 5 mL of anhydrous toluene was added. The reaction mixture was left to reflux for 72 h. Upon completion, the reaction mixture was added dropwise to MeOH to precipitate the polymer. After centrifugation, the solvent was removed *in vacuo* to give 21 mg of **P2** (58 %) as a purple/brown solid. GPC: M_n = 7,000, PDI = 1.14. ^{1}H NMR ($CDCl_3$, 500 MHz): δ 8.15-8.05 (1H), 7.75-7.60 (1H), 7.60-7.40 (1H), 7.20-7.10 (1H), 7.10-6.95 (1H), 6.85-6.75 (1H), 6.75-6.60 (1H), 4.05-3.85 (2H), 1.85-1.65 (2H), 1.50-1.35 (2H), 1.35-1.15 (8H), 0.90-0.75 (3H).

2-(Bromomethyl)-1-nitro-4-(octyloxy)benzene (6). A round bottom flask was charged with **2** (1.00 g, 3.55 mmol). The flask was evacuated and refilled with argon three times. Under argon flow, 20 mL of CH_2Cl_2 was added, and the solution was cooled to 0 °C. PBr_3 (1.06 g, 0.37 mL, 3.91 mmol) was added dropwise, and the reaction was left to stir overnight. The reaction mixture was washed with brine (1 × 200 mL) and extracted with CH_2Cl_2 (3 × 100 mL). The combined organic layers were dried over $MgSO_4$ and solvent was removed *in vacuo* to give the crude product **6** as a brown oil that solidified on standing. Flash chromatography on silica using CH_2Cl_2 as eluent gave 559 mg of **6** (46 %) as a brown solid. ^{1}H NMR ($CDCl_3$, 500 MHz): δ 8.15 (d, *J* = 9 Hz, 1H), 7.02 (d, *J* =

2.5 Hz, 1H), 6.91 (dd, *J* = 2.5 Hz, 9 Hz, 1H), 4.87 (s, 2H), 4.06 (t, *J* = 6.5 Hz, 2H), 1.85-1.80 (m, 2H), 1.50-1.44 (m, 2H), 1.38-1.27 (m, 8H), 0.90 (t, *J* = 6.5 Hz, 3H). ^{13}C NMR ($CDCl_3$, 125 MHz): δ 163.1, 140.4, 135.7, 128.4, 118.0, 114.4, 69.0, 31.8, 30.0, 29.3, 29.2, 28.9, 25.9, 22.6, 14.1.

4-(2,5-dibromothiophen-3-yl)phenol (X1). A round bottom flask was charged with 2,5-dibromo-3-(4-methoxyphenyl)thiophene (1.00 g, 2.87 mmol). The flask was evacuated and refilled with argon three times. Under argon flow, 25 mL of anhydrous CH_2Cl_2 was added, and the solution was cooled to -78 °C. Upon cooling, 1.0 M BBr_3 in anhydrous CH_2Cl_2 (3.2 mL, 3.2 mmol) was added via syringe. The reaction mixture was left to stir overnight, slowly warming to room temperature. The reaction mixture was washed with DI H_2O (1 × 200 mL) and extracted with CH_2Cl_2 (3 × 100 mL). The combined organic layers were dried over $MgSO_4$ and solvent was removed *in vacuo* to give the crude product **X1**. Flash chromatography on silica using CH_2Cl_2 as eluent gave 698 mg of **X1** (73 %) as an off-white solid. ^{1}H NMR ($CDCl_3$, 500 MHz): δ 7.40 (d, *J* = 8.5 Hz, 2H), 6.99 (s, 1H), 6.89 (d, *J* = 9 Hz, 2H), 4.84 (s, 1H). ^{13}C NMR ($CDCl_3$, 125 MHz): δ 155.38, 131.64, 129.98, 127.58, 126.81, 115.36, 111.05, 106.96. HRMS calcd for $C_{10}H_6Br_2OS$ $(M+H)^+$, 334.8562, found, 334.8564.

2,5-dibromo-3-(4-(2-nitro-5-(octyloxy)benzyloxy)phenyl)thiophene (7). A round bottom flask was charged with **X1** (484 mg, 1.45 mmol), and K_2CO_3 (547 mg, 3.96 mmol). The flask was evacuated and refilled with argon three times.

Under argon flow, compound **6** (455 mg, 1.32 mmol), dissolved in 15 mL of anhydrous DMF, was added. The reaction mixture was left to stir overnight at 50 °C. The reaction mixture was poured into DI H_2O (1 × 200 mL) and extracted with CH_2Cl_2 (3 × 100 mL). The combined organic layers were dried over $MgSO_4$ and solvent was removed *in vacuo* to give the crude product **7** as a brown oil. Flash chromatography on silica using 4:1 hexanes:CH_2Cl_2 as eluent gave 544 mg of **7** (69 %) as a viscous, clear yellow oil. ^{1}H NMR ($CDCl_3$, 500 MHz): δ 8.26 (d, *J* = 9.5 Hz, 1H), 7.47 (d, *J* = 8.5 Hz, 2H), 7.39 (d, *J* = 2.5, 1H), 7.08 (d, *J* = 8.5 Hz, 2H), 7.00 (s, 1H), 6.91 (dd, *J* = 2.5 Hz, *J* = 9 Hz, 1H), 5.56 (s, 1H), 4.06 (t, *J* = 6.5 Hz, 2H), 1.81 (m, 2H), 1.46 (m, 2H), 1.33 (m, 8H), 0.90 (t, *J* = 6.5 Hz). ^{13}C NMR ($CDCl_3$, 125 MHz): δ 163.9, 157.9, 141.5, 139.4, 137.1, 131.6, 129.9, 128.0, 127.4, 115.0, 113.6, 113.2, 111.1, 107.1, 68.9, 67.3, 31.8, 29.3, 29.2, 28.9, 25.9, 22.6, 14.1. HRMS calcd for $C_{25}H_{27}Br_2NO_4S$ $(M+NH_4)^+$, 615.0355, found, 615.0360.

NB Ether Oligo (O3). A round bottom flask was charged with $Pd(PPh_3)_4$ (12 mg, 0.01 mmol). The flask was evacuated and refilled with argon three times. Under argon flow, compound **7** (122 mg, 0.20 mmol), dissolved in 8 mL of anhydrous DMF, was added. 2-(tributylstannyl) thiophene (168 mg, 0.14 mL, 0.45 mmol) was added via syringe. The reaction was heated to 90 °C and left stirring for 48 hours. Upon cooling to room temperature, the reaction mixture was poured into DI H_2O (1 × 200 mL) and extracted with diethyl ether (3 × 100 mL). The combined organic layers were dried over $MgSO_4$ and solvent was removed *in*

vacuo to give the crude product **O3**. Flash chromatography on silica using 3:1 hexanes:CH_2Cl_2 as eluent gave 53 mg of **O3** (43 %) as a dark yellow solid. Mp: 92-94 °C. ^{1}H NMR ($CDCl_3$, 500 MHz): δ 8.25 (d, *J* = 9 Hz, 1H), 7.41 (s, 1H), 7.39 (d, *J* = 8.5 Hz, 2H), 7.24 (d, *J* = 5 Hz, 1H), 7.21 (d, *J* = 3 Hz, 1H), 7.19 (d, *J* = 5 Hz, 1H), 7.14 (s, 1H), 7.06-7.02 (m, 4H), 6.96-6.94 (m, 1H), 6.91 (d, *J* = 9 Hz, 1H), 5.55 (s, 1H), 4.07 (t, *J* = 6.5 Hz, 2H), 1.85-1.80 (m, 2H), 1.47 (d, *J* = 7.5 Hz, 2H), 1.34-1.27 (m, 8H), 0.90-0.89 (m, 3H). ^{13}C NMR ($CDCl_3$, 125 MHz): δ 163.9, 157.8, 139.4, 139.0, 137.3, 136.9, 135.7, 135.3, 130.6, 130.1, 129.3, 127.9, 127.9, 127.2, 127.0, 126.4, 125.7, 124.7, 123.9, 115.0, 113.5, 113.3, 68.9, 67.3, 31.8, 29.3, 29.2, 29.0, 25.9, 22.6, 14.1. HRMS calcd for $C_{33}H_{33}NO_4S_3$ $(M+H)^+$, 604.1644, found 604.1648.

NB Ether Polymer (P3). A round bottom flask was charged with **7** (100 mg, 0.17 mmol), tri(*o*-tolyl)phosphine (26 mg, 0.08 mmol), and $Pd_2(dba)_3$ (8 mg, 0.008 mmol). The flask was evacuated and refilled with argon three times. Under argon flow, a solution of 2,5-bis(trimethylstannyl)thiophene (69 mg, 0.17 mmol) in 5 mL of anhydrous toluene was added. The reaction mixture was left to reflux for 72 h. Upon completion, the reaction mixture was added dropwise to MeOH to precipitate the polymer. After centrifugation, the solvent was removed *in vacuo* to give 75 mg of **P3** (85 %) as a purple/red solid. GPC: M_n = 12,800, PDI = 2.14. ^{1}H NMR ($CDCl_3$, 500 MHz): δ 8.30-8.20 (1H), 7.45-7.30 (2H), 7.20-6.70 (7H), 5.60-5.50 (2H), 4.10-3.90 (2H), 1.85-1.70 (2H), 1.50-1.40 (2H), 1.30-1.10 (8H), 0.95-0.75 (3H).

NB Ether D-A Polymer (P5). A round bottom flask was charged with 2,1,3-benzothiadiazole-4,7-bis(boronic acid pinacol ester) (76 mg, 0.19 mmol), $NaHCO_3$ (48 mg, 0.57 mmol), and $Pd(PPh_3)_4$ (18 mg, 0.015 mmol). The flask was evacuated and refilled with argon three times. Under argon flow, a solution of **7** (113 mg, 0.19 mmol) in 8 mL of anhydrous toluene was added. Two drops of Aliquat 336 and 2 mL of deionized water were added. The reaction mixture was left to reflux for 72 h. Upon completion, the reaction mixture was added dropwise to MeOH to precipitate the polymer. After centrifugation, the solvent was removed *in vacuo* to give 95 mg of **P5** (80 %) as a purple solid. GPC: M_n = 46,382, PDI = 1.65. ^{1}H NMR ($CDCl_3$, 500 MHz): δ 8.40-8.10 (2H), 8.05-7.50 (3H), 7.50-7.28 (3H), 7.00-6.75 (2H), 5.60-5.40 (2H), 4.15-3.85 (2H), 1.90-1.70 (2H), 1.50-1.40 (2H), 1.40-1.20 (8H), 0.95-0.70 (3H).

2-(1-bromoethyl)-1-nitro-4-(octyloxy)benzene (8). A round bottom flask was charged with CBr_4 (773 mg, 2.33 mmol), and PPh_3 (611 mg, 2.33 mmol). The flask was evacuated and refilled with argon three times. Under argon flow, compound **5** (459 mg, 1.55 mmol) dissolved in 10 mL of anhydrous tetrahydrofuran (THF) was added. The reaction was left stirring at room temperature for two hours. The reaction mixture was filtered and the solvent was removed *in vacuo* to give the crude product **8** as a brown oil. Flash chromatography on silica using 4:1 hexanes:CH_2Cl_2 as eluent gave 290 mg of **8** (52 %) as a clear, yellow oil. ^{1}H NMR ($CDCl_3$, 500 MHz): δ 7.96 (d, *J* = 9 Hz,

1H), 7.33 (d, *J* = 3 Hz, 1H), 6.86 (dd, *J* = 2.5 Hz, *J* = 9 Hz, 1H), 6.02 (q, *J* = 7 Hz, 1H), 4.07 (m, 2H), 2.07 (d, *J* = 7 Hz, 3H), 1.84 (m, 2H), 1.52-1.46 (m, 2H), 1.36-1.30 (m, 8H), 0.92-0.89 (m, 3H). ^{13}C NMR ($CDCl_3$, 125 MHz): δ 163.1, 140.9, 140.1, 127.4, 115.7, 113.9, 68.9, 42.6, 31.8, 29.3, 29.2, 29.0, 27.2, 25.9, 22.6, 14.1.

2,5-dibromo-3-(4-(1-(2-nitro-5-(octyloxy)phenyl)ethoxy)phenyl)thiophene (9). A round bottom flask was charged with **X1** (100 mg, 0.30 mmol), and K_2CO_3 (113 mg, 0.82 mmol). The flask was evacuated and refilled with argon three times. Under argon flow, compound **8** (97 mg, 0.27 mmol), dissolved in 15 mL of anhydrous DMF, was added. The reaction mixture was left to stir overnight at 50 °C. The reaction mixture was poured into DI H_2O (1 × 200 mL) and extracted with diethyl ether (3 × 100 mL). The combined organic layers were dried over $MgSO_4$ and solvent was removed *in vacuo* to give the crude product **9** as a clear oil. Flash chromatography on silica using 3:1 hexanes:CH_2Cl_2 as eluent gave 140 mg of **9** (84 %) as a transparent, colorless oil. ^{1}H NMR ($CDCl_3$, 500 MHz): δ 8.15 (d, *J* = 9 Hz, 1H), 7.35 (d, *J* = 7.5 Hz, 2H), 7.23 (d, *J* = 2.5 Hz, 1H), 6.94 (s, 1H), 6.86-6.84 (m, 3H), 6.20 (q, *J* = 6.5 Hz, 1H), 4.00 (m, 2H), 1.79-1.74 (m, 2H), 1.72 (d, *J* = 6 Hz, 3H), 1.43-1.41 (m, 2H), 1.31-1.28 (m, 8H), 0.90-0.89 (m, 3H). ^{13}C NMR ($CDCl_3$, 125 MHz): δ 163.9, 157.2, 142.7, 141.4, 139.8, 131.6, 129.8, 127.9, 127.0, 115.4, 113.7, 112.5, 111.0, 106.9, 71.9, 68.8, 31.8, 29.3, 29.2, 28.9, 25.9, 23.5, 22.6, 14.1. HRMS calcd for $C_{26}H_{29}Br_2NO_4S$ $(M+NH_4)^+$, 629.0512, found, 629.0526.

MNB Ether Oligo (O4). A round bottom flask was charged with 2-thienylboronic acid (92 mg, 0.72 mmol), sodium bicarbonate (83 mg, 0.99 mmol), and $Pd(PPh_3)_4$ (18 mg, 0.02 mmol). The flask was evacuated and refilled with argon three times. Under argon flow, compound **9** (200 mg, 0.33 mmol), dissolved in 10 mL of deoxygenated DMF/H_2O mixture (4:1), was added. The reaction mixture was left to stir overnight at 80 °C. The reaction mixture was poured into DI H_2O (1 × 200 mL) and extracted with diethyl ether (3 × 100 mL). The combined organic layers were dried over $MgSO_4$ and solvent was removed *in vacuo* to give the crude product **O4** as a yellow oil. Flash chromatography on silica using 3:1 hexanes:CH_2Cl_2 as eluent gave 165 mg of **O4** (82 %) as a yellow oil. ^{1}H NMR ($CDCl_3$, 500 MHz): δ 8.14 (d, *J* = 9.5 Hz, 2H), 7.24-7.22 (m, 3H), 7.18 (d, *J* = 3.5 Hz, 1H), 7.16 (d, *J* = 5.5 Hz, 1H), 7.07 (s, 1H), 7.03 (dd, *J* = 4 Hz, *J* = 1 Hz, 1H), 6.97 (d, *J* = 3.5 Hz, 1H), 6.92 (dd, *J* = 4 Hz, *J* = 1 Hz, 1H), 6.85 (dd, *J* = 2.5 Hz, *J* = 6.5 Hz, 1H), 6.80 (d, *J* = 8.5 Hz, 2H), 6.20 (q, *J* = 6.5 Hz, 1H), 4.02-3.96 (m, 2H), 1.78-1.75 (m, 2H), 1.72 (d, *J* = 6 Hz, 3H), 1.45-1.42 (m, 2H), 1.33-1.28 (m, 8H), 0.89 (t, *J* = 6.5 Hz, 3H). ^{13}C NMR ($CDCl_3$, 125 MHz): δ 163.9, 156.9, 142.8, 139.9, 139.0, 136.9, 135.8, 135.2, 130.5, 130.0, 128.9, 127.9, 127.1, 126.9, 126.3, 125.7, 124.6, 123.8, 115.6, 113.8, 112.4, 71.9, 68.8, 31.8, 29.3, 29.2, 28.9, 25.9, 23.5, 22.6, 14.1. HRMS calcd for $C_{34}H_{35}NO_4S_3$ $(M+H)^+$, 618.1801, found, 618.1818.

MNB Ether Polymer (P4). A round bottom flask was charged with **9** (50 mg, 0.081 mmol), tri(*o*-tolyl)phosphine (12 mg, 0.04 mmol), and $Pd_2(dba)_3$ (4 mg, 0.004 mmol). The flask was evacuated and refilled with argon three times. Under argon flow, a solution of 2,5-bis(trimethylstannyl)thiophene (33 mg, 0.081 mmol) in 5 mL of anhydrous, deoxygenated toluene was added. The reaction mixture was left to reflux for 72 hours. Upon completion, the reaction mixture was added dropwise to MeOH to precipitate the polymer. After centrifugation, the solvent was removed *in vacuo* to give 40 mg of **P4** (92 %) as a purple solid. GPC: M_n = 14,800, PDI = 1.58. ^{1}H NMR ($CDCl_3$, 500 MHz): δ 8.20-8.00 (1H), 7.26-7.20 (2H), 7.20-7.15 (1H), 7.10-6.85 (2H), 6.85-6.65 (4H), 6.25-6.15 (1H), 4.05-3.90 (2H), 1.80-1.65 (2H), 1.45-1.35 (2H), 1.35-1.15 (8H), 0.95-0.75 (3H).

MNB Ether D-A Polymer (P6). A round bottom flask was charged with 2,1,3-benzothiadiazole-4,7-bis(boronic acid pinacol ester) (76 mg, 0.19 mmol), $NaHCO_3$ (48 mg, 0.57 mmol), and $Pd(PPh_3)_4$ (18 mg, 0.015 mmol). The flask was evacuated and refilled with argon three times. Under argon flow, a solution of **9** (119 mg, 0.19 mmol) in 8 mL of anhydrous toluene was added. Two drops of Aliquat 336 and 2 mL of deionized water were added. The reaction mixture was left to reflux for 72 h. Upon completion, the reaction mixture was added dropwise to MeOH to precipitate the polymer. After centrifugation, the solvent was removed *in vacuo* to give 90 mg of **P4** (80 %) as a purple solid. GPC: M_n = 10,200, PDI = 2.12. ^{1}H NMR ($CDCl_3$, 500 MHz): δ 8.40-8.10 (2H), 8.10-7.80 (1H), 7.60-7.40 (2H), 7.25-7.05 (2H), 7.00-6.80 (2H), 6.80-6.60 (1H), 6.30-6.10

(1H), 4.10-3.90 (2H), 1.86-1.65 (2H), 1.50-1.40 (2H), 1.40-1.20 (8H), 0.95-0.80 (3H).

Control Ester Oligomer (O5). A round bottom flask was charged with 2,5-dibromothiophene-3-carboxylic acid (150 mg, 0.52 mmol), and $Pd(PPh_3)_4$ (30 mg, 0.026 mmol). The flask was evacuated and refilled with argon three times. Under argon flow, 20 mL of anhydrous DMF was added. 2-(tributylstannyl) thiophene (431 mg, 0.37 mL, 1.2 mmol) was added via syringe. The reaction was heated to 90 °C and left stirring for 72 hours. The reaction mixture was poured into DI H_2O (1 × 200 mL) and extracted with diethyl ether (5 × 50 mL). The combined organic layers were dried over $MgSO_4$ and solvent was removed *in vacuo* to give the crude product **O5** as a yellow solid. Flash chromatography on silica using 2:1 hexanes:EtOAc as eluent gave 42 mg of **O5** (28 %) as a bright yellow solid. Mp: > 150 °C (dec.). ^{1}H NMR ($CDCl_3$, 500 MHz): δ 7.61 (s, 1H), 7.53 (dd, *J* = 1 Hz, *J* = 3.5 Hz, 1H), 7.45 (dd, *J* = 1 Hz, *J* = 5 Hz, 1H), 7.29 (dd, *J* = 0.5 Hz, *J* = 5 Hz, 1H), 7.22 (dd, *J* = 0.5 Hz, *J* = 3.5 Hz, 1H), 7.10 (dd, *J* = 3.5 Hz, *J* = 5 Hz, 1H), 7.06 (dd, *J* = 4 Hz, *J* = 5 Hz, 1H). ^{13}C NMR ($CDCl_3$, 125 MHz): δ 166.9, 143.4, 135.7, 135.5, 133.2, 129.8, 128.2, 128.0, 127.4, 126.6, 126.6, 125.5, 124.6. HRMS calcd for $C_{13}H_8O_2S_3$ $(M+H)^+$, 292.9759, found, 292.9773.

Control Ether Oligomer (O6). A round bottom flask was charged with $Pd(PPh_3)_4$ (20 mg, 0.018 mmol). The flask was evacuated and refilled with argon three times. Under argon flow, 15 mL of anhydrous, deoxygenated DMF, and 2,5-

dibromo-3-(4-(octyloxy)phenyl)thiophene (158 mg, 0.35 mmol) were added. 2-(tributylstannyl) thiophene (291 mg, 0.25 mL, 0.078 mmol) was added via syringe. The reaction was heated to 90 °C and left stirring for 72 hours. The reaction mixture was poured into DI H_2O (1 × 200 mL) and extracted with diethyl ether (5 × 50 mL). The combined organic layers were dried over $MgSO_4$ and solvent was removed *in vacuo* to give the crude product **O6** as a yellow oil. Flash chromatography on silica using 2:1 hexanes:CH_2Cl_2 as eluent gave 116 mg of **O6** (73 %) as a yellow oil. ^{1}H NMR ($CDCl_3$, 500 MHz): δ 7.30 (d, *J* = 8.5 Hz, 2H), 7.24 (dd, *J* = 1 Hz, *J* = 5 Hz, 1H), 7.21 (dd, *J* = 1 Hz, *J* = 3.5 Hz, 1H), 7.18 (dd, *J* = 1 Hz, *J* = 5 Hz, 1H), 7.12 (s, 1H), 7.04 (dd, *J* = 3.5 Hz, *J* = 5 Hz, 1H), 7.01 (dd, *J* = 1.5 Hz, *J* = 3.5 Hz, 1H), 6.94 (dd, *J* = 4 Hz, *J* = 5 Hz, 1H), 6.90 (d, *J* = 8.5 Hz, 2H), 3.99 (t, *J* = 6.5 Hz), 1.81 (m, 2H), 1.48 (m, 2H), 1.36-1.31 (m, 8H), 0.91 (t, *J* = 6.5 Hz, 3H). ^{13}C NMR ($CDCl_3$, 125 MHz): δ 158.8, 139.3, 137.0, 135.9, 135.1, 130.4, 129.9, 128.1, 127.9, 127.1, 127.1, 126.3, 125.6, 124.6, 123.8, 114.4, 68.0, 31.8, 29.4, 29.3, 29.2, 26.1, 22.7, 14.1. HRMS calcd for $C_{26}H_{28}OS_3$ $(M+H)^+$, 453.1375, found, 453.1374.

Control Ester Polymer (P7). A Schlenk tube was charged with 2,5-dibromothiophene-3-octylcarboxylate (48 mg, 0.12 mmol), 2,5-bis(trimethylstannyl)thiophene (49 mg, 0.12 mmol), tri(*o*-tolyl)phosphine (18 mg, 0.06 mmol), and $Pd_2(dba)_3$ (6 mg, 0.006 mmol). The Schlenk tube was evacuated and refilled with argon three times. Under argon flow, deoxygenated toluene was added. The reaction mixture was heated to 90 °C and left to stir for 72 hours.

Upon completion, the reaction mixture was added dropwise to MeOH to precipitate the polymer. After centrifugation, the solvent was removed *in vacuo* to give 50 mg of **P7** (86 %) as a purple solid. GPC: M_n = 6,000, PDI = 1.42. ^{1}H NMR ($CDCl_3$, 500 MHz): δ 7.70-7.40 (2H), 7.25-7.00 (1H), 4.50-4.20 (2H), 1.95-1.65 (2H), 1.45-1.15 (10H), 1.00-0.80 (3H).

Synthesized Photoproduct Ether Oligomer (O7). A round bottom flask was charged with 4-(2,2':5',2''-terthiophen-3-yl)anisole (475 g, 1.34 mmol).[33] The flask was evacuated and refilled with argon three times. Under argon flow, 12 mL of anhydrous CH_2Cl_2 was added, and the solution was cooled to -78 °C. Upon cooling, 1.0 M BBr_3 in anhydrous CH_2Cl_2 (1.47 mL, 1.47 mmol) was added via syringe. The reaction mixture was left to stir overnight, slowly warming to room temperature. The reaction mixture was washed with DI H_2O (1 × 200 mL) and extracted with Et_2O (3 × 50 mL). The combined organic layers were dried over $MgSO_4$ and solvent was removed *in vacuo* to give the crude product **O7**. Flash chromatography on silica using CH_2Cl_2 as eluent gave 57 mg of **O7** (13 %) as an off-white solid. Mp: 118-121 °C. ^{1}H NMR ($CDCl_3$, 500 MHz): δ 7.28-7.24 (m, 3H), 7.21 (dd, *J* = 1 Hz, *J* = 3.5 Hz, 1H), 7.19 (dd, *J* = 1 Hz, *J* = 5 Hz, 1H), 7.12 (s, 1H), 7.04 (dd, *J* = 4 Hz, *J* = 5 Hz, 1H), 7.01 (dd, *J* = 1 Hz, *J* = 3.5 Hz, 1H), 6.94 (dd, *J* = 3.5 Hz, *J* = 5 Hz, 1H), 6.85 (d, *J* = 8.5 Hz), 4.97 (s, 1H). ^{13}C NMR ($CDCl_3$, 125 MHz): δ 155.2, 139.1, 136.9, 135.8, 135.2, 130.7, 130.0, 128.6, 127.9, 127.2, 127.1, 126.3, 125.7, 124.6, 123.8, 115.4. HRMS calcd for $C_{18}H_{12}OS_3$ $(M+H)^+$, 341.0123, found, 341.0115.

Calculating Quantum Yield of Photocleavage

The quantum yields of photocleavage for **O1**-**O4** were determined by irradiating a sample of known concentration in a quartz cuvette with 365 nm light while monitoring the growth of peaks in the ^{1}H NMR spectra corresponding to the analogous photoproduct. Each sample was made concentrated enough (2-4 mM) that the OD of the sample was high enough to assume complete absorbance at 365 nm and concentrated enough for NMR. Aliquots were removed at several time intervals for NMR (and then returned to the bulk sample). The analogous photoproducts used were **O5** for NB ester oligomers **O1** and **O2**, and **O7** for NB ether oligomers **O3** and **O4**. The following equation was used to determine quantum yield of photocleavage:

$$\Phi_P = \frac{\text{moles of photoproduct}}{(\text{flux of absorbed photons}) \times (\%\ \text{light absorbed by NB})}$$

The moles of photoproduct were determined by NMR of the sample which was of known concentration. The flux of photons from the lamp was determined using chemical actinometry using the potassium ferrioxalate actinometer. The percentage of light absorbed by the *o*-nitrobenzyl group was determined by measuring the extinction coefficients of **O1**-**O7** and **2**. It was found that the extinction coefficients were additive. For example, the extinction coefficients of the NB group and synthesized photoproducts (**O5** or **O7**) could be added together to equal the extinction coefficient of the corresponding NB containing oligomer. This is necessitated due to the competitive absorbance at 365 nm of the oligomer

backbone and the NB group. In all cases, the NB group was found to absorb 10-13% of the overall light absorbed by the molecule at 365 nm. An example calculation for **O3** can be seen below:

$$\Phi_P = \frac{2.0 \times 10^{-6}}{(0.00017) \times (0.10)} = 0.12$$

3.12 References

1. Günes, S.; Neugebauer, H.; Sariciftci, N. S. *Chem. Rev.* **2007**, *107*, 1324.

2. Forrest, S. R. *Nature* **2004**, *428*, 911.

3. Thomas, S. W.; Joly, G. D.; Swager, T. M. *Chem. Rev.* **2007**, *107*, 1339.

4. Kline, R. J.; DeLongchamp, D. M.; Fischer, D. A.; Lin, E. K.; Richter, L. J.; Chabinyc, M. L.; Toney, M. F.; Heeney, M.; McCulloch, I. *Macromolecules* **2007**, *40*, 7960.

5. Allard, S.; Forster, M.; Souharce, B.; Thiem, H.; Scherf, U. *Angew. Chem. Int. Ed.* **2008**, *47*, 4070.

6. Huang, F.; Wu, H.; Cao, Y. *Chem. Soc. Rev.* **2010**, *39*, 2500.

7. Manceau, M.; Bundgaard, E.; Carle, J. E.; Hagemann, O.; Helgesen, M.; Sondergaard, R.; Jorgensen, M.; Krebs, F. C. *J. Mater. Chem.* **2011**, *21*, 4132.

8. Aoyama, Y.; Yamanari, T.; Koumura, N.; Tachikawa, H.; Nagai, M.; Yoshida, Y. *Polym. Degrad. Stab.* **2013**, *98*, 899.

9. Stuart, M. A. C.; Huck, W. T. S.; Genzer, J.; Muller, M.; Ober, C.; Stamm, M.; Sukhorukov, G. B.; Szleifer, I.; Tsukruk, V. V.; Urban, M.; Winnik, F.; Zauscher, S.; Luzinov, I.; Minko, S. *Nature Materials* **2010**, *9*, 101.

10. Liu, J. S.; Kadnikova, E. N.; Liu, Y. X.; McGehee, M. D.; Frechet, J. M. J. *J. Am. Chem. Soc.* **2004**, *126*, 9486.

11. Hagemann, O.; Bjerring, M.; Nielsen, N. C.; Krebs, F. C. *Sol. Energy Mater. Sol. Cells* **2008**, *92*, 1327.

12. Sondergaard, R. R.; Norrman, K.; Krebs, F. C. *Journal of Polymer Science, Part A: Polymer Chemistry* **2012**, *50*, 1127.

13. Bundgaard, E.; Hagemann, O.; Bjerring, M.; Nielsen, N. C.; Andreasen, J. W.; Andreasen, B.; Krebs, F. C. *Macromolecules* **2012**, *45*, 3644.

14. Krebs, F. C.; Norrman, K. *ACS Appl. Mater. Interfaces* **2010**, *2*, 877.

15. Johnson, R. S.; Haworth, J. J.; Finnegan, P. S.; Wheeler, D. R.; Dirk, S. M. *Macromol. Rapid Commun.* **2014**, *35*, 1116.

16. Johnson, R. S.; Finnegan, P. S.; Wheeler, D. R.; Dirk, S. M. *Chem. Commun.* **2011**, *47*, 3936.

17. Lee, S. K.; Jung, B.-J.; Ahn, T.; Song, I.; Shim, H.-K. *Macromolecules* **2003**, *36*, 9252.

18. Gumbley, P.; Koylu, D.; Pawle, R. H.; Umezuruike, B.; Spedden, E.; Staii, C.; Thomas, S. W. *Chem. Mater.* **2014**, *26*, 1450.

19. Thomas, S. W. *Macromol. Chem. Phys.* **2012**, *213*, 2443.

20. Klán, P.; Šolomek, T.; Bochet, C. G.; Blanc, A.; Givens, R.; Rubina, M.; Popik, V.; Kostikov, A.; Wirz, J. *Chem. Rev.* **2012**, *113*, 119.

21. Zhao, H.; Sterner, E. S.; Coughlin, E. B.; Theato, P. *Macromolecules* **2012**, *45*, 1723.

22. Smith, Z. C.; Pawle, R. H.; Thomas, S. W. *ACS Macro Lett.* **2012**, *1*, 825.

23. Solomek, T.; Mercier, S.; Bally, T.; Bochet, C. G. *Photoch. Photobio. Sci.* **2012**, *11*, 548.

24. McTiernan, C. D.; Chahma, M. h. *New J. Chem.* **2010**, *34*, 1417.

25. Blettner, C. G.; König, W. A.; Stenzel, W.; Schotten, T. *J. Org. Chem.* **1999**, *64*, 3885.

26. DiCesare, N.; Belletete, M.; Leclerc, M.; Durocher, G. *Synth. Met.* **1998**, *98*, 31.

27. Cook, S.; Furube, A.; Katoh, R. *Energ. Environ. Sci.* **2008**, *1*, 294.

28. Zhao, Y.; Zheng, Q.; Dakin, K.; Xu, K.; Martinez, M. L.; Li, W.-H. *J. Am. Chem. Soc.* **2004**, *126*, 4653.

29. Pawle, R. H.; Eastman, V.; Thomas, S. W. *J. Mater. Chem.* **2011**, *21*, 14041.

30. Jørgensen, M.; Norrman, K.; Krebs, F. C. *Sol. Energy Mater. Sol. Cells* **2008**, *92*, 686.

31. Lee, J.; Han, H.; Lee, J.; Yoon, S. C.; Lee, C. *Journal of Materials Chemistry C* **2014**, *2*, 1474.

32. Bouffard, J.; Watanabe, M.; Takaba, H.; Itami, K. *Macromolecules* **2010**, *43*, 1425.

33. Tovar, J. D.; Swager, T. M. *J. Polym. Sci., Part A: Polym. Chem.* **2003**, *41*, 3693.

Chapter 3 Appendix

^{1}H and ^{13}C NMR

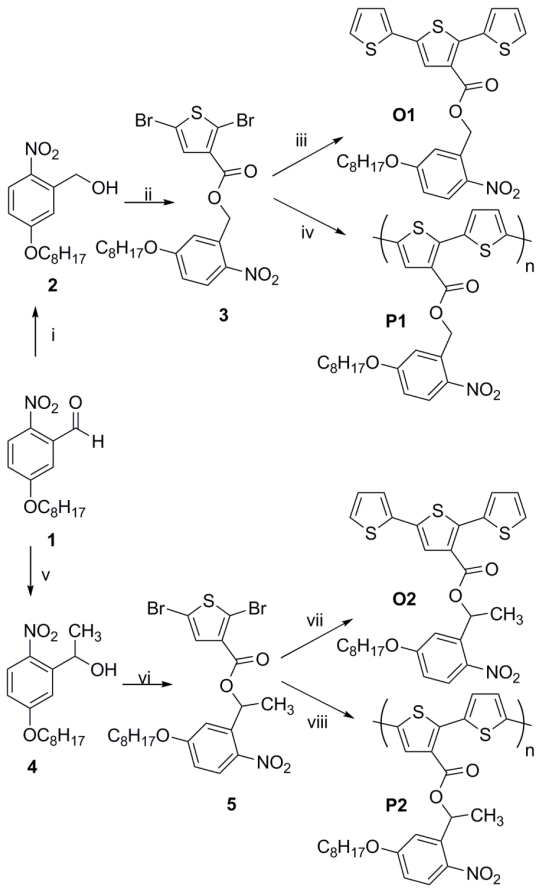

Compound **1**, ^{1}H NMR (500 MHz, $CDCl_3$)

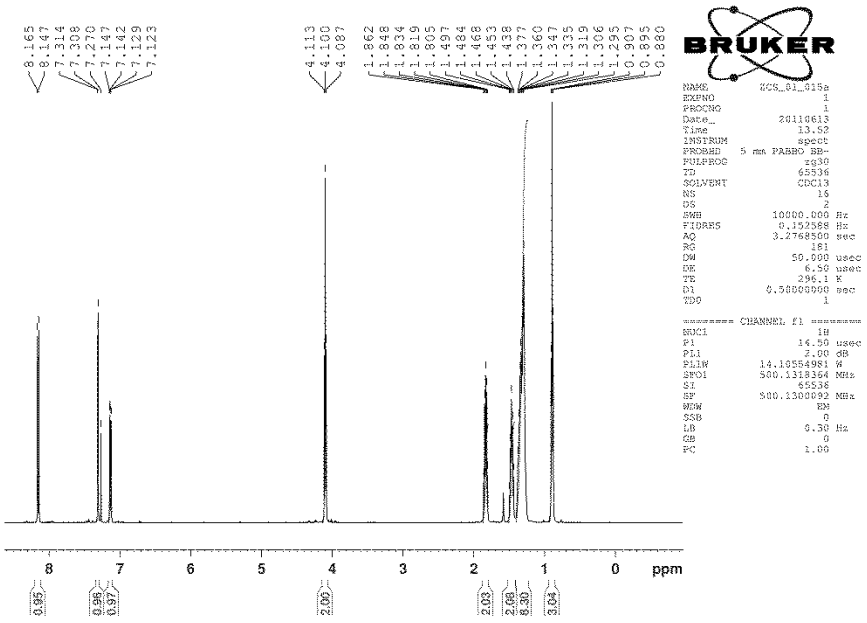

Compound **1**, ^{13}C NMR (125 MHz, $CDCl_3$)

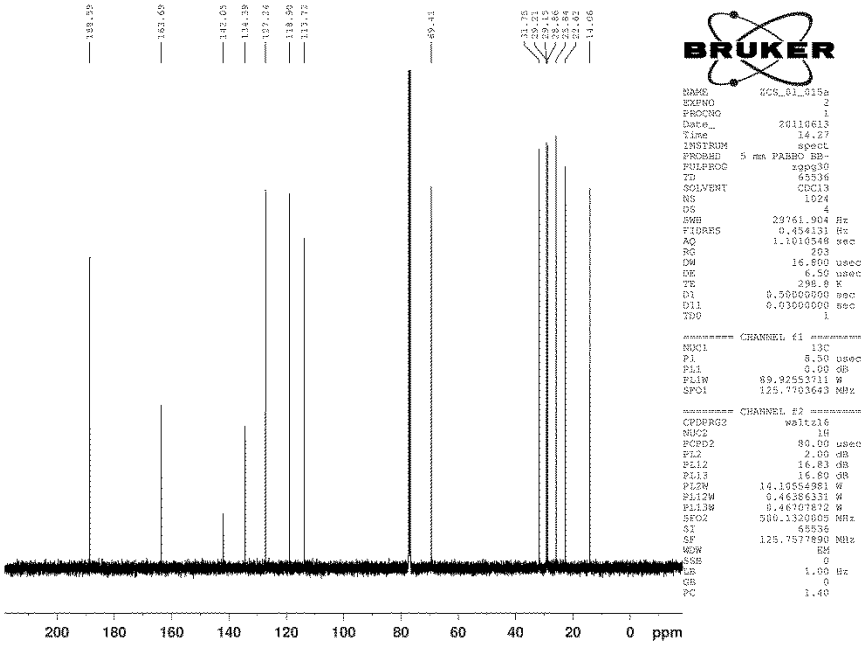

Compound **2**, ^{1}H NMR (500 MHz, $CDCl_3$)

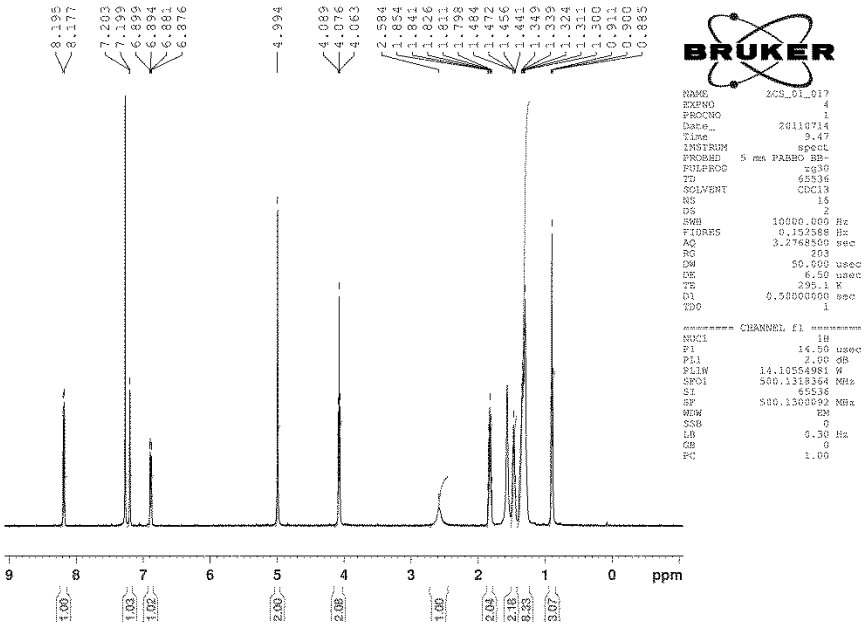

Compound **2**, ^{13}C NMR (125 MHz, $CDCl_3$)

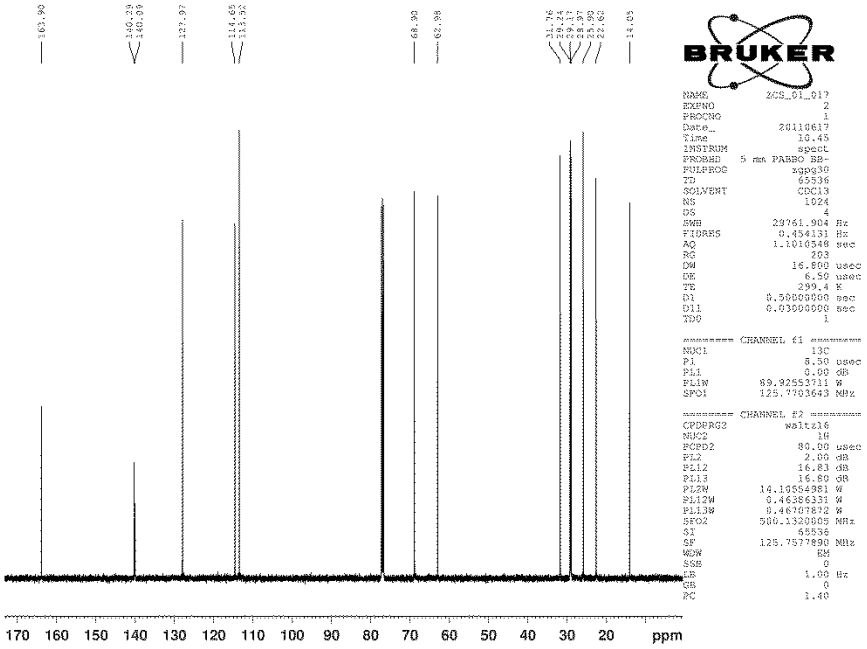

Compound **3**, ^{1}H NMR (500 MHz, $CDCl_3$)

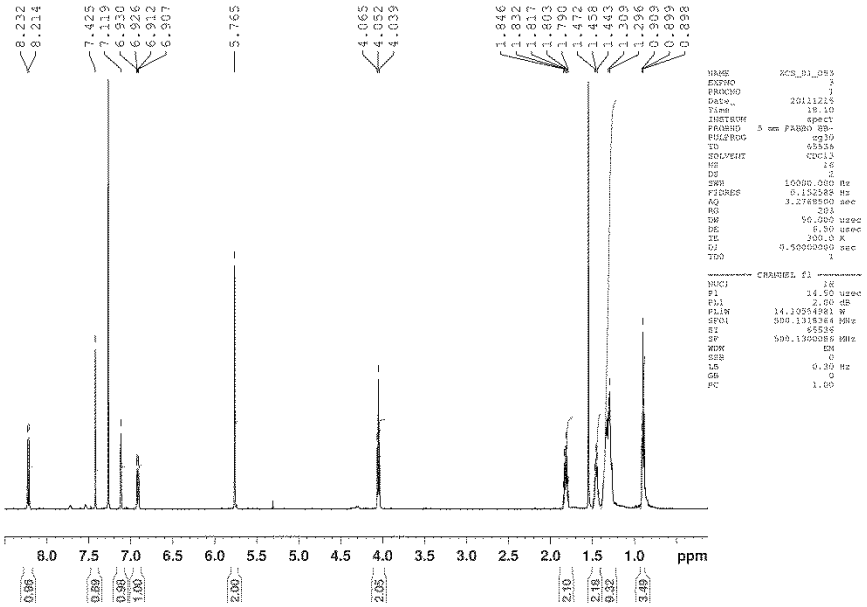

Compound **3**, ^{13}C NMR (125 MHz, $CDCl_3$)

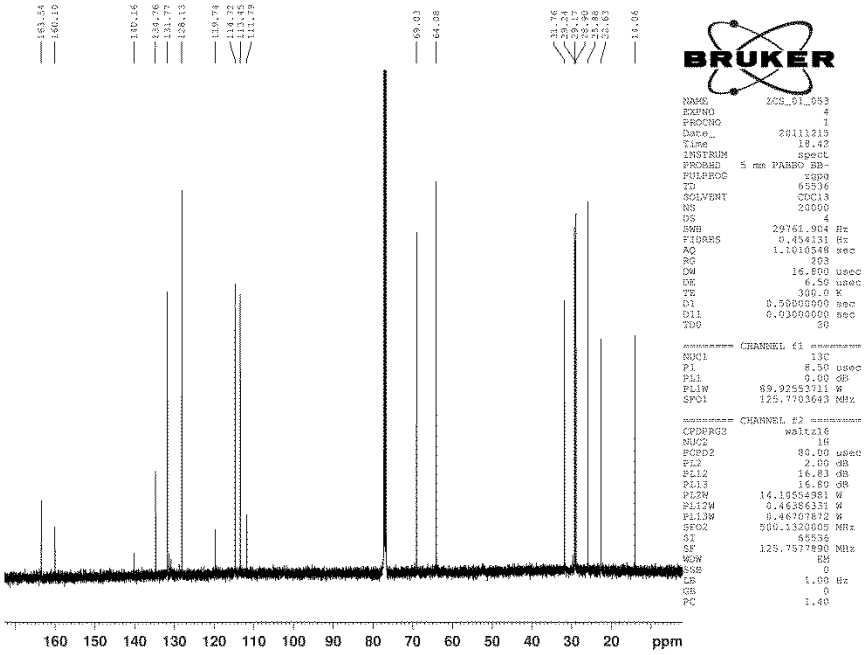

Compound **O1**, ^{1}H NMR (500 MHz, $CDCl_3$)

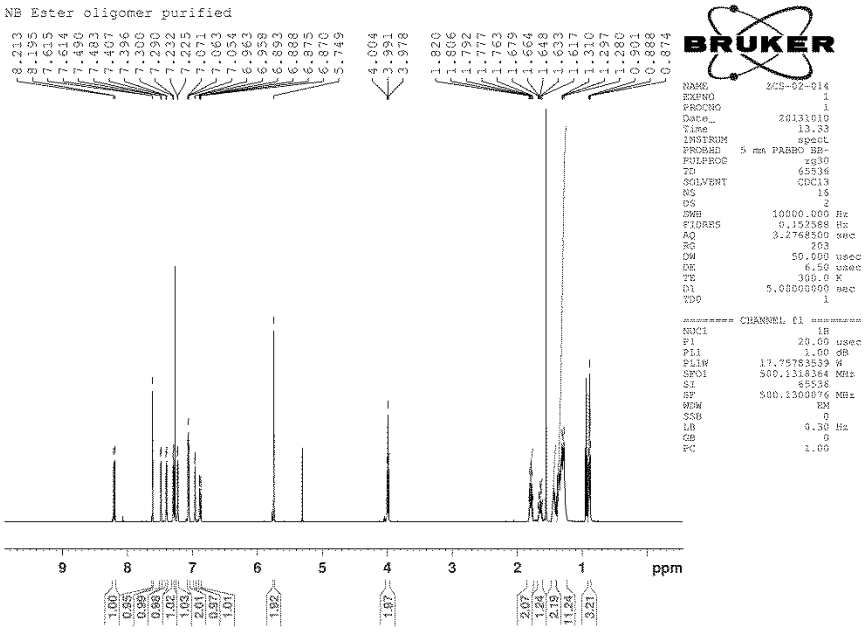

Compound **O1**, ^{13}C NMR (125 MHz, $CDCl_3$)

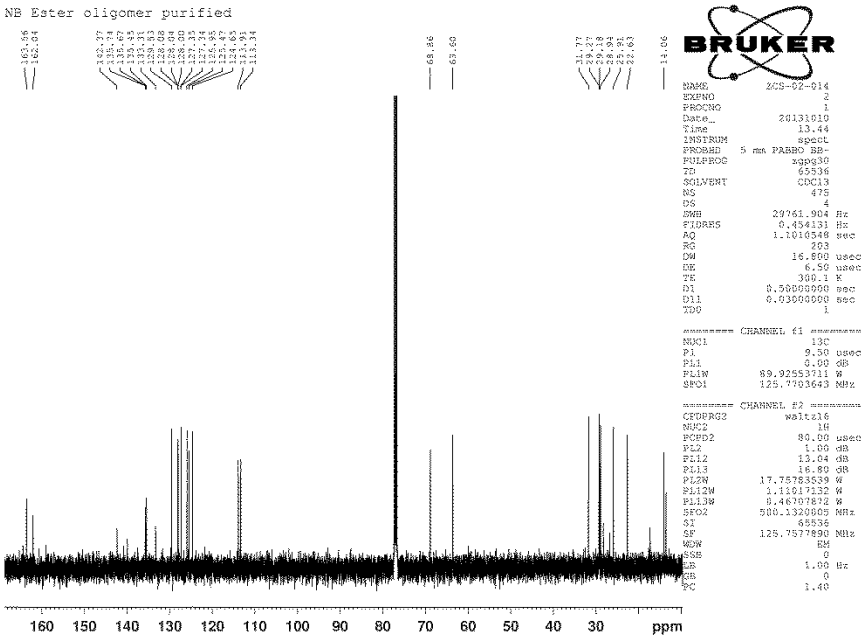

Compound **P1**, ^{1}H NMR (500 MHz, $CDCl_3$)

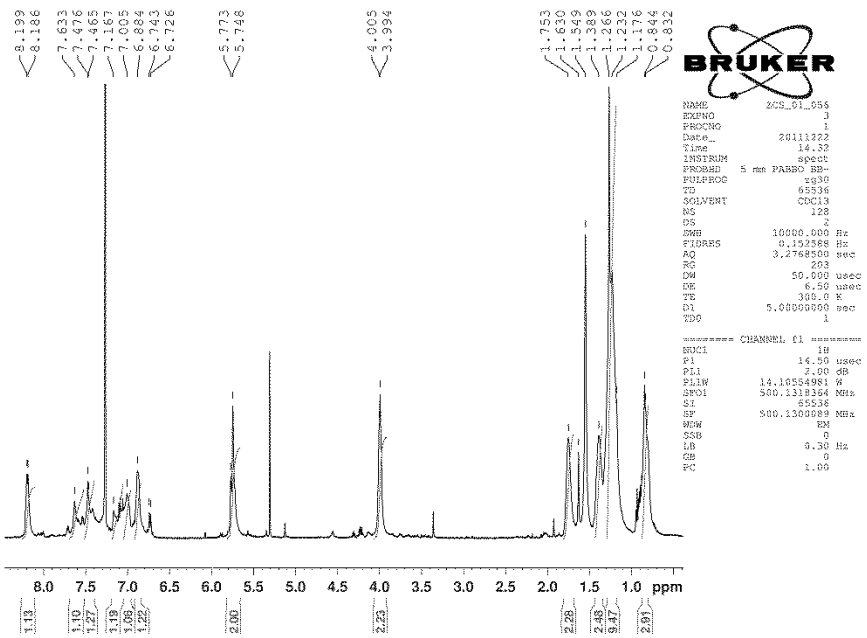

Compound **4**, ^{1}H NMR (500 MHz, $CDCl_3$)

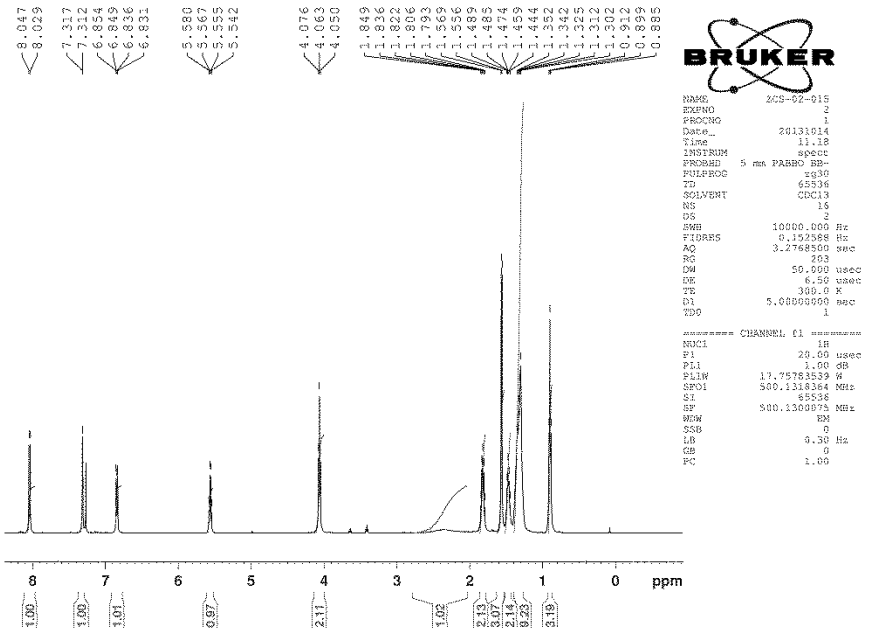

Compound **4**, ^{13}C NMR (125 MHz, $CDCl_3$)

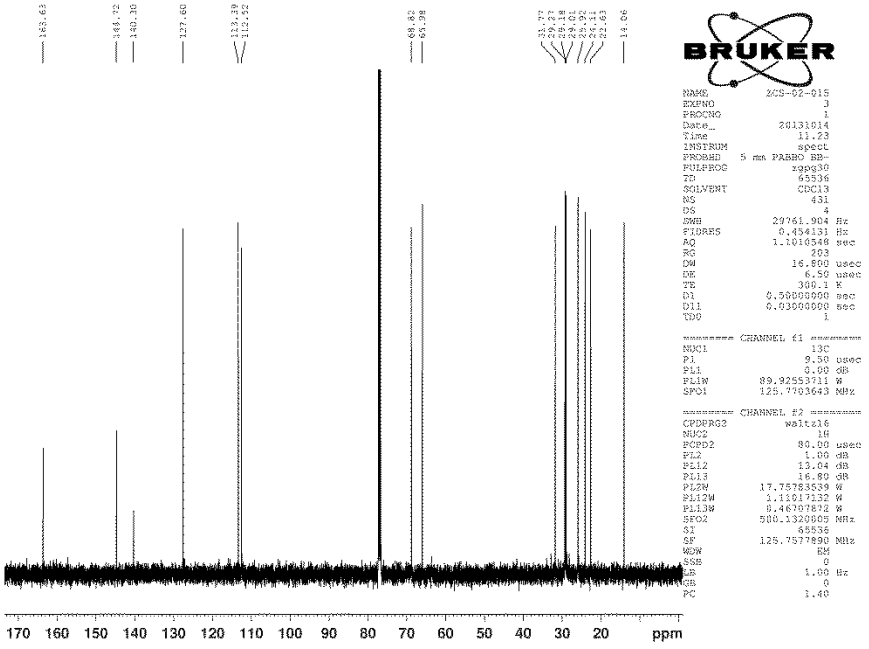

Compound **5**, ^{1}H NMR (500 MHz, $CDCl_3$)

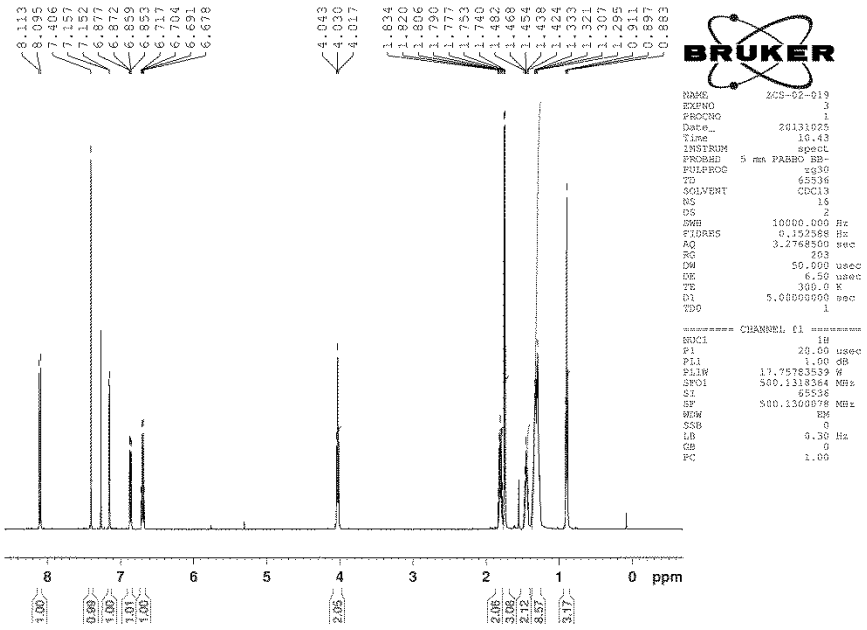

Compound **5**, ^{13}C NMR (125 MHz, $CDCl_3$)

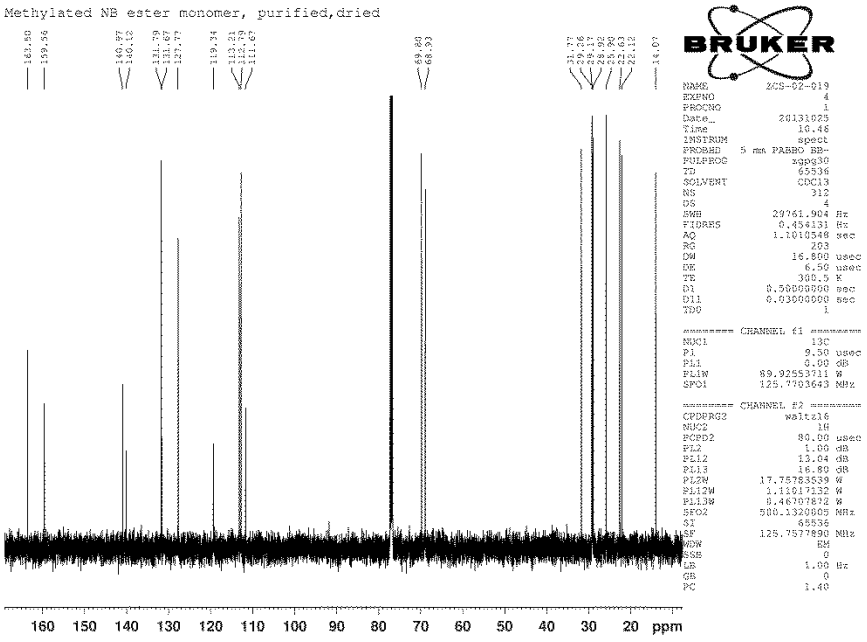

Compound **O2**, ^{1}H NMR (500 MHz, $CDCl_3$)

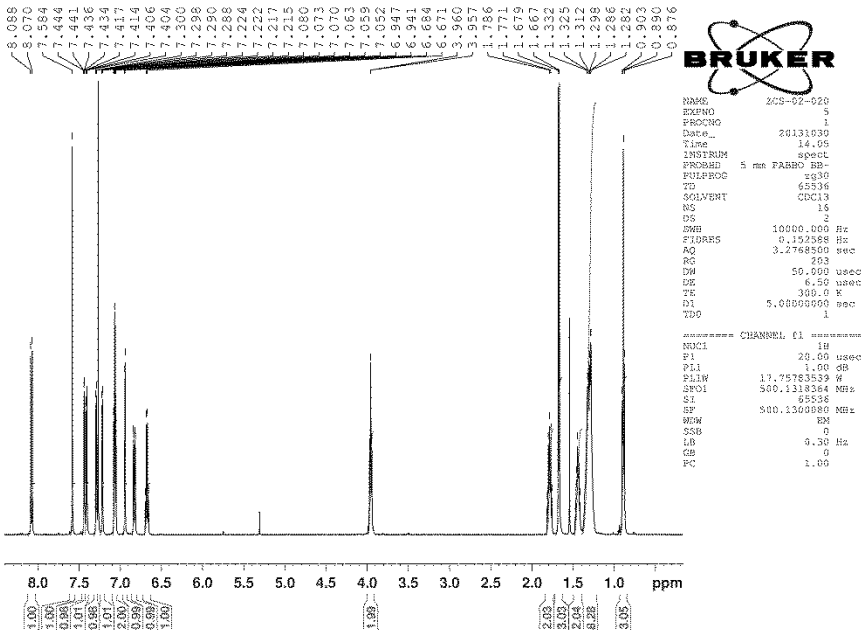

Compound **O2**, ^{13}C NMR (125 MHz, $CDCl_3$)

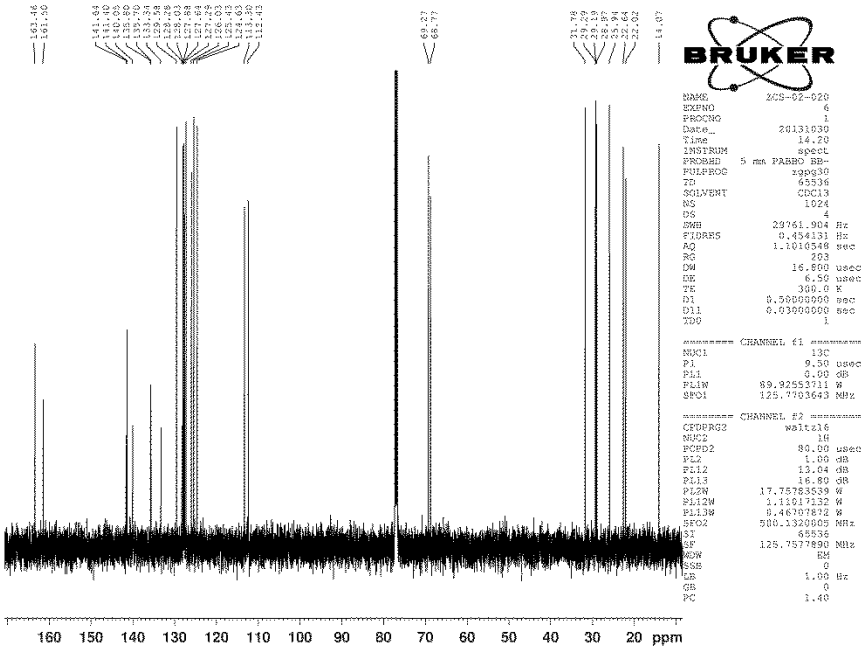

Compound **P2**, ^{1}H NMR (500 MHz, $CDCl_3$)

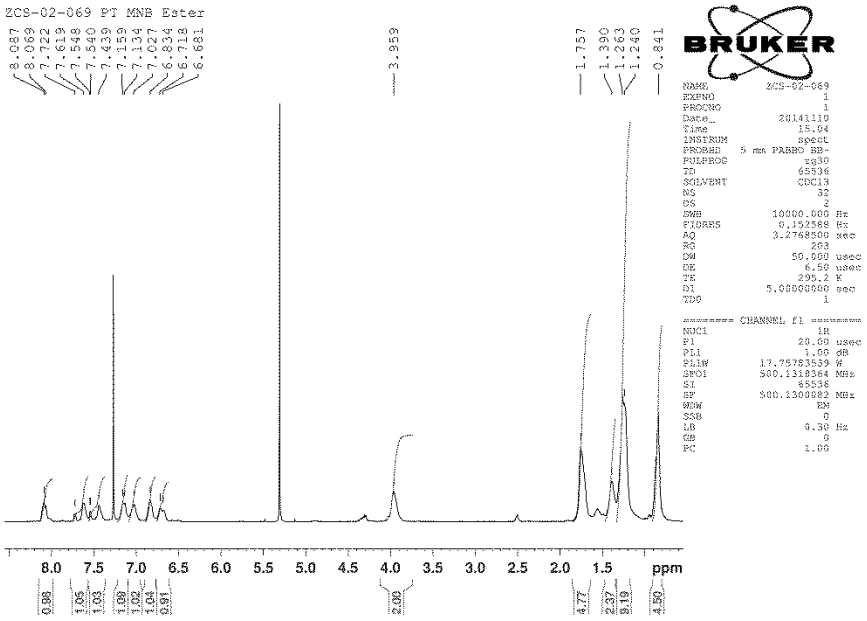

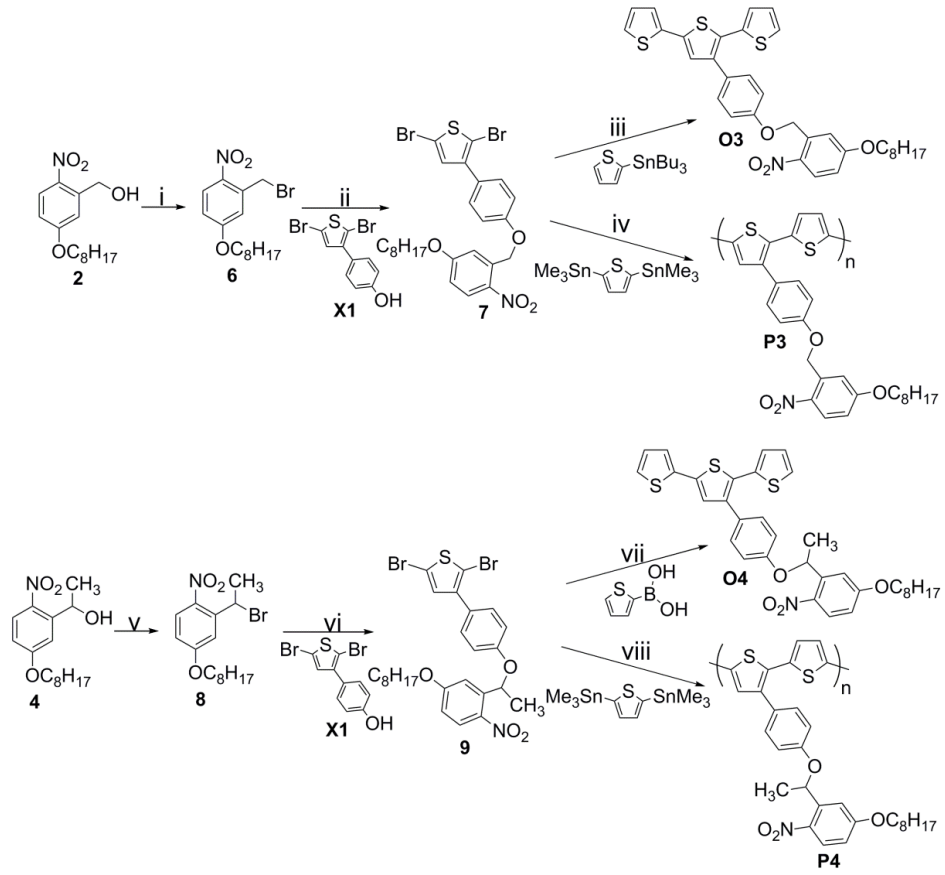

Compound **6**, ^{1}H NMR (500 MHz, $CDCl_3$)

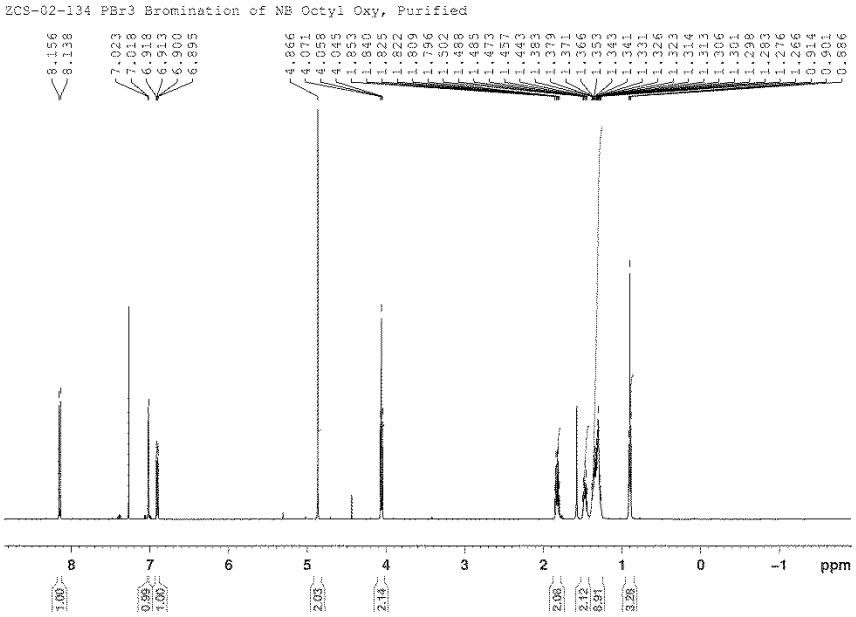

Compound **6**, ^{13}C NMR (125 MHz, $CDCl_3$)

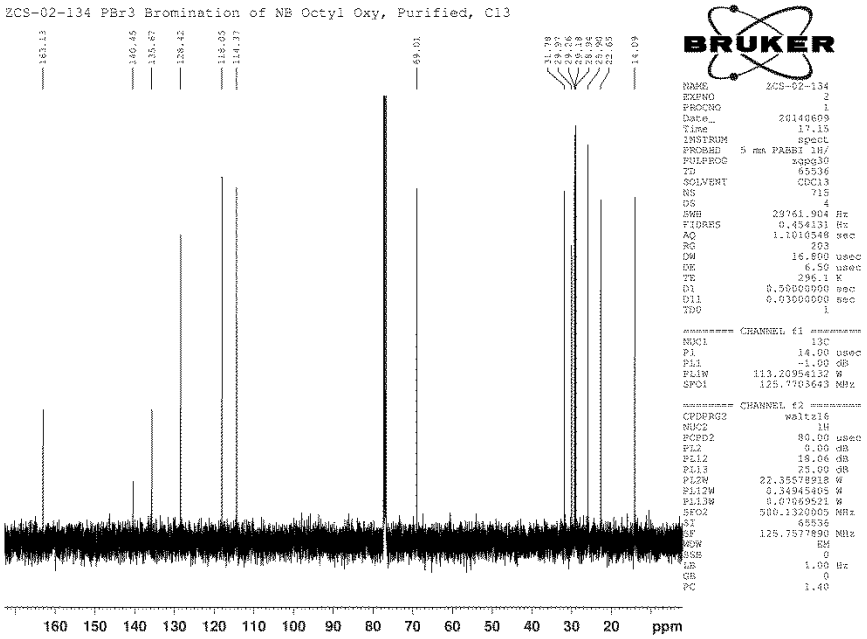

Compound **X1**, ^{1}H NMR (500 MHz, $CDCl_3$)

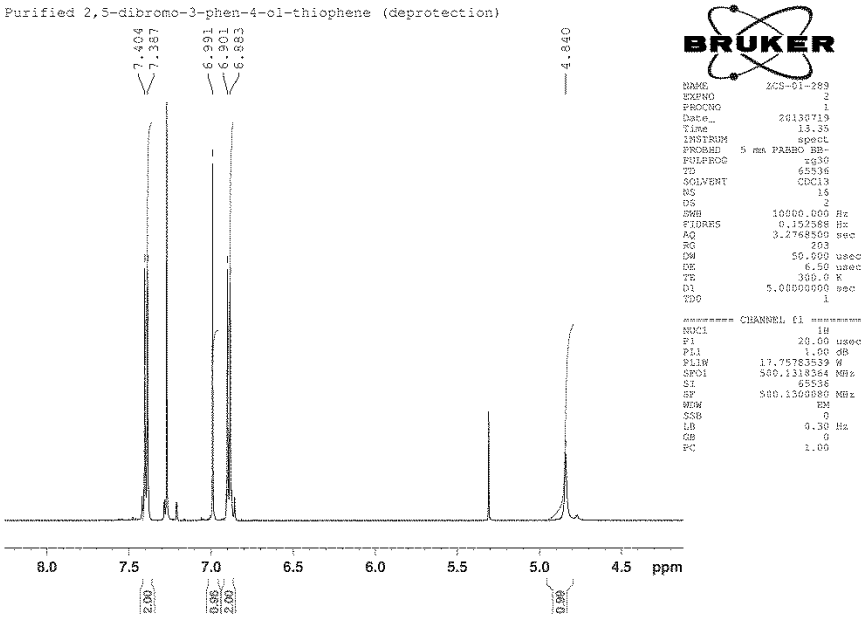

Compound **X1**, ^{13}C NMR (125 MHz, $CDCl_3$)

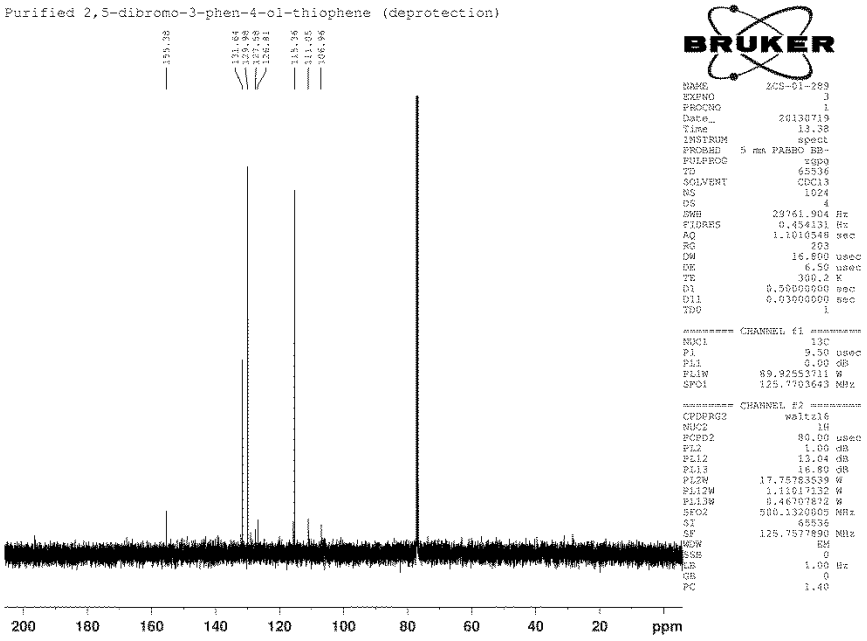

Compound **7**, ^{1}H NMR (500 MHz, $CDCl_3$)

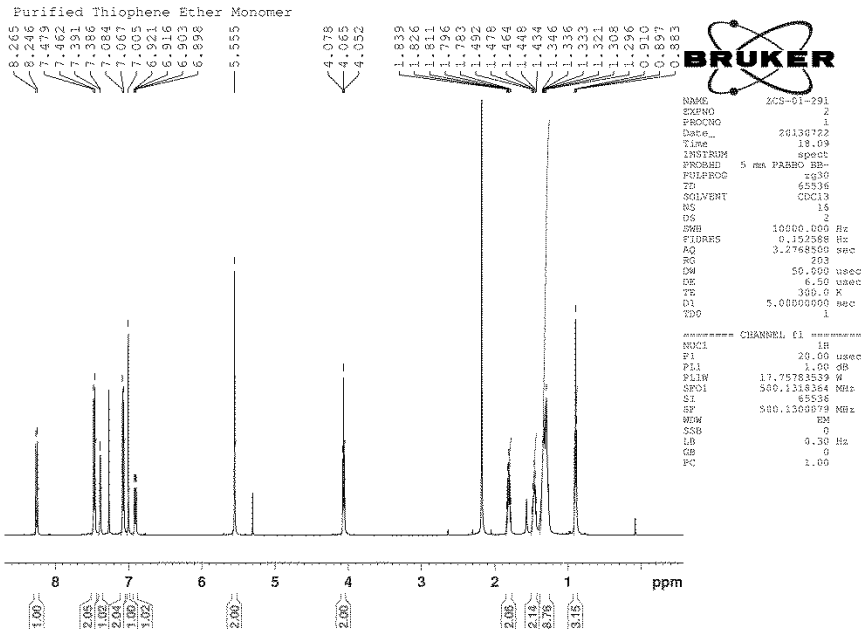

Compound **7**, ^{13}C NMR (125 MHz, $CDCl_3$)

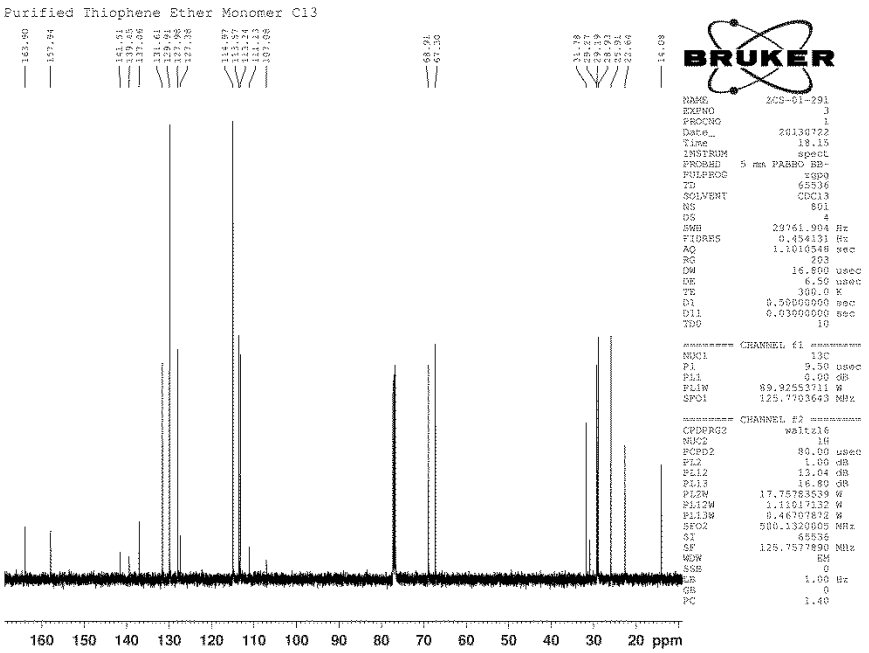

Compound **O3**, ^{1}H NMR (500 MHz, $CDCl_3$)

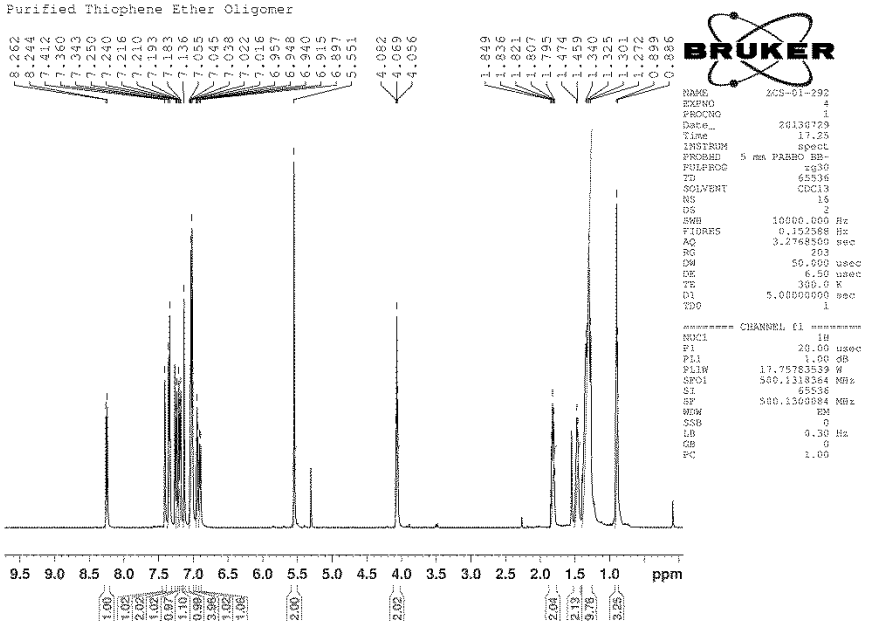

Compound **O3**, ^{13}C NMR (125 MHz, $CDCl_3$)

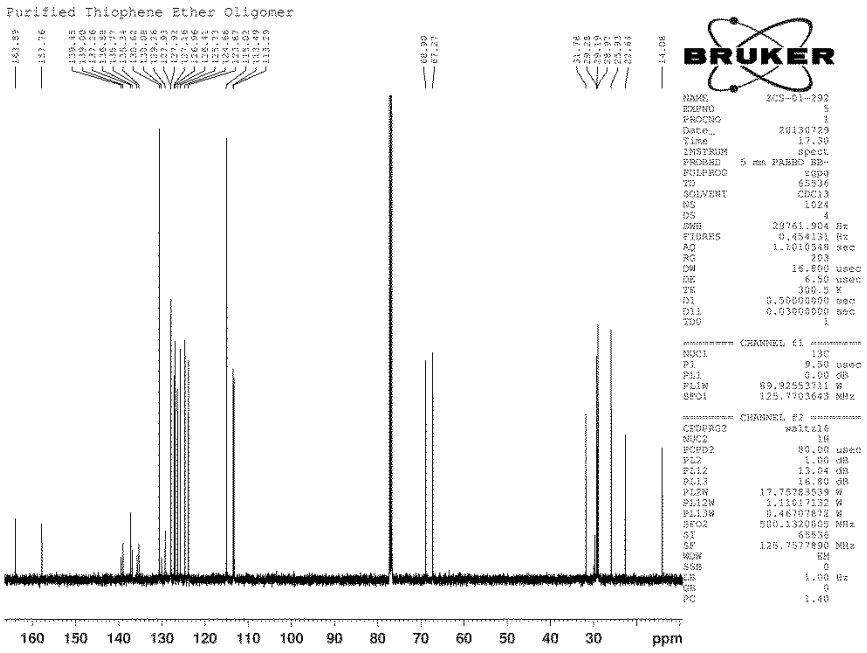

Compound **P3**, ^{1}H NMR (500 MHz, $CDCl_3$)

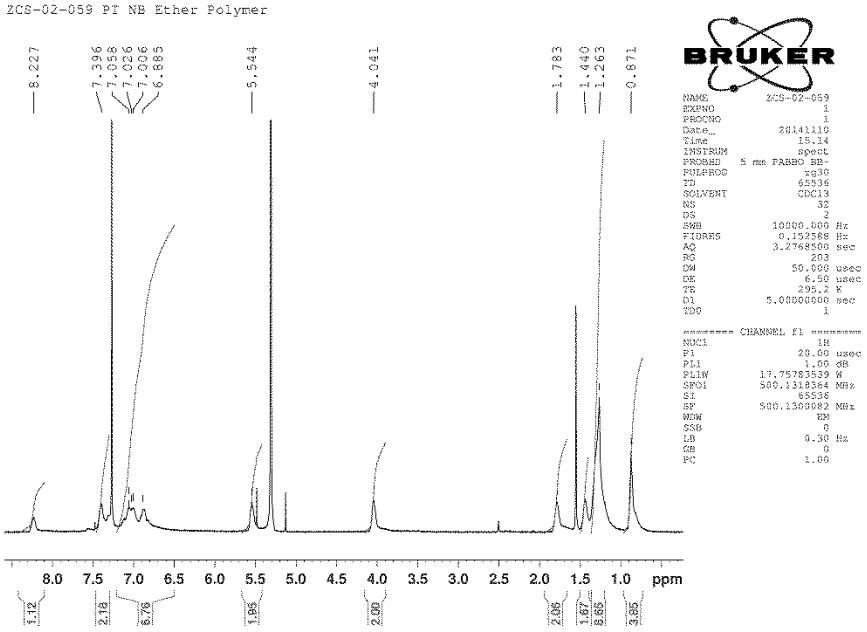

Compound **P5**, ^{1}H NMR (500 MHz, $CDCl_3$)

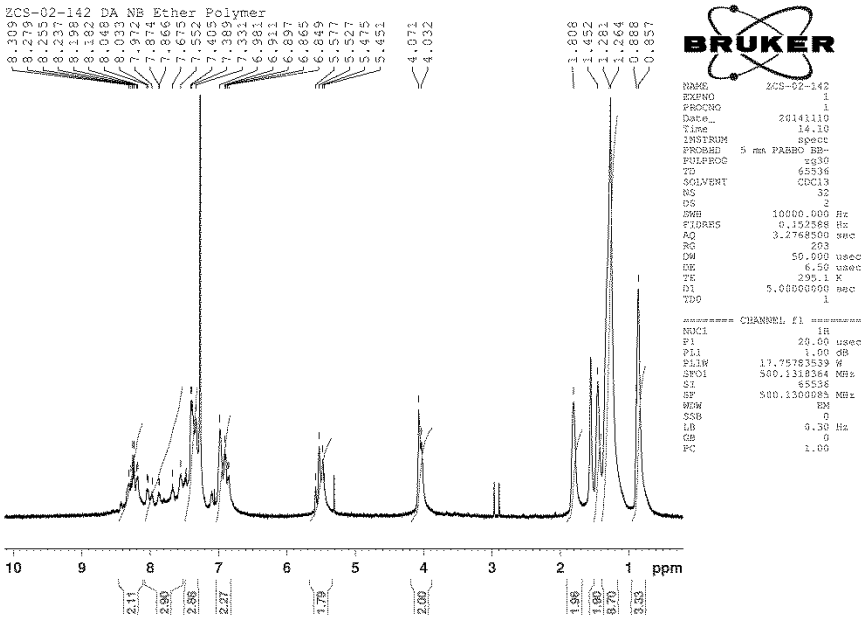

Compound **8**, ^{1}H NMR (500 MHz, $CDCl_3$)

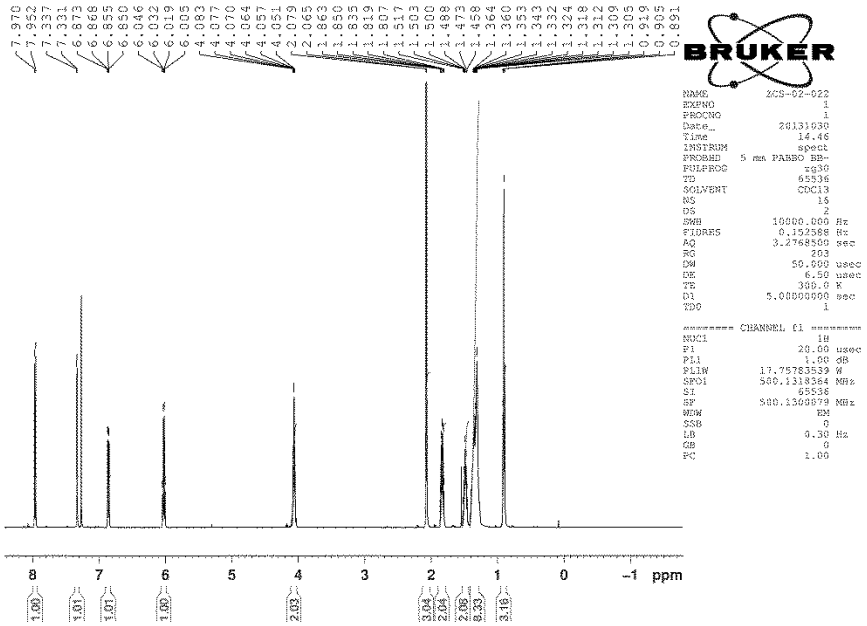

Compound **8**, ^{13}C NMR (125 MHz, $CDCl_3$)

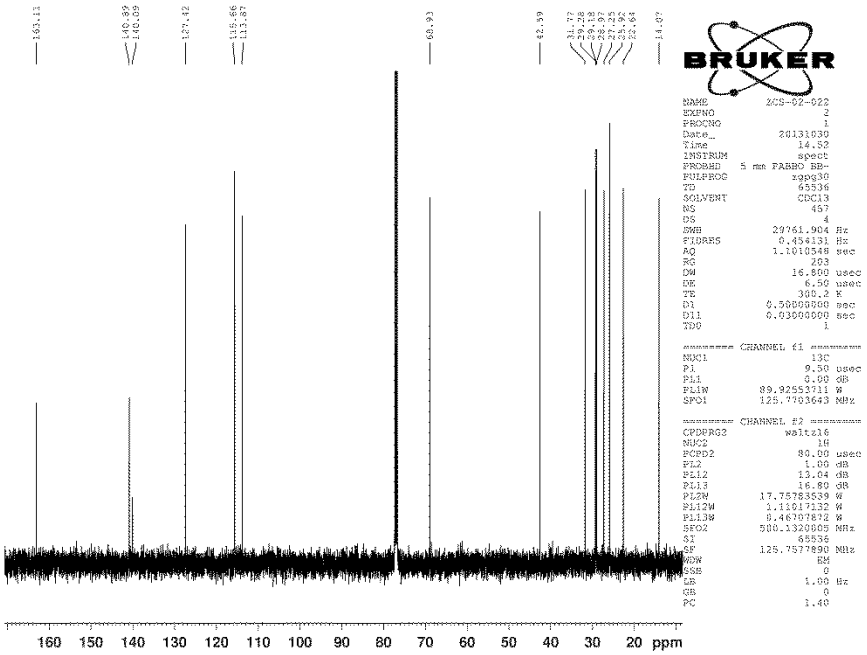

Compound **9**, ^{1}H NMR (500 MHz, $CDCl_3$)

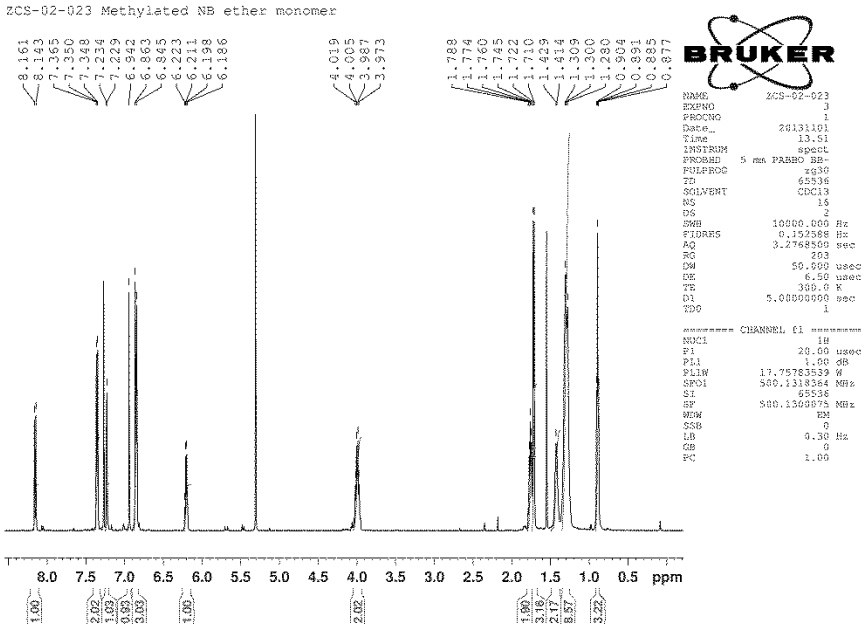

Compound **9**, ^{13}C NMR (125 MHz, $CDCl_3$)

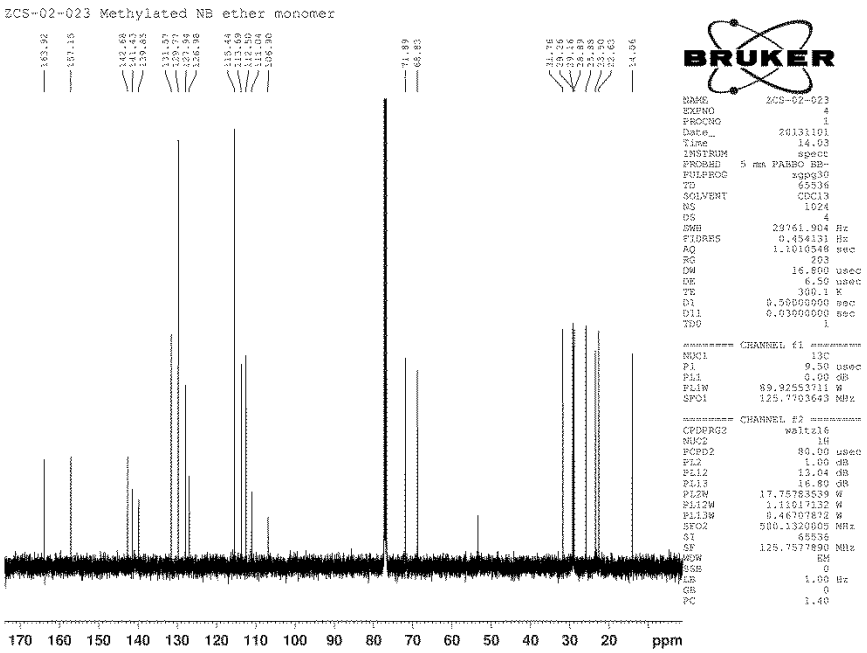

Compound **O4**, ^{1}H NMR (500 MHz, $CDCl_3$)

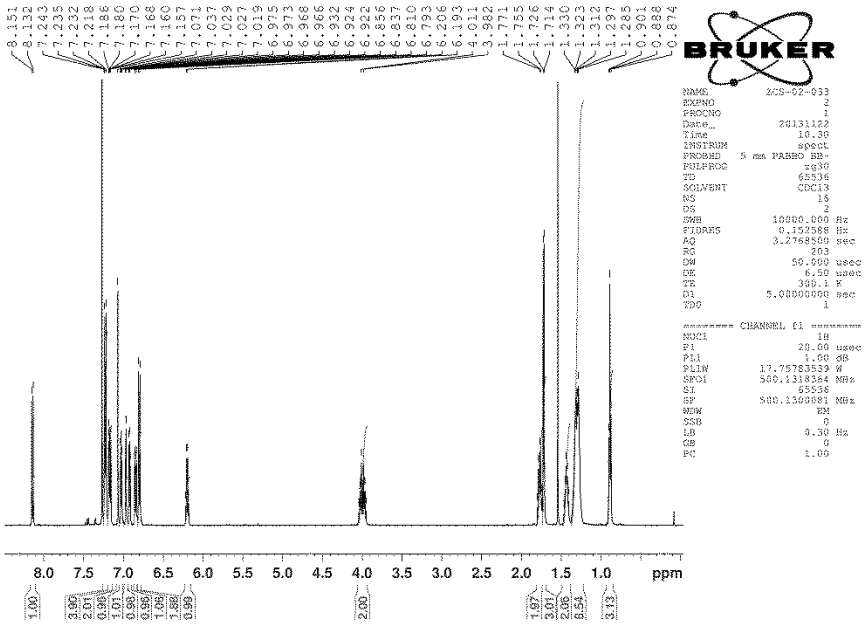

Compound **O4**, ^{13}C NMR (125 MHz, $CDCl_3$)

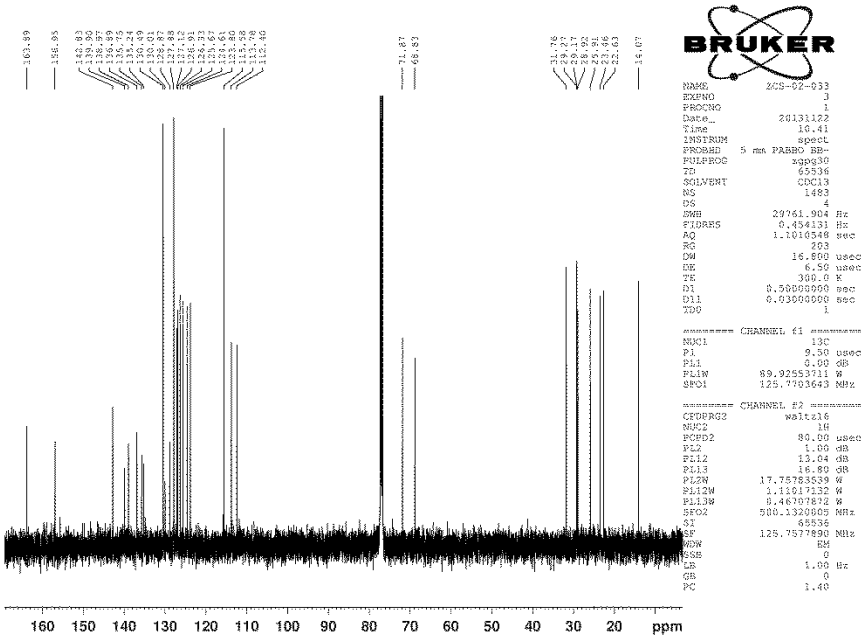

Compound **P4**, ^{1}H NMR (500 MHz, $CDCl_3$)

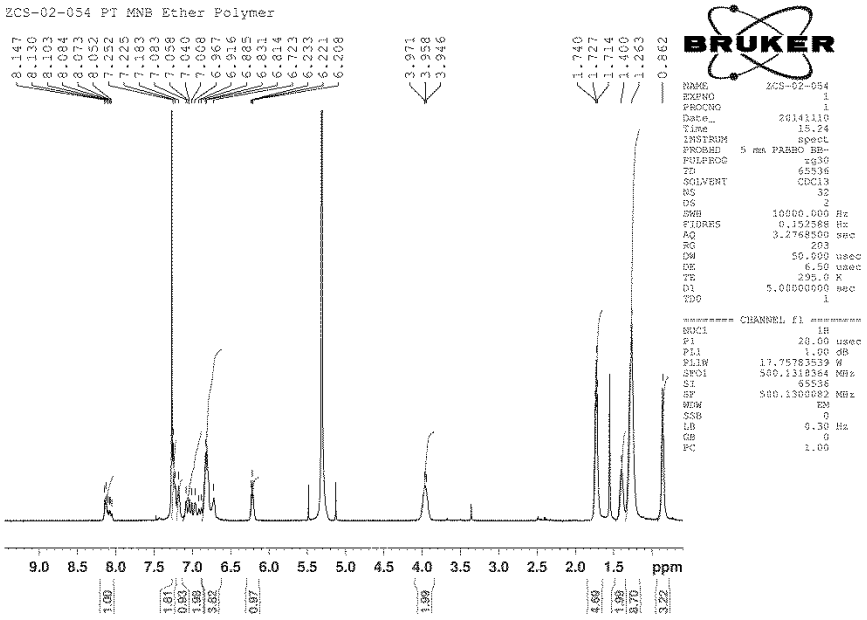

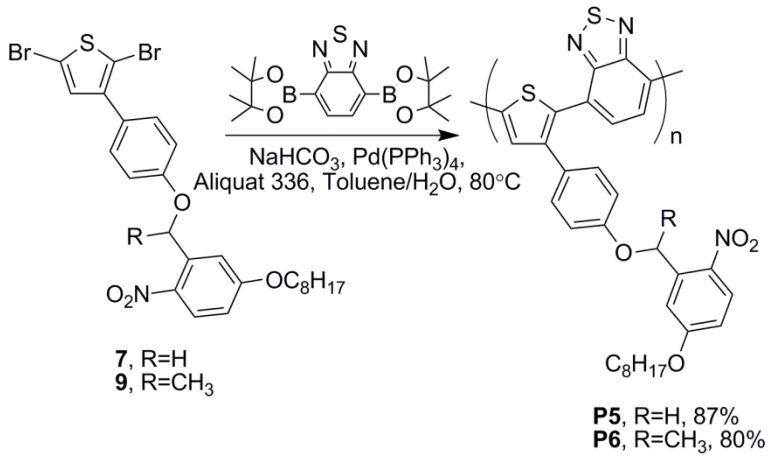

Compound **P6**, ^{1}H NMR (500 MHz, $CDCl_3$)

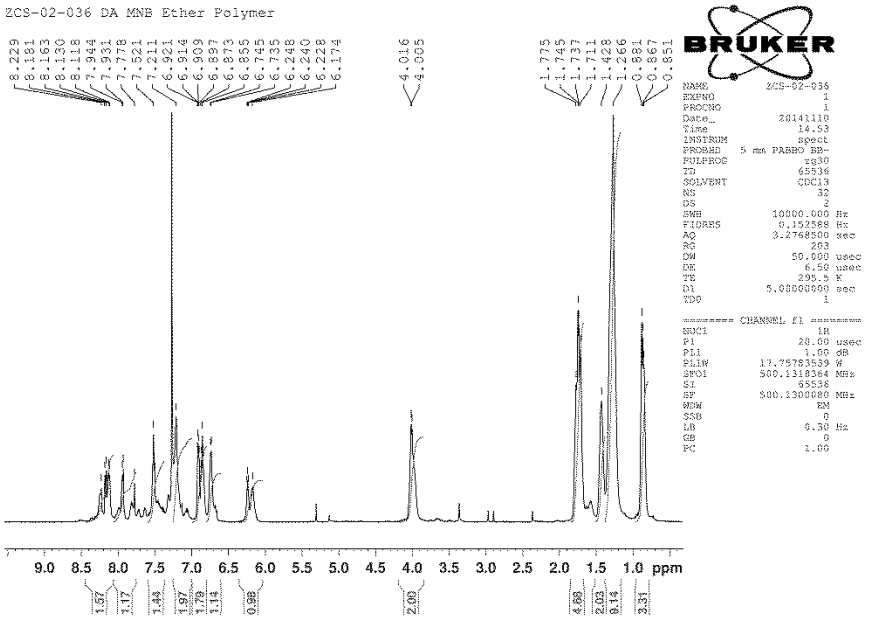

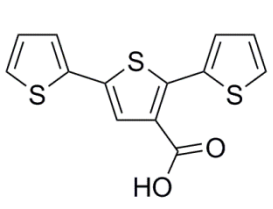

O5

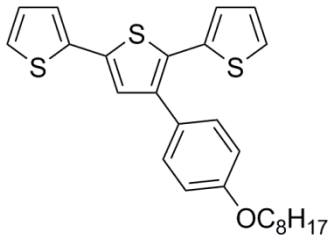

O6

Compound **O5**, ^{1}H NMR (500 MHz, $CDCl_3$)

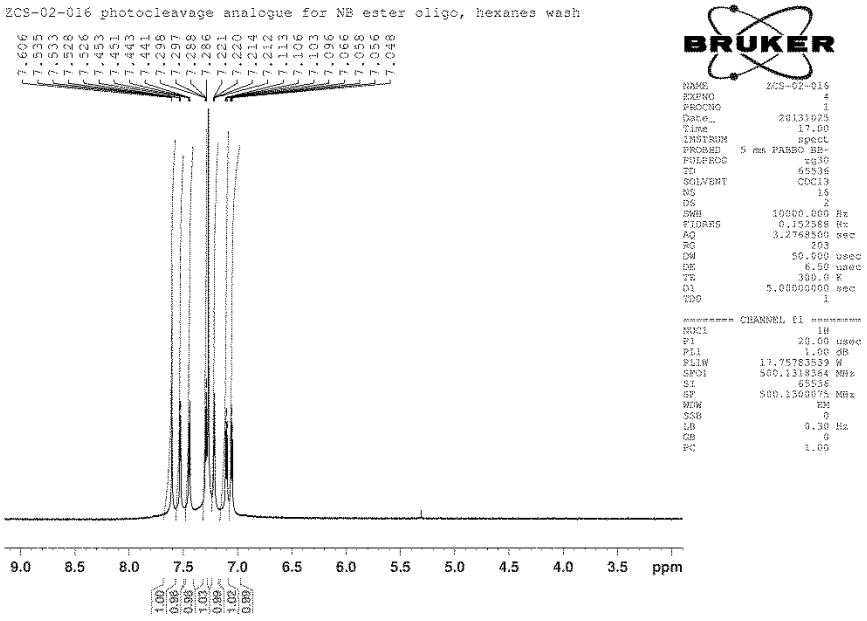

NAME	ZCS-02-016
EXPNO	4
PROCNO	1
Date_	20131025
Time	17.00
INSTRUM	spect
PROBHD	5 mm PABBO BB-
PULPROG	zg30
TD	65536
SOLVENT	CDCl3
NS	16
DS	2
SWH	10000.000 Hz
FIDRES	0.152588 Hz
AQ	3.2768500 sec
RG	203
DW	50.000 usec
DE	6.50 usec
TE	300.0 K
D1	5.00000000 sec
TD0	1
======== CHANNEL f1 ========	
NUC1	1H
P1	20.00 usec
PL1	1.00 dB
PL1W	17.75783539 W
SFO1	500.1318384 MHz
SI	65536
SF	500.1300075 MHz
WDW	EM
SSB	0
LB	0.30 Hz
GB	0
PC	1.00

Compound **O5**, ^{13}C NMR (125 MHz, $CDCl_3$)

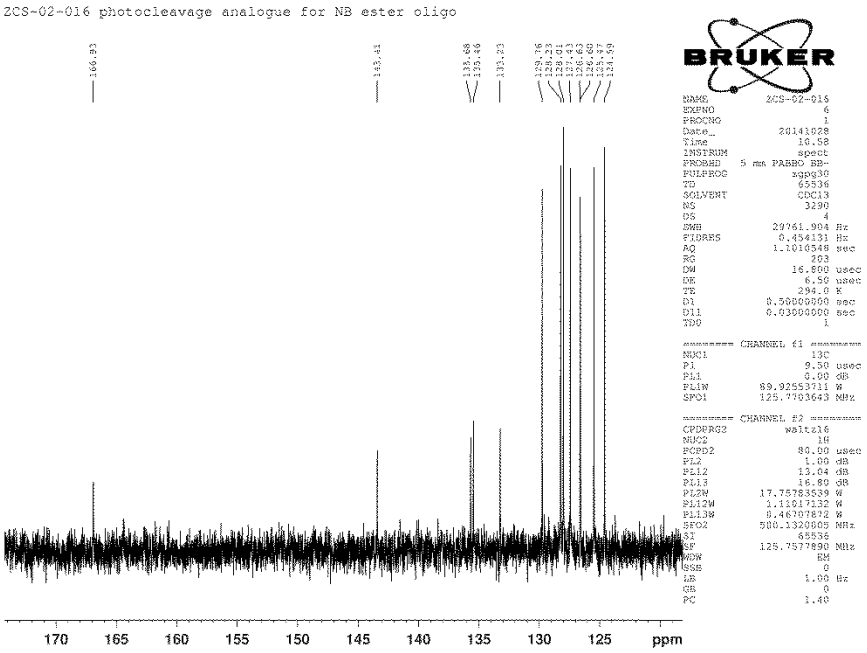

Compound **O6**, ^{1}H NMR (500 MHz, $CDCl_3$)

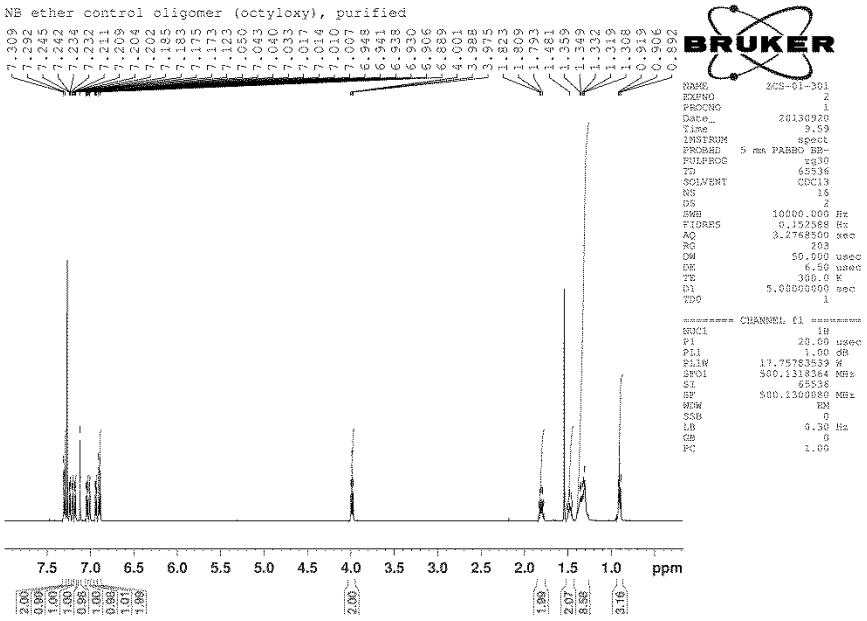

Compound **O6**, ^{13}C NMR (125 MHz, $CDCl_3$)

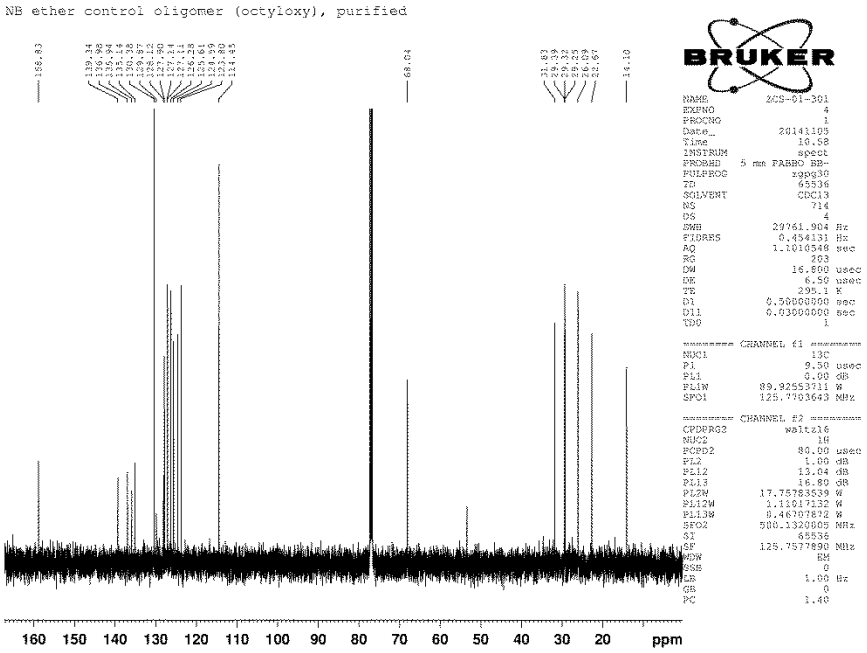

Compound **P7**, ^{1}H NMR (500 MHz, $CDCl_3$)

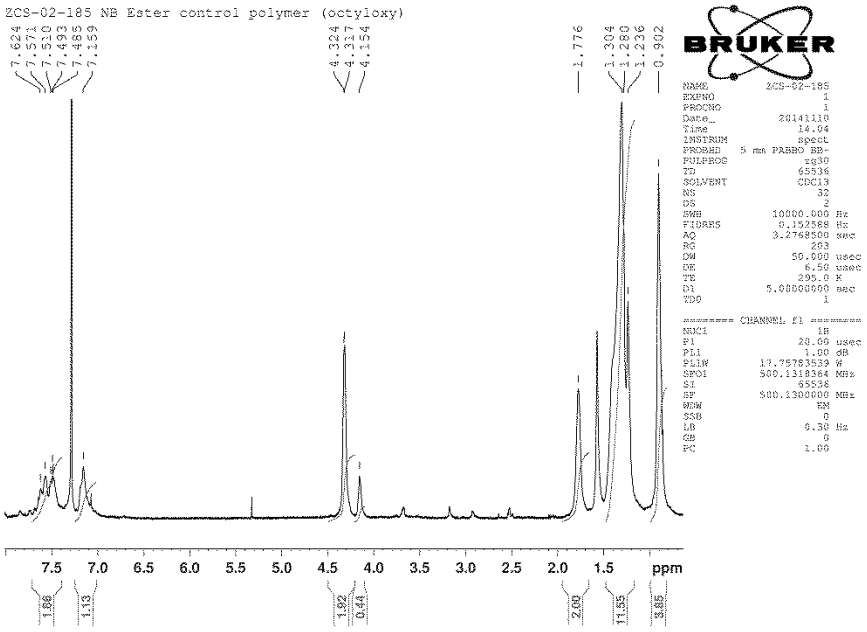

Compound **O7**, ^{1}H NMR (500 MHz, $CDCl_3$)

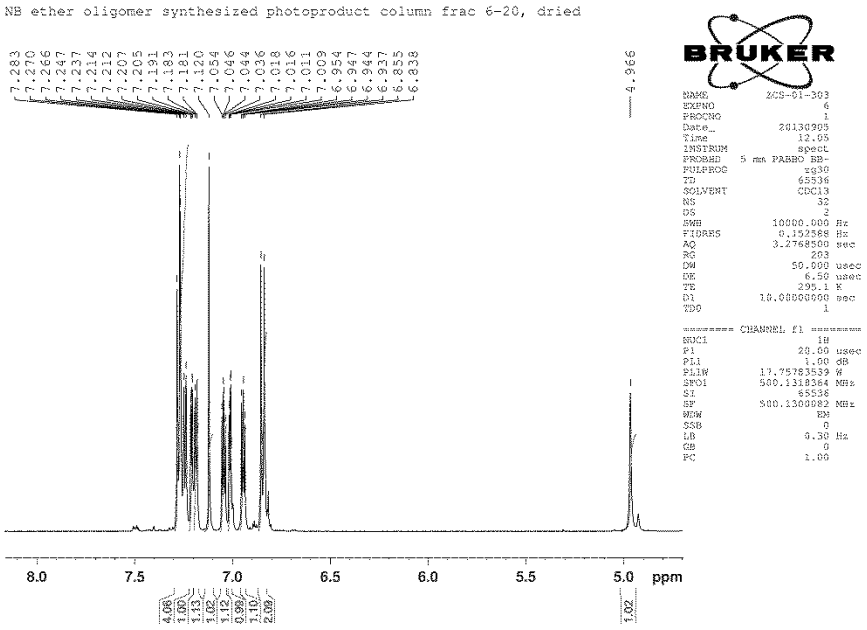

Compound **O7**, ^{13}C NMR (125 MHz, $CDCl_3$)

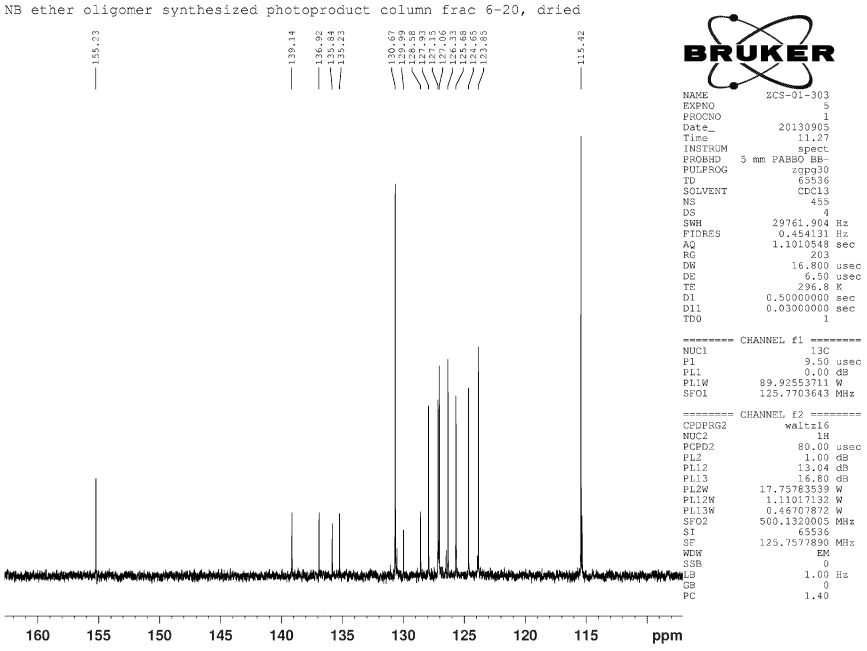

Absorbance and Emission Spectra

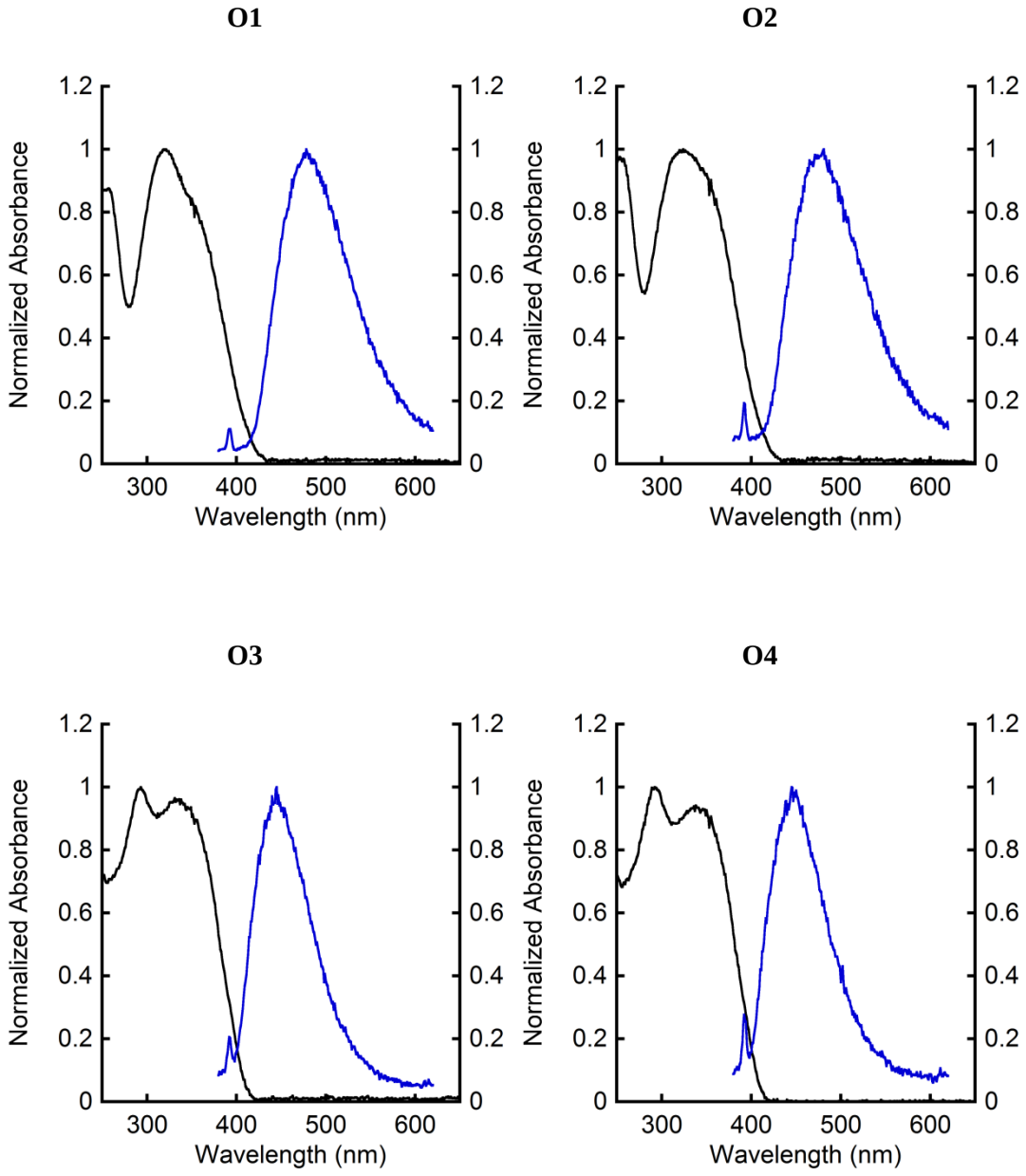
O1
O2
O3
O4
Normalized Absorbance
Wavelength (nm)
0
0.2
0.4
0.6
0.8
1
1.2
300
400
500
600

O5

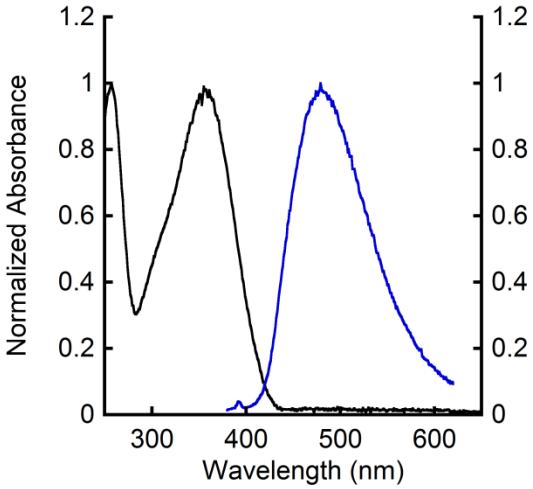
Normalized Absorbance
Wavelength (nm)
0
0.2
0.4
0.6
0.8
1
1.2
300
400
500
600

O6

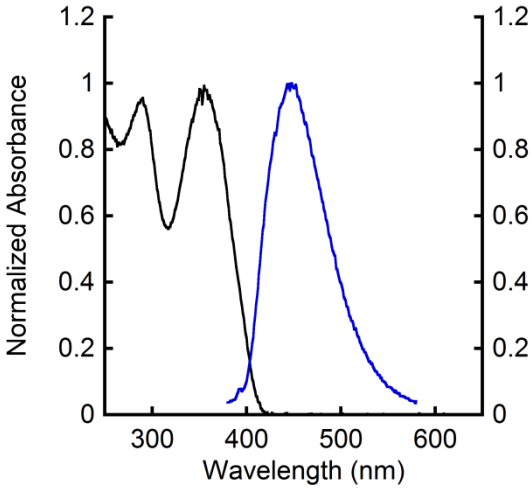
Normalized Absorbance
Wavelength (nm)
0
0.2
0.4
0.6
0.8
1
1.2
300
400
500
600

P1

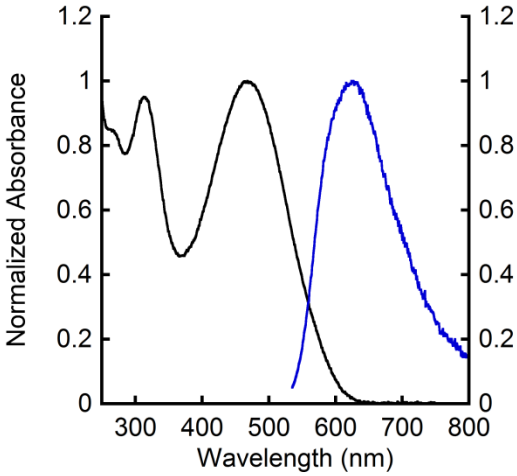
Normalized Absorbance
Wavelength (nm)
0
0.2
0.4
0.6
0.8
1
1.2
300
400
500
600
700
800

P2

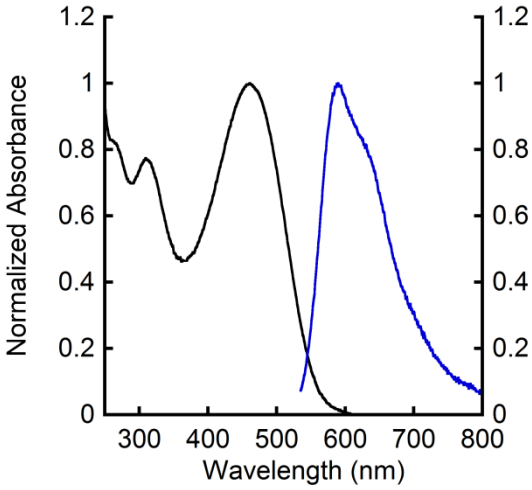
Normalized Absorbance
Wavelength (nm)
0
0.2
0.4
0.6
0.8
1
1.2
300
400
500
600
700
800

P3

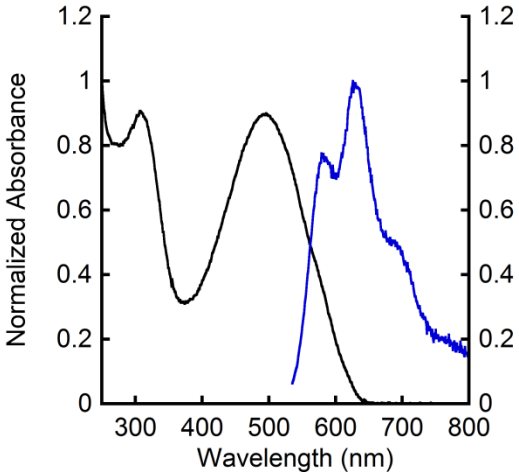
Normalized Absorbance
Wavelength (nm)
0
0.2
0.4
0.6
0.8
1
1.2
300
400
500
600
700
800

P4

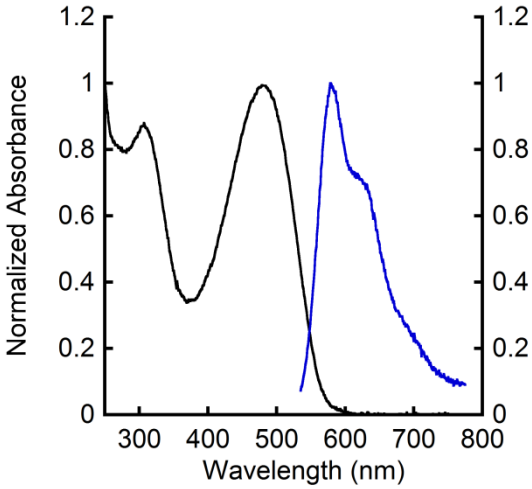
Normalized Absorbance
Wavelength (nm)
0
0.2
0.4
0.6
0.8
1
1.2
300
400
500
600
700
800

P5

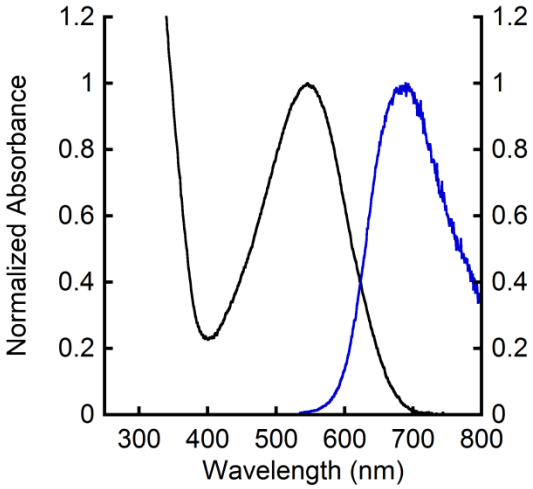
Normalized Absorbance
Wavelength (nm)
0
0.2
0.4
0.6
0.8
1
1.2
300
400
500
600
700
800

P6

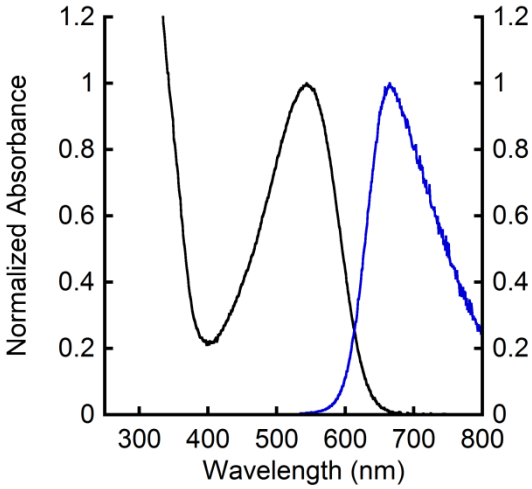
Normalized Absorbance
Wavelength (nm)
0
0.2
0.4
0.6
0.8
1
1.2
300
400
500
600
700
800

P7

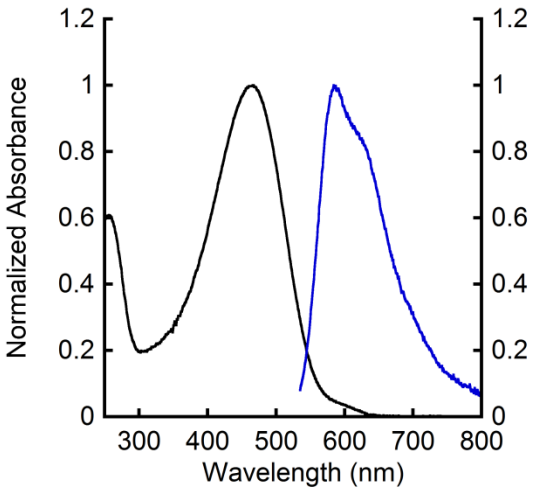
Normalized Absorbance
1.2
1
0.8
0.6
0.4
0.2
0
300
400
500
600
700
800
Wavelength (nm)

Chapter 4:

Photopatternable Low-Bandgap Conjugated Polymers

4.1 Developing Novel Low-Bandgap Polymers

Low-bandgap conjugated polymers (LBCPs) have received much attention in recent years due to their unique optoelectronic properties which differentiate them from most conjugated polymers, such as the ability to act as semiconductors and the ability to absorb light at longer wavelengths than typical CPs; these properties are due to the low-bandgap of the polymer which can be achieved by synthesizing a polymer consisting of alternating electron rich (donor) and electron poor (acceptor) units. This donor-acceptor motif lowers the bandgap of the material by creating a partial charge separation along the backbone of the polymer.[1]

LBCPs are roughly defined as polymers with a bandgap smaller than 2 eV.[2] In terms of absorbance, this can be defined as polymers that absorb light at wavelengths longer than 620 nm.[2] This means that LBCPs are ideal for applications that benefit from less energy required for excitation of an electron or applications where absorbance of light beyond 620 nm is advantageous. The use of low-bandgap conjugated polymers in organic photovoltaics (OPVs) has led to much of the interest in these materials.[3]

In a simplified description, OPVs are devices fabricated from predominantly organic materials that absorb photons emitted by the sun and convert the absorbed energy into a current. There is a subset of OPVs that utilize polymers for the active layers of the solar cell.[4] Much of the light emitted from the sun fails to make it to the surface of the earth due to the earth's atmosphere.

The intensity of the light that reaches the earth's surface can be seen in the air mass 1.5 solar spectrum (Figure 4.1).

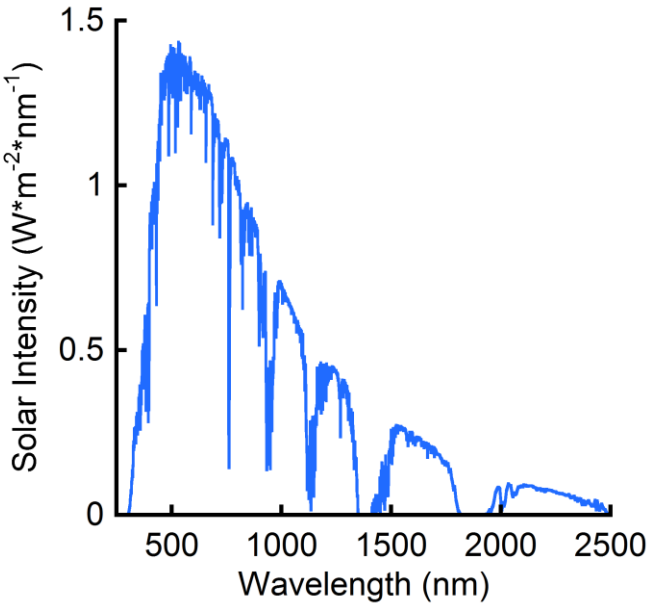

Figure 4.1 The air mass 1.5 solar spectrum depicting the intensity of the light reaching earth's surface at different wavelengths. Data provided by the National Renewable Energy Laboratory (NREL).

However, the photons that penetrate the earth's atmosphere best are photons of lower energy (longer wavelength). Therefore, it is often beneficial to utilize LBCPs in OPVs because there are more photons available to harvest in the near-infrared (NIR) region of the electromagnetic spectrum. To further broaden the absorbed wavelengths, tandem solar cells have been developed that combine multiple solar cells with different absorbance bands. The best reported polymer based tandem solar cells utilize LBCPs along with CPs that absorb light at shorter wavelengths (~300-600 nm).[5]

The maximum potential photon absorption for a material can be estimated based on the bandgap of the material. For example, poly(3-hexylthiophene)

(P3HT) has a bandgap of 1.9 eV or 650 nm and thus has the potential to absorb 22.4% of the light that reaches the earth's surface. However, if the material utilized has a bandgap of 1.2 eV or 1000 nm, it has the potential to absorb 53.0% of the light that reaches the earth's surface.[2] While these figures are based on idealized performance and surroundings, it is clear that low-bandgap materials can harvest more photons than materials with larger bandgaps.

While many of the characteristics of LBCPs are very appealing from an applications perspective, one issue with LBCPs is that they are often made using bulkier and more rigid monomers than other CPs, so solubility of the polymer is harder to achieve.[6,7] This is likely due to incompatibility of the physical properties of the LBCPs, such as the Hansen Solubility Parameter.[8] However, the ideal processing of LBCP materials is solution based, and thus solubility in organic solvents is required. That is why we have developed LBCPs functionalized with photocleavable NB linked solubilizing side chains.

4.2 Experimental Design

Our initial design for our low-bandgap polymer was based around the iso-indigo (Chart 4.1) monomer which has become popular in recent years due to its low-bandgap properties and due to its relative ease of synthesis.[9-11] However, the last step of the monomer synthesis, the linking of the NB group to the monomer, failed. This led to a shift from the iso-indigo design to a thiadiazoloquinoxaline (TQ, Chart 4.1) based system. The synthesis of the TQ monomer was adapted from several previously published studies.[12-15]

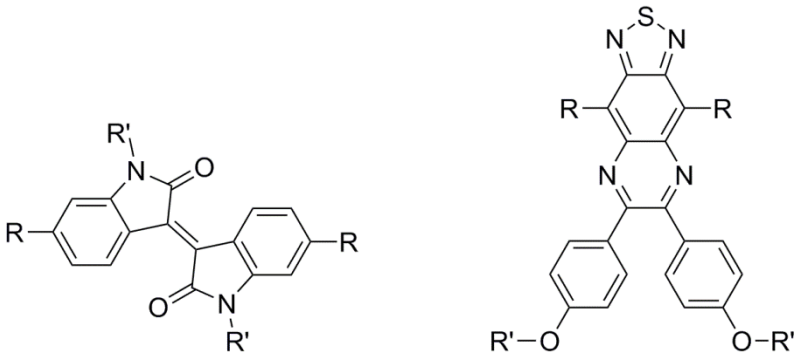

Iso-Indigo **TQ**

Chart 4.1 The two monomer designs pursued in this research. The Iso-indigo monomer was quickly phased out in favor of the TQ monomer due to the ease of attachment of the NB side chains. In each structure R is where the polymer backbone extends from and R' is where the NB solubilizing side-chain would be attached.

The TQ monomer was chosen due to the presence of ether solubilizing chains normally present in the TQ moiety and previous work that had shown that its copolymerization with thiophene led to conjugated polymers with very low-bandgaps.[16] The presence of an ether side-chain was an ideal location for attaching the NB ether photocleavable group. However, we found that placing the NB group in that position (R' in Chart 4.1) resulted in a 20 % decrease in absorbance of the polymer upon irradiation. This decrease upon irradiation is indicative of degradation of the conjugated polymer backbone. This led to the synthesis of a control polymer which, upon irradiation, showed less than 5 % degradation. This indicated that the NB group would need to not be directly attached to the TQ moiety in our low-bandgap polymer. The revelation that the NB group needed to be separate from the TQ moiety led to the copolymerization of the control TQ monomer with a NB containing thiophene monomer similar to

those previously developed in our lab. These polymers were then studied in patterning and multilayer experiments.

4.3 Synthesis of Low-Bandgap Oligomers and Polymers

We initially prepared the dinitrobenzyl ether substituted TQ monomer (**10**) in order to synthesize the thiophene-*co*-TQ polymer (**P1**). This overall synthesis can be broken down into several parts, starting with the NB substituted diketone (**6**, Scheme 4.1).

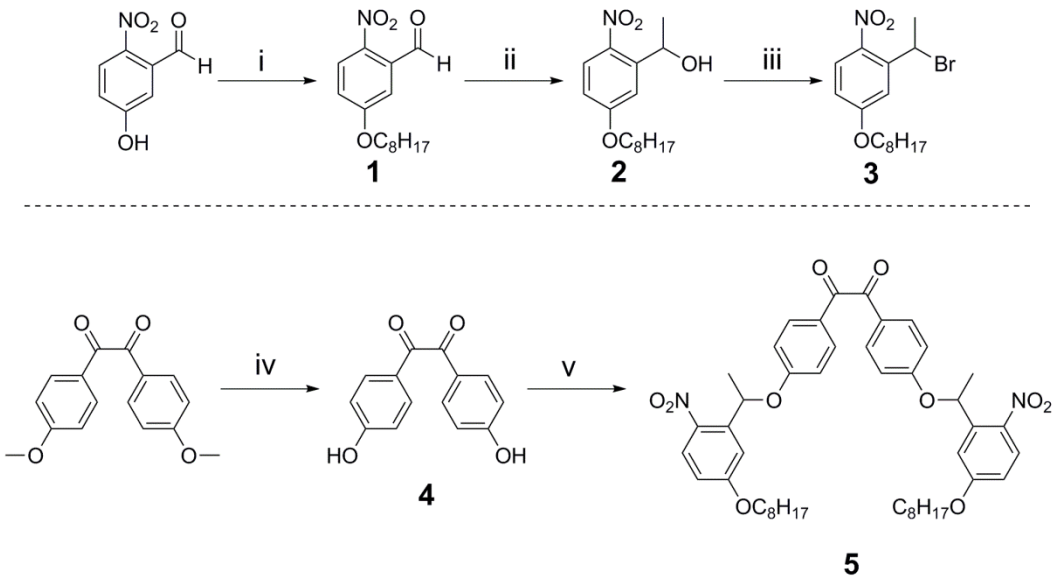

Scheme 4.1 i) *n*-$C_8H_{17}Br$, K_2CO_3, DMF, 50 °C, >95 %; ii) $TiCl_4$, CH_3MgBr, Et_2O, -78°C, 95 %; iii) CBr_4, PPh_3, 52 %; iv) 48% HBr, acetic acid, reflux, 60 %; v) **3**, K_2CO_3, DMF, 50 °C, 63 %.

The synthetic route begins with the alkylation of 5-hydroxy-2-nitrobenzaldehyde using *n*-bromooctane to yield **1**. Alkylation of **1** with $CH_3MgBr/TiCl_4$ gave the corresponding secondary nitrobenzyl alcohol **2**. A halo-de-hydroxylation reaction of methylated benzyl alcohol **2** yielded the corresponding benzyl bromide with

PPh_3/CBr_4 (**3**). This benzyl bromide could then be coupled with diphenol **4**, synthesized via deprotection of anisil by 48% HBr, to yield nitrobenzyl functionalized diketone **5**. Diketone **5** represents one half of the eventual monomer needed for the NIR absorbing polymer

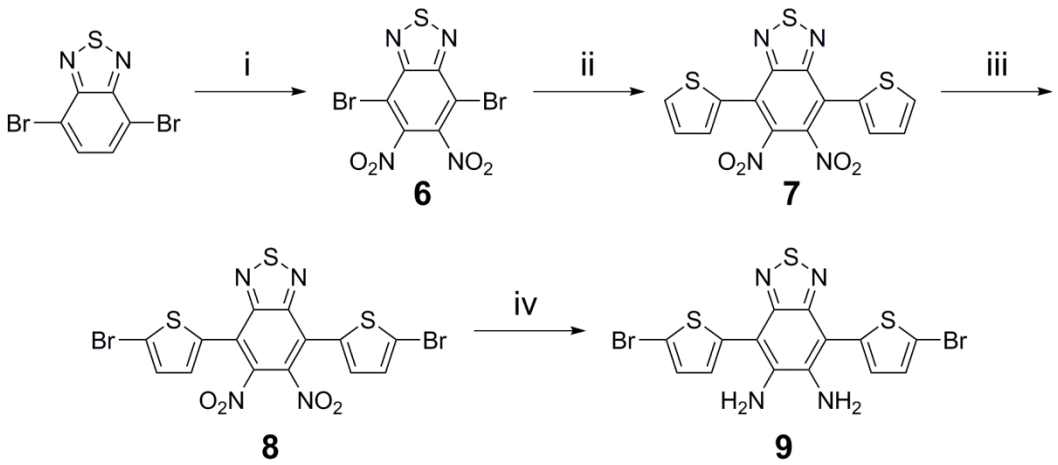

Scheme 4.2 i) conc. H_2SO_4, fuming HNO_3, 0 °C, 48 %, ii) 2-(tributylstannyl)thiophene, $PdCl_2(PPh_3)_2$, THF, 60 °C, 70 %, iii) NBS, DMF, 60 °C, 93 %; iv) Fe (0), acetic acid, 80 °C, 90 %.

The second half of the NIR monomer synthesis, which was adapted from previously reported procedures[14,16], began with the nitration of 4,7-dibromobenzo[*c*]-1,2,5-thiadiazole via fuming nitric acid to yield **6**, which was then used in a Stille reaction with 2-(tributylstannyl)thiophene to yield **7** (Scheme 4.2). The terminal thiophene rings were then brominated at the 5-position via *n*-bromosuccinimide (NBS) to yield **8**. The nitro groups of **8** were then reduced with Fe (0) to yield diamine **9**.

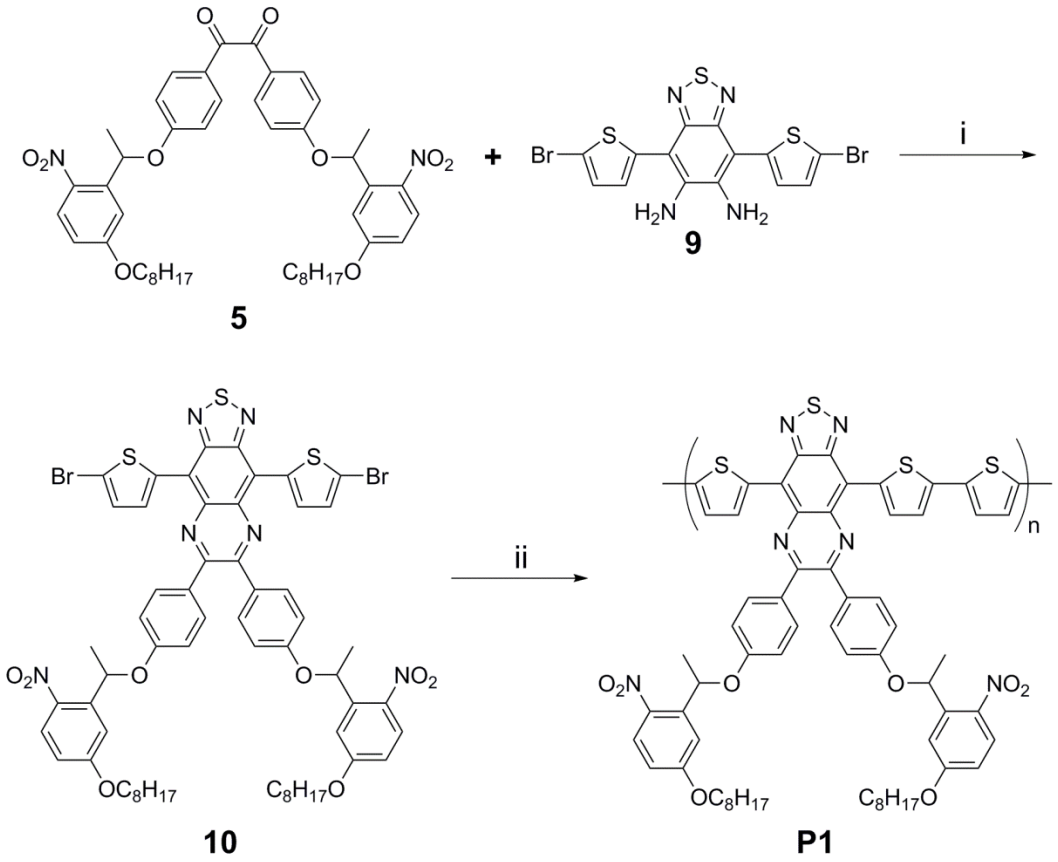

Scheme 4.3 i) acetic acid, reflux, 46 %; ii) 2,5-bis(trimethylstannyl) thiophene, $Pd_2(dba)_3$, tri-*o*-tolylphosphine, toluene, 90°C, 64 %.

Diamine **9** and diketone **5** were combined via condensation reaction in acetic acid to yield NIR monomer **10** (Scheme 4.3). Monomer **10** was then reacted with 2,5-bis(trimethylstannyl) thiophene under Stille conditions to yield the low-bandgap polymer **P1**.

To further probe our ability to change the solubility of **P1** using light, a control polymer, **P2**, was necessary (Scheme 4.4). Polymer **P2** is structurally identical to **P1** with one key difference: the nitro group is not present on the side chain, thus removing the photoreactivity of the side chain.

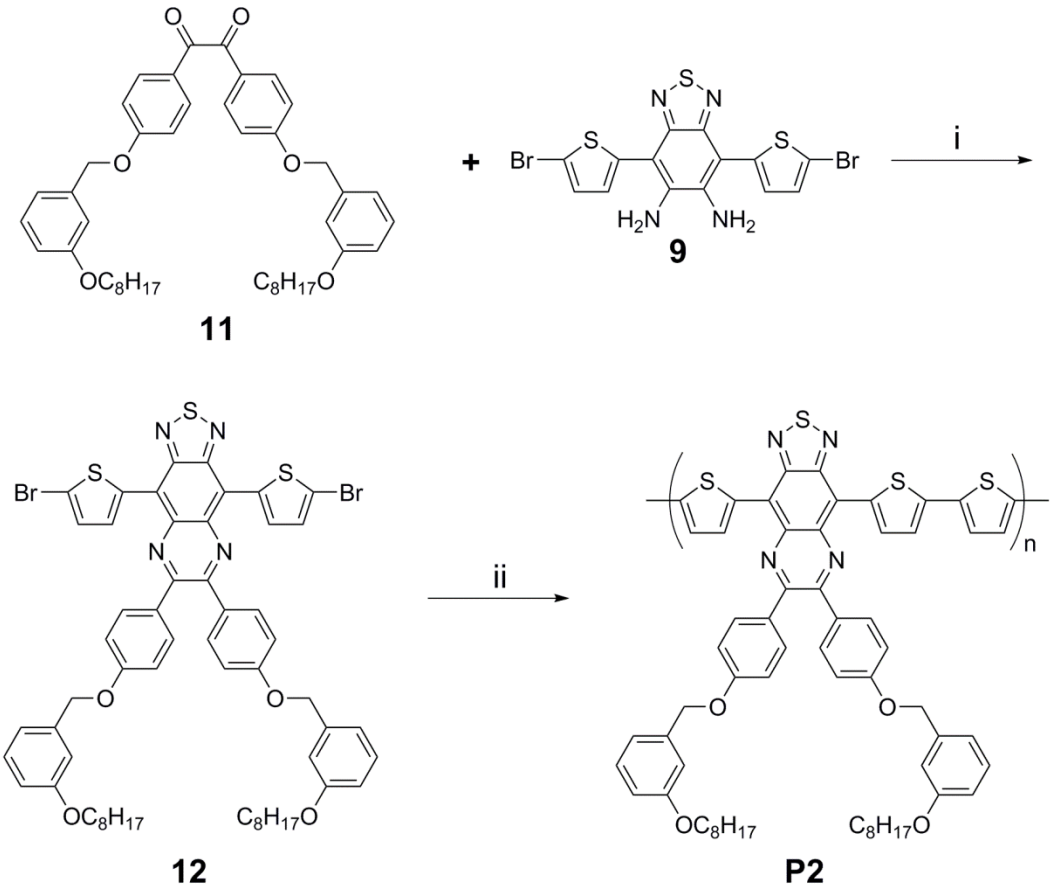

Scheme 4.4 i) acetic acid, reflux, 46 %; ii) 2,5-bis(trimethylstannyl) thiophene, $Pd_2(dba)_3$, tri-*o*-tolylphosphine, toluene, 90 °C, 26 %.

Compound **11** was synthesized via Williamson ether synthesis between **4** and 1-(bromomethyl)-3-(octyloxy)-benzene. Control monomer **12** was then synthesized via condensation reaction between **9** and **11**. Monomer **12** was polymerized via Stille cross-coupling conditions with 2,5-bis(trimethylstannyl) thiophene to yield **P2**.

To better understand the degradation pathway of our polymeric materials, we synthesized polymers using control TQ monomer **12** as well as a NB ether containing thiophene monomer **16**. These polymers (**P3** and **P4**) were designed to

still be photoreactive like **P1**, but the photocleavable group would be attached to the thiophene-based monomer instead of the TQ monomer (Scheme 4.5).

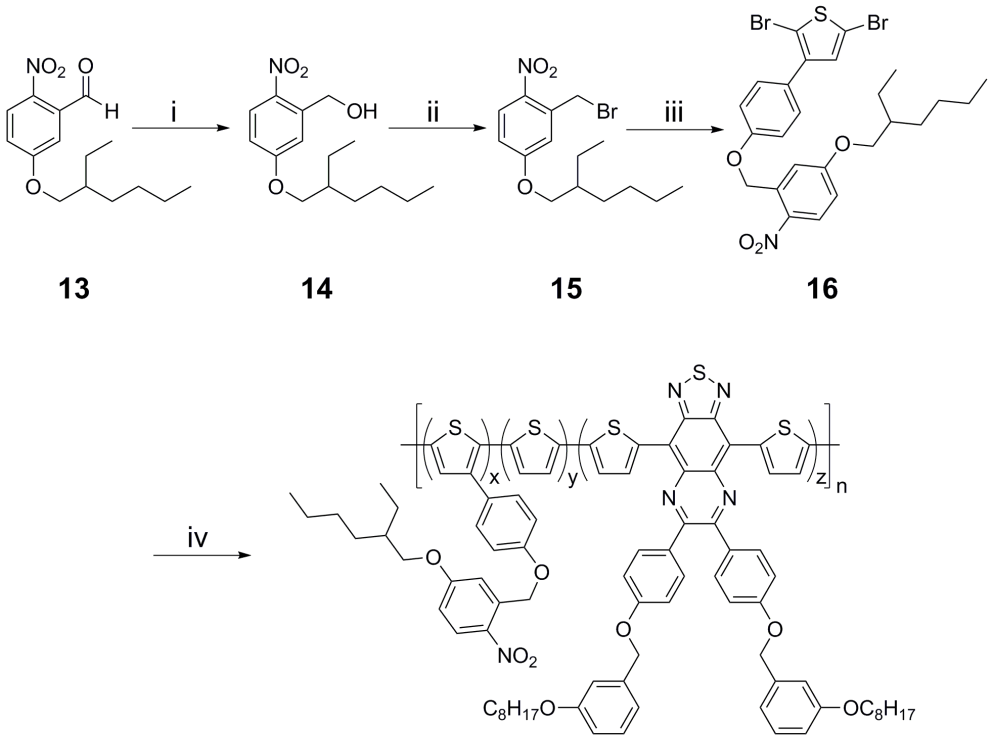

P3: x=0.50, y=1.0, z=0.50
P4: x=0.82, y=1.0, z=0.18

Scheme 4.5 i) $NaBH_4$, MeOH, 99 %; ii) PBr_3, 0°C, 34 %; iii) 4-(2,5-dibromothiophen-3-yl)phenol, K_2CO_3, DMF, 50°C, 36 %; iv) **12**, 2,5-bis(trimethylstannyl) thiophene, $Pd_2(dba)_3$, tri-*o*-tolylphosphine, toluene, 90 °C, **P3:** 33 %, **P4:** 37 %.

Compound **13** was synthesized via Williamson ether synthesis between 5-hydroxy-2-nitrobenzaldehyde and 2-ethylhexyl bromide. The aldehyde in **13** was then reduced with $NaBH_4$ to yield **14**, which was then converted to the NB bromide **15** via PBr_3. A Williamson ether synthesis was then used to combine **15** with 4-(2,5-dibromothiophen-3-yl)phenol to make the NB ether functionalized

thiophene monomer **16**. Monomer **16** was then used to synthesize **P3** and **P4** via Stille cross-coupling polymerization with 2,5-bis(trimethylstannyl) thiophene.

The system used in **P3** and **P4** was further refined in **P5** which was functionalized with a methylated nitrobenzyl (MNB) side-chain that is more reactive than the original NB side-chain (Scheme 4.6).

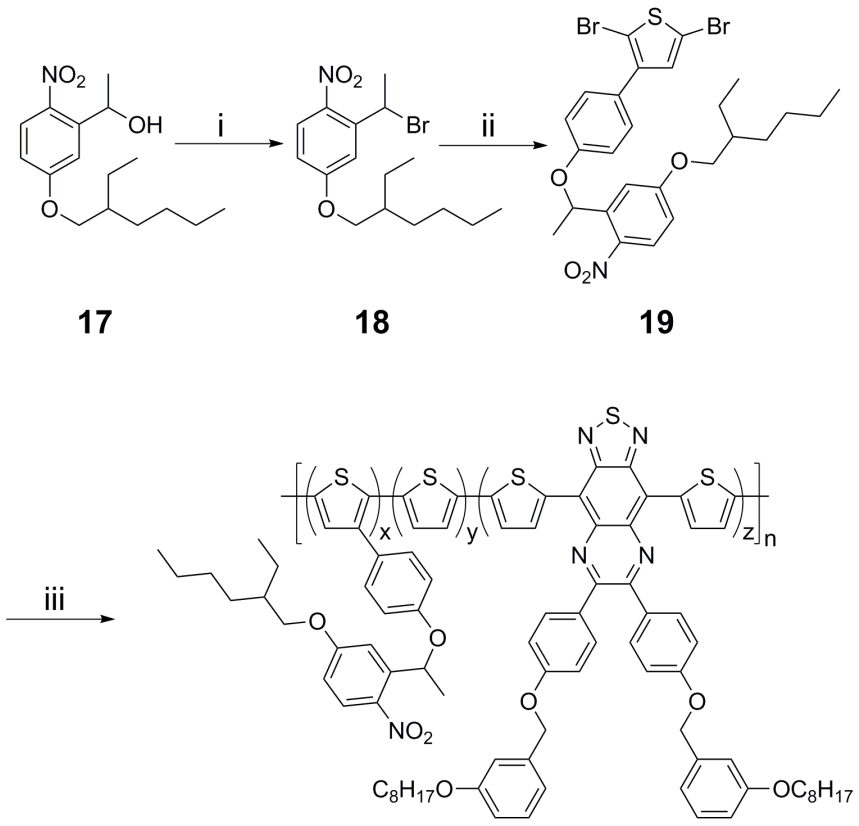

Scheme 4.6 i) CBr_4, PPh_3, 97 %; ii) 4-(2,5-dibromothiophen-3-yl)phenol, K_2CO_3, DMF, 50°C, 34 %; iii) **12**, 2,5-bis(trimethylstannyl) thiophene, $Pd_2(dba)_3$, tri-*o*-tolylphosphine, toluene, 90 °C, 37 %.

Compound **17** was synthesized via a modified Grignard reaction of **13** using CH_3MgBr and $TiCl_4$. **17** was converted to the MNB bromide via an Appel reaction using CBr_4 and triphenylphosphine to yield **18**. A Williamson ether

synthesis was used to combine **18** with 4-(2,5-dibromothiophen-3-yl)phenol to yield MNB ether functionalized thiophene monomer **19**. Monomer **19** was then used to synthesize **P5** via Stille cross-coupling polymerization with 2,5-bis(trimethylstannyl) thiophene.

4.4 Spectral Properties of Synthesized Low-Bandgap Materials

Table 4.1 summarizes the properties of absorbance of the LBCPs studied here, while Figure 4.2 shows the normalized absorbance spectra of LBCPs **P1**-**P5**.

Table 4.1 The optical and physical properties of polymers **P1**-**P5**.

	λ_{max} (abs), nm	M_n, g/mol	PDI
P1	1030	12,200	4.60
P2	876	2,700	1.73
P3	887	6,400	3.06
P4	835	9,400	3.05
P5	897	7,600	2.59

The absorbance spectra of all of the synthesized polymers exhibit three distinct bands (Figure 4.2). The first band, found around 300 nm, likely corresponds to NB side-chain, or, in the case of control polymer **P2**, the benzyl side-chain. This band is often observed in molecules functionalized with NB groups.[17-20] The second band, found around 500 nm, is typical of donor-acceptor polymers.[16] The third band, found in the NIR region (λ_{max} 850-1100 nm for **P1**-**P5**), corresponds to the TQ portion of the polymer. This absorbance is typical of TQ containing conjugated polymers which tend to exhibit an absorbance band in the 800-2000 nm range.[12,13,16]

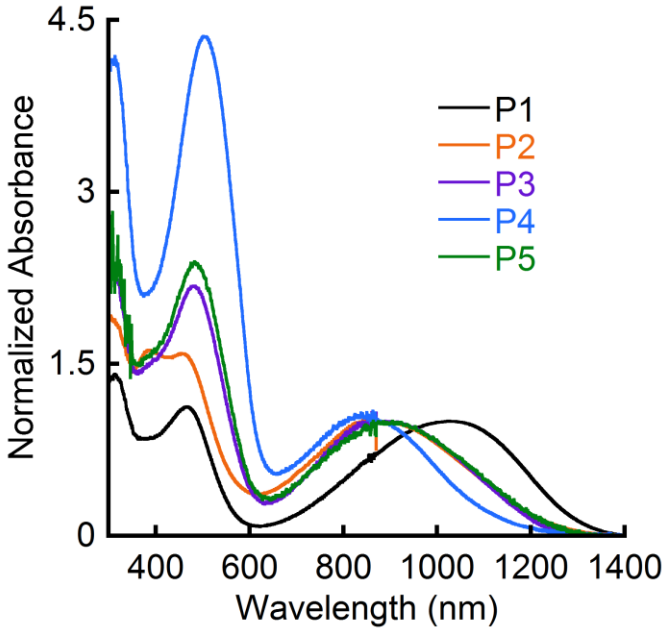

Figure 4.2 The absorbance spectra of films of **P1**-**P5**, normalized with respect to the NIR band.

The combination of the two major bands from the absorbance spectra show that all of these polymers exhibit good coverage over a broad range of wavelengths, which is advantageous for OPV applications.[21-23]

4.5 Photoinduced Film Insolubility

In order to test photoinduced film insolubility of **P1**-**P5**, films of the polymers were irradiated with UV light and then washed with chloroform. The absorbance of the film was measured before irradiation, after irradiation, and after washing. The main characteristics that were focused on during these experiments were the decrease in absorbance of the NIR band after irradiation and after washing with chloroform. The initial decrease after irradiation is indicative of the degradation of the polymer, while the decrease in the absorbance after the

chloroform wash is indicative of the retention of the polymer film. The results of the irradiation experiment of **P1** can be seen in Figure 4.3.

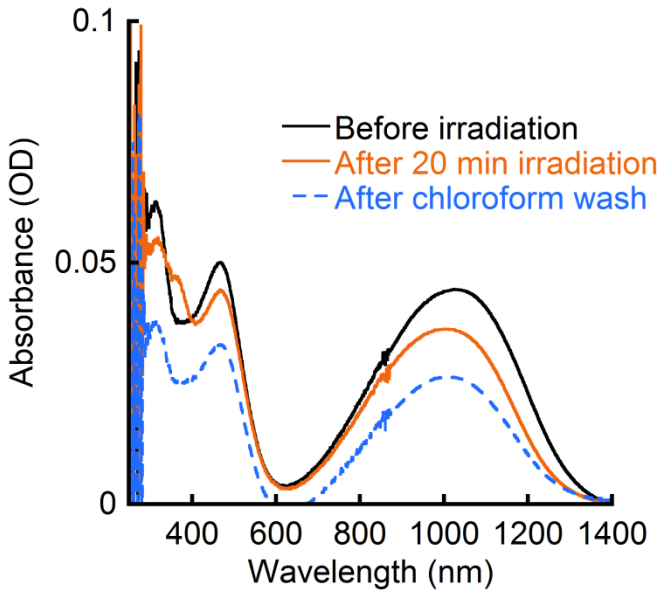

Figure 4.3 Absorbance spectra of the NIR MNB Ether polymer **P1** (black), which was irradiated at 365 nm for 20 minutes (orange), and washed with chloroform (blue dashed).

Before irradiation the film displays the aforementioned three characteristic bands observed when analyzing these materials. After irradiation (20 min, 365 nm) there is a decrease in absorbance of all three bands and the growth of a new band around 400 nm. The decrease in absorbance of the NB moiety (300 nm band), coupled with the growth of a band at 400 nm is indicative of photocleavage of the NB side chain, with the new band corresponding to the NB photocleavage byproduct. However, the decrease in the two bands corresponding to the polymer backbone is indicative of degradation of the conjugated polymer backbone. This was thought to be due to photo-oxidation of the backbone. To test this, films of

P1 were irradiated in the presence of oxygen, and in the absence of oxygen to observe any difference in the degradation of the films (Figure 4.4).

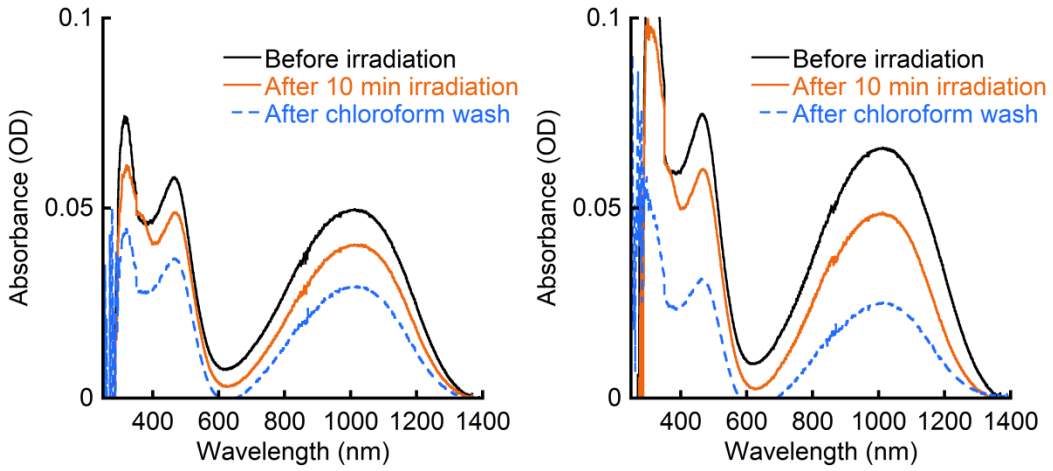

Figure 4.4 Absorbance spectra of the NIR MNB Ether polymer **P1** (black), which was irradiated with a 365 nm spotlight (39 mW/cm^2) for 10 minutes (orange), and washed with chloroform (blue dashed). The experiment was carried out in the presence of air (*Left*) and in the absence of air (*Right*).

The degradation observed was not lessened by the absence of air. Therefore, the degradation of the conjugated polymer backbone is likely to occur through a pathway other than photo-oxidation. To further probe this degradation and in order to establish the necessity of the photocleavable group in order to change solubility, a control polymer (**P2**) was made.

Films of **P2** were subjected to the same irradiation and wash conditions as the initial experiments with **P1**. The spectra for the irradiation experiment of **P2** can be seen in Figure 4.5.

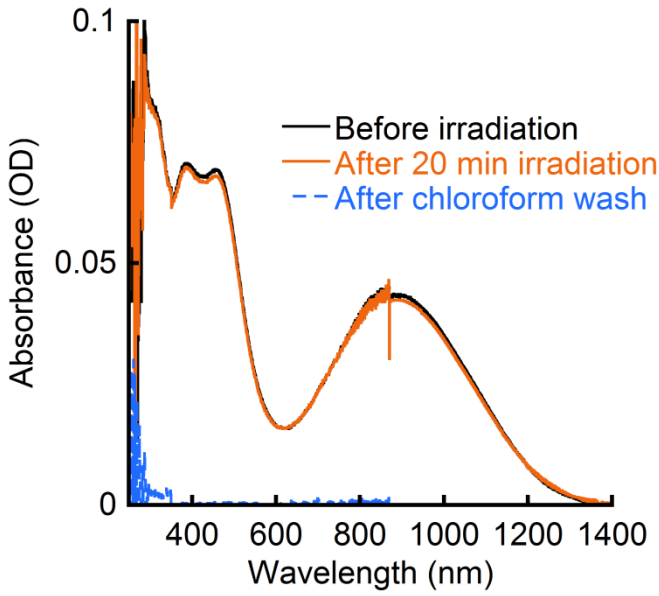

Figure 4.5 Absorbance spectra of the Control NIR polymer **P2** (black), which was irradiated with 295-395 nm light for 20 minutes (orange), and washed with chloroform (blue dashed).

The irradiation of films of **P2** demonstrated that the NB side-chains were in fact necessary for changing the solubility of the polymer. The retention of **P1** after irradiation and washing was determined to be 52-73 %, while the retention of **P2** was less than one percent. Also, the irradiation of films of **P2** resulted in only 2-4 % degradation after 20 minutes of irradiation. This is in stark contrast to the irradiation of **P1** which resulted in 19-26 % degradation. This result indicated that the degradation of the conjugated polymer backbone was at least partially due to the direct linkage of the NB group to the TQ moiety.

This discovery led to the synthesis of **P3** and **P4** which were synthesized via the copolymerization of 2,5-bis(trimethylstannyl) thiophene, the NIR control monomer (**12**), and a thiophene based monomer containing a NB-linked solubilizing side-chain (**16**). Polymer **P3** was made with equal amounts of the two

synthesized monomers (50:50), while **P4** was made with more than four times as much of the NB containing monomer as the NIR control monomer (82:18). The absorbance spectra from the irradiation experiments of **P3** and **P4** can be seen in Figure 4.6.

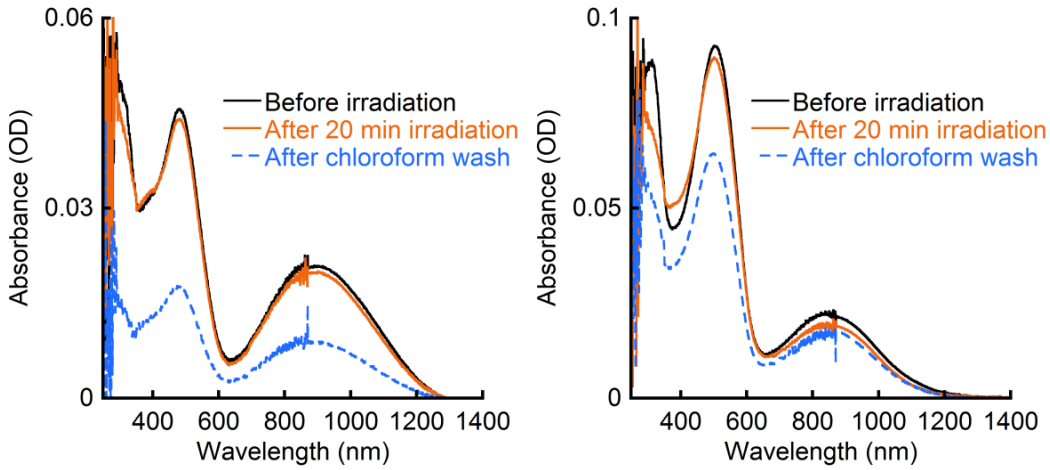

Figure 4.6 Absorbance spectra of the 50-50 NIR-co-thiophene NB Ether polymer **P3** (*Left*) and the 18-82 NIR-co-thiophene NB Ether polymer **P4** (*Right*). The absorbance spectra were measured for the polymers before irradiation (black), after irradiation with 295-395 nm light for 20 minutes (orange), and after washing with chloroform (blue dashed).

During irradiation experiments, **P3** exhibited much less degradation (4 %) than **P1**, which is further evidence that the NB side-chain being directly connected to the NIR monomer was a large contributor to the degradation of **P1**. While **P3** exhibited slightly lower retention (44 %) than **P1**, the decrease in degradation was quite substantial. These results indicated that even after irradiation much of the polymer chains remained soluble, which suggested that more NB character was necessary to induce a solubility change upon irradiation. **P4**, which had a 4:1 ratio of NB containing monomer to NIR monomer, displayed less degradation (11 %) than **P1** and more than double the retention (93 %) of **P3**.

In order to keep the degradation of the conjugated polymer low, the irradiation time and intensity should be kept to a minimum. Thus **P5** was synthesized to undergo photocleavage more efficiently than the NB ether used in **P3** and **P4** due to its MNB ether solubilizing side-chain. This design enabled better retention with the same irradiation conditions and maintained the low degradation as seen in **P3** and **P4**. The spectra obtained from the irradiation experiment of **P5** can be seen in Figure 4.7.

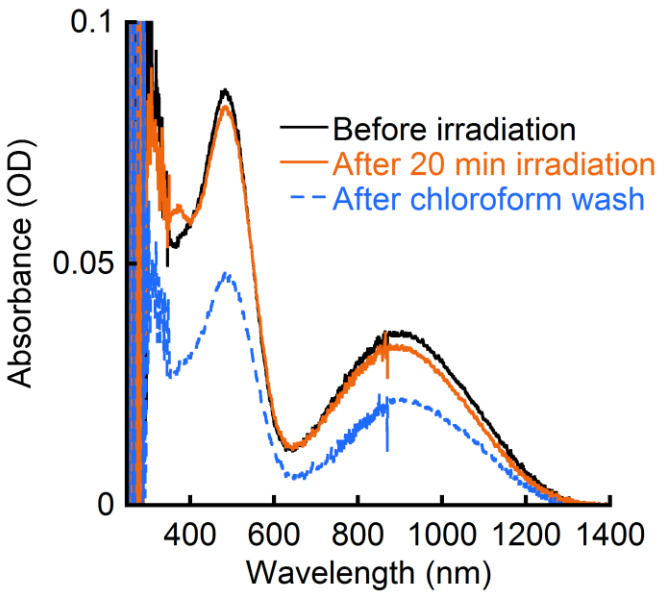

Figure 4.7 Absorbance spectra of the 50-50 NIR-co-thiophene MNB Ether polymer **P5**. The absorbance spectra were measured for the polymer before irradiation (black), after irradiation with 295-395 nm light for 20 minutes (orange), and after washing with chloroform (blue dashed).

During irradiation experiments, **P5** exhibited low degradation (10 %) and higher retention than **P3** (55 % vs 44 %) while maintaining a larger amount of TQ character in the polymer backbone, thus increasing the NIR absorbance of the polymer.

4.6 Multilayer Low-Bandgap Polymer Films

One of the benefits of photoinduced aggregation is the ability to make multilayer films without the need for orthogonal solubility or crosslinking. This is accomplished by spin coating a layer of the desired polymer, irradiating it to render it insoluble, and then repeating these steps until the desired thickness or layers are attained. The results of a multilayer experiment with **P4** can be seen in Figure 4.8.

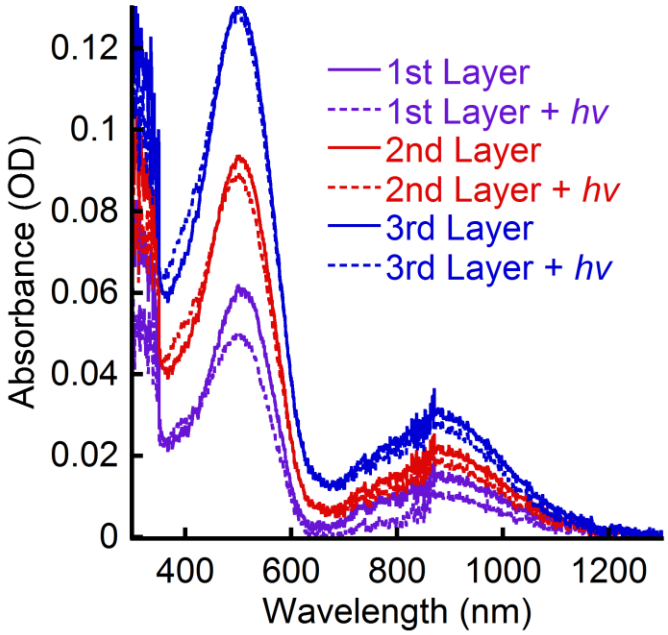

Figure 4.8 Thin film multi-layer of **P4** made by sequentially spin coating and irradiating layers for three deposition steps.

The spectra in Figure 4.7 show that each layer is made insoluble upon irradiation and that sequential layers can then be added. However, it is important to note that the irradiation step is critical to multilayer deposition of these types of polymers. As a control, the same experiment was repeated except without the irradiation

step between each deposition. The spectra obtained from the control experiment can be seen in Figure 4.9.

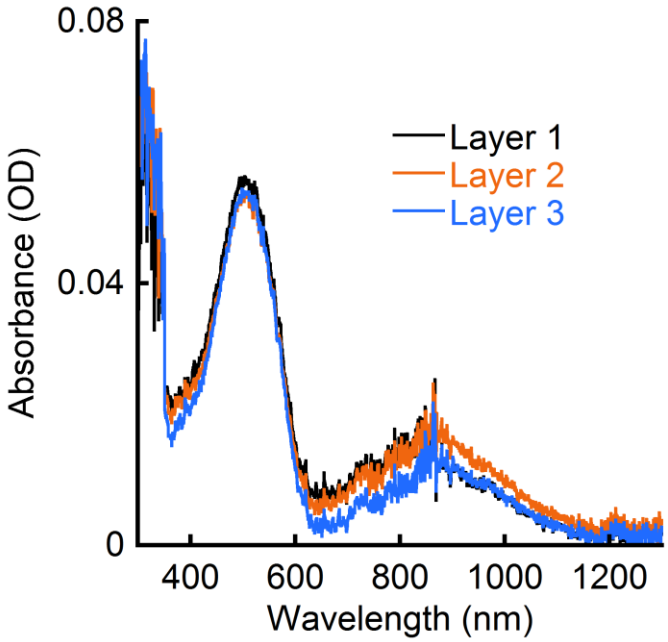

Figure 4.9 Thin film multilayer experiment of **P4** without irradiation between layer depositions.

The spectra in Figure 4.8 show that the addition of each subsequent layer does not increase the absorbance of the film. This is likely due to each deposition dissolving the previous un-irradiated layer due to its solubility in chloroform that is used for the spin coating of each additional layer.

4.7 Photopatterning of Low-Bandgap Polymer Films

As discussed in Chapter 3, the ability to photopattern conjugated polymers has potential for organic electronics applications. Previously, we have shown the ability to photopattern conjugated polymers functionalized with NB solubilizing side-chains.[17] We applied this same approach to some of the novel LBCPs

described in this chapter. Initial results show that **P4** is able to be photopatterned using a chrome photomask. Optical microscopy images obtained from the photopatterning experiments can be seen in Figure 4.10.

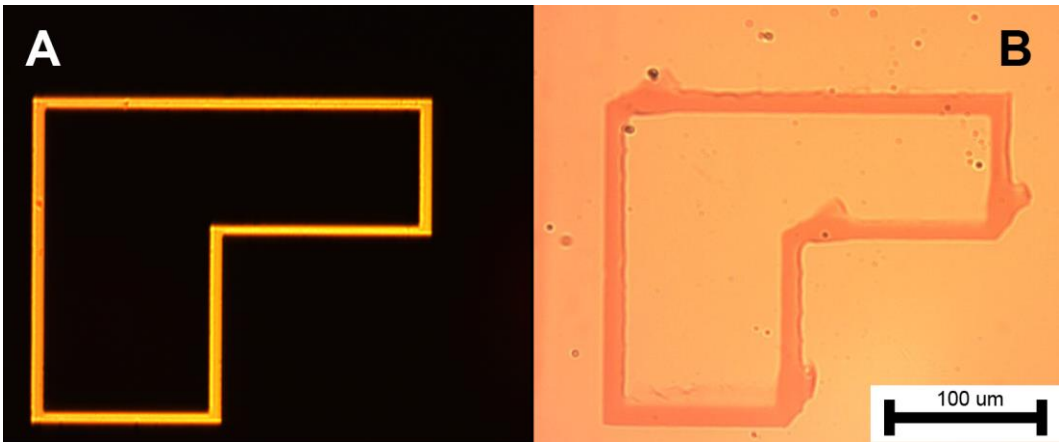

Figure 4.10 Optical microscopy images of the photomask used in the photopatterning experiment (*Left*), and of a film of **P4** after irradiation with 295-395 nm light for 35 minutes (*Right*).

The slight broadening of the patterned lines seen in Figure 4.9 is likely due to our non-optimized setup for photopatterning. Subsequent experiments will likely address this minor flaw.

4.8 Conclusions

The polymers developed in this study have shown that our design for photo-patternable conjugated polymers can be applied to more polymer architectures than just polythiophene and that this approach enables the creation of many novel and unique photo-patternable polymers. Also, the synthetic space for these polymers has been greatly expanded by the discovery that this approach still works when using a three monomer system where only one monomer is functionalized with the photolabile side-chain. This means that any conjugated

dibromide could theoretically be polymerized with a NB of MNB functionalized monomer to produce a photo-patternable conjugated polymer. The main source of experimentation in these future experiments will include: i) fine tuning the ideal ratio of the two dibromide monomers, ii) optimizing the amount of any non-photocleavable solubilizing group present along the polymer backbone, and iii) utilizing monomers that are relatively resistant to degradation upon UV irradiation.

4.9 Experimental Considerations

All synthetic manipulations were performed under standard air-free conditions under an atmosphere of argon gas with magnetic stirring unless otherwise mentioned. Flash chromatography was performed using silica gel (230-400 mesh) as the stationary phase. NMR spectra were acquired on a Bruker Avance III 500 or Bruker DPX-300 spectrometer. Chemical shifts are reported relative to residual protonated solvent (7.27 ppm for $CHCl_3$). High-resolution mass spectra (HRMS) were obtained at the MIT Department of Chemistry Instrumentation Facility using a peak-matching protocol to determine the mass and error range of the molecular ion. All reactants and solvents were purchased from commercial suppliers and used without further purification, unless otherwise noted.

Solid state absorbance spectra were acquired with a Jasco V-570 UV/Vis/NIR Spectrophotometer in double-beam mode using a blank glass cover slip for background subtraction spectra. Molecular weight distribution

measurements of the polymers were conducted with a Shimadzu Gel Permeation Chromatography (GPC) system equipped with a Tosoh TSKgel GMHhr-M mixed-bed column and guard column (5 μm), in addition to both UV and refractive index detectors. The column was calibrated with low polydispersity poly(styrene) standards (Tosoh, PSt Quick Kit) with THF as the mobile phase eluting at 0.75 mL/min. Irradiations of samples to cleave nitrobenzyl ether groups were performed with a 200W Hg/Xe lamp (Newport-Oriel) equipped with a condensing lens, recirculating water filter, manual shutter, and a 365 nm interference filter (Semrock) or 295 nm + UG 11 filter (Newport, 295-395 nm) in the light path. Thin films were fabricated using chloroform solutions of **P1**-**P5** (1–10 mg/mL) that were spun-cast onto glass cover slips using a Laurell Technologies Corporation spin coater (Model WS-400E-6NPP-Lite) at 1000 rpm for 1 minute.

Synthesis and Characterization

2-Nitro-5-(octyloxy)benzaldehyde (1). A round bottom flask was charged with 5-hydroxy-2-nitrobenzaldehyde (5.00 g, 29.9 mmol) and potassium carbonate (12.4 g, 89.8 mmol). The flask was evacuated and refilled with argon three times. Under argon flow, 100 mL of dimethyl formamide (DMF) and 1-bromooctane (7.8 mL, 8.7 g, 45 mmol) were added. The mixture was left to stir overnight at 50 °C. The reaction mixture was poured into 1M NaOH (1×100 mL) and extracted with diethyl ether (3×100 mL). The combined organic layers were then washed with saturated aqueous $NaHCO_3$ (1×100 mL), deionized (DI) water (1×100 mL),

and brine (1×100 mL). Drying over $MgSO_4$ and removal of solvent *in vacuo* gave the crude product **1** as a yellow-orange solid. Flash chromatography on silica using 2:1 hexanes:CH_2Cl_2 as eluent gave 8.35 g of **1** (99 %) as a pale yellow solid. This compound has been reported.[18] Mp: 55-56 °C. ^{1}H NMR ($CDCl_3$, 500 MHz): δ 10.49 (s, 1H), 8.16 (d, *J* = 9 Hz, 1H), 7.31 (d, *J* = 3 Hz, 1H), 7.14 (dd, *J* = 9 Hz, 3 Hz, 1H), 4.10 (t, *J* = 7 Hz, 2H), 1.83 (m, 2H), 1.50-1.44 (m, 2H), 1.38-1.30 (m, 8H), 0.91-0.88 (m, 3H). ^{13}C NMR ($CDCl_3$, 125 MHz): δ 188.6, 163.7, 142.0, 134.4, 127.2, 118.9, 113.7, 69.4, 31.8, 29.2, 29.2, 28.9, 25.8, 22.6, 14.1. HRMS calcd for $C_{15}H_{21}NO_4$ $(M+Na)^+$, 302.1363, found, 302.1370.

1-(2-nitro-5-(octyloxy)phenyl)ethanol (2). A round bottom flask was evacuated and refilled with argon three times. The flask was charged with 40 mL of anhydrous diethyl ether and cooled to -78 °C. $TiCl_4$ (0.12 mL, 1.0 mmol) was added via syringe, followed by the addition of 3.0 M CH_3MgBr in anhydrous diethyl ether (0.35 mL, 1.1 mmol). The solution was left to stir for 30 minutes at -78 °C. **1** (223 mg, 0.80 mmol) was then added and the reaction was left to stir for 3 hours while the reaction gradually warmed to room temperature. The reaction mixture was poured into DI H_2O (1 × 200 mL) and extracted with diethyl ether (3 × 100 mL). The combined organic layers were dried over $MgSO_4$ and solvent was removed *in vacuo* to give 223 mg of **2** (95 %) as a brown oil that was used without further purification. ^{1}H NMR ($CDCl_3$, 500 MHz): δ 8.04 (d, *J* = 9 Hz, 1H), 7.31 (d, *J* = 2.5 Hz, 1H), 6.84 (dd, *J* = 2.5 Hz, *J* = 9 Hz, 1H), 5.56 (q, *J* = 6.5 Hz, 1H), 4.06 (t, *J* = 6.5 Hz, 2H), 2.35 (s, 1H), 1.82 (m, 2H), 1.56 (d, *J* = 6.5 Hz,

3H), 1.49-1.44 (m, 2H), 1.35-1.30 (m, 8H), 0.91-0.88 (m, 3H). ^{13}C NMR ($CDCl_3$, 125 MHz): δ 163.6, 144.7, 140.3, 127.6, 113.4, 112.5, 68.8, 66.0, 31.8, 29.3, 29.2, 29.0, 25.9, 24.1, 22.6, 14.1.

2-(1-bromoethyl)-1-nitro-4-(octyloxy)benzene (3). A round bottom flask was charged with CBr_4 (773 mg, 2.33 mmol), and PPh_3 (611 mg, 2.33 mmol). The flask was evacuated and refilled with argon three times. Under argon flow, compound **2** (459 mg, 1.55 mmol) dissolved in 10 mL of anhydrous tetrahydrofuran (THF) was added. The reaction was left stirring at room temperature for two hours. The reaction mixture was filtered and the solvent was removed *in vacuo* to give the crude product **3** as a brown oil. Flash chromatography on silica using 4:1 hexanes:CH_2Cl_2 as eluent gave 290 mg of **8** (52 %) as a clear, yellow oil. ^1H NMR ($CDCl_3$, 500 MHz): δ 7.96 (d, *J* = 9 Hz, 1H), 7.33 (d, *J* = 3 Hz, 1H), 6.86 (dd, *J* = 2.5 Hz, *J* = 9 Hz, 1H), 6.02 (q, *J* = 7 Hz, 1H), 4.07 (m, 2H), 2.07 (d, *J* = 7 Hz, 3H), 1.84 (m, 2H), 1.52-1.46 (m, 2H), 1.36-1.30 (m, 8H), 0.92-0.89 (m, 3H). ^{13}C NMR ($CDCl_3$, 125 MHz): δ 163.1, 140.9, 140.1, 127.4, 115.7, 113.9, 68.9, 42.6, 31.8, 29.3, 29.2, 29.0, 27.2, 25.9, 22.6, 14.1. HRMS calcd for $C_{21}H_{25}Br_2NO_5S$ $(M+NH_4)^+$, 581.0147, found, 581.0145.

4,4'-Dihydroxybenzil (4). A round bottom flask was charged with anisil (1000 mg, 3.70 mmol). The flask was evacuated and refilled with argon three times. Under argon flow, acetic acid (15 mL) and 48 % HBr (15 mL) were added. The reaction was left to reflux overnight. Upon cooling to room temperature, the

reaction mixture was poured into DI H_2O (1 × 100 mL) and extracted with ethyl acetate (3 × 50 mL). The combined organic layers were dried over $MgSO_4$ and solvent was removed *in vacuo* to give the crude product **4** as a brown solid. Flash chromatography on silica using 5:1 CH_2Cl_2:acetone as eluent gave 536 mg of **4** (60 %) as a white/yellow solid. ^{1}H NMR (acetone-d_6, 500 MHz): δ 7.78 (d, J = 9 Hz, 4H), 6.95 (d, J = 9 Hz, 4H). ^{13}C NMR (acetone-d_6, 125 MHz): δ 194.3, 164.3, 132.8, 125.9, 116.5.

Dinitrobenzyl-diketone (5). A round bottom flask was charged with **4** (180 mg, 0.74 mmol) and potassium carbonate (511 mg, 3.70 mmol). The flask was evacuated and refilled with argon three times. Under argon flow, compound **3** (532 mg, 1.48 mmol), and 12 mL of dry DMF were added. The reaction was heated to 50 °C and left to stir for 48 hours. Upon cooling to room temperature, the reaction mixture was poured into DI H_2O (1 × 100 mL) and extracted with diethyl ether (5 × 50 mL). The combined organic layers were dried over $MgSO_4$ and solvent was removed *in vacuo* to give the crude product **5** as a brown oil. Flash chromatography on silica using 1:1 hexanes:CH_2Cl_2 as eluent gave 372 mg of **5** (63 %) as a yellow oil. ^{1}H NMR ($CDCl_3$, 500 MHz): δ 8.15 (d, J = 9 Hz, 2H), 7.83 (d, J = 9 Hz, 4H), 7.09 (d, J = 3 Hz, 2H), 6.85 (m, 6H), 6.26 (q, J = 6 Hz, 2H), 4.00-3.91 (m, 4H), 1.77-1.71 (m, 4H), 1.43-1.40 (m, 4H), 1.32-1.27 (m, 16H), 0.90-0.87 (m, 6H). ^{13}C NMR ($CDCl_3$, 125 MHz): δ 193.1, 164.0, 162.5, 141.6, 139.7, 132.4, 128.1, 126.6, 115.7, 113.6, 112.5, 72.2, 68.9, 31.8, 29.3, 29.1, 28.9, 25.9, 23.3, 22.6, 14.1.

4,7-Dibromo-5,6-dinitrobenzo[*c*][1,2,5]thiadiazole (6). A round bottom flask was charged with concentrated H_2SO_4 (25 mL) and fuming HNO_3 (25 mL). Upon cooling to 0 °C, 4,7-dibromobenzo[*c*]-1,2,5-thiadiazole (4540 mg, 15.44 mmol) was slowly added. The reaction was left to stir for 48 hours. The reaction mixture was poured over ice and the product crashed out as an off white solid. The solid was filtered off to yield 2824 mg of **6** (48 %) that was used without further purification. Mp: 201 °C. ^{13}C NMR ($CDCl_3$, 125 MHz): δ 151.4, 144.9, 110.3.

5,6-dinitro-4,7-di-2-thienyl-benzo[*c*][1,2,5]thiadiazole (7). A round bottom flask was charged with **6** (493 mg, 1.28 mmol), and $PdCl_2(PPh_3)_2$ (45 mg, 0.006 mmol). The flask was evacuated and refilled with argon three times. Under argon flow, 2-(tributylstannyl)thiophene (1198 mg, 1.0 mL, 3.21 mmol), and anhydrous THF (12 mL) were added. The reaction was left to reflux for 48 hours. Upon cooling to room temperature, a brownish orange precipitate formed. The precipitate was isolated through filtration and then washed with DI water and hexanes. After washing, the solid was dried *in vacuo* to yield 351 mg of **7** (70%) which was used without further purification. ^{1}H NMR ($CDCl_3$, 500 MHz): δ 7.75 (dd, J = 1 Hz, J = 5 Hz, 2H), 7.53 (dd, J = 1 Hz, J = 4 Hz, 2H), 7.25 (dd, J = 4 Hz, J = 5 Hz, 2H). ^{13}C NMR ($CDCl_3$, 125 MHz): δ 152.2, 141.9, 131.4, 131.0, 129.6, 128.0, 121.5.

4,7-bis(5-bromo-2-thienyl)-5,6-dinitro-benzo[*c*][1,2,5]thiadiazole (8). A round bottom flask was charged with **7** (1295 mg, 3.32 mmol), and *n*-bromosuccinimide (2954 mg, 16.6 mmol). The flask was evacuated and refilled with argon three times. Under argon flow, anhydrous DMF (50 mL) was added. The reaction was heated to 60 °C and left to stir overnight. Upon cooling to room temperature, the reaction mixture was poured into 1M HCl, which resulted in the precipitation of a reddish orange solid. The solid was then washed with DI H_2O and methanol, before being dried *in vacuo* to yield 1688 mg of **8** (93%) which was used without further purification. ^{1}H NMR ($CDCl_3$, 500 MHz): δ 7.27 (d, J = 4 Hz, 2H), 7.20 (d, J = 4 Hz, 2H). ^{13}C NMR ($CDCl_3$, 125 MHz): δ 151.8, 131.3, 131.0, 130.9, 120.3, 119.9.

4,7-bis(5-bromo-2-thienyl)-5,6-diamine-benzo[*c*][1,2,5]thiadiazole (9). A round bottom flask was charged with **8** (526 mg, 0.96 mmol), Fe (0) (643 mg, 11.5 mmol), and acetic acid (40 mL). The reaction was heated to 80 °C and left to stir overnight. Upon cooling to room temperature, the reaction mixture was poured into 1M NaOH (1 × 100 mL) and extracted with diethyl ether (3 × 50 mL). The combined organic layers were dried over $MgSO_4$, filtered, and solvent was removed *in vacuo* to give the pure product **9** as a reddish brown solid. ^{1}H NMR ($CDCl_3$, 500 MHz): δ 7.20 (d, J = 4 Hz, 2H), 7.12 (d, J = 4 Hz, 2H), 4.42 (broad singlet, 4H). ^{13}C NMR ($CDCl_3$, 125 MHz): δ 150.4, 139.4, 136.9, 130.2, 128.9, 114.2, 106.6.

MNB Ether NIR Monomer (10). A round bottom flask was charged with **9** (227 mg, 0.46 mmol), **5** (372 mg, 0.46 mmol), and acetic acid (20 mL). The reaction was left to reflux overnight. Upon cooling to room temperature, the reaction mixture was poured into DI H_2O (1 × 100 mL) and extracted with diethyl ether (3 × 50 mL). The combined organic layers were dried over $MgSO_4$, filtered, and solvent was removed *in vacuo* to give crude product **10** as a blackish green solid. Flash chromatography on silica using 1:1 hexanes:CH_2Cl_2 as eluent gave 267 mg of **10** (46 %) as a blackish green solid. ^{1}H NMR ($CDCl_3$, 500 MHz): δ 8.64 (dd, *J* = 1.5 Hz, *J* = 2.5 Hz, 2H), 8.17 (t, *J* = 9.5 Hz, 2H), 7.55 (dd, *J* = 4 Hz, *J* = 9 Hz, 4H), 7.08 (dd, *J* = 1.5 Hz, *J* = 4.5 Hz, 2H), 6.87-6.83 (m, 6H), 6.29 (m, 2H), 4.02-4.0 (m, 4H), 1.77 (d, *J* = 6.5 Hz, 6H), 1.42-1.40 (m, 4H), 1.28-1.21 (m, 16H), 0.82 (m, 6H). ^{13}C NMR ($CDCl_3$, 125 MHz): δ 164.0, 158.8, 152.8, 150.9, 142.4, 139.8, 137.2, 133.9, 133.2, 132.4, 130.6, 129.5, 128.0, 120.2, 119.7, 115.3, 113.6, 112.8, 71.9, 68.9, 31.8, 29.3, 29.2, 29.0, 25.9, 23.4, 22.6, 14.1.

MNB Ether NIR Polymer (P1). A Schlenk tube was charged with **10** (50 mg, 0.04 mmol), 2,5-bis(trimethylstannyl)thiophene (16 mg, 0.04 mmol), tri(*o*-tolyl)phosphine (6 mg, 0.02 mmol), and $Pd_2(dba)_3$ (2 mg, 0.002 mmol). The Schlenk tube was evacuated and refilled with argon three times. Under argon flow, deoxygenated anhydrous toluene (5 mL) was added. The reaction was heated to 90 °C and left to stir for 72 hours. Upon cooling to room temperature, the reaction mixture was added dropwise to MeOH to precipitate the polymer. After centrifugation, the polymer was washed via Soxhlet extraction with MeOH,

hexanes, and chloroform. The solvent was removed *in vacuo* to give 30 mg of **P1** (64 %) as a brown solid. GPC: M_n = 12,200, PDI = 4.60. ^{1}H NMR ($CDCl_3$, 500 MHz): δ 8.50-8.00 (1H), 8.00-7.50 (2H), 7.25-6.50 (4H), 6.50-6.00 (2H), 4.50-3.75 (2H), 2.30-1.75 (4H), 1.50-1.00 (8H), 1.00-0.30 (3H).

Control diketone (11). A round bottom flask was charged with **4** (232 mg, 0.96 mmol) and potassium carbonate (633 mg, 4.80 mmol). The flask was evacuated and refilled with argon three times. Under argon flow, compound 1-(bromomethyl)-3-(octyloxy)-benzene (601 mg, 2.01 mmol), and 20 mL of dry DMF were added. The reaction was heated to 60 °C and left to stir for 24 hours. Upon cooling to room temperature, the reaction mixture was poured into DI H_2O (1 × 100 mL) and extracted with diethyl ether (5 × 50 mL). The combined organic layers were dried over $MgSO_4$ and solvent was removed *in vacuo* to give the crude product **11** as a yellowish white solid. Flash chromatography on silica using 1:1 hexanes:CH_2Cl_2 as eluent gave 488 mg of **11** (75 %) as a white solid. ^{1}H NMR ($CDCl_3$, 500 MHz): δ 7.94 (d, *J* = 9 Hz, 4H), 7.30 (t, *J* = 8 Hz, 2H), 6.97 (d, *J* = 9 Hz, 4H), 6.87 (m, 2H), 5.12 (s, 2H), 3.96 (t, *J* = 6.5 Hz, 4H), 1.79 (m, 4H), 1.46 (m, 4H), 1.33 (m, 16H), 0.90 (m, 6H). ^{13}C NMR ($CDCl_3$, 125 MHz): δ 193.4, 164.0, 160.0, 137.3, 132.4, 129.8, 126.5, 119.4, 115.1, 114.3, 113.6, 70.2, 68.0, 31.8, 29.4, 29.3, 29.2, 26.1, 22.7, 14.1.

Control NIR Monomer (12). A round bottom flask was charged with **9** (144 mg, 0.29 mmol), **11** (200 mg, 0.29 mmol), and acetic acid (20 mL). The reaction was

left to reflux overnight. Upon cooling to room temperature, the reaction mixture was poured into DI H_2O (1 × 100 mL) and extracted with diethyl ether (3 × 50 mL). The combined organic layers were dried over $MgSO_4$, filtered, and solvent was removed *in vacuo* to give crude product **12** as a blackish green solid. Flash chromatography on silica using 1:1 hexanes:CH_2Cl_2 as eluent gave 154 mg of **12** (46 %) as a blackish green solid. ^{1}H NMR ($CDCl_3$, 500 MHz): δ 8.82 (m, 2H), 7.72 (m, 4H), 7.34 (m, 2H), 7.21 (m, 2H), 7.06 (m, 6H), 6.91 (m, 2H), 5.14 (m, 4H), 4.01 (m, 4H), 1.82 (m, 4H), 1.49 (m, 4H), 1.34 (m, 16H), 0.91 (m, 6H). ^{13}C NMR ($CDCl_3$, 125 MHz): δ 160.3, 159.5, 153.1, 151.1, 138.0, 137.4, 134.2, 133.2, 132.5, 130.5, 129.7, 129.6, 120.3, 119.9, 119.6, 114.6, 114.2, 113.7, 70.1, 68.1, 31.8, 29.4, 29.3, 29.2, 26.1, 22.6, 14.1.

Control NIR Polymer (P2). A Schlenk tube was charged with 2,5-bis(trimethylstannyl)thiophene (18 mg, 0.044 mmol), tri(*o*-tolyl)phosphine (7 mg, 0.02 mmol), and $Pd_2(dba)_3$ (2 mg, 0.002 mmol). The Schlenk tube was evacuated and refilled with argon three times. Under argon flow, deoxygenated anhydrous toluene (5 mL) and **12** (50 mg, 0.044 mmol) were added. The reaction was heated to 90 °C and left to stir for 72 hours. Upon cooling to room temperature, the reaction mixture was added dropwise to MeOH to precipitate the polymer. After centrifugation, the polymer was washed via Soxhlet extraction with MeOH, hexanes, and chloroform. The solvent was removed *in vacuo* to give 12 mg of **P2** (26 %) as a brown solid. GPC: M_n = 2,700, PDI = 1.73. ^{1}H NMR ($CDCl_3$, 500 MHz): δ 7.80-7.70 (4H), 7.60-7.50 (2H), 7.20-6.70 (8H), 5.20-5.00 (2H), 4.90-

4.70 (2H), 4.10-3.90 (2H), 3.80-3.50 (2H), 1.90-1.70 (4H), 1.50-1.00 (18H), 1.00-0.70 (6H).

2-Nitro-5-(2-ethylhexyl)benzaldehyde (13). A round bottom flask was charged with 5-hydroxy-2-nitrobenzaldehyde (5.00 g, 29.9 mmol) and potassium carbonate (12.4 g, 89.8 mmol). The flask was evacuated and refilled with argon three times. Under argon flow, 30 mL of dimethyl formamide (DMF) and 2-ethylhexyl bromide (7.8 mL, 8.7 g, 45 mmol) were added. The mixture was left to stir for 48 hours at 50 °C. Upon cooling to room temperature, the reaction mixture was poured into DI H_2O (1 × 100 mL) and extracted with dichloromethane (3 × 50 mL). The combined organic layers were dried over $MgSO_4$ and solvent was removed *in vacuo* to give the crude product **13** as a yellowish brown oil. Flash chromatography on silica using 2:1 hexanes:CH_2Cl_2 as eluent gave 8311 mg of **13** (99 %) as a colorless oil. ^{1}H NMR ($CDCl_3$, 500 MHz): δ 10.50 (s, 1H), 8.16 (d, *J* = 9 Hz, 1H), 7.32 (d, *J* = 3 Hz, 1H), 7.15 (dd, *J* = 3 Hz, *J* = 9 Hz, 1H), 3.99 (q, *J* = 4 Hz, 2H), 1.78 (m, 1H), 1.44 (m, 4H), 1.32 (m, 4H), 0.93 (m, 6H). ^{13}C NMR ($CDCl_3$, 125 MHz): δ 189.7, 163.9, 142.0, 134.4, 127.2, 118.9, 113.8, 71.8, 39.2, 30.4, 29.0, 23.7, 23.0, 14.0, 11.0.

(2-nitro-5-(2-ethylhexyl)phenyl)methanol (14). A round bottom flask was charged with $NaBH_4$ (541 mg, 14.32 mmol). The flask was evacuated and refilled with argon three times. Under argon flow, **13** (2000 mg, 7.16 mmol), and 40 mL of MeOH were added. The reaction was left to stir overnight at room temperature.

The reaction mixture was poured into DI H_2O (1 × 100 mL) and extracted with diethyl ether (3 × 50 mL). The combined organic layers were dried over $MgSO_4$ and solvent was removed *in vacuo* to give 2000 mg of **14** (99 %) as a colorless oil. ^{1}H NMR ($CDCl_3$, 500 MHz): δ 8.18 (d, *J* = 9 Hz, 1H), 7.21 (d, *J* = 2.5 Hz, 1H), 6.89 (dd, *J* = 2.5 Hz, *J* = 9 Hz, 1H), 5.00 (s, 2H), 3.96 (q, *J* = 3.5 Hz, 2H), 2.62 (broad singlet, 1H), 1.77 (m, 1H), 1.51-1.41 (m, 4H), 1.33 (m, 4H), 0.92 (m, 6H). ^{13}C NMR ($CDCl_3$, 125 MHz): δ 164.1, 140.2, 140.1, 128.1, 114.8, 113.6, 71.3, 63.1, 39.2, 30.4, 29.0, 23.8, 23.0, 14.0, 11.1.

2-(Bromomethyl)-1-nitro-4-(2-ethylhexyl)benzene (15). A round bottom flask was evacuated and refilled with argon three times. Anhydrous dichloromethane (40 mL), and **14** (2000 mg, 7.16 mmol) were added. The solution was cooled to 0 °C and PBr_3 (2132 mg, 0.75 mL, 7.88 mmol) was added. The reaction was left to stir overnight. The reaction mixture was poured into DI H_2O (1 × 100 mL) and extracted with dichloromethane (3 × 50 mL). The combined organic layers were dried over $MgSO_4$ and solvent was removed *in vacuo* to give the crude product **15** as a yellowish brown oil. Flash chromatography on silica using 3:1 hexanes:CH_2Cl_2 as eluent gave 831 mg of **15** (34 %) as a yellow oil. ^{1}H NMR ($CDCl_3$, 300 MHz): δ 8.15 (d, *J* = 9 Hz, 1H), 7.02 (d, *J* = 3 Hz, 1H), 6.92 (dd, *J* = 3 Hz, *J* = 9 Hz, 1H), 4.87 (s, 2H), 3.94 (d, *J* = 6 Hz, 2H), 1.76 (m, 1H), 1.49 (m, 4H), 1.33 (m, 4H), 0.94 (m, 6H). ^{13}C NMR ($CDCl_3$, 75 MHz): δ 163.3, 140.4, 135.6, 128.4, 118.0, 114.4, 71.4, 39.2, 30.4, 30.0, 29.0, 23.8, 23.0, 14.0, 11.1.

NB Ether Thiophene Monomer (16). A round bottom flask was charged with 4-(2,5-dibromothiophen-3-yl)phenol (887 mg, 2.66 mmol) and potassium carbonate (1001 mg, 7.24 mmol). The flask was evacuated and refilled with argon three times. Under argon flow, anhydrous DMF (25 mL) and **15** (831 mg, 2.41 mmol) were added. The reaction was heated to 50 °C and left for 48 hours. Upon cooling to room temperature, the reaction mixture was poured into DI H_2O (1 × 100 mL) and extracted with diethyl ether (3 × 50 mL). The combined organic layers were dried over $MgSO_4$ and solvent was removed *in vacuo* to give crude product **16** as a brown oil. Flash chromatography on silica using 4:1 hexanes:CH_2Cl_2 as eluent gave 515 mg of **16** (36 %) as a viscous golden oil. ^{1}H NMR ($CDCl_3$, 300 MHz): δ 8.25 (d, *J* = 9 Hz, 1H), 7.47 (d, *J* = 9 Hz, 2H), 7.41 (d, *J* = 3 Hz, 1H), 7.09 (d, *J* = 9 Hz, 2H), 6.99 (s, 1H), 6.92 (dd, *J* = 3 Hz, *J* = 9 Hz, 1H), 5.53 (s, 2H), 3.97 (d, *J* = 9 Hz, 2H), 1.75 (m, 1H), 1.42 (m, 4H), 1.35 (m, 4H), 0.94 (m, 6H). ^{13}C NMR ($CDCl_3$, 75 MHz): δ 164.1, 157.9, 141.5, 139.3, 137.0, 131.6, 129.9, 128.0, 127.3, 115.0, 113.6, 113.2, 111.2, 107.0, 71.3, 67.3, 39.2, 30.4, 29.1, 23.8, 23.1, 14.2, 11.1.

50:50 NB Ether Thiophene-*co*-NIR Control Polymer (P3). A Schlenk tube was charged with 2,5-bis(trimethylstannyl)thiophene (18 mg, 0.044 mmol), tri(*o*-tolyl)phosphine (7 mg, 0.02 mmol), and $Pd_2(dba)_3$ (2 mg, 0.002 mmol). The Schlenk tube was evacuated and refilled with argon three times. Under argon flow, deoxygenated anhydrous toluene (4 mL), **16** (13 mg, 0.022 mmol), and **12** (25 mg, 0.022 mmol) were added. The reaction was heated to 90 °C and left to stir

for 72 hours. Upon cooling to room temperature, the reaction mixture was added dropwise to MeOH to precipitate the polymer. After centrifugation, the polymer was washed via Soxhlet extraction with MeOH, hexanes, and chloroform. The solvent was removed *in vacuo* to give 21 mg of **P3** (33 %) as a reddish brown solid. GPC: M_n = 6,400, PDI = 3.06. ^{1}H NMR ($CDCl_3$, 500 MHz): δ 8.30-8.20 (2H), 7.90-7.70 (3H), 7.60-7.28 (4H), 7.25-6.60 (13H), 5.60-5.50 (2H), 5.20-5.10 (2H), 4.10-3.70 (4H), 1.90-1.60 (5H), 1.50-1.10 (28H), 1.00-0.50 (14H).

82:18 NB Ether Thiophene-*co*-NIR Control Polymer (P4). A Schlenk tube was charged with 2,5-bis(trimethylstannyl)thiophene (18 mg, 0.044 mmol), tri(*o*-tolyl)phosphine (7 mg, 0.02 mmol), and $Pd_2(dba)_3$ (2 mg, 0.002 mmol). The Schlenk tube was evacuated and refilled with argon three times. Under argon flow, deoxygenated anhydrous toluene (4 mL), **16** (22 mg, 0.036 mmol), and **12** (9 mg, 0.011 mmol) were added. The reaction was heated to 90 °C and left to stir for 72 hours. Upon cooling to room temperature, the reaction mixture was added dropwise to MeOH to precipitate the polymer. After centrifugation, the polymer was washed via Soxhlet extraction with MeOH, hexanes, and chloroform. The solvent was removed *in vacuo* to give 24 mg of **P4** (37 %) as a reddish brown solid. GPC: M_n =9,400, PDI = 3.05. ^{1}H NMR ($CDCl_3$, 500 MHz): δ 8.30-8.10 (2H), 7.60-7.30 (3H), 7.20-6.60 (11H), 5.65-5.35 (2H), 4.00-3.60 (4H), 1.90-1.60 (3H), 1.55-1.35 (6H), 1.35-1.00 (15H), 1.00-0.60 (12H).

1-(2-nitro-5-(2-ethylhexyl)phenyl)ethanol (17). A round bottom flask was evacuated and refilled with argon three times. The flask was charged with 120 mL of anhydrous diethyl ether and cooled to -78 °C. $TiCl_4$ (1698 mg, 1 mL, 8.95 mmol) was added via syringe, followed by the addition of 3.0 M CH_3MgBr in anhydrous diethyl ether (3.13 mL, 9.38 mmol). The solution was left to stir for 30 minutes at -78 °C. **13** (1900 mg, 6.80 mmol) was then added and the reaction was left to stir overnight while the reaction gradually warmed to room temperature. The reaction mixture was poured into DI H_2O (1 × 200 mL) and extracted with diethyl ether (3 × 100 mL). The combined organic layers were dried over $MgSO_4$ and solvent was removed *in vacuo* to give crude product **17** as a brownish green oil. Flash chromatography on silica using 2:1 hexanes:CH_2Cl_2 as eluent gave 1106 mg of **17** (55 %) as a yellow oil. ^{1}H NMR ($CDCl_3$, 500 MHz): δ 8.06 (d, *J* = 9 Hz, 1H), 7.32 (d, *J* = 2.5 Hz, 2H), 6.86 (dd, *J* = 2.5 Hz, *J* = 9 Hz, 1H), 5.58 (q, *J* = 6 Hz, 1H), 3.95 (m, 2H), 2.34 (broad singlet, 1H), 1.76 (m, 1H), 1.58 (d, *J* = 6 Hz, 3H), 1.52-1.42 (m, 4H), 1.33 (m, 4H), 0.94 (m, 6H). ^{13}C NMR ($CDCl_3$, 125 MHz): δ 163.9, 144.7, 140.3, 127.6, 113.4, 112.5, 71.2, 66.0, 39.2, 30.4, 30.4, 29.0, 24.1, 23.8, 23.0, 14.0, 11.1.

2-(1-bromoethyl)-1-nitro-4-(2-ethylhexyl)benzene (18). A round bottom flask was charged with CBr_4 (1860 mg, 5.61 mmol), and PPh_3 (1471 mg, 5.61 mmol). The flask was evacuated and refilled with argon three times. Under argon flow, anhydrous THF (25 mL) and **17** (1106 mg, 3.74 mmol) were added. The reaction was left to stir at room temperature for 48 hours. The reaction mixture was

filtered and solvent removed *in vacuo* to give the crude product **18** as a brown oil that solidified on standing. Flash chromatography on silica using 4:1 hexanes:CH_2Cl_2 as eluent gave 1304 mg of **18** (97 %) as a yellow oil. ^{1}H NMR ($CDCl_3$, 500 MHz): δ 7.96 (d, *J* = 9 Hz, 1H), 7.33 (d, *J* = 3 Hz, 1H), 6.87 (dd, *J* = 3 Hz, *J* = 9 Hz), 6.03 (q, *J* = 7 Hz, 1H), 3.95 (m, 2H), 2.08 (d, *J* = 7 Hz, 3H), 1.79-1.774 (m, 1 H), 1.56-1.43 (m, 4H), 1.36 (m, 4H), 0.92 (m, 6H). ^{13}C NMR ($CDCl_3$, 125 MHz): δ 163.3, 140.9, 140.0, 127.4, 115.6, 113.9, 71.3, 42.6, 29.3, 30.4, 29.1, 27.2, 23.8, 23.0, 14.1, 11.1.

MNB Ether Thiophene Monomer (19). A round bottom flask was charged with 4-(2,5-dibromothiophen-3-yl)phenol (270 mg, 0.81 mmol) and potassium carbonate (336 mg, 2.43 mmol). The flask was evacuated and refilled with argon three times. Under argon flow, anhydrous DMF (15 mL) and **18** (263 mg, 0.73 mmol) were added. The reaction was heated to 50 °C and left for 48 hours. Upon cooling to room temperature, the reaction mixture was poured into DI H_2O (1 × 100 mL) and extracted with diethyl ether (3 × 50 mL). The combined organic layers were dried over $MgSO_4$ and solvent was removed *in vacuo* to give crude product **19** as a brown oil. Flash chromatography on silica using 3:1 hexanes:CH_2Cl_2 as eluent gave 154 mg of **19** (34 %) as a viscous yellow oil. ^{1}H NMR ($CDCl_3$, 500 MHz): δ 8.16 (d, *J* = 9 Hz, 1H), 7.36 (d, *J* = 9 Hz, 2H), 7.23 (d, *J* = 3 Hz, 1H), 6.94 (s, 1H), 6.86 (m, 3H), 6.21 (q, *J* = 6 Hz, 1H), 3.87 (m, 2H), 1.72 (d, *J* = 6 Hz, 3H), 1.42 (m, 4H), 1.29 (m, 4H), 0.90 (m, 6H). ^{13}C NMR ($CDCl_3$, 125 MHz): δ 164.2, 157.2, 142.7, 141.4, 139.8, 131.6, 129.8, 128.0,

127.0, 115.5, 113.7, 112.5, 111.0, 106.9, 72.0, 71.3, 39.1, 30.3, 29.0, 23.7, 23.5, 23.0, 14.0, 11.1.

50:50 MNB Ether Thiophene-*co*-NIR Control Polymer (P5). A Schlenk tube was charged with 2,5-bis(trimethylstannyl)thiophene (14 mg, 0.042 mmol), tri(*o*-tolyl)phosphine (7 mg, 0.02 mmol), and $Pd_2(dba)_3$ (2 mg, 0.002 mmol). The Schlenk tube was evacuated and refilled with argon three times. Under argon flow, deoxygenated anhydrous toluene (4 mL), **19** (13 mg, 0.021 mmol), and **12** (24 mg, 0.021 mmol) were added. The reaction was heated to 90 °C and left to stir for 72 hours. Upon cooling to room temperature, the reaction mixture was added dropwise to MeOH to precipitate the polymer. After centrifugation, the polymer was washed via Soxhlet extraction with MeOH, hexanes, and chloroform. The solvent was removed *in vacuo* to give 24 mg of **P5** (37 %) as a reddish brown solid. GPC: M_n = 7,600, PDI = 2.59. ^{1}H NMR ($CDCl_3$, 500 MHz): δ 8.30-8.00 (2H), 8.00-7.40 (4H), 7.20-6.60 (8H), 6.50-6.10 (2H), 5.25-4.75 (2H), 4.30-3.60 (4H), 2.00-1.65 (5H), 1.55-1.00 (16H), 1.00-0.60 (8H).

4.10 References

1. van Mullekom, H. A. M.; Vekemans, J.; Havinga, E. E.; Meijer, E. W. *Mater. Sci. Eng. R-Rep.* **2001**, *32*, 1.

2. Bundgaard, E.; Krebs, F. C. *Sol. Energy Mater. Sol. Cells* **2007**, *91*, 954.

3. Ide, M.; Koizumi, Y.; Saeki, A.; Izumiya, Y.; Ohkita, H.; Ito, S.; Seki, S. *The Journal of Physical Chemistry C* **2013**, *117*, 26859.

4. Li, G.; Zhu, R.; Yang, Y. *Nat Photon* **2012**, *6*, 153.

5. Dou, L.; You, J.; Yang, J.; Chen, C.-C.; He, Y.; Murase, S.; Moriarty, T.; Emery, K.; Li, G.; Yang, Y. *Nat Photon* **2012**, *6*, 180.

6. Deng, Y.; Li, W.; Liu, L.; Tian, H.; Xie, Z.; Geng, Y.; Wang, F. *Energy & Environmental Science* **2015**, *8*, 585.

7. Qi, J.; Zhou, X.; Yang, D.; Qiao, W.; Ma, D.; Wang, Z. Y. *Adv. Funct. Mater.* **2014**, *24*, 7605.

8. Park, C.-D.; Fleetham, T. A.; Li, J.; Vogt, B. D. *Org. Electron.* **2011**, *12*, 1465.

9. Lei, T.; Wang, J.-Y.; Pei, J. *Acc. Chem. Res.* **2014**, *47*, 1117.

10. Grenier, F.; Berrouard, P.; Pouliot, J.-R.; Tseng, H.-R.; Heeger, A. J.; Leclerc, M. *Polymer Chemistry* **2013**, *4*, 1836.

11. Robb, M. J.; Ku, S. Y.; Brunetti, F. G.; Hawker, C. J. *J. Polym. Sci. Pol. Chem.* **2013**, *51*, 1263.

12. Perzon, E.; Wang, X.; Admassie, S.; Inganäs, O.; Andersson, M. R. *Polymer* **2006**, *47*, 4261.

13. Yi, H.; Johnson, R. G.; Iraqi, A.; Mohamad, D.; Royce, R.; Lidzey, D. G. *Macromol. Rapid Commun.* **2008**, *29*, 1804.

14. Perzon, E.; Zhang, F. L.; Andersson, M.; Mammo, W.; Inganas, O.; Andersson, M. R. *Adv. Mater.* **2007**, *19*, 3308.

15. Steckler, T. T.; Fenwick, O.; Lockwood, T.; Andersson, M. R.; Cacialli, F. *Macromol. Rapid Commun.* **2013**, *34*, 990.

16. Steckler, T. T.; Henriksson, P.; Mollinger, S.; Lundin, A.; Salleo, A.; Andersson, M. R. *J. Am. Chem. Soc.* **2013**, *136*, 1190.

17. Smith, Z. C.; Meyer, D. M.; Simon, M. G.; Staii, C.; Shukla, D.; Thomas, S. W. *Macromolecules* **2015**, *48*, 959.

18. Smith, Z. C.; Pawle, R. H.; Thomas, S. W. *ACS Macro Lett.* **2012**, *1*, 825.

19. Pawle, R. H.; Eastman, V.; Thomas, S. W. *J. Mater. Chem.* **2011**, *21*, 14041.

20. Thomas, S. W. *Macromol. Chem. Phys.* **2012**, *213*, 2443.

21. Lee, Y.; Russell, T. P.; Jo, W. H. *Org. Electron.* **2010**, *11*, 846.

22. Boudreault, P.-L. T.; Najari, A.; Leclerc, M. *Chem. Mater.* **2011**, *23*, 456.

23. Cao, W.; Xue, J. *Energy & Environmental Science* **2014**, *7*, 2123.

Chapter 4 Appendix

^{1}H and ^{13}C NMR

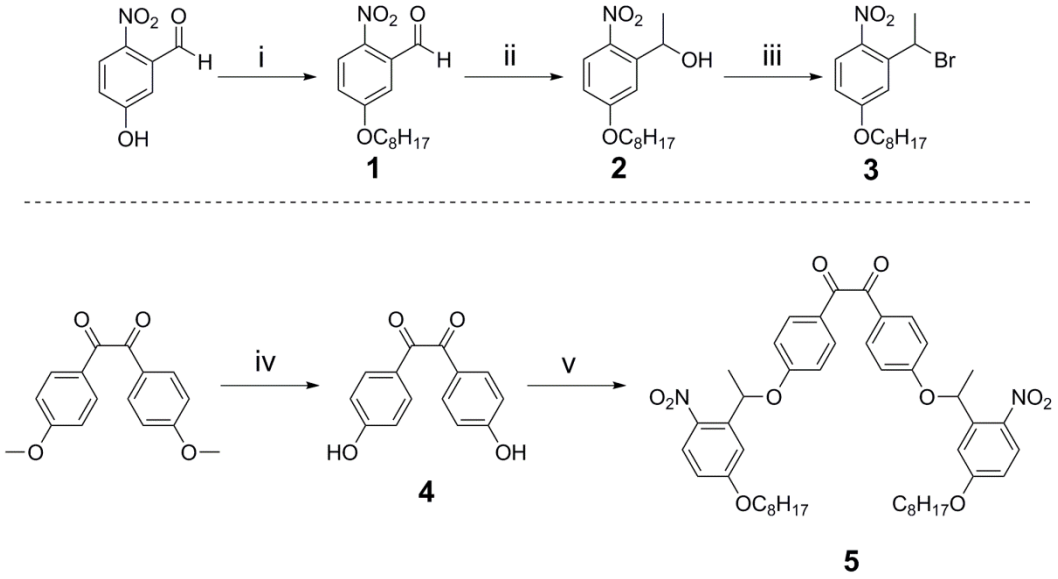

Compound **1**, ^{1}H NMR (500 MHz, $CDCl_3$)

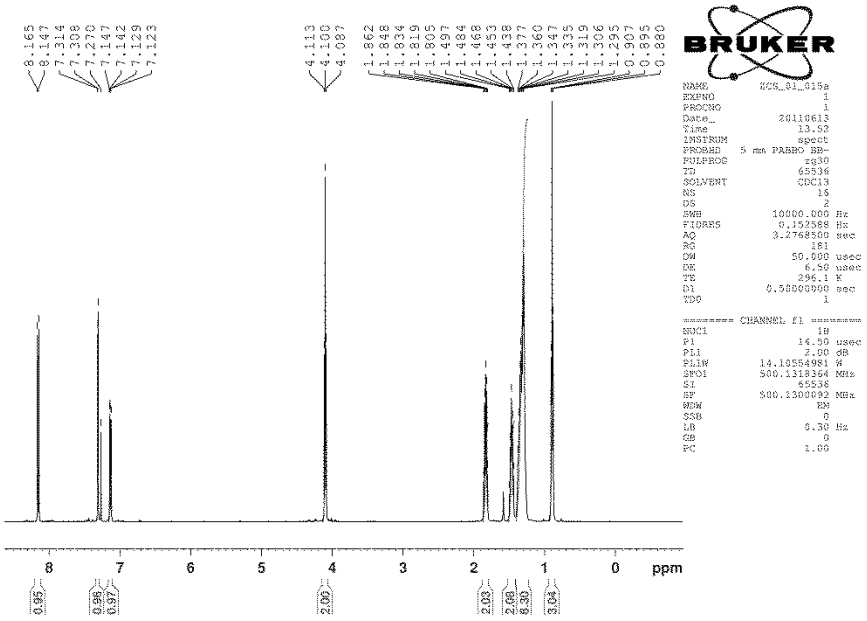

Compound **1**, ^{13}C NMR (125 MHz, $CDCl_3$)

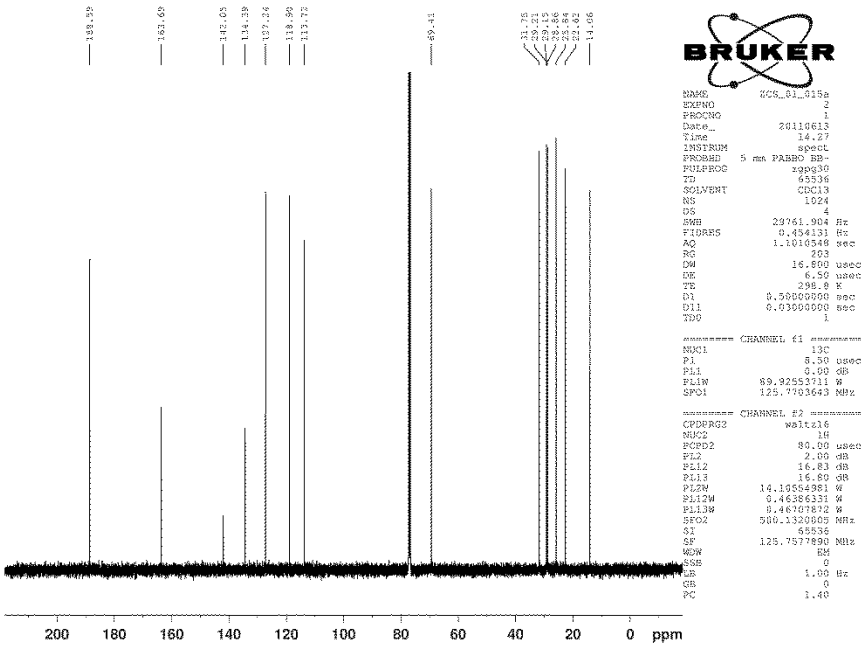

Compound **2**, ^{1}H NMR (500 MHz, $CDCl_3$)

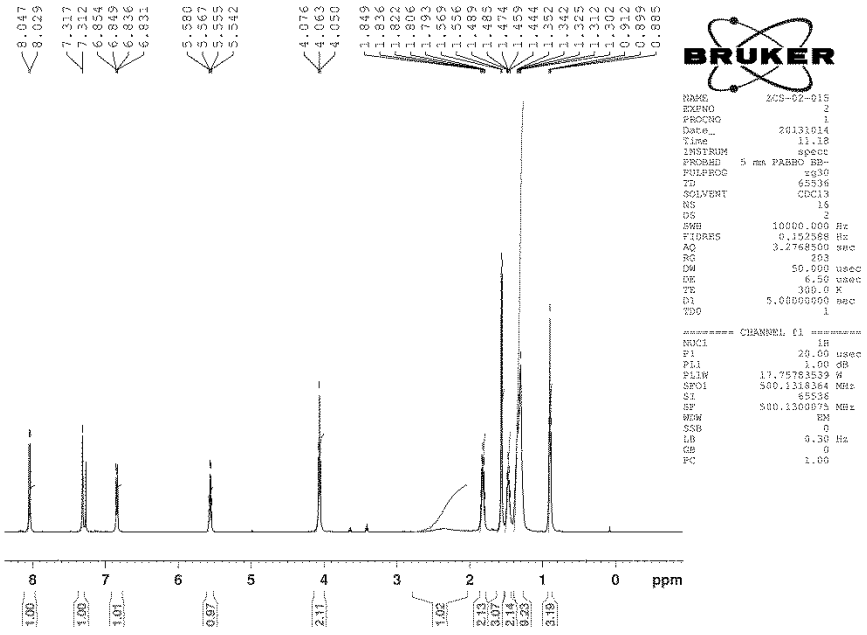

Compound **2**, ^{13}C NMR (125 MHz, $CDCl_3$)

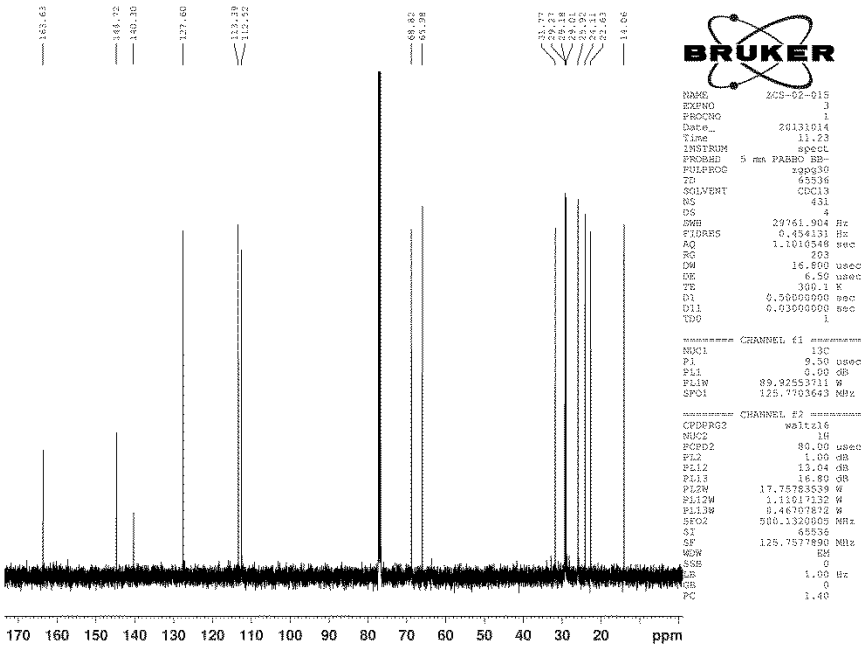

Compound **3**, ^{1}H NMR (500 MHz, $CDCl_3$)

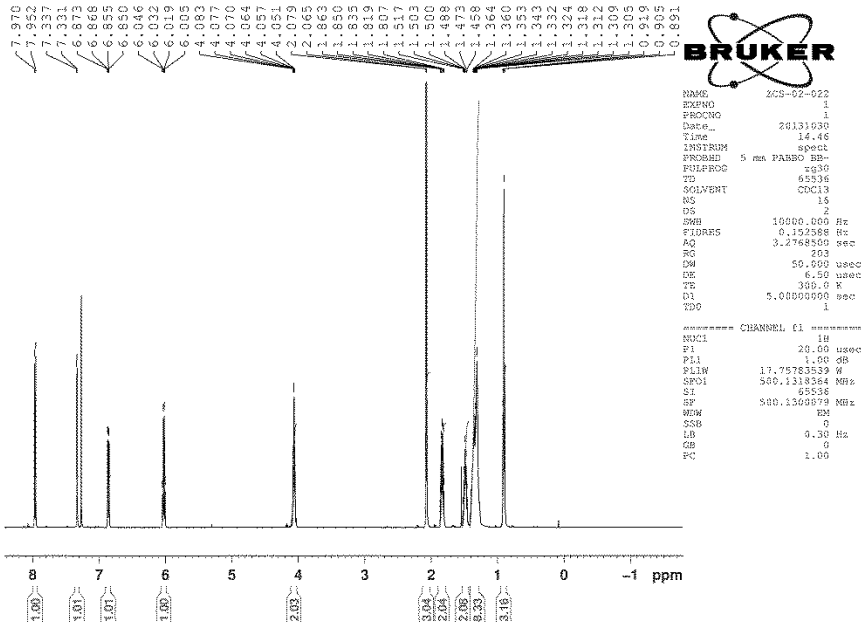

Compound **3**, ^{13}C NMR (125 MHz, $CDCl_3$)

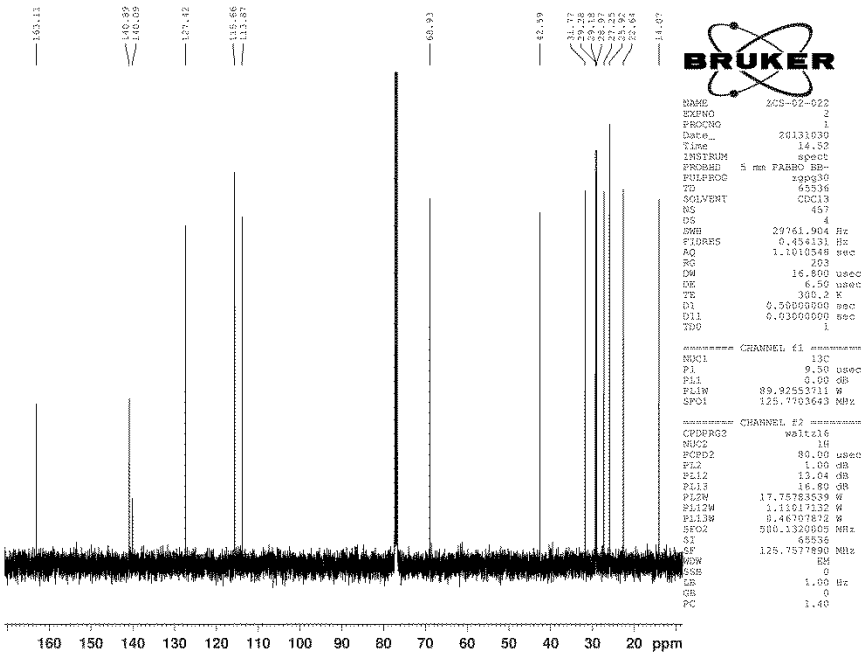

Compound **4**, ^{1}H NMR (500 MHz, $CDCl_3$)

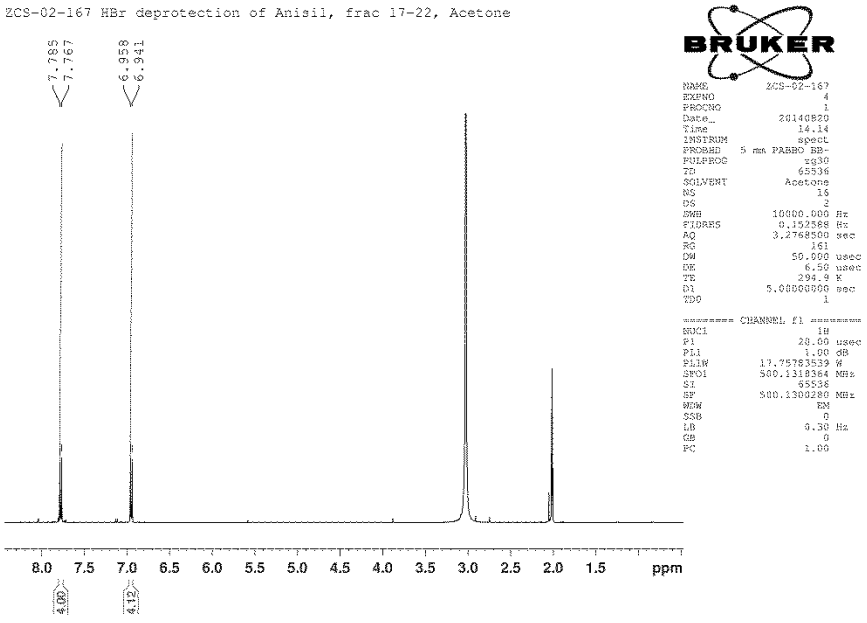

Compound **4**, ^{13}C NMR (125 MHz, $CDCl_3$)

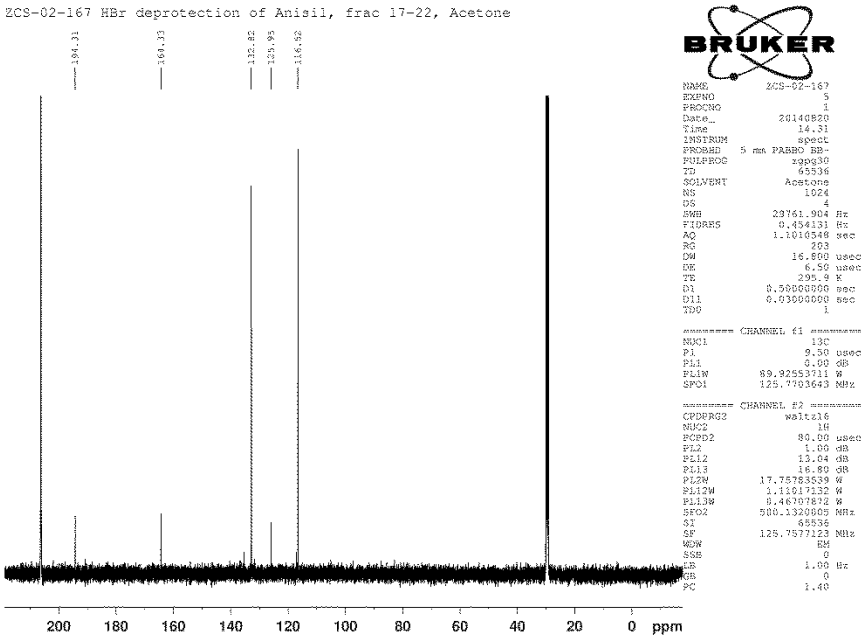

Compound **5**, ^{1}H NMR (500 MHz, $CDCl_3$)

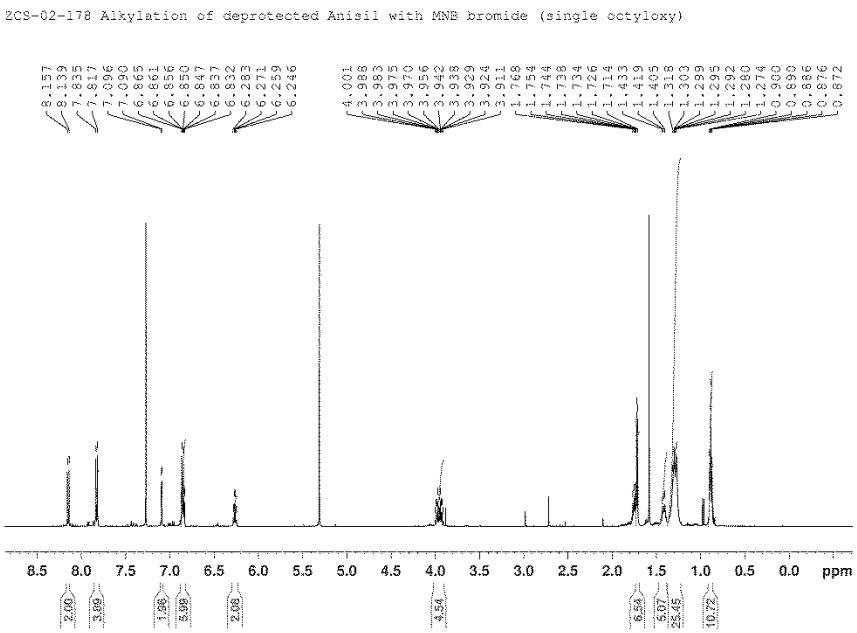

Compound **5**, ^{13}C NMR (125 MHz, $CDCl_3$)

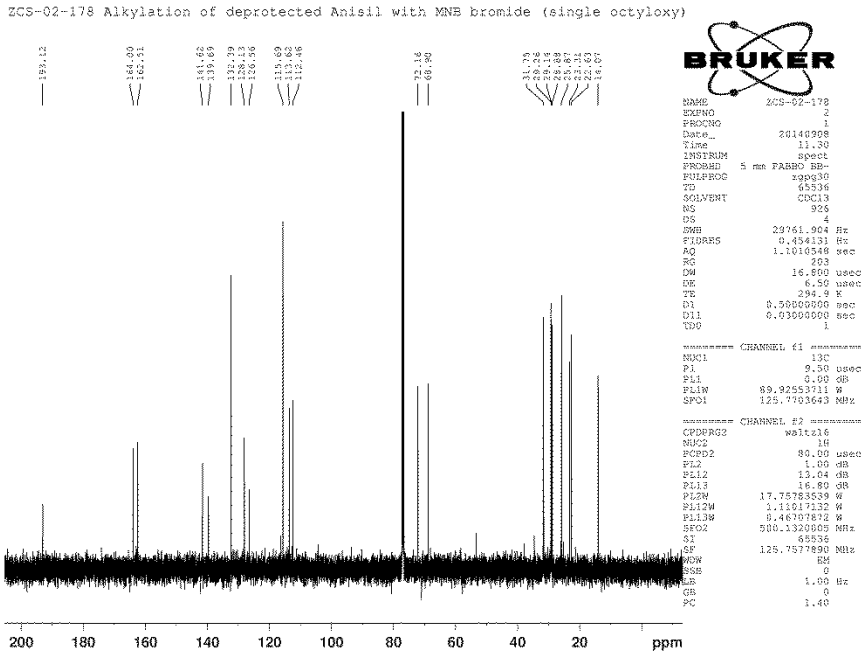

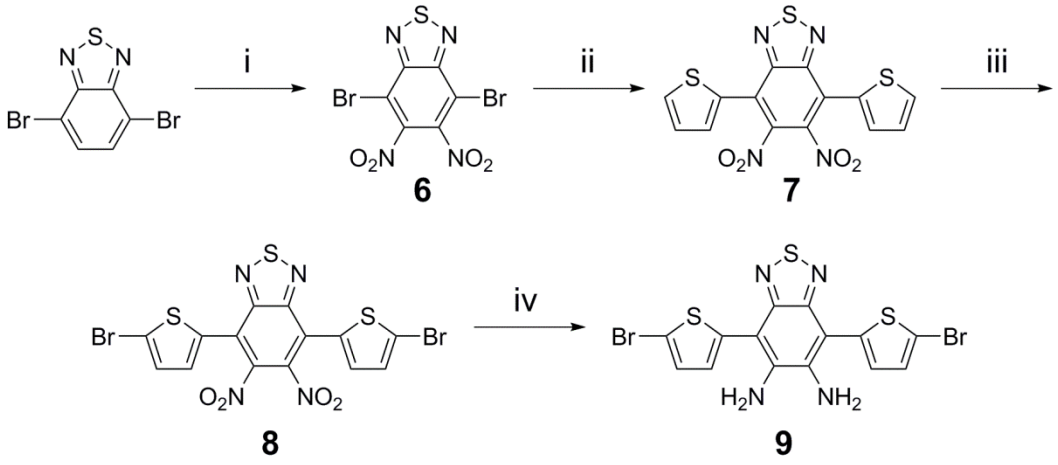

Compound **6**, ^{13}C NMR (125 MHz, $CDCl_3$)

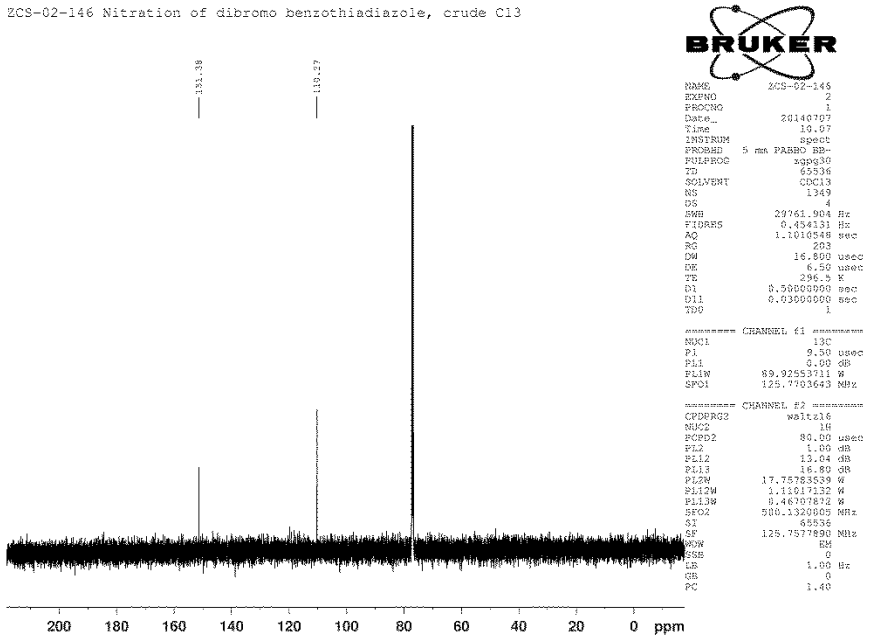

Compound **7**, ^{1}H NMR (500 MHz, $CDCl_3$)

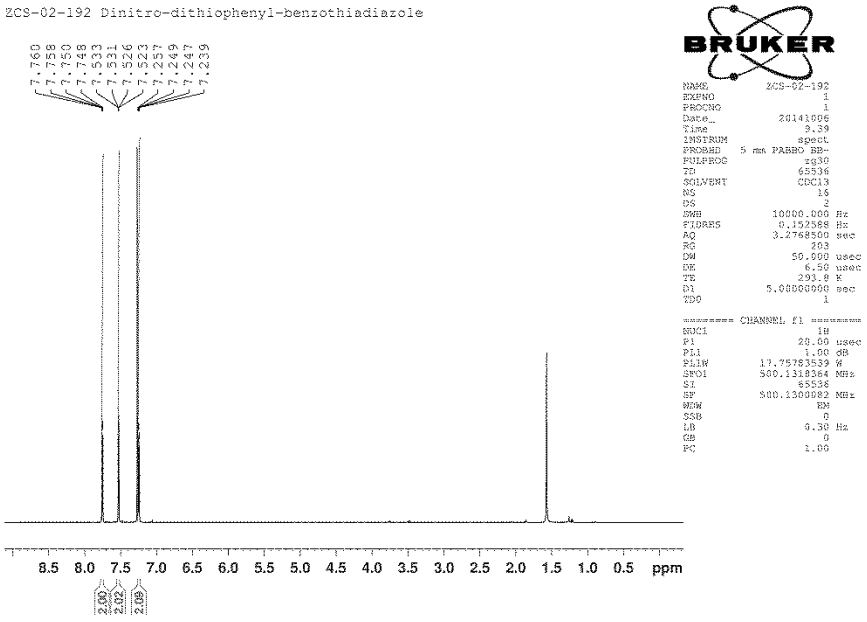

Compound **7**, ^{13}C NMR (125 MHz, $CDCl_3$)

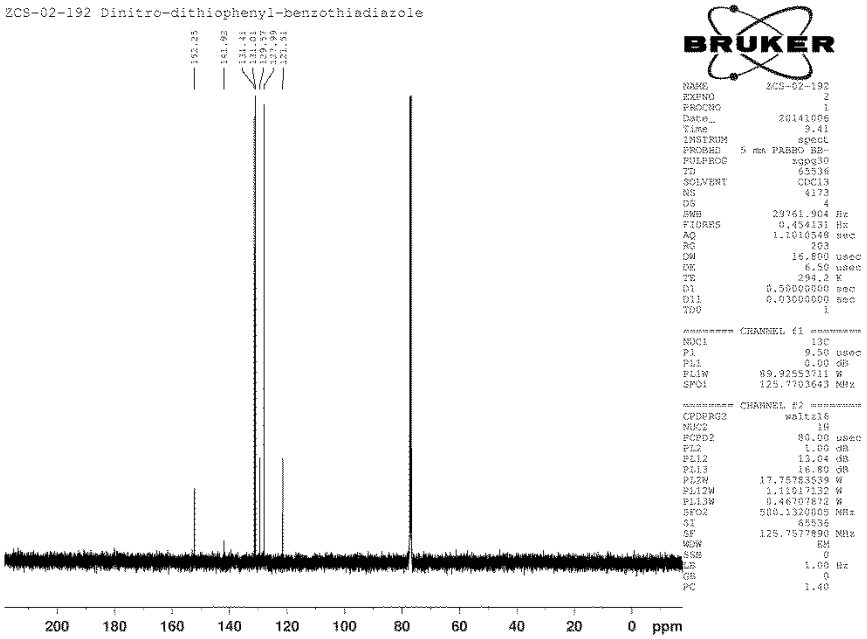

Compound **8**, ^{1}H NMR (500 MHz, $CDCl_3$)

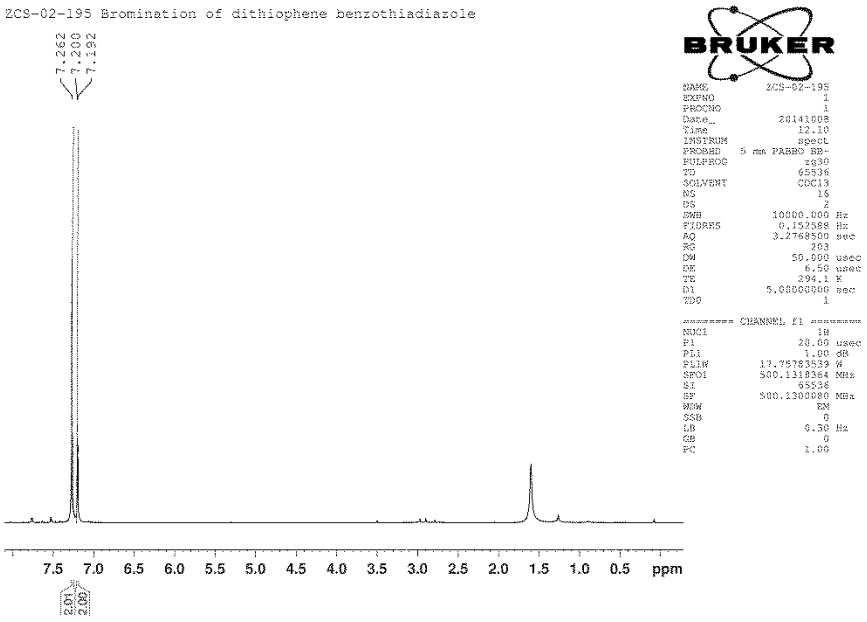

Compound **8**, ^{13}C NMR (125 MHz, $CDCl_3$)

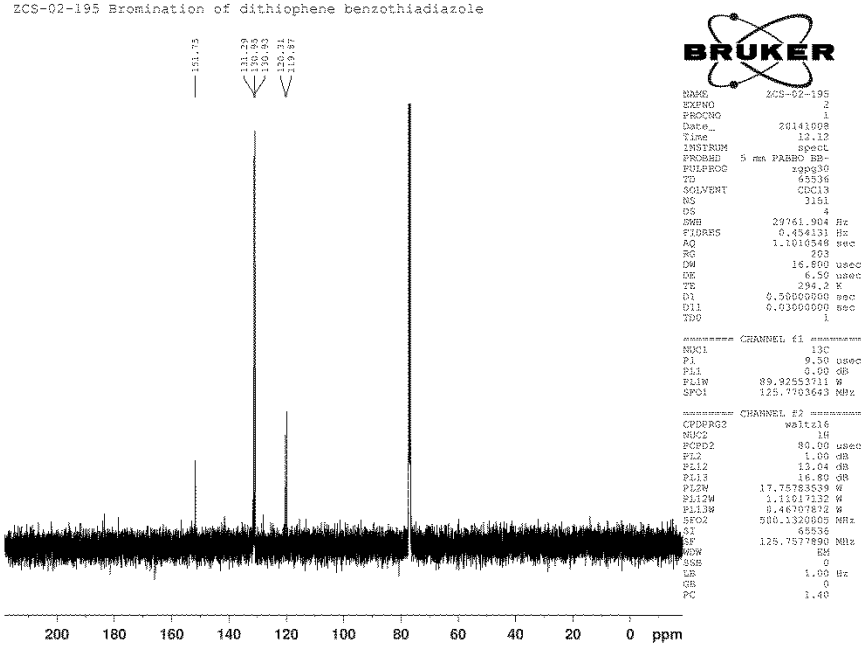

Compound **9**, ^{1}H NMR (500 MHz, $CDCl_3$)

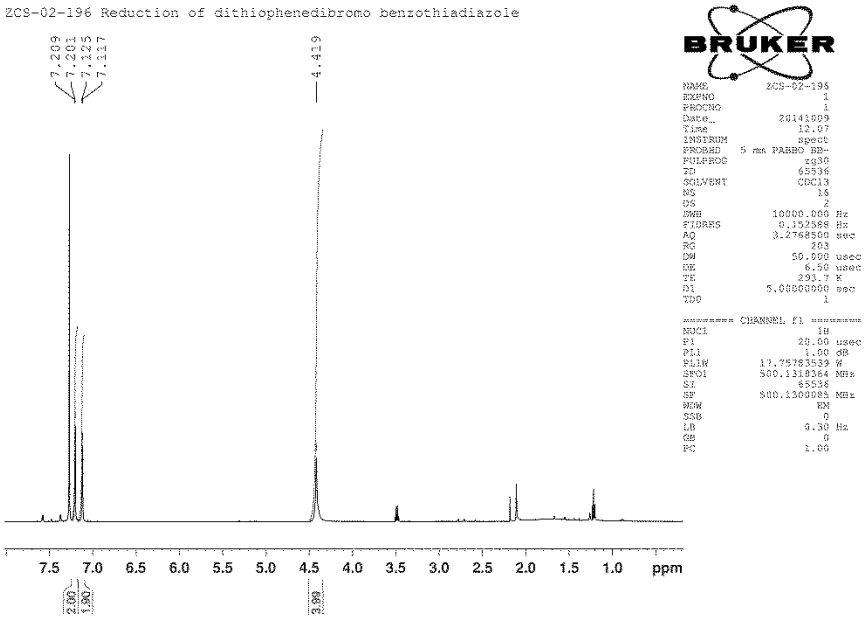

Compound **9**, ^{13}C NMR (125 MHz, $CDCl_3$)

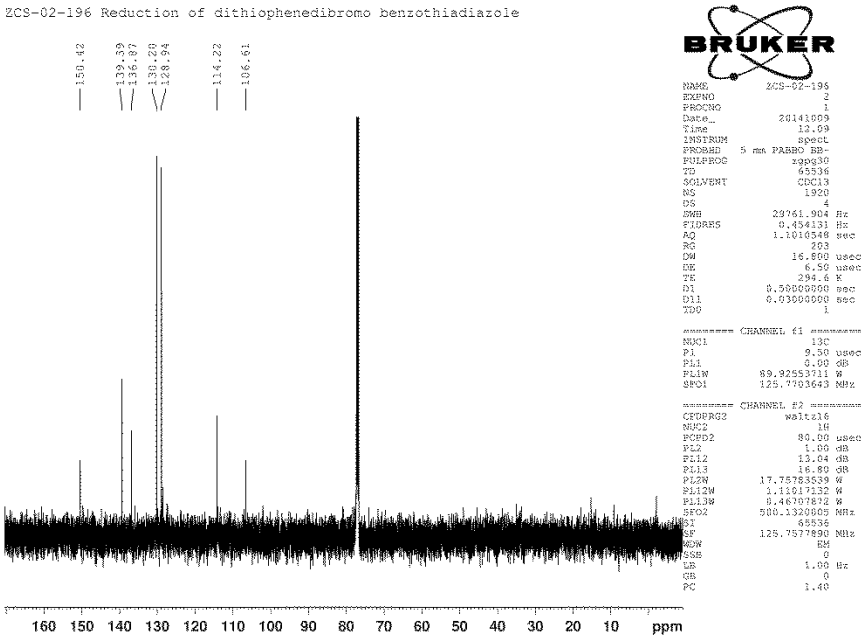

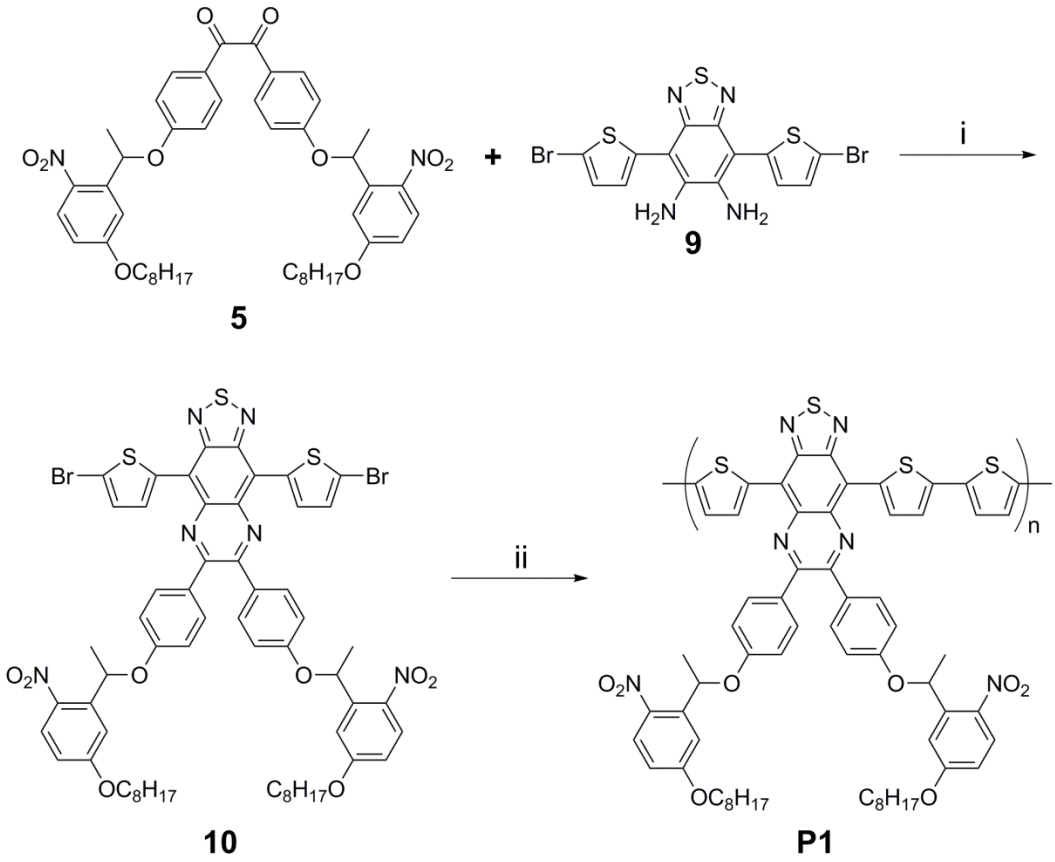

Compound **10**, ^{1}H NMR (500 MHz, $CDCl_3$)

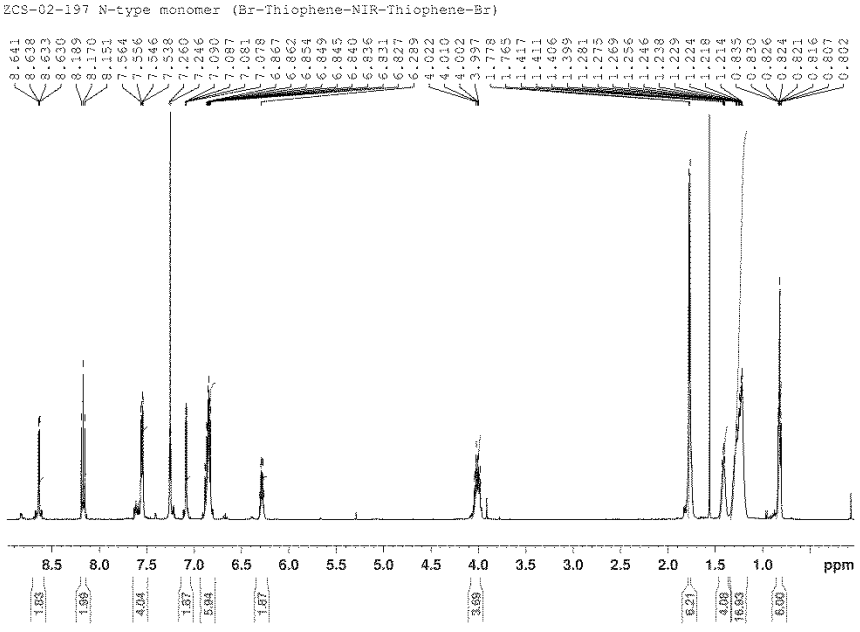

Compound **10**, ^{13}C NMR (125 MHz, $CDCl_3$)

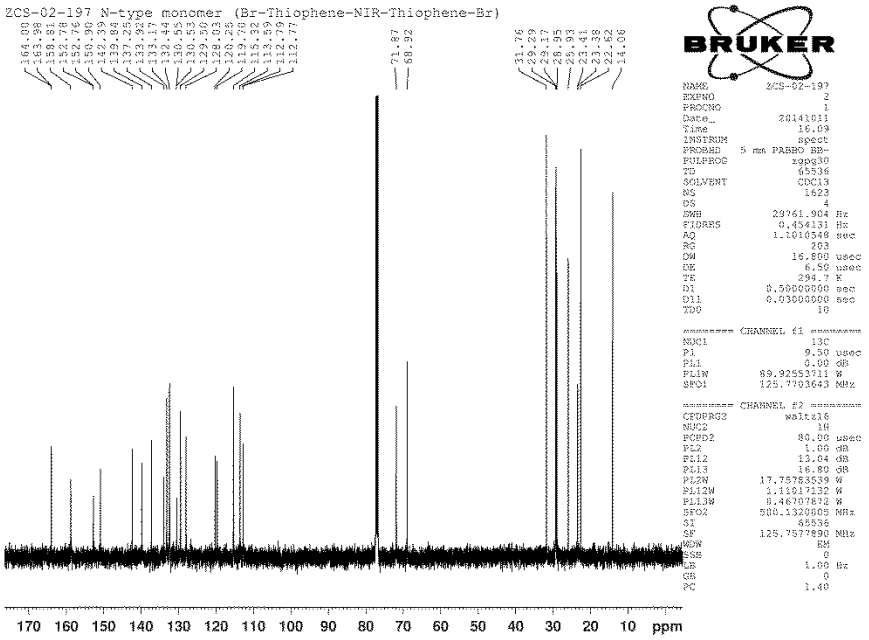

Compound **P1**, ^{1}H NMR (500 MHz, $CDCl_3$)

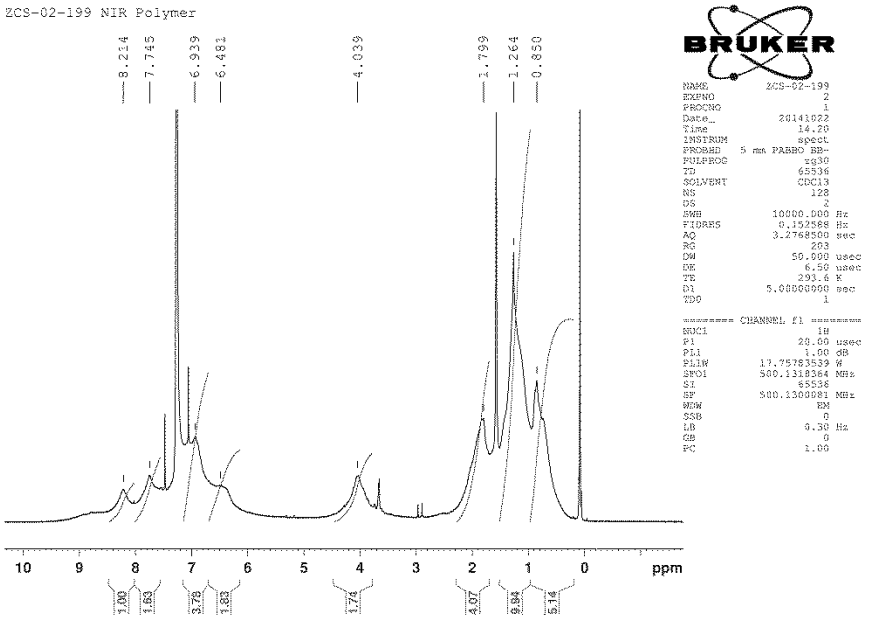

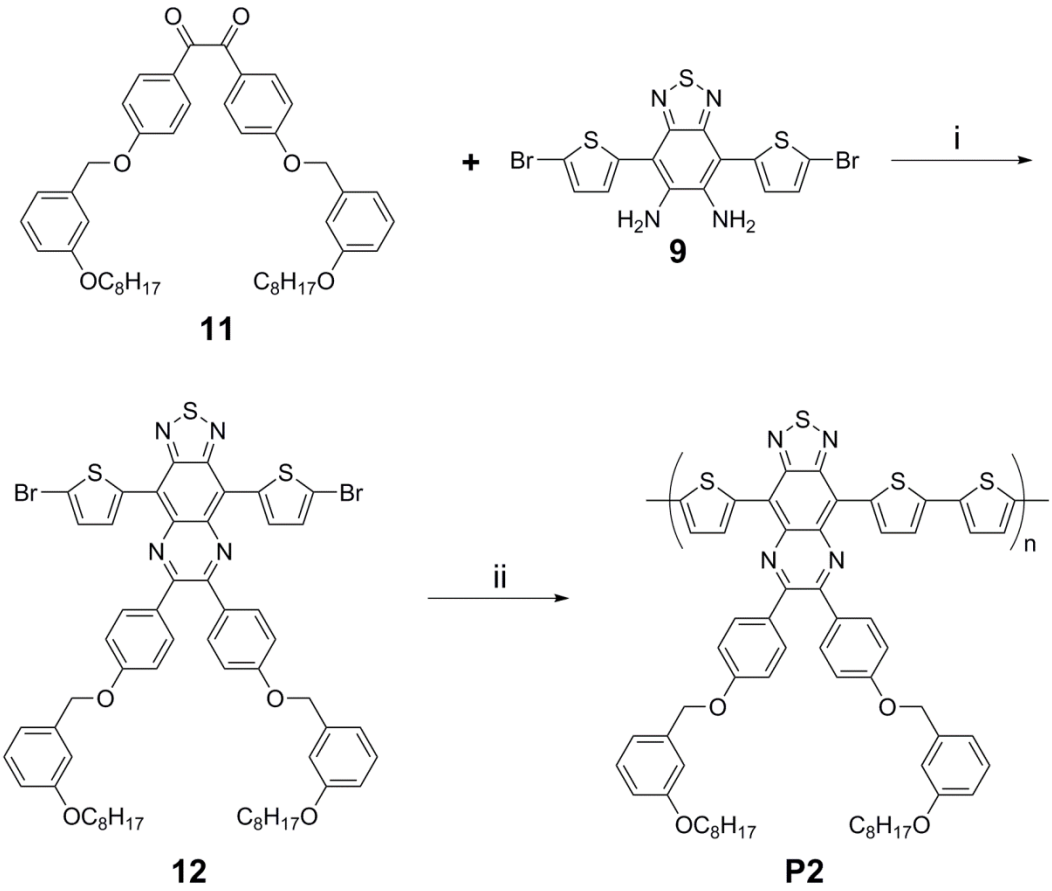

Compound **11**, ^{1}H NMR (500 MHz, $CDCl_3$)

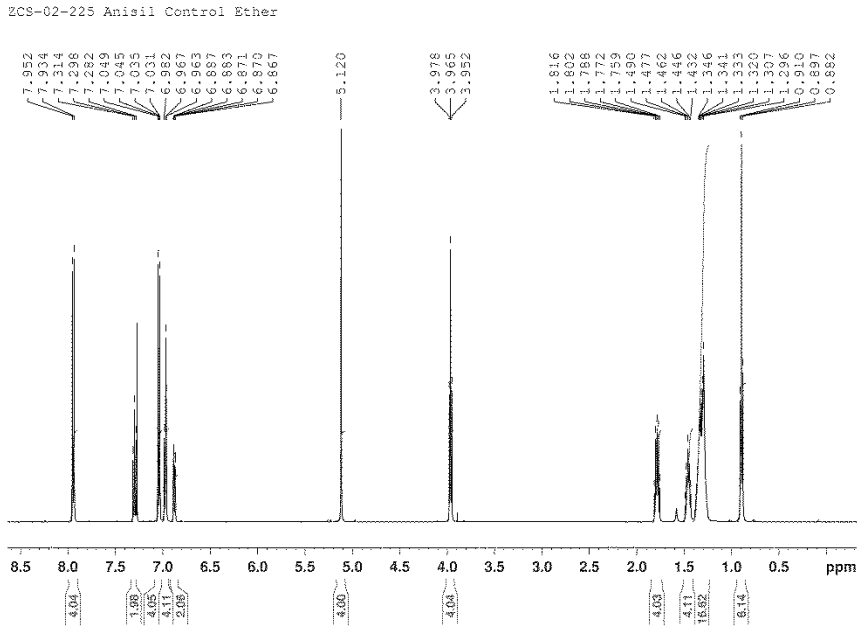

Compound **11**, ^{13}C NMR (125 MHz, $CDCl_3$)

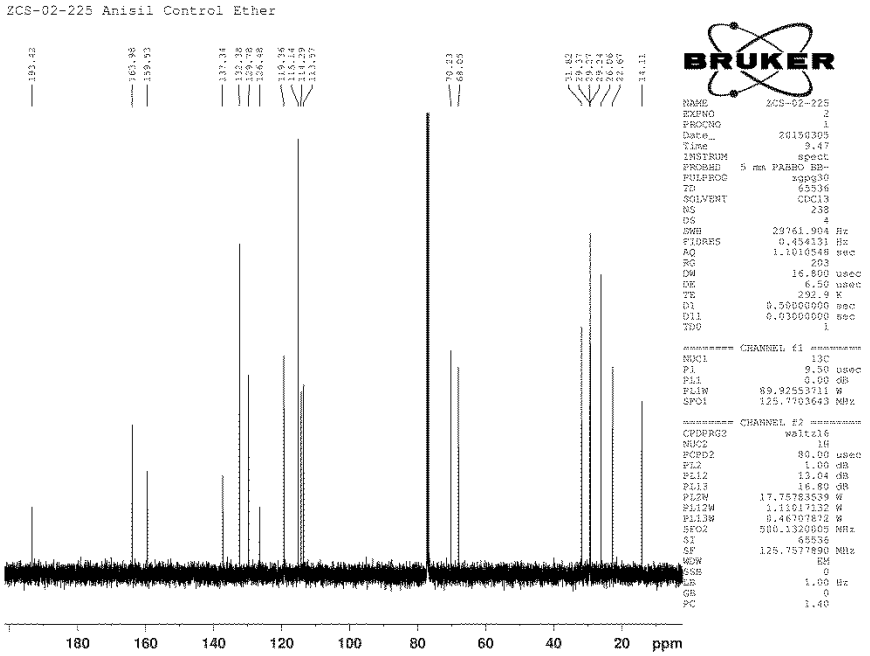

Compound **12**, ^{1}H NMR (500 MHz, $CDCl_3$)

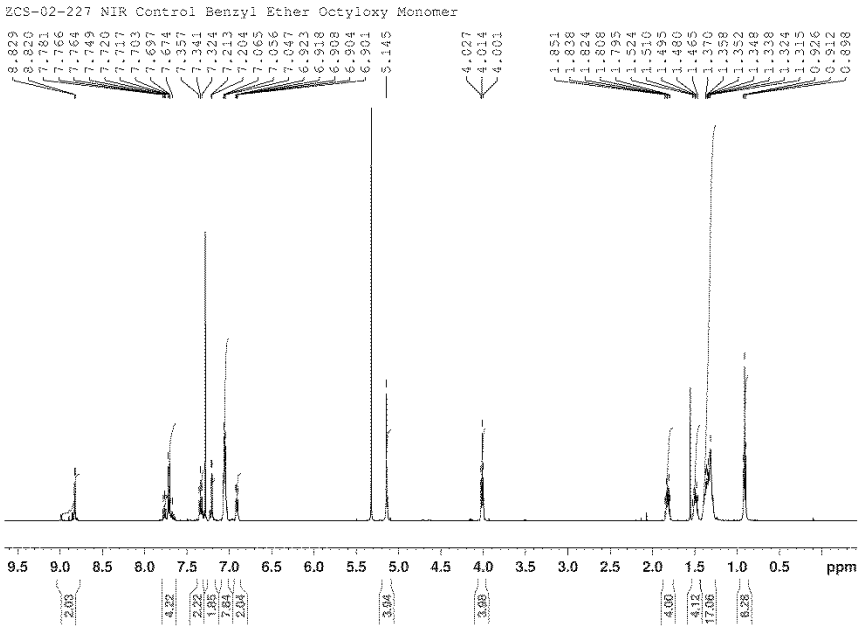

Compound **12**, ^{13}C NMR (125 MHz, $CDCl_3$)

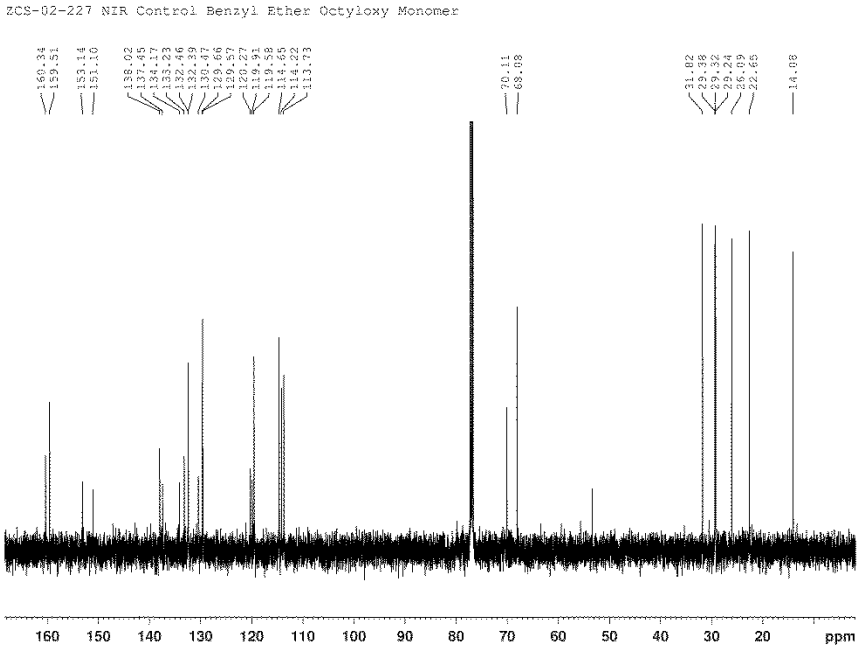

Compound **P2**, ^{1}H NMR (500 MHz, $CDCl_3$)

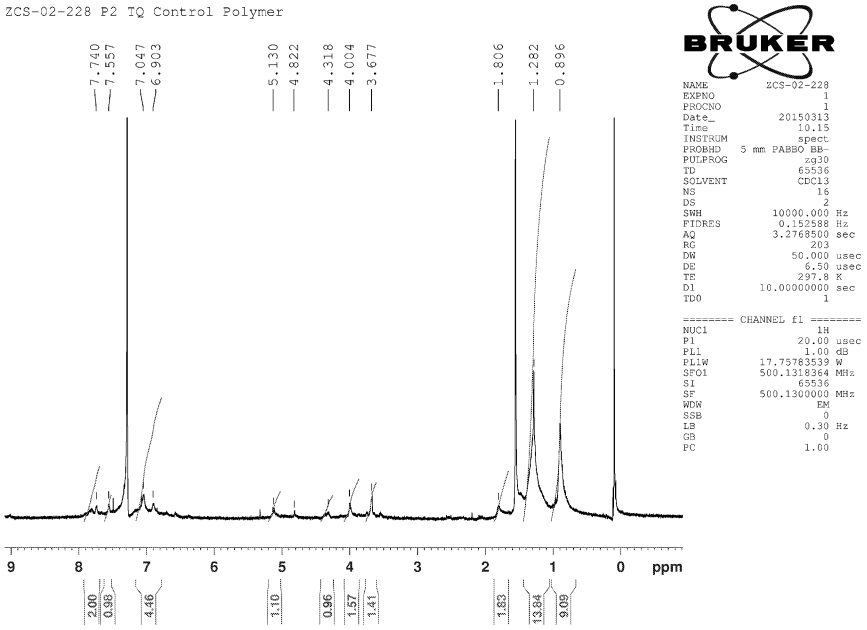

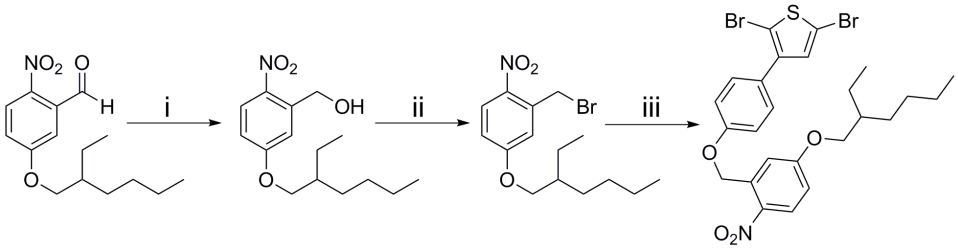

13 **14** **15** **16**

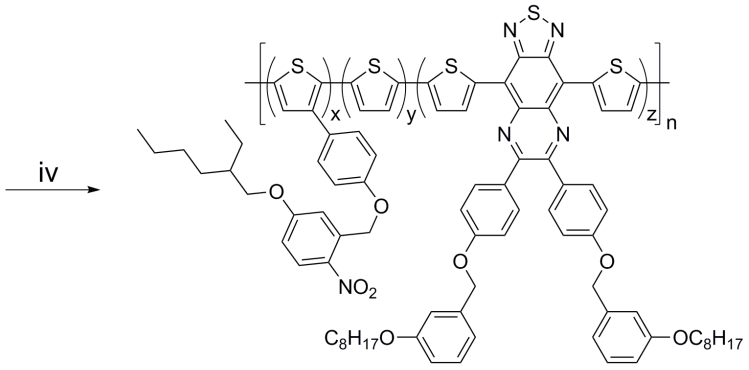

P3: x=0.50, y=1.0, z=0.50
P4: x=0.82, y=1.0, z=0.18

Compound **13**, ^{1}H NMR (500 MHz, $CDCl_3$)

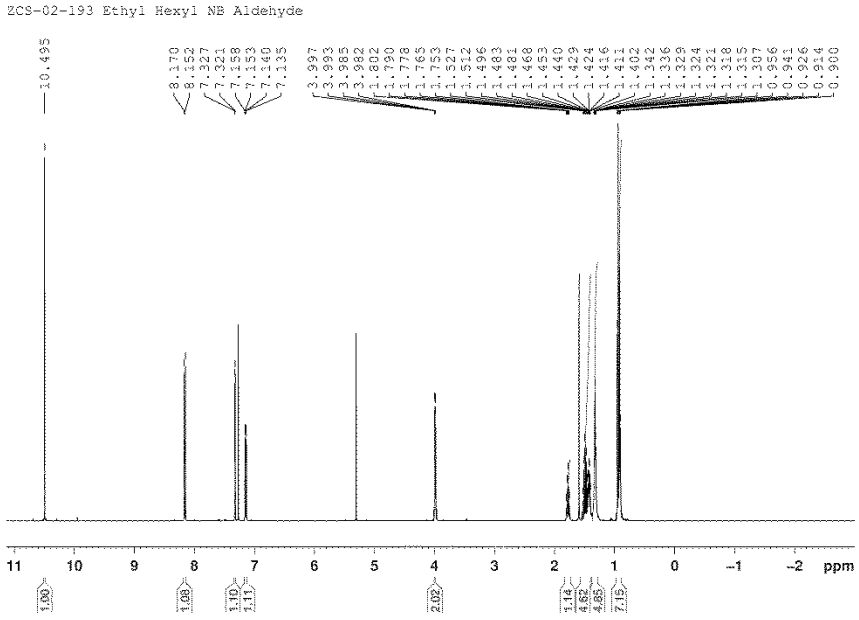

Compound **13**, ^{13}C NMR (125 MHz, $CDCl_3$)

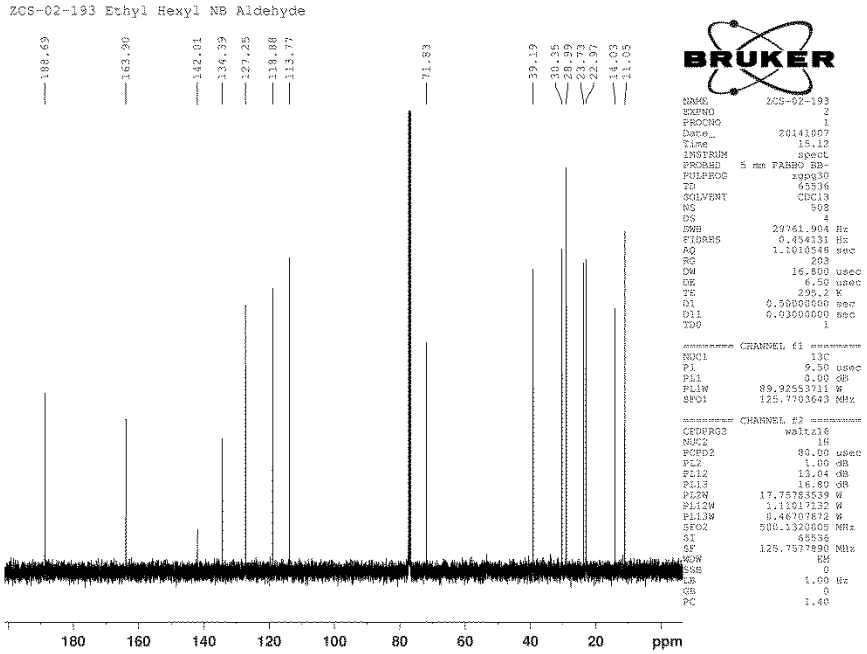

Compound **14**, ^{1}H NMR (500 MHz, $CDCl_3$)

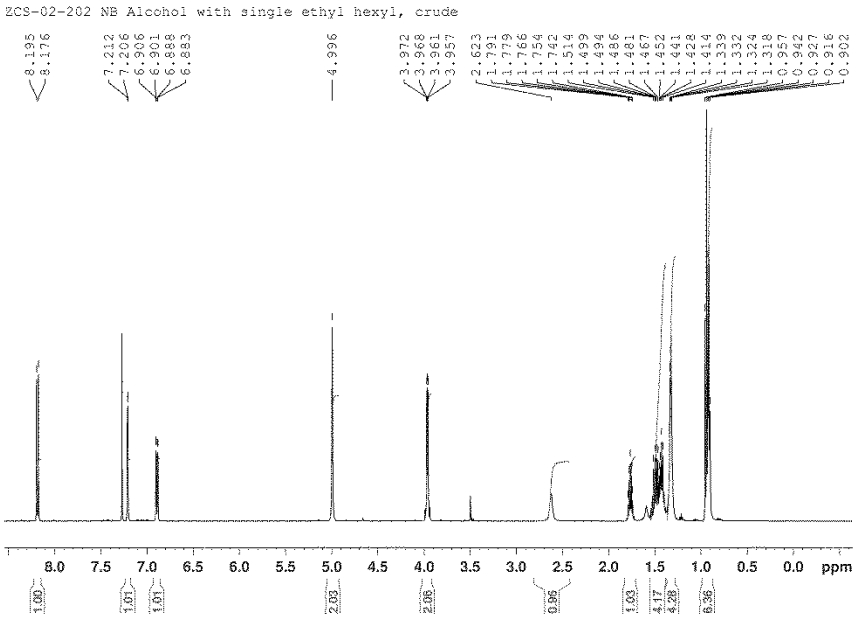

Compound **14**, ^{13}C NMR (125 MHz, $CDCl_3$)

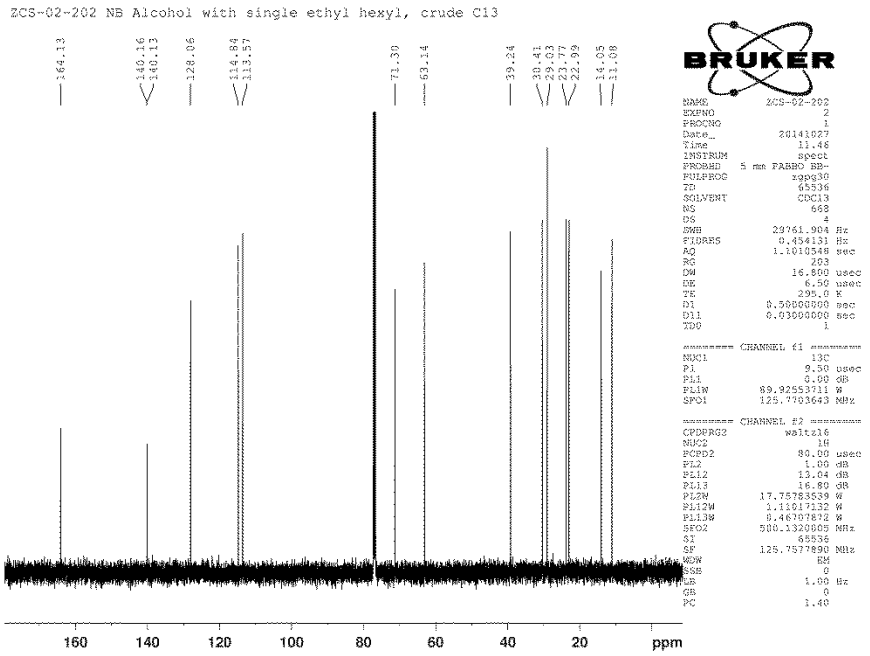

Compound **15**, ^{1}H NMR (300 MHz, $CDCl_3$)

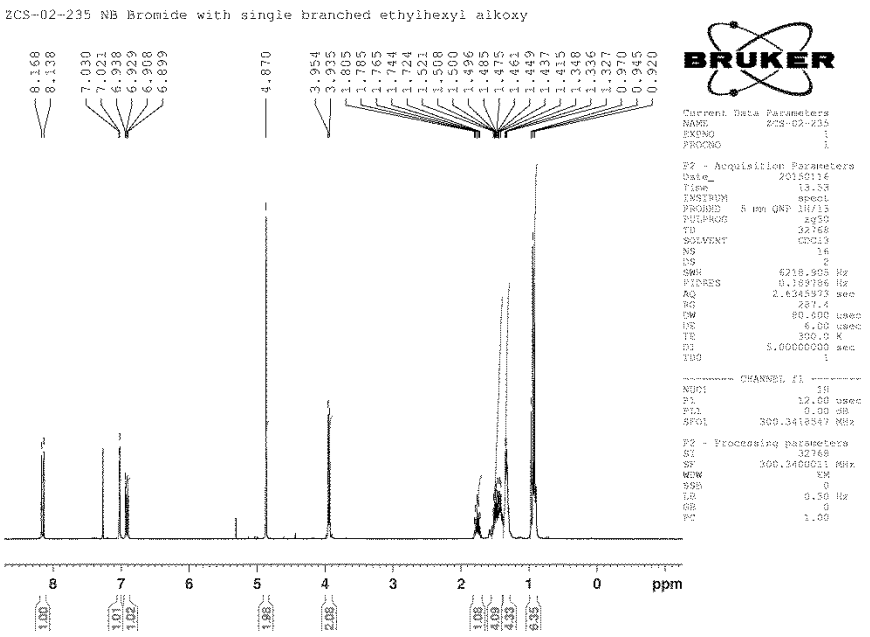

Compound **15**, ^{13}C NMR (75 MHz, $CDCl_3$)

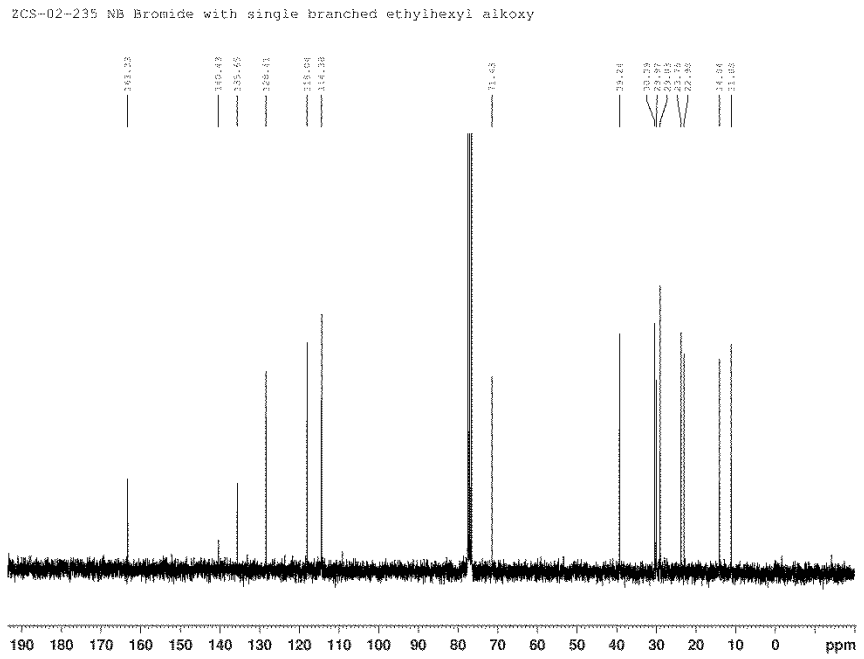

Compound **16**, ^{1}H NMR (300 MHz, $CDCl_3$)

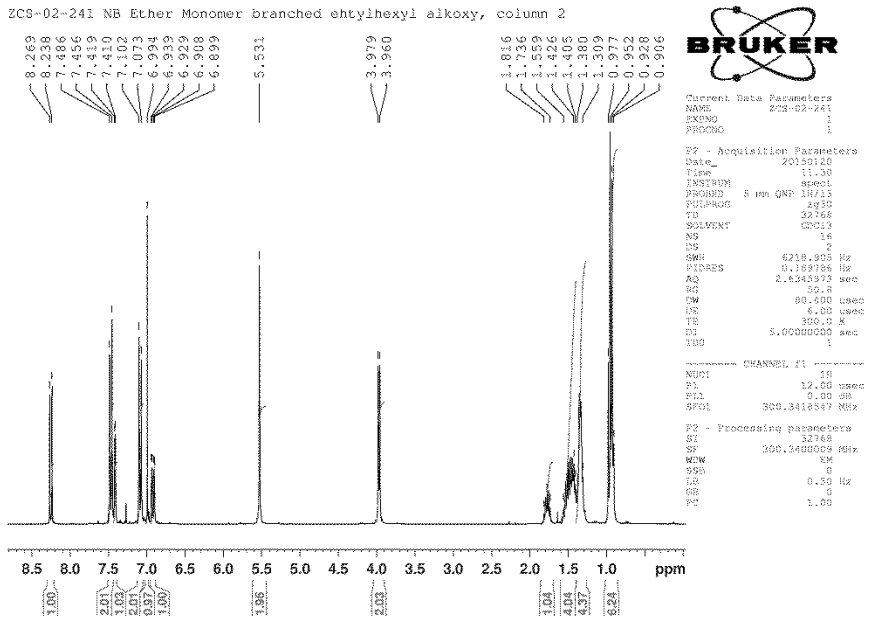

Compound **16**, ^{13}C NMR (75 MHz, $CDCl_3$)

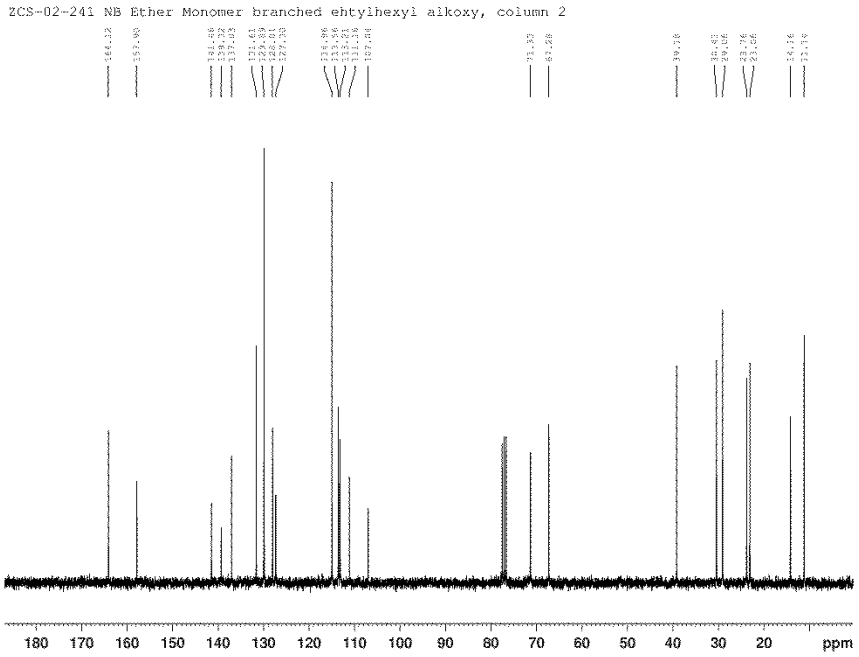

Compound **P3**, ^{1}H NMR (500 MHz, $CDCl_3$)

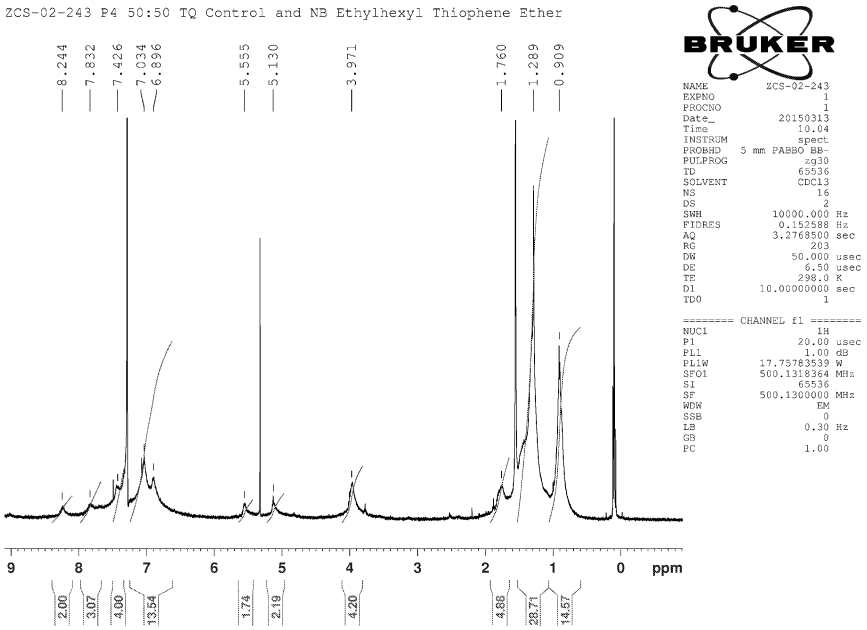

Compound **P4**, ^{1}H NMR (500 MHz, $CDCl_3$)

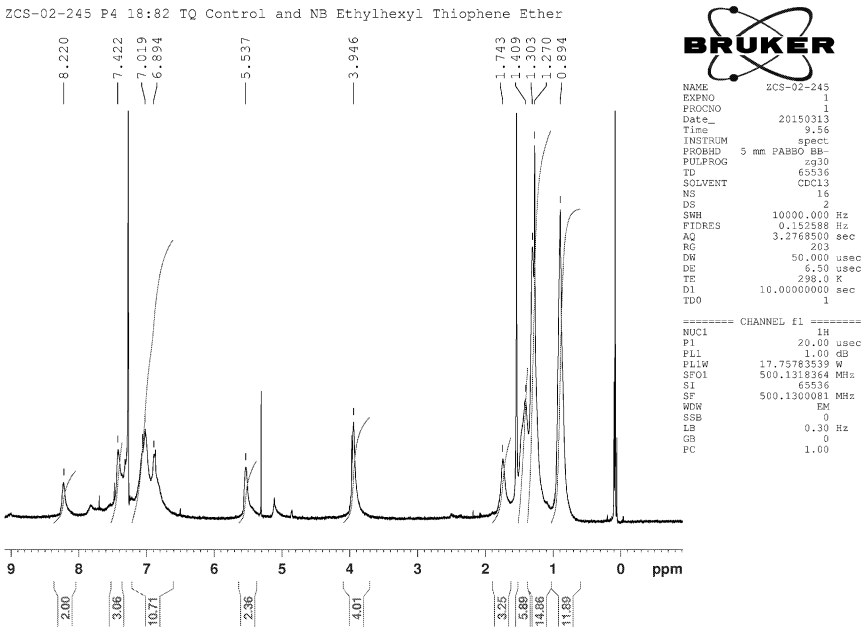

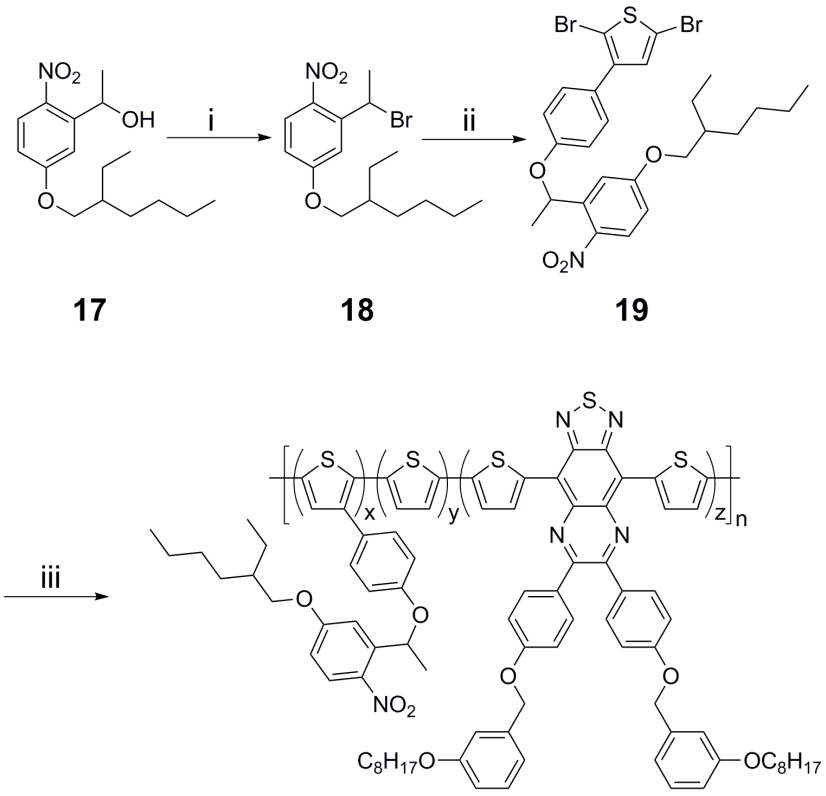

P5: x=0.50, y=1.0, z=0.50

Compound **17**, ^{1}H NMR (500 MHz, $CDCl_3$)

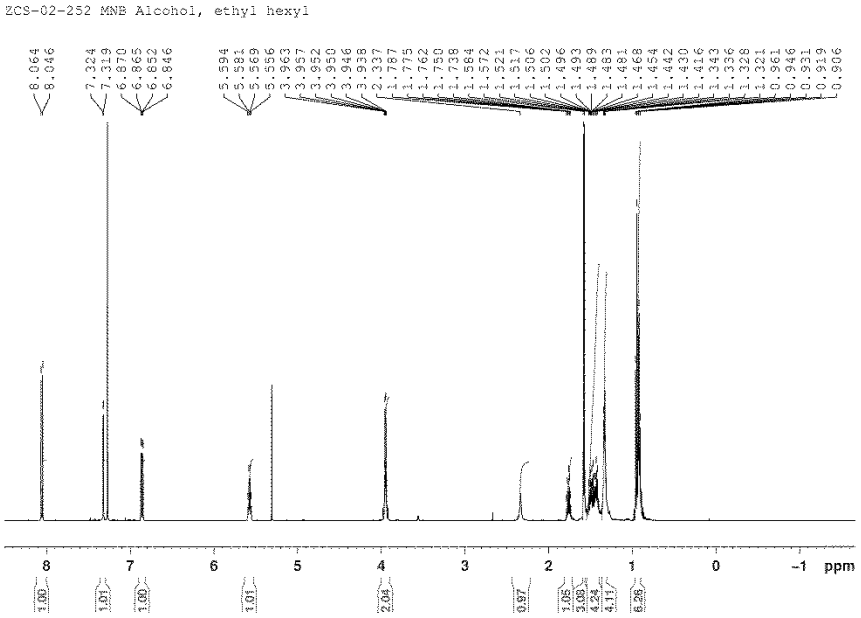

Compound **17**, ^{13}C NMR (125 MHz, $CDCl_3$)

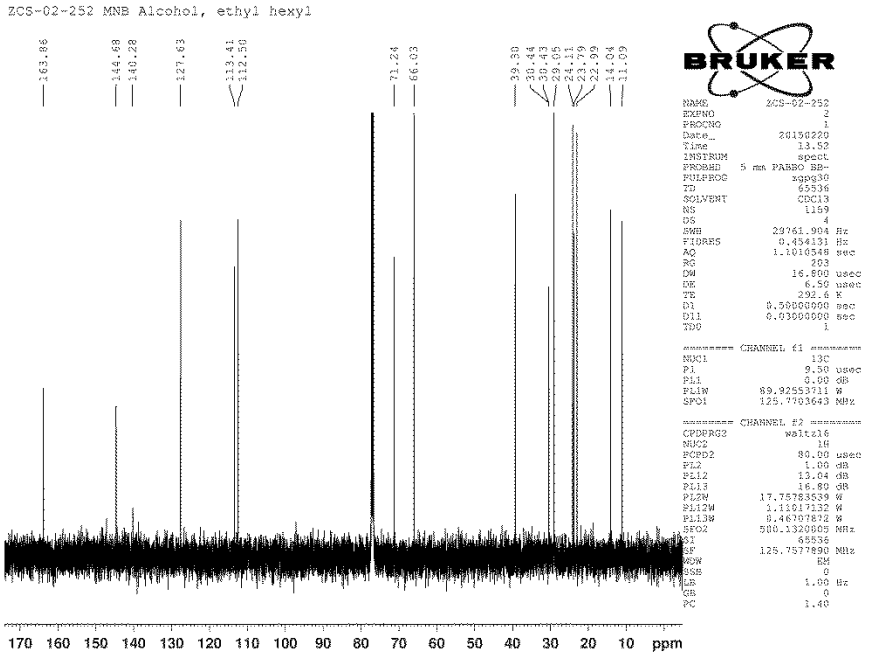

Compound **18**, ^{1}H NMR (500 MHz, $CDCl_3$)

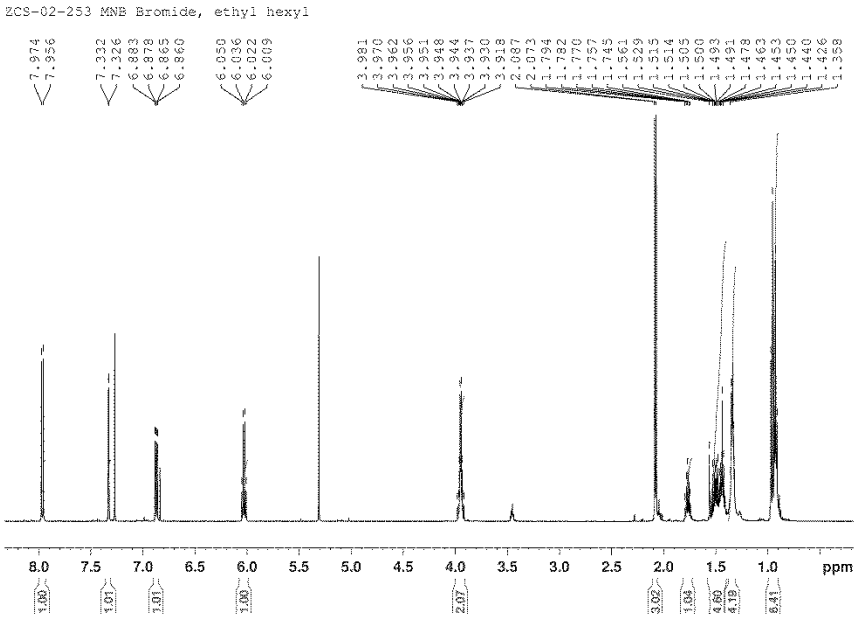

Compound **18**, ^{13}C NMR (125 MHz, $CDCl_3$)

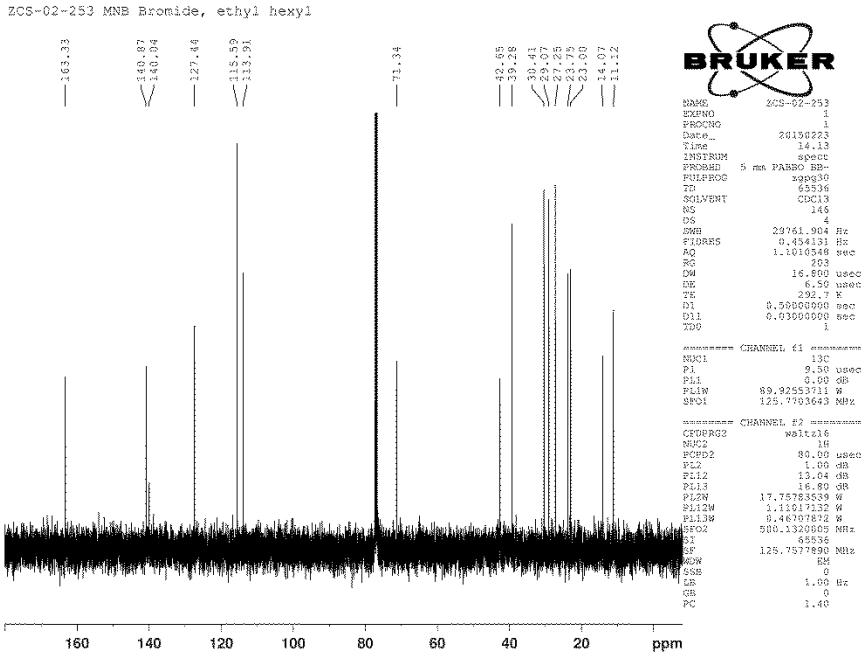

Compound **19**, ^{1}H NMR (500 MHz, $CDCl_3$)

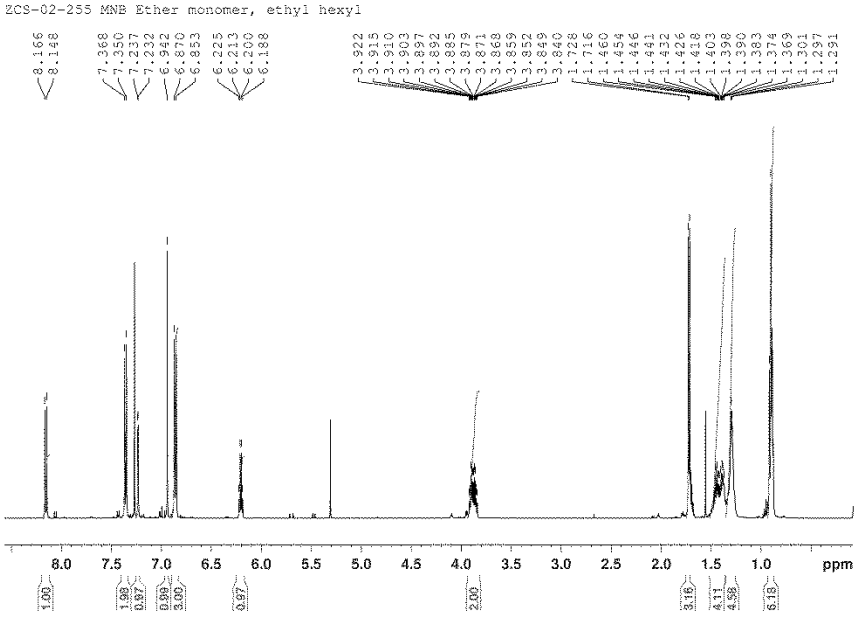

Compound **19**, ^{13}C NMR (125 MHz, $CDCl_3$)

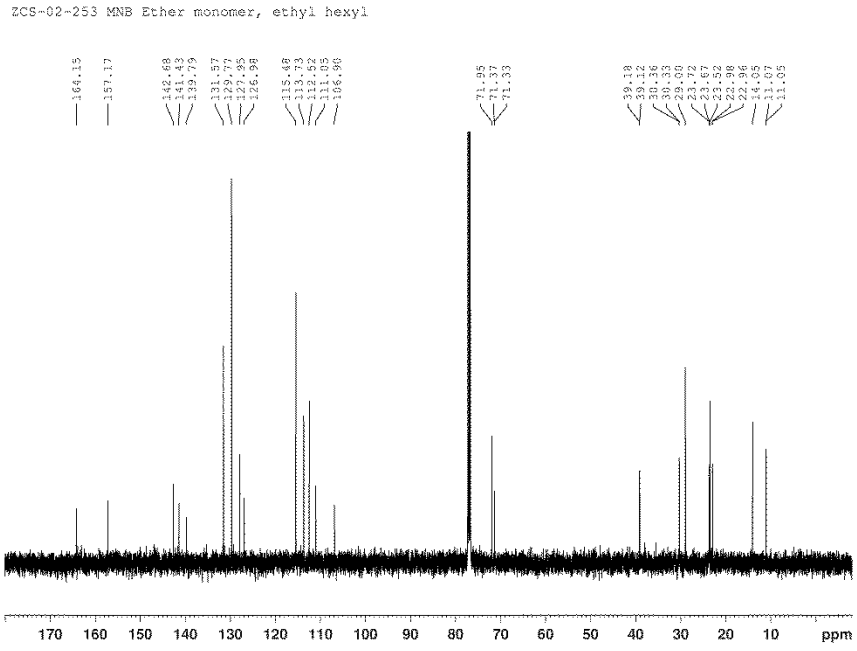

Compound **P5**, ^{1}H NMR (500 MHz, $CDCl_3$)